The University Of Sheffield.

Elucidating the impact of loss of function of AP-2 endocytic adaptor complex of *Candida albicans* in hyphal morphology switch and virulence during host - pathogen interactions.

Stella Christou

A thesis submitted in partial fulfilment of the requirements for the degree of Doctor of Philosophy.

The University of Sheffield

Department of Biomedical Sciences

Faculty of Science

December 2021

Abstract

Recently AP-2 endocytic adaptor complex was determined to have an important role in the endocytosis of an important *Candida albicans* cell wall synthase, chitin synthase 3 (Chs3). Loss of function of AP-2 cells cannot endocytose Chs3 resulting in increased cell wall composition changes and defects during polarized growth. The cell wall and hyphal switch are two important *C. albicans* virulence factors so studying the impact of AP-2 was of interest. In this study, the importance of AP-2 for the host – pathogen interactions of the human pathogenic fungus *C. albicans* were investigated. Three infection models were used (macrophages, epithelial and zebrafish embryos) to investigate the significance of AP-2 during host-pathogen interactions. This investigation shows that the cell wall composition changes in *C. albicans* with loss of function of AP-2 resulting in increased phagocytosis by macrophages, decreased host adhesion and decreased virulence in both macrophage and zebrafish models. *C. albicans* with loss of function of AP-2 complex are less virulent however they are not cleared by the host immune system but rather proliferate in the host cells. The mutant *C. albicans* cells were less invasive than wild type cells during epithelial infections, suggesting reduced host cell damage and virulence. This thesis concludes that the AP-2 is critical for the virulence of *C. albicans* cells due to its role in cell wall remodelling, hyphal morphology switch and hyphal maintenance.

Acknowledgements

I would like to sincerely thank my supervisors. Kathryn, thank you so much for being patient with me, being encouraging and checking that I am doing well. You always reminded me to take a step back and relax. Thank you for going through all my bad writing and not being annoyed at how dissociated everything sounded. Simon, thank you for all the encouragement and your overall positive vibe through the entire PhD. Thank you both for teaching me how to be a proper scientist. It was amazing to meet and work with both of you.

To my KASWER lab past and present, thank you all for being around to help and hear me excessively mumble all about pathogens for the past 4 plus years. Steve and Elena thank you for your constructive criticism during my lab talks. Iwona and Harriet, thank you for teaching me all about *Candida* and being my lab support. Mona, Adam, Ben and Sarah we all started this experience together, and I have to say that my experience would have not been the same without you there. I learned a lot from all of you; from things like keeping calm to Yorkshire slang. Hopefully you will all remember me as the short one running around in distress every time her timer was beeping. The rest of my PhD gang Montse, Nan, Bian it has been great to be around you guys, I don't know if things would have been as great without you, I will most definitely miss you. See you all in Austria! My little ones Shahd, Sherry, Rachele and Haya it was nice to have you around during this writing process.

To my Johnstons assemble group, I will miss you all so much! Thank you for teaching me loads of things and taking me for walks and brunch when I was stressed. Jaime, Jacob, Topher, Jacqui and Mahrukh I will miss you guys a lot with all your "great" taste in music, silly chats and loads of random skin care conversations. Thank you to all the past Johnston lab members (Kate and Josie) for being welcoming and overall amazing lab friends. I would like to also thank the Cake and Science lab meeting group for their engagement during my lab talks and the great suggestions. Ffion my injection buddy, our chats during injections were always amazing and I don't think I can inject embryos again without you next to me chatting about random tv shows. Walking buddy Jelle, thank you for being there and keeping me company during lockdown, will miss you my little one.

I would also like to thank my advisor Dan Humphreys for all his support and suggestions through the past 4 years. Thank you to the aquarium facility for keeping our zebrafish embryos happy and also to the LMF facility for their help specifically Nick and Darren. Thank you to BBSRC White rose for funding this PhD and giving me the opportunity to do this.

My friends both from back home, Sheffield and the world thank you for your support, even the smallest funny video or pet video has helped me through the process. Stella and Sophia, I love you guys. My friends in Sheffield (Danielle, Laura, Eve and my lab mates) thank you for all the emotional support, for going on pub trips around Sheffield and making things fun, I am hoping to see much much more of all of you in the future. Mireia, thank you for being my family here and really caring about my wellbeing. My friends who are abroad Barbara, Irene and Noura I miss you guys and thank you for staying in touch.

My cousins plus sister group chat Guardians of the Vaccine formerly known as Ιός ανέστη formerly known as Πανδημιόγενέθλια and other names, thank you for being my flatmates during lockdown and sending me weird video of the day updates Taso, Salomi and Panagiota I love you my babies, thank you for making me laugh and being my virtual family (besides the fact that you are my actual family hahaha). Thank you to my big fat Cyprus family (my uncles, aunties, cousins and of course my dad) for all their support through the years, I cannot name all of you because you are just too many and this would literally take ages. Special love and a big thank you to the two most important women in my life my mum and my granny, you both raised me and brought me up to the person I am today. With no exaggeration at all I am here and me because of you. This thesis is dedicated to both of you.

Contents

List of figures

List of tables

List of abbreviations

%	Percentage
µg	Micrograms
µL	Microliter
µm	Micrometer
AFM	Atomic Force Microscopy
Akt	A serine threonine kinase
Als	Agglutinin like sequence
ANOVA	Analysis of variance
AP-2	Adaptor protein 2
ATP	Adenosine triphosphate
bp	Base pairs
C. albicans	*Candida albicans*
C’	Carboxy terminal
CARD-9	Caspase recruitment domain-containing protein 9
cfu	Colony forming units
CFW	Calcofluor white
Chs	Chitin synthase
Cht	Chitinase
Clod	Clodronate
CO_2	Carbon dioxide
CW	Cell wall
CWI	Cell wall integrity
dH_2O	Distilled water
DIC	Differential interference contrast microscopy
dpf	Days post fertilization
dpi	Days post infection
EDTA	ethylenediaminetetraacetic acid
EGFR	Epidermal Growth Factor Receptor

ER	Endoplasmic reticulum
ERK	Extracellular signal-regulated protein kinase
ESCRT	Endosomal-sorting complex required for transport
F-actin	Filamentous actin
FBS	Fetal bovine serum
FIJI	FIJI Is Just ImageJ
fL	Femtoliter
g	Gravity
g	Grams
GDP/GTP	Guanosine diphosphate/ uanosine trisphosphate
GFP	Green fluorescent protein
GOI	Gene of interest
HCl	Hydrochloric acid
HOG	High Osmolarity Glycerol
hpi	Hours post infection
hr	Hour
Hwp1	Hyphal wall protein 1
IgG	Immunoglobulin G
ILx	Interleukin
IκB	Inhibitor of kappa-light-chain-enhancer of activated B-cells
JNK	c-Jun N terminal kinase
kDa	Kilodalton
kV	Kilovolt
LiOAc	Lithium acetate
Lipo	PBS liposome
M	Molar
MAPK	Mitogen Activated protein kinase
mg	Milligrams
MKP1	Mitogen-activated protein kinase phosphatase 1
mM	Millimolar

MPa	Megapascals
mTOR	Mammalian target of rapamycin
n	Number of replicates / animals in the experiment
N’	Amino terminal
NaCl	Sodium chloride
NaOH	Sodium hydroxide
NET	Neutrophil extracellular traps
NFκB	Nuclear Factor kappa-light-chain-enhancer of activated B-cells
ng	Nanograms
NGY	Neopeptone glucose yeast extract
nL	Nanoliter
nm	Nanometer
ns	Nanoseconds
^{o}	Degrees
O_2	Oxygen
^{o}C	Degrees Celsius
OD	Optical density
p	Statistical probability number
PAMP	Pathogen Associated Molecular Patterns
PBS	Phosphate buffered saline
PBSTw	Phosphate buffered saline with Tween
PCR	Polymerase Chain Reaction
PEG	Polyethylene glycol
PKA	Protein Kinase A
PKC	Protein Kinase C
PM	Plasma membrane
PRR	Pathogen Recognition Receptors
ROS	Reactive oxygen species
S. cerevisiae	*Saccharomyces cerevisiae*
Saps	Secretes aspartic peptidases

SEM	Scanning Electron Microscopy
spp.	Species
ssDNA	Single stranded deoxyribose nucleic acid
TAE	Tris, acetic acid and EDTA
TBST	Tris-buffered saline with Tween
TE	Tris EDTA
TEM	Transmission Electron Microscopy
TGFβ	Transforming growth factor beta
TIFF	Tagged Image File Format
TLR	Toll-like Receptor
TNFα	Tumor necrosis factor α
UDP	Uridine disphosphate
V	Volts
w/v	Weight/volume
w/w	Weight/weight
Wt	Wild type
YPD	Yeast extract peptide dextrose
Δ	Heterogeneous deletion
ΔΔ	Homogeneous deletion

Different abbreviations have been used to describe the *C. albicans* strains in the study:

SN76, SN148 and SN148- eno1GFP are the wild type strains have been abbreviated as Wt.

The homozygous deletion of *apm4* in all three Wt backgrounds has been abbreviated as *apm4Δ/Δ.*

Homozygous deletion of *apm4* with a single deletion of *chs3* has been abbreviated as *apm4Δ/Δ,chs3Δ*.

Chapter 1: Introduction

1.1 *Candida albicans* a commensal human pathogen.

Candida albicans (*C. albicans*) is a eukaryotic organism within the kingdom of Fungi and more specifically in the Ascomycota phylum. *C. albicans* is closely related to *Saccharomyces* and there are multiple species in the *Candida* genus. The name *albicans* means white in Latin and is derived from the colour of the fungus when it grows on plates or tissue. *C. albicans* cells form lemon shaped yeast. The species has been characterised based on the morphology, fermentation, metabolism, virulence and the phenotype exhibited in serum (McCullough et al., 1996, Barnett, 2008).

C. albicans is an opportunistic fungal pathogen which means that it resides within humans as part of the microbial flora and when there is injury, or the host becomes immunocompromised the fungus becomes pathogenic. *C. albicans* resides in various areas within the host including the oral, gut and vaginal epithelia. The *C. albicans* cells interact with microbes that reside on host tissues, with tissue resident immune cells as well as bloodstream phagocytes. *C. albicans* are fit to survive conditions such as interactions with the microbial flora, changes in pH and nutrient depletion due to the adaptation to interact with different host cell types. The interactions were recently reviewed (Brown et al., 2012, Brown & May, 2017, da Silva Dantas et al., 2016).

C. albicans is the most prevalent out of the *Candida spp* and is widely considered to be the leading cause of Candidiasis. The other non-*albicans Candida spp* can also cause disease but they are not as prevalent (Neppelenbroek et al., 2014). Candidiasis describes all the disease caused by *Candida spp*. The fungus can initially colonise tissue due to changes in the immune cells or the microenvironment and the infection can result in a severe bloodstream invasion called Candidemia. It is noteworthy that a patient can be colonised by two different *Candida* strains at the same time in different tissue which could potentially increase the severity if there is an imbalance within the host immune system leading to reduced clearance (McCullough et al, 1996, Singh et al., 2020).

C. albicans is the leading cause of over 400 000 cases of Candidiasis per year (Desai, Lionakis, 2019, Singh et al., 2020). According to the CDC website more than 3.6 million US dollars are spent annually on healthcare for Candidiasis patients. There are treatments

available, but it is challenging for the treatments to be effective. The challenge with drugs against fungal pathogens is that they are targeting a eukaryotic organism which means that potential drug targets could be shared with the host. One of the major fungal cell structures that is not shared with the host is the cell wall and the cell wall components. The antifungal drugs currently available and under development target cell wall components and cell wall biosynthesis pathways. These have been reviewed recently (Lima et al., 2019). However due to the genome plasticity of *C. albicans* the cells can readily develop resistance to the drug target sites or compensate for the stress induced from the antifungals by activating persistence mechanisms (Balashov et al., 2006, Wiederhold et al., 2005, Desnos-Ollivier et al., 2008, Rueda et al., 2014, Whaley et al., 2017, Walker, L. et al., 2018, Walker et al., 2010).

The large financial burden as well as the resistance challenges mean that there is an ongoing need to identify further targets. To establish better therapeutics, it is critical to understand the cell biology and how the pathogen interacts with the host cells. A deep understanding of the interactions and responses will result in more informed decisions for treatment and selecting the next drug that will enter clinical trials.

1.2 *Candida albicans* cell biology.

C. albicans are diploid organisms with high genetic plasticity. The *C. albicans* genetics are closely related to *S. cerevisiae*, this has led to a quick progression in the field and a good understanding of overall cell biology. The cell biology aspects of *C. albicans* major virulence factors; morphology switching, cell wall, adhesion and the production of the lytic fungal toxin Candidalysin will be discussed in this section.

1.2.1 Phenotypic switching

C. albicans has been shown to switch between 3 morphologies: yeast, pseudohyphae and hyphae. The fungus switches between morphologies under different conditions and these environments stimulate this switching. (Barnett, 2008, Noble et. al, 2017). In this section the mechanism of morphology switch and maintenance as well as the differences between morphologies will be discussed.

1.2.1.1 What are the three major morphologies of Candida albicans?

The yeast morphology cells are lemon shaped and grow only as yeast at temperatures close to 30^{o}C, higher temperatures can stimulate growth of the other *C. albicans* morphologies.

During growth and division, the yeast cells form daughter buds. The septa form at the mother daughter neck constriction and the nuclear division occurs at the septa. Following cytokinesis, the cells carry birth scars enriched in chitin. The cell cycle of the mother and daughter cell is synchronized (figure 1.1) (Sudbery, P. et al., 2004).

The pseudohyphal morphology is characterised as a morphology between yeast and hyphae (figure 1.1). No completely stable conditions to grow pseudohyphae have been identified but temperatures close to 35^{o}C and pH 6 enrich for this form (Chen et al., 2020). Pseudohyphal cells form the first septa at the neck region, between the mother and the stem. Cell division occurs at the septa similarly to the yeast morphology. Like in the yeast morphology the cell cycle is synchronized for the mother and the stem. Pseudohyphal stems are not even in width and compartment size along the stem can be variable (Sudbery, P. et al., 2004, Sudbery, P. E., 2011, Noble et al., 2017).

The hyphal morphology is the invasive structure of *C. albicans*. The mother cell switches to the hyphal morphology and grows a hyphal stem (figure 1.1). Different conditions can stimulate hyphal morphology switch including the presence of serum, temperature of 37^{o}C, hypoxia, low pH and nutrient depletion. Multiple pathways are involved in hyphal induction and maintenance, and the appearance of a membrane trafficking organelle, the Spitzenkörper, is associated with fast rates of membrane growth at the hyphal tip. This organelle is not found in the yeast or pseudohyphal form of cells. The hyphal septa are distinct from yeast and pseudohyphal septa, they form on the hyphal tube away from the mother cell and nuclear division also occurs within the stem. The hyphal tube and mother have asynchronous cell cycles. Unlike pseudohyphae, hyphal cells have a uniform hypha width across the cell (Sudbery, P. et al., 2004, Sudbery, P. E., 2011, Noble et al., 2017).

The vacuoles of hyphal and pseudohyphal cells move across the stem and in some instances are retained at the septa. The hyphal mother and non-growing parts of the stem become vacuolated over time and the sections are no longer live (Veses & Gow, 2008).

The different *C. albicans* morphologies under some conditions (presence of a surface and in polymicrobial environments) can be present simultaneously to promote adaptation, an example of such interactions are biofilms. In biofilms all three *C. albicans* morphologies are observed. If the host surface (live or artificial) provides a favourable environment for growth

and nutrients biofilms start to form as there is an increase in the expression of genes involved in matrix formation. The surface can either be biological or synthetic. In a hospital setting *C. albicans* are known to form biofilms on catheters. *C. albicans* biofilm formation has been reviewed by other researchers (Pereira et al., 2021). Recent work suggested that biofilms can be created as soon as 8 hours post adhesion and the biofilm matrix forms in about 20 hours. The genes described as the most important for biofilm formation are the adhesion genes *als1* and *als3* (Pujol et al., 2015, Rodriguez-Cerdeira et al., 2019). Biofilms are critical for survival in harsh environmental conditions and adaptation to stress (Pereira et al., 2021).

Morphological switch is one of the most important responses during *C. albicans* host infection and adaptation. The next sections will focus on pathways resulting in hyphal morphology switch as well as the responses important in maintaining polarity.

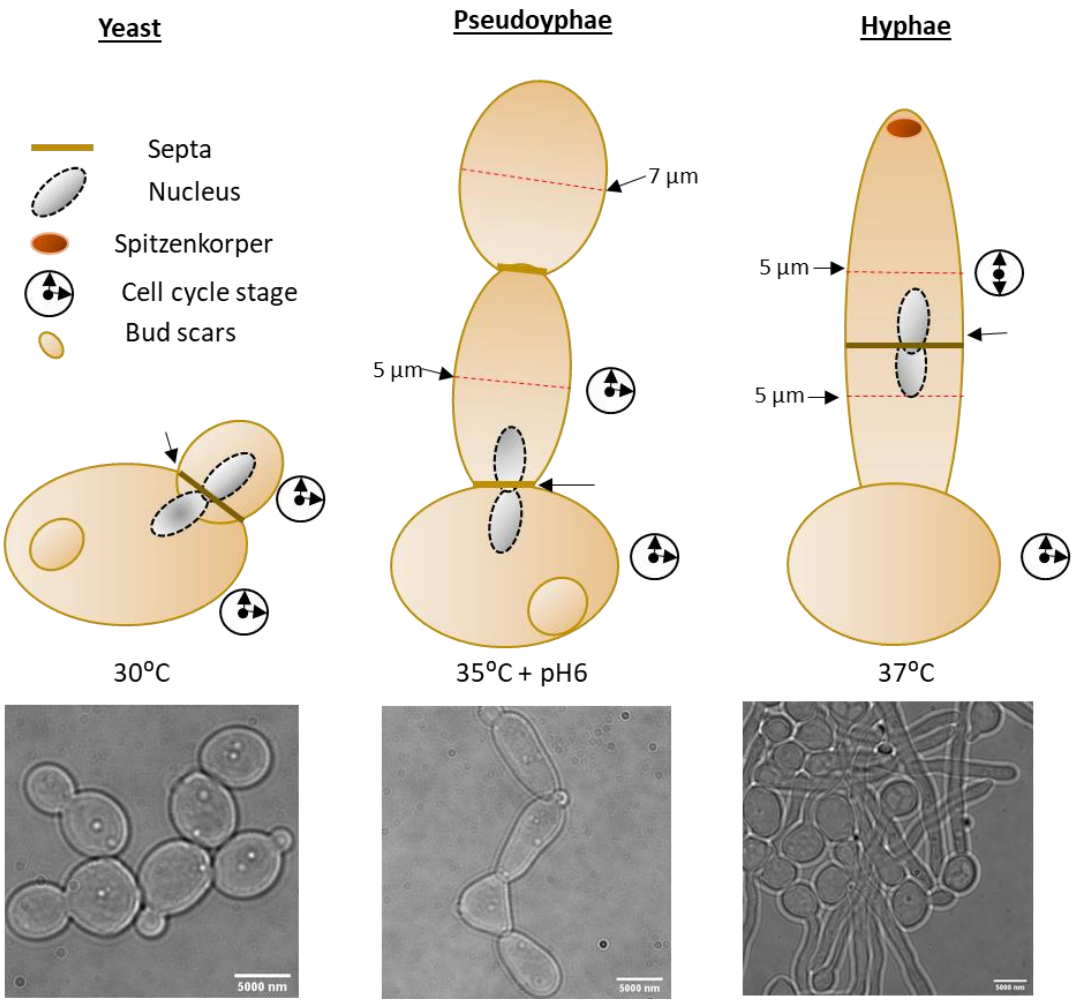

Figure 1.1: The Candida albicans morphologies: *The three morphologies of C. albicans are illustrated. Characteristics of each morphology are highlighted: gold line: septa, white circle: nucleus, red circle: Spitzenkörper, clock: cell cycle stage, gold circle: bud scars. Microscopy images of the morphologies are presented. Adapted from: (Sudbery, P. et al., 2004, Sudbery, P. E., 2011, Noble et al., 2017).*

1.2.1.2 Hyphal switch modulation

Hyphal morphology switch is an important part of *C. albicans* survival and host adaptation. This is highlighted further by the complexity of pathways regulating the response. The main transcription factors stimulating hyphal switch are Ume6, Efg1 and Rim101. Regulation of hyphal switch has been recently reviewed (Noble et al., 2017). The different pathways involved in hyphal switch modulation will be briefly discussed here (figure 1.2).

One of the main stimuli of hyphal switch is a change in the environmental pH. Changes in pH activate the Mitogen Activated Protein Kinase (MAPK) Cascade through Dfg1 and Rim21. The downstream activation of the pathway results in transcription factor *RIM101* expression through the Endosomal-sorting complex required for transport (ESCRT) pathway (transport of machinery at active growth sites) (Noble et al., 2017). Rim101 induces hyphal switch through the regulation of cell surface glycosidase acting on β glucan crosslinking that is secreted during filamentation Phr1/2 (Chen et al., 2020).

During different stresses such as changes in carbon dioxide, low nitrogen, presence of serum and increased temperatures, the Protein Kinase A (PKA) pathway is stimulated through a MAPK cascade initiated by Cyr1 phosphorylation. Metabolic changes of arginine, ornithine, proline and methionine trigger the PKA pathway (Arkowitz & Bassilana, 2019). During PKA activation both *EFG1* and *UME6* are upregulated. Hyphal genes are expressed, and morphology switch is successful (Noble et al., 2017).

Osmotic stress is another important stimulus that can trigger hyphal switch through the High Osmolarity pathway (HOG) which is activated. Hog1 activation results in *UME6* expression resulting in hyphal switch (Noble et al., 2017).

Hyphal morphology is repressed using the expression of different DNA binding proteins such as Nrg1 and Rfg1. The proteins bind on the promoters of the main hyphal morphology transcription factors. Efg1 protein binds to *EFG1* promoter to repress hyphal morphology when hyphal morphology is achieved (Tebarth et al., 2003). The HOG pathway can inhibit hyphal switch by upregulating *RFG1* and *HOG1* expression resulting in an inhibition of hyphal induction genes (Noble et al., 2017).

Regulation of the hyphal morphology is critical for *C. albicans* adaptation to different environments.

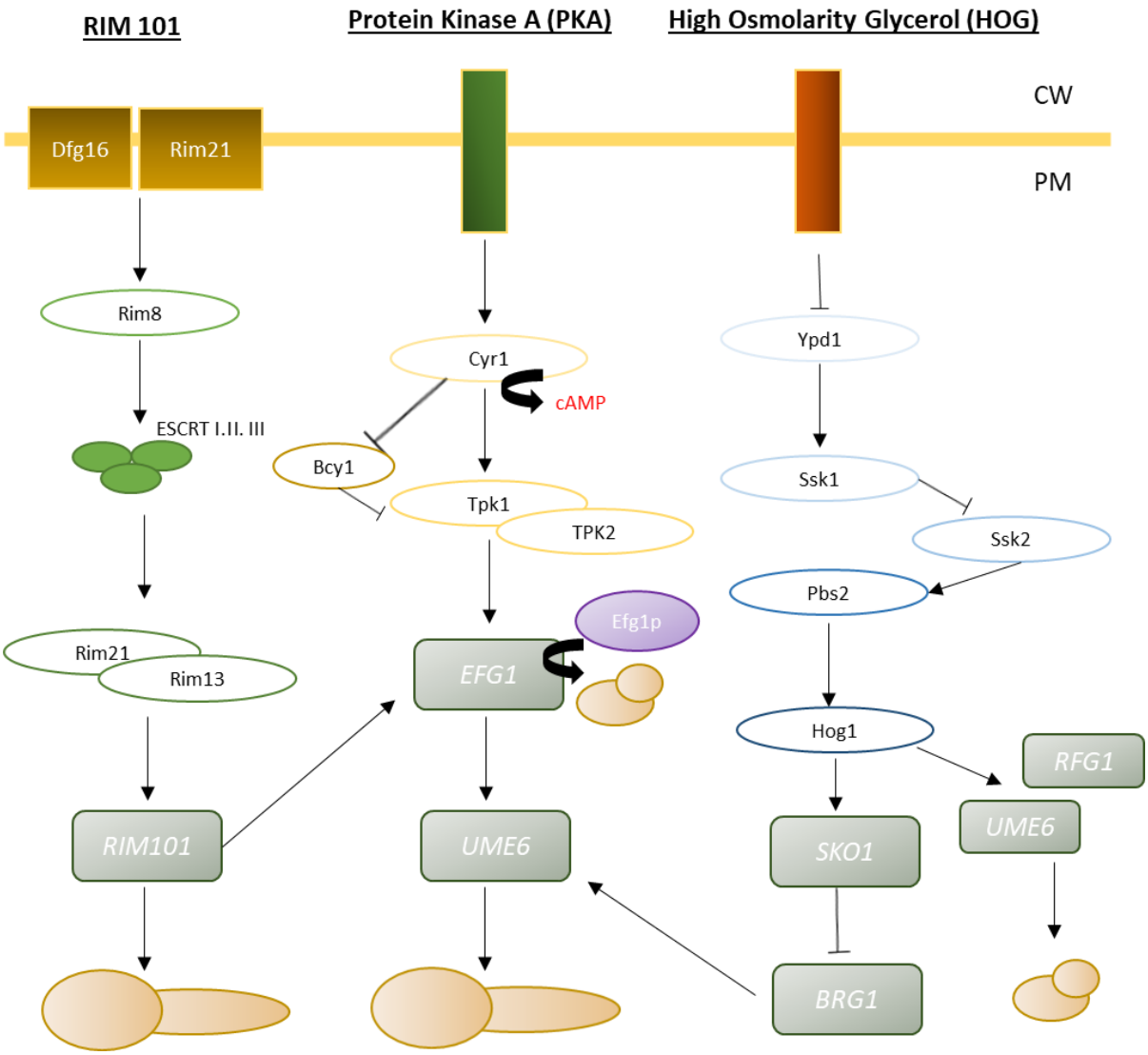

Figure 1.2: The Candida albicans hyphal switch modulation: *The pathways regulating hyphal morphology switch are illustrated, the figure is adapted from:* (Sudbery, P. E., 2011, Noble et al., 2017). *Rim101, PKA and the HOG pathway are illustrated in the figure. The transcription factors responsible for the regulation of morphology switch are in green squares. Efg1 protein can repress hyphal morphology and it is illustrated in purple. The fate of cells after the activation of transcription factors is illustrated with sketches of cells.*

1.2.1.3 Trafficking at the hyphal tip and polarity maintenance

Hyphal growth involves focused polarised growth on the mother cell. A hyphal tube/stem starts growing from the mother, the tube elongates further away from the mother cell. The sites of active growth are at the tip. Membrane expansion coupled with protein secretion and cell wall addition are critical for hyphal growth. The *C. albicans* hyphae have developed

a trafficking system that allows fast transport of components that are critical for hyphal growth (Arkowitz & Bassilana, 2019) (figure 1.3).

The Endoplasmic Reticulum (ER) and the Golgi are localised close to the hyphal tip to allow for faster and more efficient transport of vesicles to the tip. The vesicles are transported from the Golgi to a hypha specific organelle called the Spitzenkörper (figure 1.1). The Spitzenkörper is an organelle composed of different vesicles involved in membrane and cell wall expansion, the morphology of the Spitzenkörper was recently studied using Transmitted Electron Microscopy (Weiner et al., 2019). Vesicles are transported to the Spitzenkörper via actin cables, and a type V myosin. The hyphal tip polarity is maintained through the activity of the Spitzenkörper and the polarisome. The small GTPase Cdc42 is responsible for establishing the polarisome at the hyphal tip. Proteins within the tip include the formins which can nucleate new actin filaments. The polarisome also associates with the exocyst, the complex of proteins that allow docking and fusion of vesicles to allow tip growth (Crampin et al., 2005).

A balance between secretion and endocytosis are essential for growth at the tip. The balance is important to ensure that components are recycled when they no longer need to be active so that the cells can effectively respond to the environmental stimuli. Actin aids endocytic invaginations and helps with the recycling of essential enzymes as well as with trafficking of molecules (Robertson et al., 2009).

Endocytosis in yeast including *C. albicans* involves the sequential recruitment and assembly of complexes that recognise and bind to cargo such as proteins to be recycled or degraded. Actin is polymerised at sites and is required to support the invagination of membrane. These invaginations then undergo scission to generate vesicles containing the endocytosed material. Cargoes are sorted to be degraded in the vacuoles or recycled. In hyphal growth recycling of cell wall enzymes allows growth of new cell wall to be focussed at the tip region. The endocytic adaptor protein AP-2 is involved in recognition and endocytosis of the chitin synthase Chs3 to ensure that the enzyme activity is removed from the hyphal stem and recycled back to the tip (Figure 1.3) (Knafler et al., 2019).

The hyphal polarity maintenance through secretion and endocytosis is critical for adaptation of cells to different environments.

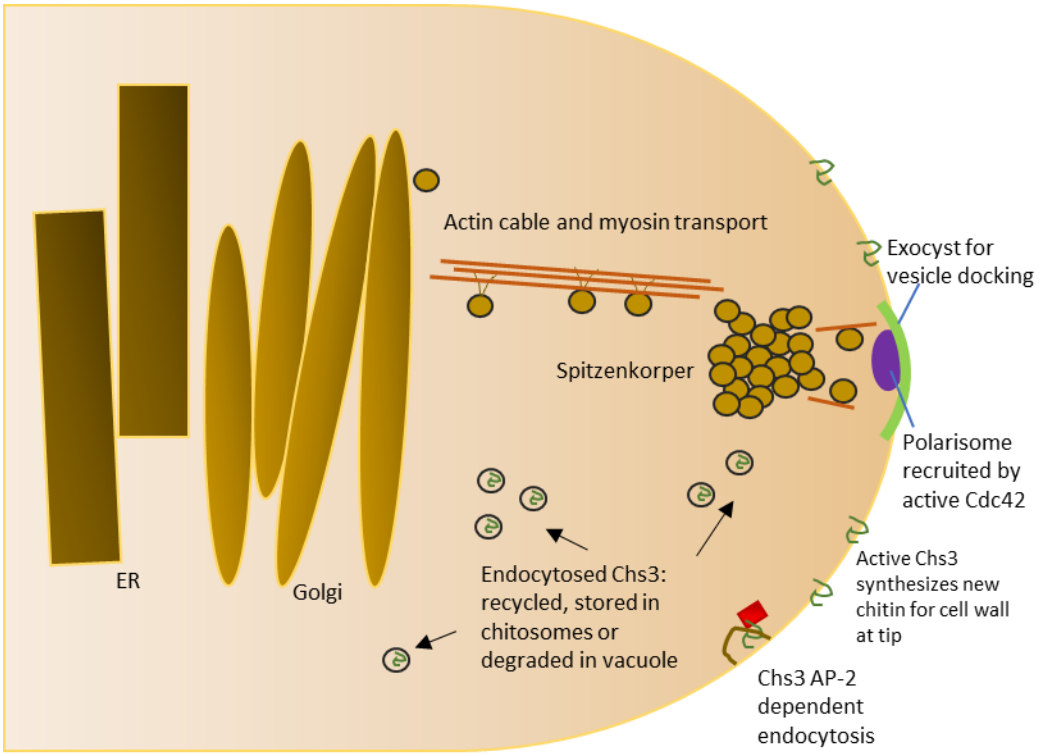

Figure 1.3: Candida albicans trafficking at the tip. *At the hyphal tip of C. albicans vesicles are transported from the Endoplasmic reticulum (ER) to the Trans Golgi network. Components essential for membrane and cell wall expansion are transported in vesicles via actin cables and myosin transport to an organelle called the Spitzenkörper. The Spitzenkörper associates with the polarisome at the hyphal tip through the recruitment of active Cdc42, their activity maintains polarised growth and the localization is important for vesicle docking through the exocyst activity. Active components at the cell surface are endocytosed by the cells for recycling, storing or degradation. Chs3 is a transmembrane protein that is endocytosed due to the activity of the endocytic cargo binding adaptor AP-2. After the membrane invagination Chs3 is in vesicles called chitosomes. The figure was made using information from:* (Arkowitz & Bassilana, 2019, Knafler et al., 2019, Bassilana et al., 2020).

1.2.1.4 Importance of hyphal polarity maintenance on environmental adaptation

The components involved in polarity maintenance such as the Spitzenkörper can be important in sensing the environment the hyphal cell is interacting with. For example, *C. albicans* has been reported to respond to external signals by contact sensing and electric fields stimulation. *C. albicans* hyphae change their direction according to signals. These

responses can either be Calcium/ Calcineurin dependent (figure 1.2) or independent (Brand et al., 2007). The cells regulate the direction of growth according to stimuli. For example, during physical restrictions the cells can sense their topology through proteins, Rsr1/Bud1 (a GTP/GDP cycling required for selection of polar bud sites). The proteins are reported to have a role in hyphal growth guidance and are interacting with the Spitzenkörper. The Spitzenkörper directs the growth through the activity of those proteins. This was shown genetically through deletion of the genes encoding the proteins (Thomson et al., 2015).

The hyphal tip is sensitive and responds to the external environment highlighting further the importance of endocytosis and secretion of components, to and from the tip ensuring that the components critical for sensing and adaptation are active at the cell surface.

1.2.1.5 The role of AP-2 in Candida albicans.

AP-2 is a cargo binding complex involved in the process of endocytosis (figure 1.3). Endocytosis is the process of recruiting proteins at the cell surface to a specific spot where a material needs to be taken into the cell from the outer surface. The proteins are recruited to the surface via actin polymerisation. The proteins recruited are important for the cargo recognition and tethering to the outer surface. The cargo is internalised in a vesicle which is pinched off the membrane via the activity of the recruited proteins and then the outer cell membrane recovers from the internalisation (Sudbery, P.E, 2011). AP-2 binds and recognises the cargo stimulating downstream effects of endocytosis. The protein contains 4 subunits with different molecular weights, α, β, μ and σ. In mammalian cells the role of AP-2 is well characterised. The protein is responsible for recruiting cargoes to the clathrin coated endocytic vesicles. In yeast the role of the protein is less well characterised due to the mild phenotypes of deletion strains when studied under normal lab growth conditions, data from *S. cerevisiae* studies suggest AP-2 binds to lipids and is involved in the type of endocytosis that requires clathrin. Deletion of the *apm4* gene encoding the μ subunit of AP-2 in *S. cerevisiae* led to a complete disruption of the AP-2 complex but did not cause severe defects in cell growth rates nor in the uptake of lipophilic dye (FM4-64) (Chapa-Y-Lazo & Ayscough, 2014).

However it was shown in fungi that the AP-2 complex is important for the endocytosis of cell wall damage sensors such as Mid2 and for the endocytosis of lipid flippases (Chapa-y-Lazo et

al., 2014, Martzoukou et al., 2017). Deletion of the *apm4* gene in *C. albicans* resulted in a reduction of cell switching towards hyphal morphology and strains acquired a more pseudohyphal morphology. Yeast cells had more random budding sites indicating defective polarised growth of cells (Chapa-Y-Lazo & Ayscough, 2014).

More extensive recent investigations showed a*pm4* deletion results in larger and rounder yeast cells. The hyphal morphology has a different phenotype compared to the Wt, the hyphae are shorter with larger width. There is a polarization deficiency leading to defects during hyphal growth and the mutant cells can have multiple buds. Knafler (2019) demonstrated that AP-2 is the key endocytic adaptor for Chs3 endocytosis. It is also important for the overall polarity maintenance in *C. albicans*. Cells with an AP-2 deletion have increased cell wall chitin levels but no other overall changes on the cell wall (Knafler et al., 2019). Generation of a series of mutants led to identification of Chs3 key motifs for uptake by AP-2. The importance of chitin synthase as a cargo was shown when deletion of one copy of *CHS3* (in the absence of *apm4*) led to the rescue of several of the phenotypes associated with the *apm4* deletion. These strains present an opportunity to investigate the importance of chitin in some host-pathogen interactions and is the focus of most of the work presented in this thesis.

1.2.2 The fungal cell wall

The cell wall is a *C. albicans* virulence factor. It is the outermost structure of the cells composed primarily of chitin, β glucan, mannans and proteins presented on figure 1.4. The ultrastructure and composition of the cell wall are critical for interactions with the host as well as for responses against stress. There are multiple pathways dedicated to cell wall integrity thus indicating even further the importance of the structure. The cell wall is recognised by host immune cells and elicits host responses. It is a unique structure for fungi which has led to the cell wall being targeted by many antifungal drugs (Gow et al., 2017). In this section the cell wall structure, maintenance and recognition by the host phagocytic cells will be discussed.

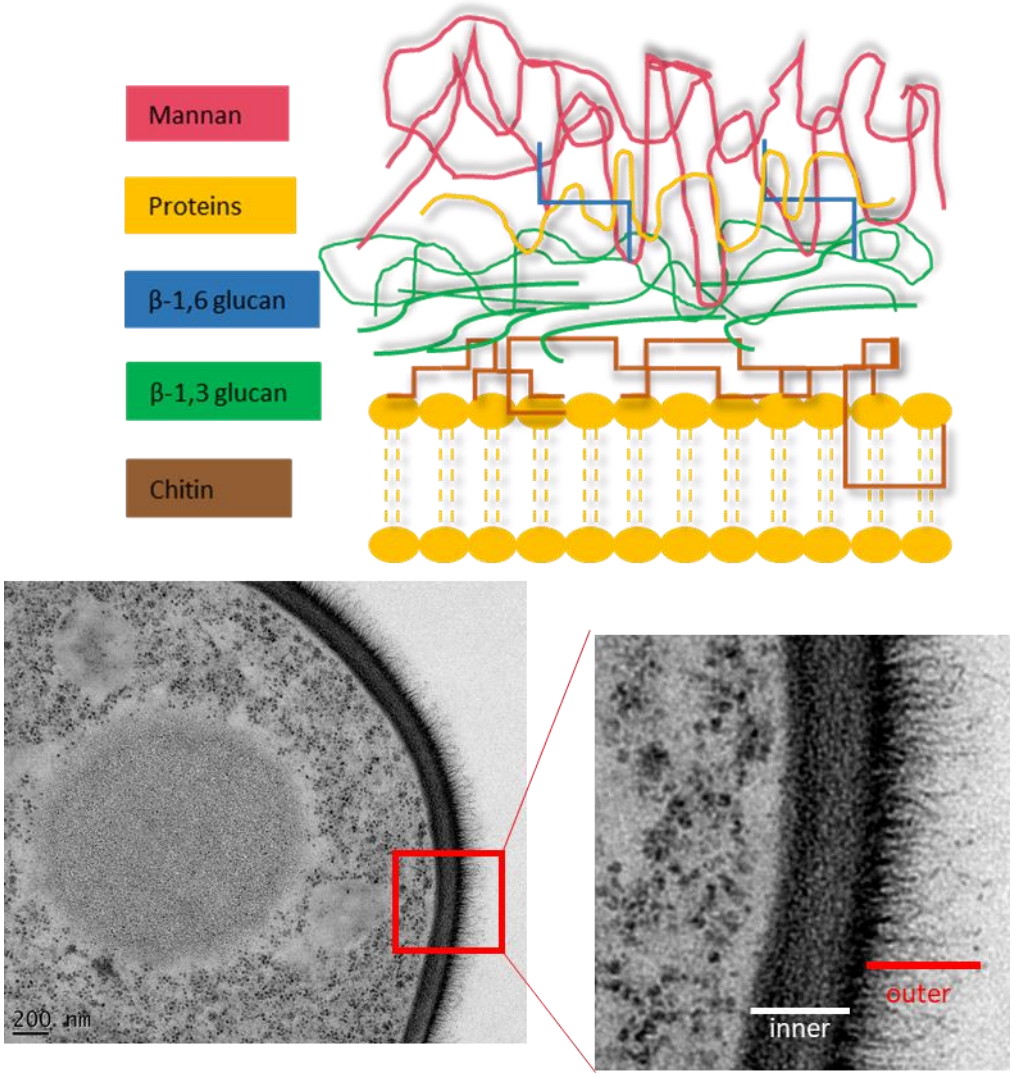

Figure 1.4: The Candida albicans cell wall. *The cell wall composition is described through the schematic diagram. The cell wall components are chitin (brown), β-1,3 glucan (green), β-1,6 glucan (blue), proteins such as adhesion proteins (yellow) and the mannans (pink). TEM images from unpublished work in the Ayscough lab in collaboration with the Gow lab (University of Exeter) are presented. The zoomed panel shows the cell wall structure; the inner (white) and outer (red) cell wall layer. The inner layer is composed of chitin and β glucan and the outer layer has mannans and different proteins. The figure is adapted from* (Gow et al., 2017).

1.2.2.1 The cell wall ultrastructure

The cell wall composition has been well studied and characterised, there are multiple reviews highlighting the importance of different cell wall components for the cell wall ultrastructure (Klis et al., 2001, Garcia-Rubio et al., 2020). Here, a discussion of each of the main cell wall components will be presented.

Chitin is part of the inner cell wall closest to the plasma membrane. The chitin composition and synthesis have been reviewed (Lenardon et al., 2010, Gow et al., 2017). UDP -N-acetylglycosamine localised in the cytoplasm is used to make chitin. Chitin is synthesised via enzymes called Chitin synthases (Chs) which are transmembrane proteins. Chs extrudes chitin to make the cell wall. An illustration of Chitin production is shown in figure 1.5. Chitin provides rigidity to the cell wall and maintains the cell shape. In the yeast morphology chitin can make up 1-2% of the dry cell wall weight (Chattaway et al., 1968). Once in the cell wall, chitin can be organised and cleaved to form different structures through the activity of Chitin cleaving enzymes called Chitinases (Cht). Cht cleave chitin forming chitin fibrils and can influence the cell shape. The activity of Chs and Cht is important for the cell wall ultrastructure. Deletion of Chts can result in abnormal budding patterns as well as problems during cytokinesis (Selvaggini et al., 2004). Genetic deletion of Chs can in some cases be fatal to *C. albicans* cells, an example of this, is deletion of *Chs1* which is an essential gene. Chitin is a very important component for *C. albicans* survival and adaptation in (Hall, 2015, Hopke et al., 2018).

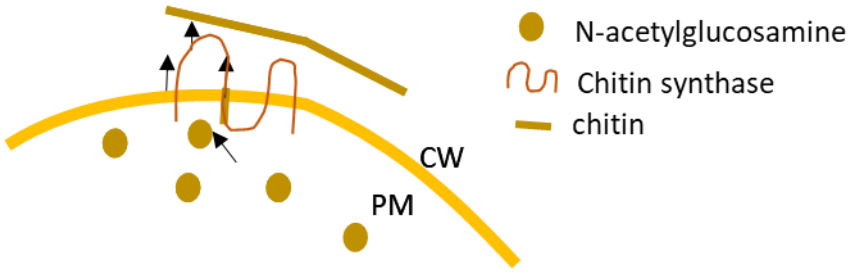

Figure 1.5: Chitin synthesis. *The process of chitin synthesis is illustrated, N-acetylglucosamine from the cytoplasm passes from the cytoplasm and is processed by the transmembrane protein Chitin synthase to make chitin filaments in the cell wall.*

B glucan is another component that is part of the inner cell wall reviewed by Gow (2017). β glucan associates with chitin on the cell wall. UDP-glucose from the cytoplasm is extruded in the cell wall as β glucan through the activity of transmembrane proteins. Fks1 is the transmembrane protein that synthesises β glucan (figure 1.6). Fks1 is a target for antifungals due to the importance of β glucan for cell wall integrity. After synthesis β glucan is crosslinked on the cell wall either as β-1,3 glucan or a β-1,6 glucan. The crosslinking has an impact on their activity in the cell wall. β-1,3 glucan forms crosslinks with chitin in the inner cell wall layer (figure 1.4) while β-1,6 glucan is crosslinked by Kre6 and Skn1. The β-1,6 glucan interacts with β-1,3 glucan and cell wall proteins such as adhesion proteins (Herrero et al., 2004, Garcia-Rubio et al., 2020, Liu et al., 2020). β glucan as part of the cell wall is important for the maintenance of cell structure and shape in concert with other cell wall components allowing for adaptation to different environments. During harsh environmental conditions such as increased pH, cell wall β glucan levels increase to promote survival and adaptation to the environment (Sherrington et al., 2017). Cell wall adaptation to stress is reviewed by other researchers (Hall, 2015, Hopke et al., 2018).

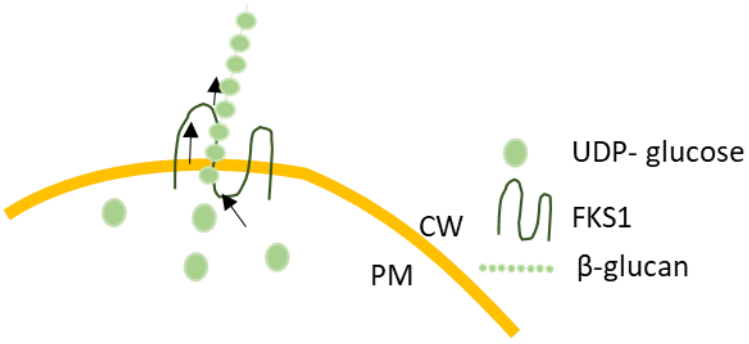

Figure 1.6: β glucan synthesis. *The process of β glucan synthesis is illustrated. UDP-glucose in the cytoplasm passes from the cytoplasm and β glucan is synthesised through the activity of transmembrane protein FKS1.*

Mannans are an important cell wall component of the outer cell wall (figure 1.4). Mannans are made from GDP mannose and are synthesised in the ER lumen (figure 1.7). The mannan can either be N (Asparagine) linked or O (Pyrrolysine) linked. The mannoprotein is processed in the ER before transport to the Golgi. Mannans are added to glycoproteins and more mannan residues are added. The mannans are transported to the cell membrane where they are secreted to the cell wall (Gow et al., 2017). Mannans are less rigid than chitin but are critical for the interactions with other cells. Mannans have roles in sensing the environment and responding to stimuli. The role of mannans for *C. albicans* cell biology was studied through the deletion of enzymes important for mannan production (Prill et al., 2005, Mora-Montes et al., 2010, Kruppa et al., 2011, Bates et al., 2013, Bain et al., 2014, Hernandez-Chavez et al., 2019).

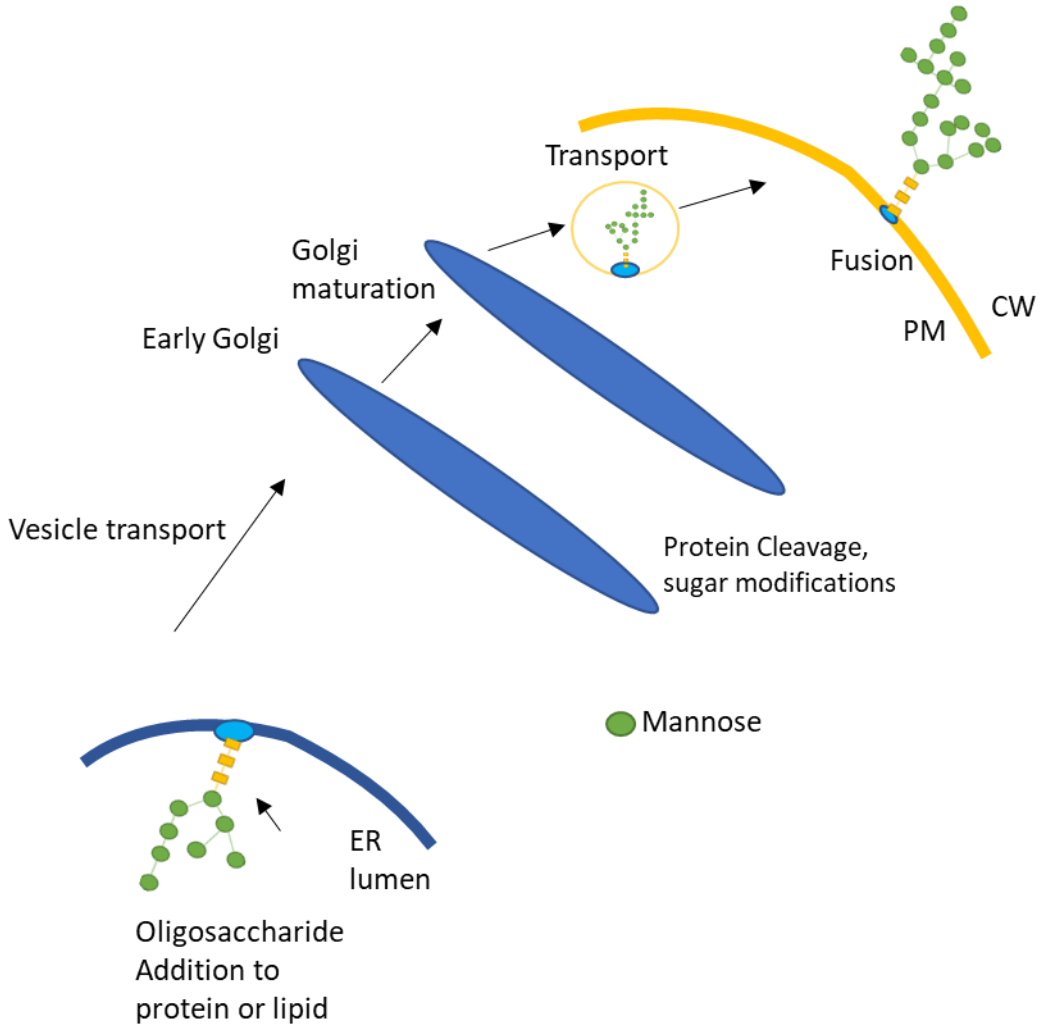

Figure 1.7: Mannan synthesis and trafficking to the cell wall. *Mannans are synthesized in the Endoplasmic reticulum (ER) lumen, then trafficked to the Golgi for maturation and the addition of more mannose. The cell wall mannan is transported to the cell membrane and fuses with the cell wall.*

The main cell wall components interact with each other to promote adaptation and to respond to the different environments. The processes of endocytosis and secretion are essential for maintaining the cell wall ultrastructure (Arkowitz & Bassilana, 2019).

1.2.2.2 Chitin synthases

Chitin synthases (Chs) are transmembrane proteins that extrude N-acetylglucosamine from the plasma membrane into the cell wall producing Chitin. There are different chitin synthases with distinct roles which will be discussed in this section. Chitin synthases were classed into different families by Bowen and colleagues according to their sequence similarity (Bowen et al., 1992). The Chs enzymes were first identified and studied in *S. cerevisiae*. The genetic similarities between *S. cerevisiae* and *C. albicans* allowed better understanding of Chs activity in *C. albicans* cells due to all the previous research focused on *S. cerevisiae* Chs. Here, the *C. albicans* Chs enzymes will be reviewed.

Chs1 is a Class II chitin synthase, it is essential for survival and responsible for septa formation. Chs1 was the first enzyme identified due to its increased activity levels in cells as well as because of its role in septa formation (Bulawa et al., 1995). Chs1 is expressed in both yeast and hyphae; its deletion is lethal (figure 1.8) (Chen-Wu et al., 1992, Munro et al., 1998).

Chs2 and Chs8 are Class I chitin synthases, both localizing at the septa. Chs2 was imaged as two very bright and distinct spots on the septa while Chs8 was identified as only one spot on the septa. Chs2 is also localized at the tips of hyphal cells and small buds for polarized growth. It has been reported that Chs2 is expressed in higher levels in hyphae compared to yeast (Chen-Wu et al., 1992, Bulawa et al., 1995, Mio et al., 1996, Munro et al., 1998, Preechasuth et al., 2015). Genetic mutations in *CHS2* do not influence cell viability (Bulawa

et al., 1995). Deletion of *CHS8* results in reduced chitin levels but has no impact on cell viability (Epp et al., 2010).

Chs3 is a class IV chitin synthase, producing the majority of cell wall chitin. Chs3 is upregulated during hyphal growth (Sudoh et al., 1993, Bulawa et al., 1995, Mio et al., 1996). Chs3 localises to the hyphal tip and is also involved in the formation of chitin rings marking where the septa will be formed (Walker, L. A. et al., 2013). A genetic deletion of *CHS3* results in reduced levels of overall chitin but the cells are still viable (Bulawa et al., 1995). Trafficking and recycling of Chs3 is illustrated on figure 1.3. The activities of other Chs enzymes (Chs 4-7) are important for the trafficking and localization of Chs3 (Rowbottom et al., 2004, Sanz et al., 2005, Munro et al., 2007, Anton et al., 2018).

Deletion of Chs genes can result in increased sensitivity to stress. Cell wall integrity pathways control the expression of Chs genes. When the Chs genes are deleted or disrupted, the cell wall integrity pathways are activated and respond to the increased cell wall stress resulting in cell adaptation (Ueno et al., 2011, Walker, L. A. et al., 2013, Jiang et al., 2018, Han et al., 2019). Single genetic deletions of *CHSx* genes mostly result in cell adaptation through the activities of other Chs proteins. The other Chs enzymes compensate for the enzymes lost during the mutation. The *C. albicans* cells respond to the stress and maintain cell wall integrity.

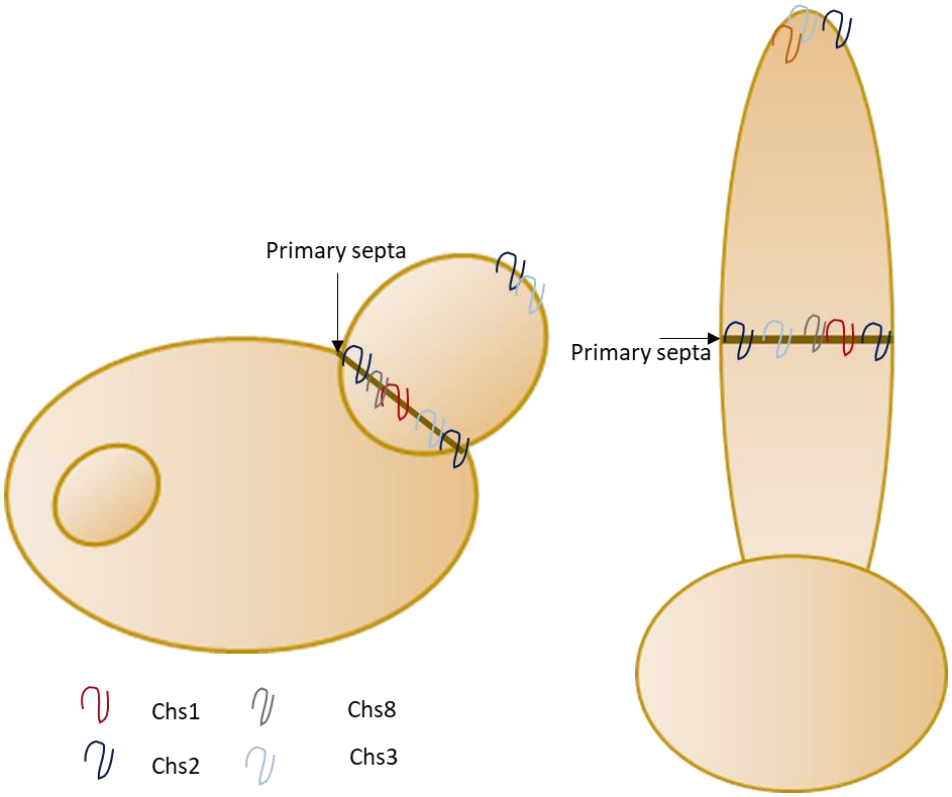

Figure 1.8: The localization of Chitin synthase enzymes in yeast and hyphal cells. *The diagram illustrates the localization of Chitin synthase (Chs) enzymes in C. albicans. Chs1 (red), Chs2 (dark blue), Chs3 (light blue/grey) and Chs8 (light brown).*

1.2.2.3 Environmental changes and cell wall adaptation to stress

The cell wall is an important structure for *C. albicans* therefore maintenance of the structure as well as ensuring that the structure is not compromised is critical. Cell wall remodelling is important for *C. albicans* especially during stress conditions. This is established through a balance between endocytosis and secretion of the cell wall synthases and break down enzymes. Cell wall integrity (CWI) pathways are important for the response during stress. In this section High osmolarity glycerol (HOG) pathway, Calcium / Calcineurin pathway and the Protein kinase C (PKC) pathway will be discussed (figure 1.9). The pathways have also been reviewed extensively (Heinisch & Rodicio, 2018, Chen et al., 2020, Ibe & Munro, 2021).

Oxidative stress, cell wall damage and caspofungin treatment are conditions that can initiate a response by the Calcium/ Calcineurin pathway. The stress is sensed by cells activating the pathway. Calmodulin is activated by calcium resulting in the activation of Calcineurin. Calcineurin dephosphorylates Crz1 (a MAPK) resulting in activation. The activation of the

pathway results in an upregulation of *CHS* genes producing more chitin on the cell wall. Mitochondria and redox regulation are stimulated by the Calcium/ Calcineurin activation to promote adaptation and cell survival (Ibe & Munro, 2021).

Osmotic stress results in the activation of the HOG pathway. When osmotic stress is sensed, the activity of Ypd1 protein is inhibited allowing for Ssk1 activation. The activation of Ssk1 is important as it inhibits the activity of Ssk2 allowing for Pbs2 expression and Hog1 (MAPK) activation. Activation of Hog1 inhibits hyphal switch allowing stress adaptation. During HOG pathway activation *C. albicans CHS* genes are upregulated (Munro et al., 2007, Correia et al., 2017).

PKC pathway is activated during *C. albicans* treatment with Caspofungin, nutritional stress and membrane stress resulting in pathway activation. Rom2 is activated by the stress resulting in downstream activation of Rho1. Rho1 activates Pkc1 resulting in Mkc1 (MAPK) activation and the activation of the PKC pathway. The PKC pathway stimulates both *CHS* gene expression and β glucan synthesis. PKC is responsible for cell wall repair and membrane growth with a role on hyphal regulation (Navarro-Garcia et al., 1995, Munro et al., 2007, LaFayette et al., 2010, Heilmann et al., 2013, Dichtl et al., 2016, Han et al., 2019).

Maintaining the cell wall integrity is one of the most important processes for *C. albicans* and it is critical for survival. The importance is highlighted further by the complexity and number of pathways that are important for CWI. Cell wall integrity pathways can combine activities with organelles to regulate the cell wall. The regulation of growth strongly depends on ATP production by the mitochondria. ATP is used for the MAPK pathway activation and regulation. An example of mitochondria being important for CWI regulation is during growth in hypoxic environments. The mitochondria can regulate the exposure of chitin and β glucan in the environment through the activity of CWI pathways (Duvenage et al., 2019). A similar example is during pH changes in the environment, the Rim101 pathway (figure 1.2) (hyphal morphology switch pathway) can help with cell wall integrity maintenance by influencing the cell wall composition of cells. There is an increase in chitin and β glucan levels which is independent of the Calcium/ Calcineurin pathway (Sherrington et al., 2017). The pH response on the cell wall composition is time dependent. The cell wall composition changes over time by the regulation of different CWI pathways. The hyphal transcription factor Efg1

is a key player as it regulates *CHT2* expression and thus chitin exposure (Cottier et al., 2019). More examples of such responses have been recently reviewed by Cottier (2020) (Cottier, Hall, 2020). These findings stress the complexity of *C. albicans* responses and the significance of adaptation for *C. albicans* cell biology.

1.2.2.4 Antifungal compounds target cell wall integrity

Antifungal drugs are often used to target the fungal cell wall as it is a unique structure for fungi and not present in the human host. The antifungals available and the fungal cell responses against their activity will be briefly discussed here. The antifungals were recently reviewed (Bhattacharya et al., 2020).

The β glucan synthase Fks1 is targeted by Echinocandins (Caspofungin and Micafungin). To survive the response of Echinocandins a small proportion of *C. albicans* mutate the site of activity. Another survival mechanism is persistence of the antifungal treatment via the activity of CWI pathways upregulating the cell wall chitin levels (Deresinski & Stevens, 2003, Wiederhold et al., 2005, Desnos-Ollivier et al., 2008, Walker et al., 2010, Lee et al., 2012).

The ergosterol biosynthesis is an important antifungal target. Mutations on the ergosterol biosynthesis components are used as resistance mechanisms by *C. albicans*. Another resistance mechanism against ergosterol targeting antifungals is increased expression of Azole transmembrane transporters that remove the antifungal from the cell resisting its activity. Recently a delivery method for Amphotericin B (antifungal activity through membrane pore formation) antifungal through the AmBisome, a lipid capsule used to deliver Amphotericin B to fungi has demonstrated less *C. albicans* resistance. *C. albicans* has developed mechanisms of resistance against the entry of Amphotericin B in cells, the AmBisome capsule surrounds Amphotericin B to allow for delivery of the drug in the fungus and fungal clearance (Walker, L. et al., 2018, Bhattacharya et al., 2020).

The examples of antifungals show the dynamic response of *C. albicans* to survive the stress and adapt to the conditions highlighting further the importance of CWI and cell sensing.

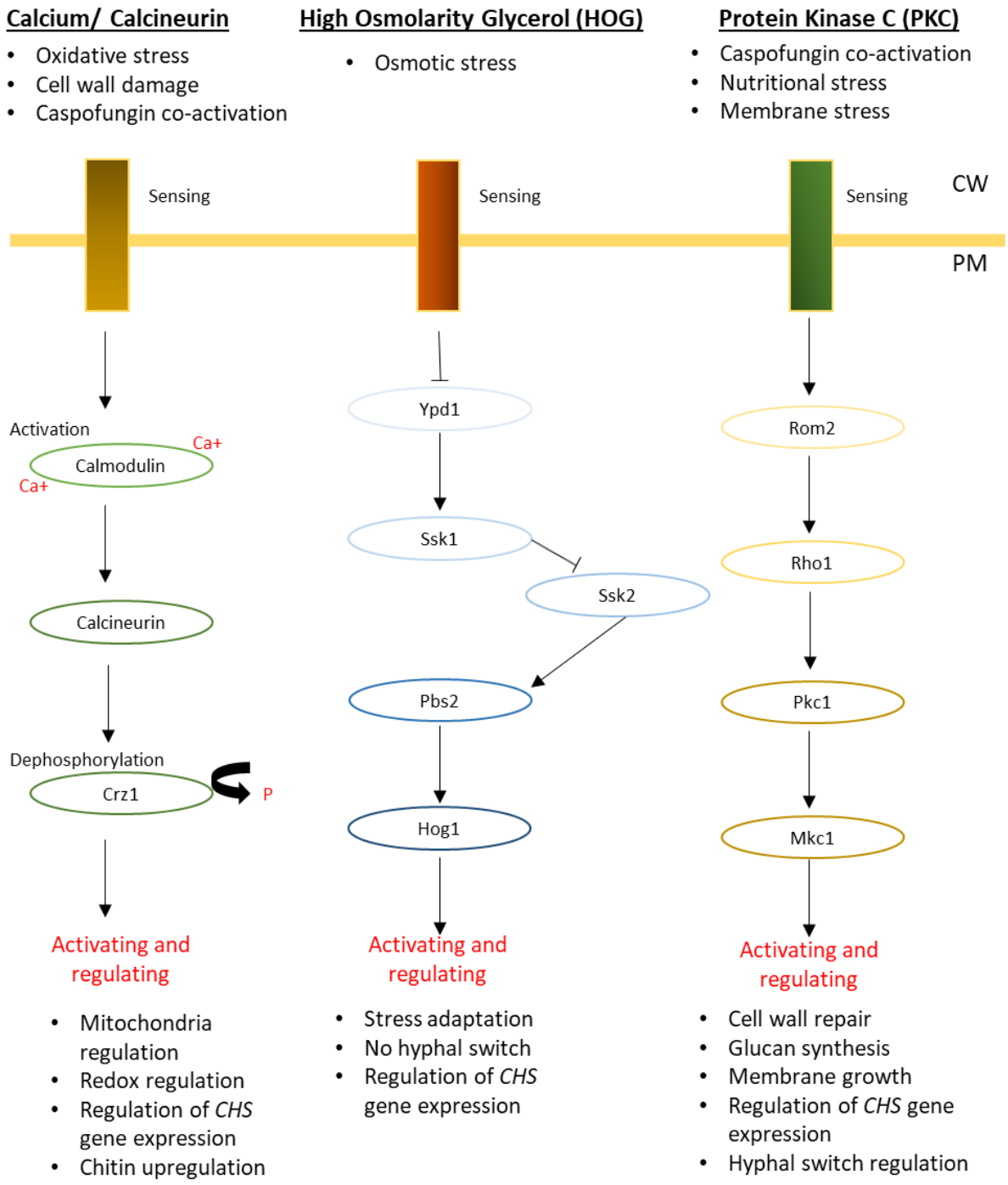

Figure 1.9: The cell wall integrity pathways. *The stimulants for the activation of three cell wall integrity pathways: Calcium/ Calcineurin, HOG and PKC. The activation of the pathways is schematically illustrated. The effects on cell biology after the pathway activation are highlighted in the diagram.*

1.2.3 *Candida albicans* adhesion

Another *C. albicans* virulence factor that is important during host interaction is adhesion. Adhesion can be either on to other *C. albicans* cells or with host surfaces. *C. albicans* cells express adhesion proteins, the proteins are secreted to the cell wall to promote cell attachment. The most studied adhesins are Agglutinin Like Sequence (Als) family proteins, Hyphal wall protein 1 (Hwp1) and secreted aspartic peptidases (Saps). The adhesion proteins are secreted to the cell wall during interactions with different surfaces (other pathogens, host cells, synthetic surfaces) (Mourer et al., 2021, Romo & Kumamoto, 2020, Richardson et al., 2018).

The Als proteins have different structures, the N-terminal of the ALS protein family is important for the adhesion interactions (Fan et al., 2013, Moyes et al., 2015). The N-terminal of Als3 contains a peptide binding cavity domain that has a role in *C. albicans* cell aggregate formation (Lin et al., 2014). Nuclear magnetic resonance (NMR) was used to elucidate the structure of the Als3 C-terminus. The C-terminus is a flexible structure allowing for different cross linking in the cell wall and possibly explaining how *C. albicans* cells can attach to different tissue (Cota & Hoyer, 2015).

Deletion of adhesion genes such as *als1*, *als3, sap10* and *hwp1* results in a reduction of epithelial adhesion with an overall phenotype of decreased virulence and more cell sensitivity to cell wall stimulant such as Congo red, calcofluor white and antifungals. The adhesion proteins are important for both virulence and cell wall integrity (Richardson et al., 2018).

During host interactions with epithelial cells *C. albicans* yeast are attached to the host cells because of electrostatic attractions and the interactions of β glucan with the host cell surface. The adhesion protein Als3 is expressed in both the yeast and hyphal morphology and helps with the initial interactions. Once *C. albicans* yeast cells are attached to a surface, the pathways for hyphal switch are activated and hyphal induction begins. Hyphal cells grow on the surface and grow through the host cell surface during invasion. During attachment Als proteins and Hwp1 are secreted to the cell wall from hyphal cells. In invasion the adhesion proteins Sap2 and Sap5 are critical for the process degrading host material and

different proteins are released from hyphal cells (Candidalysin, Lipases and phospholipases) to cause host cell damage (figure 1.10) (Richardson et al., 2018).

Adhesion is an important process for *C. albicans* cells as it allows for interactions with other cells and can promote cell growth.

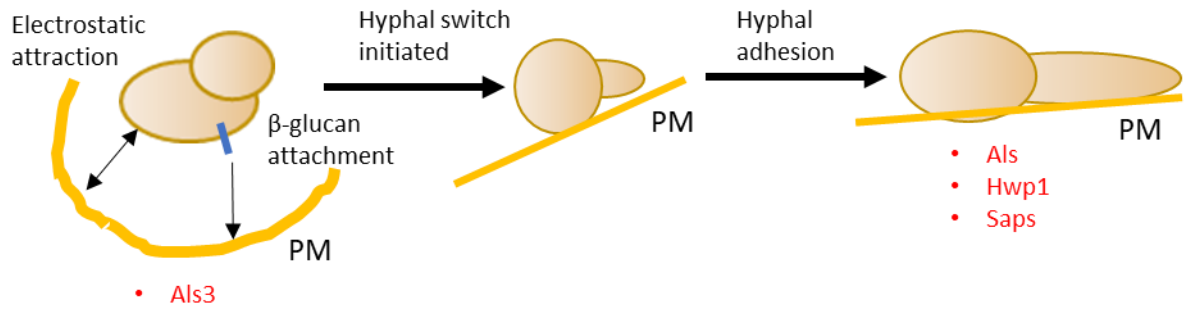

Figure 1.10: Candida albicans adhesion. *The diagram illustrates the adhesion of C. albicans cells to epithelial surfaces. Yeast cells attach to host epithelial initially due to the properties of the cell wall and electrostatic attraction. In the yeast morphology Als3 adhesion protein is expressed promoting adhesion. Once the yeast cells are attached to epithelia hyphal switch signalling pathways are activated resulting in hyphal transition. In the hyphal morphology adhesion proteins of the Als family, Hwp1 and Saps are expressed to promote adherence and host invasion. Figure adapted from (Richardson et al., 2018).*

1.2.4 The fungal toxin Candidalysin production

Candidalysin is the first cytolytic toxin identified in a fungal pathogen. The protein is encoded by the *ECE1* gene. *ECE1* is a gene associated with hyphae, expressed only in the hyphal morphology of *C. albicans*. The Ece1 protein is 28.9kDa, is encoded by 271 amino acids and is cleaved by the enzyme Kex2. The active site for Candidalysin is between amino acids 62 - 93, it is critical for the immune activation and the cytolytic activity (Moyes et al., 2016). This is a 32 amino acid region that is processed further by the cleavage of the terminal Arginine through the activity of Kex1 enzyme, this cleavage results in a 31 amino

acid active protein. The Ece1 protein is processed at the Golgi by Kex1/2 enzymes to ensure activation of the toxin (Richardson et al., 2018).

Candidalysin is secreted by *C. albicans* hyphae to induce host cell damage and host immune activation. The importance of Candidalysin for the cell biology of *C. albicans* is not fully understood but it is critical for the host virulence. Candidalysin is secreted from hyphal cells to induce host cell damage. The toxin creates pores on the host cell surface which are responsible for both host damage and immune system activation. The host immune response is only activated against high concentrations of Candidalysin so it is possible that individual cells produce Candidalysin for commensalism as well as pathogenicity. The activity of the toxin could be useful for acquiring nutrients from the environment or even to stop interactions with other microbes in polymicrobial environments. Work on the expression of Candidalysin has been recently reviewed (Naglik et al., 2019).

1.3 *Candida albicans* host-pathogen interactions.

C. albicans as an opportunistic fungal pathogen interacting with the host as a commensal and as an invasive pathogen. The pathogen resides on mucosal tissues and when the host is compromised *C. albicans* disseminates and invades host tissue. In this section the host and *C. albicans* responses during the interaction with macrophages, neutrophils and epithelial cells will be discussed.

1.3.1 *Candida albicans* interactions with macrophages

Macrophages are the first cells to respond to pathogens and are part of the innate immune system (immune system that is not specifically adapted towards a pathogen). Macrophages take up pathogens and then release compounds into the phagolysosome to clear the infection. The phagolysosome can produce multiple stress responses in *C. albicans*, however the *C. albicans* cells have developed mechanisms of adaptation to survive these stresses. Here, the interactions between *C. albicans* and macrophages will be discussed.

The first step of the interaction is phagocytosis. The process of phagocytosis involves sensing of the pathogen by the host phagocytes and this results in movement towards the pathogen via chemotaxis (Playfair J. H. L. & Chain B. M., 2012). Phagocytosis consists of recognition of the pathogen by Pattern Recognition Receptors (PRRs). PRRs are recruited to the surface via actin polymerization. Receptors assemble on the membrane of the

macrophage to recognize the pathogen associated molecular patterns (PAMPs) on the cell wall of *C. albicans* (figure 1.11). Actin localises near the membrane and drives formation of extensions, inducing more binding of the pathogen to macrophages and a strong pull for engulfment. The pathogen is bound to the macrophages through the PRRs and then engulfed via actin-induced host cell membrane extensions. The phagosome pinches off the macrophage membrane through actin activity while still bound to the PRRs. The pattern of PRRs interacting with the pathogen influences the recognition and the response that is exhibited (Netea et al., 2008, Goodridge et al., 2012).

C. albicans PAMPs are present on the cell wall and different immune receptors are involved in the recognition of the pathogen (figure 1.11). The cell wall components mostly considered to be involved for recognition are mannans and β glucan. The recognition ensures appropriate immune stimulation (figure 1.12). The PRRs recognising different PAMPs and the immune responses elicited are reviewed below.

Recognition of the cell wall β glucan has been described as important for the host cell response. β glucan associates with the PRR Dectin-1 (Figure 1.11). Dectin-1 is the most important PRR for yeast recognition by macrophages but has low activity towards the hyphal morphology (Hohl et al., 2008, Netea et al., 2008, Bain et al., 2014, Roman et al., 2016, Gow et al., 2017). Dectin-1 has a cytoplasmic subunit involved in the activation of macrophages (Taylor et al., 2002, Herre et al., 2004, Goodridge et al., 2012). During recognition of the PAMP, the receptor is activated via protein Syk. The receptor activation has two responses. One is the activation of CARD9 resulting in dimerization of NFκB and NF-AT leading to the production of IL-10 and IL-2. The other pathway is to switch off the inhibition of NFκB by the IκB thus promoting more NFκB activity in the host cell (figure 1.12). The activation of Dectin-1 results in the stimulation of an inflammatory response and the activation of T cells which are part of the adaptive immune response. The TNF pathway activated by Dectin-1 via NFκB activity promotes tissue healing and caspase activation for apoptosis of damaged host cells (Playfair J. H. L. & Chain B. M., 2012). The activity of the Dectin-1 receptor is critical for the immune response, the receptor binds to the cells to promote phagocytosis (Herre et al., 2004, Mansour et al., 2013, Bain et al., 2014, Hasim et al., 2016, Sem et al., 2016).

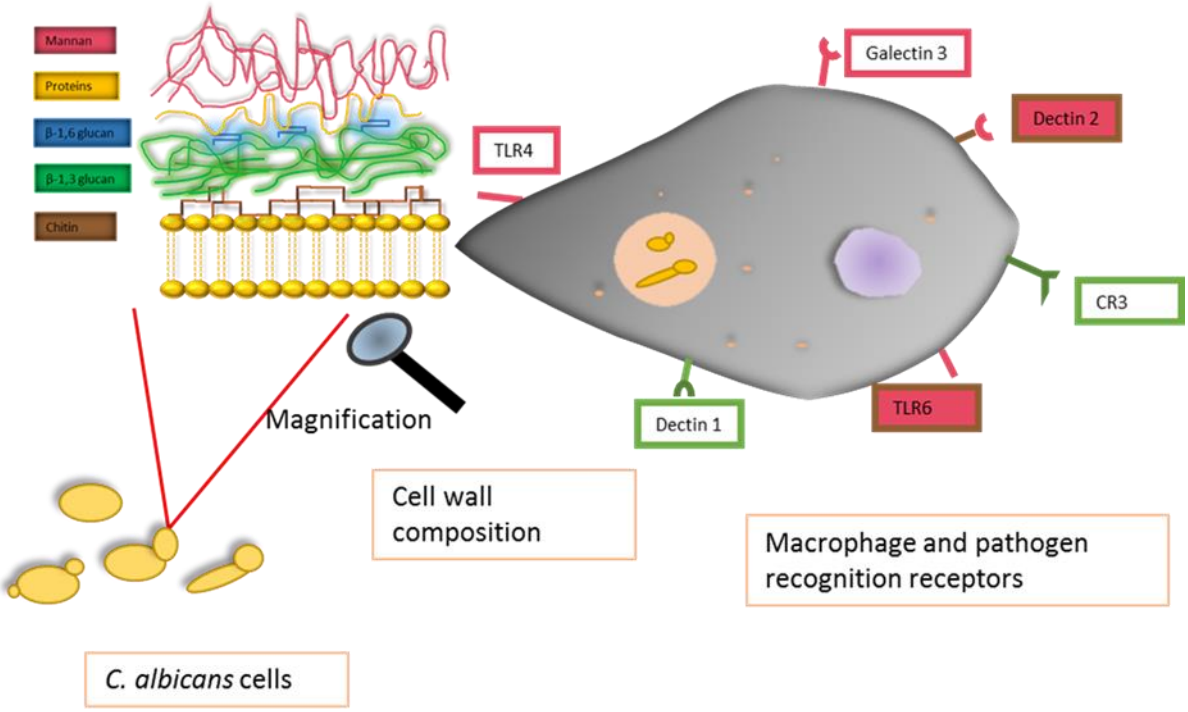

Figure 1.11: The Candida albicans cell wall composition and the main host Pathogen recognition receptors. *The organisation of cell wall components adapted from (Gow et al., 2017) is presented. The cell wall components are recognised by different pathogen recognition receptors of the host immune cells. The recognition receptors are colour coordinated with the cell wall components that they recognise.*

Mannans are also an important PAMP for recognition by immune cells. Different PRRs are involved in mannan recognition and in some cases, there is co-recognition of mannans with other PAMPs. There are 10 different Toll-like receptors (TLRs) in humans with different activation and recognition domains. TLRs have been associated with the recognition of mannans. TLR4 primarily recognises mannans and is activated via two proteins Mal and MyD88 resulting in activation of NFκB via dissociation of the inhibitor IκB. The activation results in a TNF and IL-10 (cytokine interleukin 10) response. The TLR4 response results in tissue healing, activation of the adaptive immune response, caspase and inflammatory activation, similar to the Dectin-1 response (figure 1.12). TLR3 and 6 have an impact on each other's activation and are stimulated with mannan and β glucan. TLR3 activation and response has a core pathway similar to TLR4 with some differences, for TLR3 to be activated the Mal protein also needs to bind to TLR6 leading to co-activation. TLR3 similar to TLR4 can

activate the NFκB response but can also result in the activation of the ERK pathway resulting in the expression of TGFβ and IL-10 and ultimately the expression of Regulatory T cell and B cell activation (figure 1.12). This means that the adaptive immune system is stimulated, and more immune cells will be recruited at the site. Galectin 3 is also involved in TLR3 activation, Galectin 3 recognises mannans (figure 1.11) and stimulates the TLR3 response (figure 1.12) (Netea et al., 2008, Goodridge et al., 2012, Munawara et al., 2017).

Chitin is a PAMP present on the inner cell wall of *C. albicans* (figure 1.4). Currently no chitin specific PRRs have been identified however the PAMP has been reported to be co-recognised with mannans during the activity of TLRs (Plaine et al., 2008, Mora-Montes et al., 2011, Sem et al., 2016, Tams et al., 2020). Dectin-2 has also been reported to be involved in the co-recognition of chitin and mannan. Activation of Dectin-2 is similar to the Dectin-1 activation as it results in TNFα expression involved in the activation of NFκB and has similar downstream effects on immune activation (Netea et al., 2008, Playfair J. H. L. & Chain B. M., 2012, Snarr et al., 2017).

The interactions of PAMPs and PRRs are complex as the pathogen attempts to promote survival via different cell wall remodelling mechanisms regulated by the CWI pathways of *C. albicans* (figure 1.9). Once phagocytosed *C. albicans* cells are subjected to different host stimuli that attempt pathogen clearance while the *C. albicans* cells attempt to respond to these environmental changes.

The complexity of the interactions is highlighted in the illustration on figure 1.13. The phagosome environment is nutrient poor, acidic and hypoxic. (May & Casadevall, 2018). The antimicrobials, the acidic environment, reduced respiration and the Reactive oxygen species are released in the phagosome to induce pathogen clearance. The nutrient deprivation and the micronutrient depletion aim to inhibit pathogen growth (Case & Samuel, 2016). All the phagosome mechanisms induced are important for pathogen clearance (figure 1.13).

During interactions with macrophages *C. albicans* use mechanisms to escape the environment and/or adapt to the conditions. *C. albicans* can switch to the hyphal morphology after the stimulation by the phagosome environment. This results in macrophage lysis (Scherer et al., 2020). *C. albicans* hyphal switch also result in Candidalysin

production that cause host cell damage and induces an IL-1β (inflammation) response (Kasper et al., 2018).

C. albicans cells can alter their gene expression and adapt to the harsh environmental conditions inside the phagosome. The reduced respiration in the phagosome activates the CWI pathways of *C. albicans* resulting in increased cell wall thickness with no changes in the overall cell wall composition. The cells upregulate the glyoxylate cycle, glycolysis and gluconeogenesis leading to changes in the lipid metabolism with more exposure of β glucan and chitin (Duvenage et al., 2019). The acidic phagosome pH activates the CWI pathways resulting in increased chitin and β glucan levels through the Rim101 pathway activation and hyphal morphology switch. The cell wall changes caused by the acidic pH can result in increased cytokine expression by host cells (Sherrington et al., 2017).

It has been reported that *C. albicans* cells have mechanisms to adapt in the phagosome and alkalinise the acidic pH of the environment. This response is linked to the hyphal morphology of *C. albicans*. Host macrophages are auxotrophic for the amino acid L-arginine which is critical for the Nitric Oxide production and pathogen clearance. *C. albicans* cells have arginases that hijack the nitric oxide production pathway. *C. albicans* take up the L-arginine from the environment and use the amino acid to produce carbon dioxide and urea resulting in host phagosome alkalinization and inhibit Nitric oxide production by the host (Jimenez-Lopez et al., 2013, Vylkova & Lorenz, 2014, Vesely et al., 2017, Wagener et al., 2017). Another factor contributing to phagosome alkalinization is the hyphal growth in the phagosome leading to mechanical tension on the phagosome membrane resulting in alkalinisation (Westman et al., 2018).

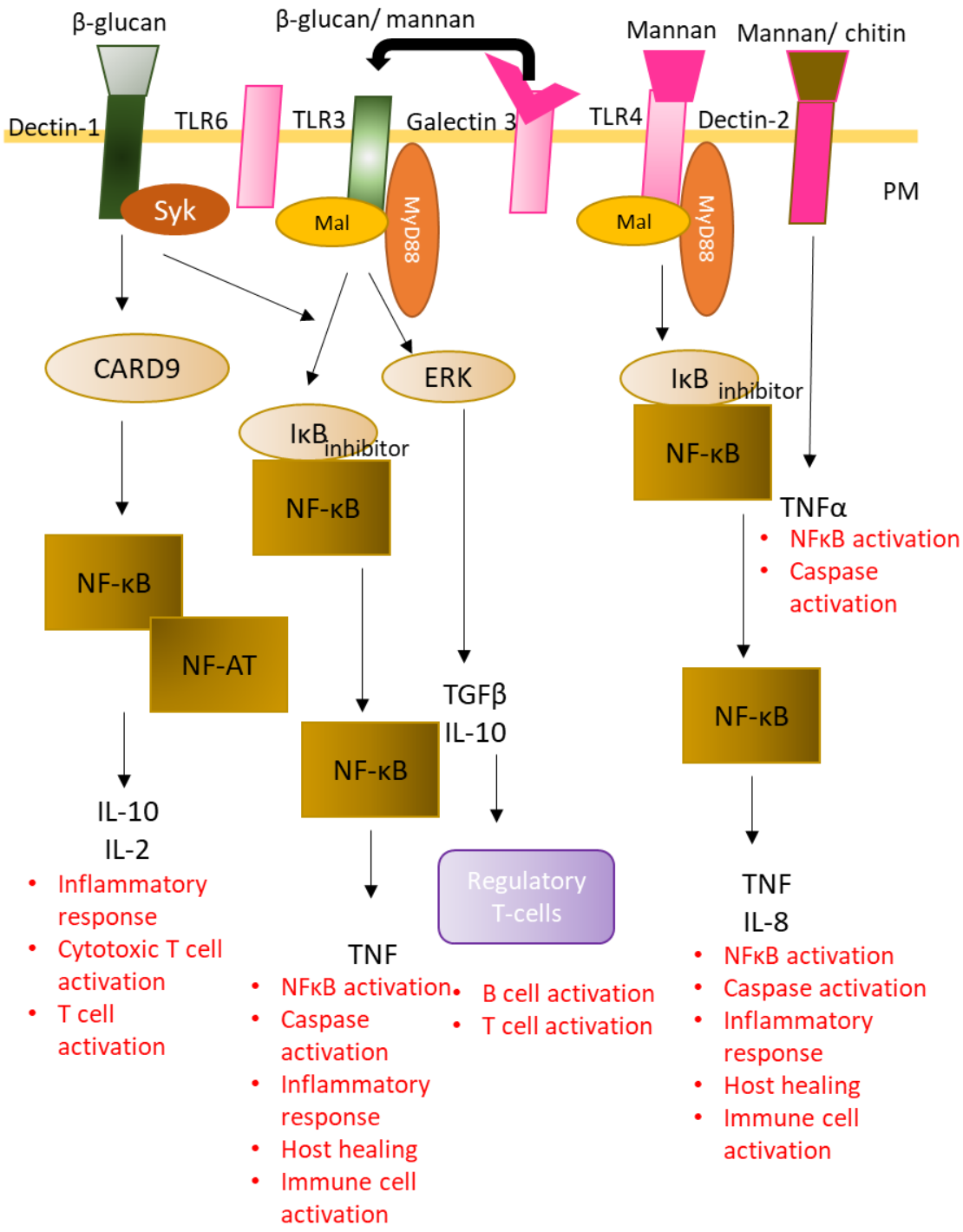

Figure 1.12: Activation of host pathogen recognition receptors results in downstream immune activation. *The diagram describes the downstream effects of the activation of Pathogen recognition receptors by C. albicans pathogen associated molecular patterns. The diagram also highlights the immune responses that are stimulated inside an innate immune cell after the recognition of C. albicans cell wall components. The illustration is colour coded*

based on the cell wall components on figure 1.11. The figure is adapted from (Netea et al., 2008) with information from (Playfair J. H. L. & Chain B. M., 2012).

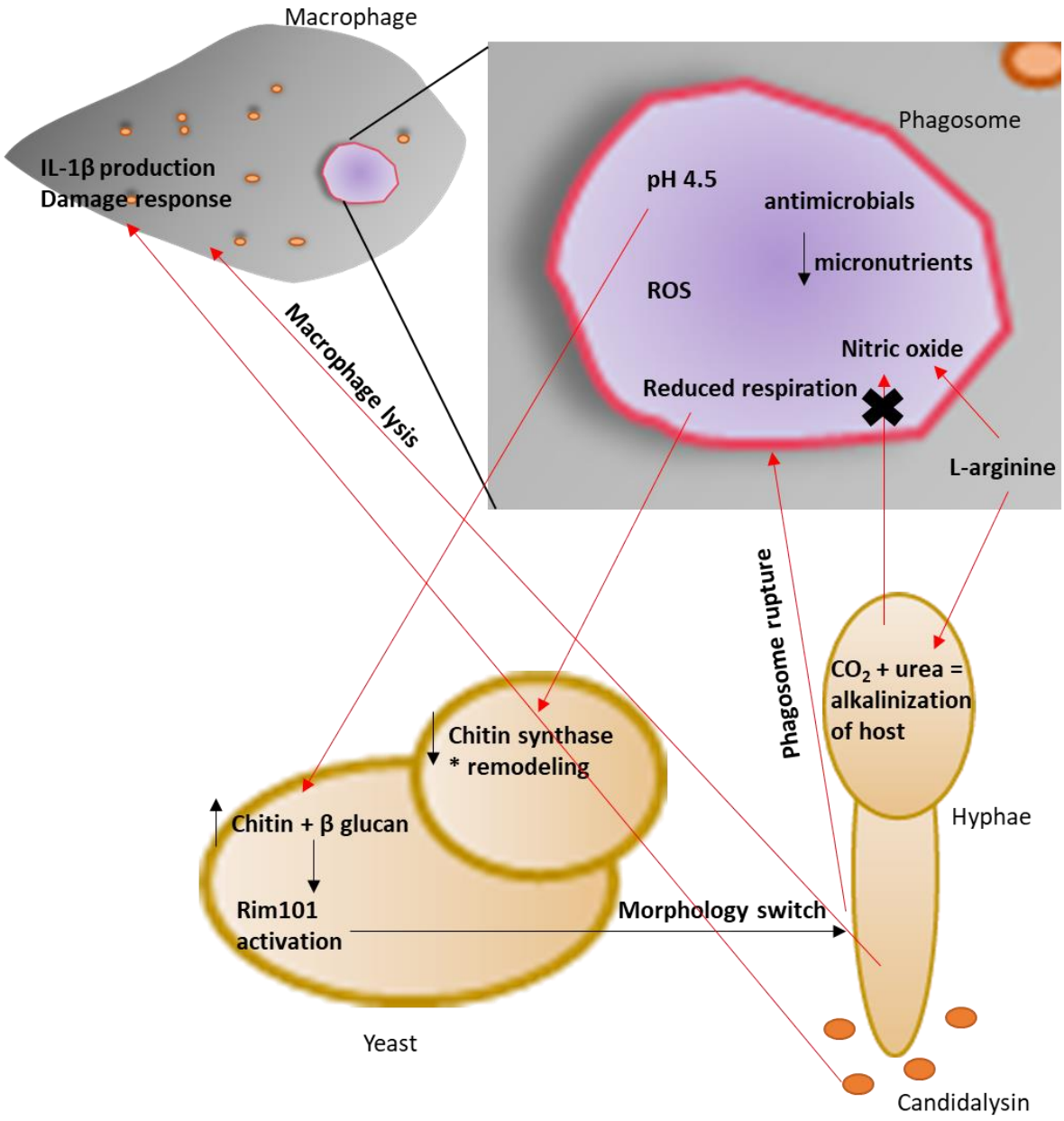

Figure 1.13: The Candida albicans to macrophage interactions. *The diagram illustrates the environmental conditions inside the phagosome and the responses elicited by C. albicans after the stimulation by the phagosome environment. The responses of C. albicans against the macrophage are also highlighted in this diagram.*

1.3.2 Interactions of *Candida albicans* with neutrophils

Neutrophils are part of the innate immune response and are a connection to the adaptive immune system. The neutrophils are important for the interactions with *C. albicans* as they can respond to both yeast and hyphae, while as mentioned, macrophages are generally more effective against yeast. Neutrophils are stimulated and recruited during infections with *C. albicans* regardless of the fungal burden and interact with other immune cells to initiate a response (Gratacap et al., 2013).

Phagocytosis occurs in a similar way to what has previously been outlined for macrophages. Similar PRRs are present in neutrophils to the ones shown in figures 1.11 – 1.12. Unlike macrophages however, neutrophil PRRs are different for hyphae and yeast cells but the response towards the activation of the adaptive immune response and the release of cytokines post PRR activation is similar (Duggan et al., 2015). During neutrophil interactions with *C. albicans* the Dectin-1 receptor is not as critical as it is during macrophage interactions however the CARD-9 (downstream effector) (figure 1.12) is important for the regulation of neutrophils. The CARD-9 activation has been reported to work independently of the Dectin-1 receptor and is important for the T-cell and inflammatory activation. In neutrophils TLR2 has been shown to be more important than Dectin-1. Activation of the TLR2 pathway results in phagocytosis by neutrophils but it has also been reported to have a role in neutrophil chemotaxis, macrophage recruitment and nitric oxide production. These activities are possibly due to the induction of cytokines and antimicrobial peptides after receptor activation (Tessarolli et al., 2010, Duggan et al., 2015). Two PRRs that were not mentioned during the review of macrophage phagocytosis but are important for neutrophil phagocytosis are CR3 (Luo et al., 2013, Johnson et al., 2016, Luo et al., 2018) and Mincle (Vijayan et al., 2012). Activation of these receptors results in downstream adaptive immune response activation as well as clearance through pro-inflammatory signalling.

Studies comparing capacity of macrophages and neutrophils to clear the infection led to the conclusion that neutrophils have a higher phagocytosis level however cannot clear the pathogen more compared to macrophages and are more susceptible to *C. albicans* killing than macrophages. In co-cultures of macrophages and neutrophils it was shown by Rudkin (2013) that the macrophages are promoted to phagocytose more hyphal cells compared to

single cell cultures of macrophages, this results in loss of macrophage death (Rudkin et al., 2013). These findings suggest that the macrophages and neutrophils have different properties and interact with each other during infections.

Neutrophils have different responses to promote clearance of *C. albicans*. Neutrophil activation results in recruitment of the NADPH oxidase complex to the phagosome to promote pathogen clearance. This is responsible for the oxidative environment inside the phagosome. Neutrophils form a structure called a granulocyte that contains different cytotoxic proteins and peptides that are released when the granulocyte fuses with the phagosome containing the pathogen (Gazendam et al., 2016, Gazendam et al., 2016). *C. albicans* respond by stimulating the HOG pathway (figure 1.9) to resist the neutrophil response. *C. albicans* cells release a superoxide dismutase called Sod5 to detoxify the Reactive Oxygen Species (ROS) in the environment and promote pathogen survival (Miramon et al., 2012). Responses in figure 1.13 occur inside the neutrophil phagosomes (Gazendam et al., 2016, Alves de Lima et al., 2018).

An important response unique to neutrophils is the formation of Neutrophil extracellular traps (NETs) for the clearance of hyphal *C. albicans*. NETs are made from DNA, histones and other proteins (Johnson et al., 2016, Kenny et al., 2017). NETs are formed by loading intracellular vesicles with nuclear material that will eventually be expelled upon stimulation by pathogens (Byrd et al., 2013). NETs against *C. albicans* form slower than what was observed during interactions with other pathogens and their induction can be inhibited through the PKC pathway (CWI pathway figure 1.9) possibly because of the changes of the cell wall composition or the hyphal morphology proteins (Kenny et al., 2017). NETs can cause cell wall damage resulting in more exposed β glucan and changes in the chitin deposition. The HOG CWI pathway (figure 1.9) is stimulated by the cell wall stress and activates a Chs3-mediated response to aid with cell adaptation to the stress. The cell wall remodelling for β glucan is achieved via the secretion of Phr1 (a cell surface protein involved in β glucan linkage) and the cell membrane and cell wall organization are restored via the activity of Sur7 (protein required for cell wall and membrane organization) (Hopke et al., 2016).

The host neutrophils have multiple responses which are distinct to macrophages to promote pathogen clearance. *C. albicans* has adapted to respond to the macrophage and neutrophil stimuli to promote survival within the host. The complexity of the interactions and the multiple signalling pathways show that the signalling system for environmental adaptation of *C. albicans* cells is robust and linked.

1.3.3 *Candida albicans* interactions with epithelial tissue

C. albicans resides on mucosal epithelia (oral, gut and vaginal) resulting in Candidiasis. The different epithelial cells respond differentially to the *C. albicans* infection stress, upregulating distinct combinations of cytokines and chemokines (Whiley et al., 2012). In this section the interactions of *C. albicans* with epithelial cells (immune response, adhesion and Candidalysin production) will be discussed. Understanding these interactions can be critical to identify alternative targets for therapeutic development and to understand the *C. albicans* pathogenicity.

Classically recognition of pathogens by host cells involves pattern recognition receptors recognising cell wall components of *C. albicans* that initiate a response. During interactions with epithelia cells classical recognition receptors are not used. Epithelial cells respond to damage not pathogen associated molecular patterns. The *C. albicans* adhesion proteins on its cell surface and cell wall are important for attachment to the host receptors and for the activation of pathways upon recognition. The pathways activated have downstream activity on transcription factors: 1) NFκB 2) c Jun and c Fos 3) the mTOR response for damage protection (figure 1.14) (Naglik et al., 2017). Epithelial cells can sense which *C. albicans* morphology they are interacting with and induce a different response to it. Response against hyphal cells is stronger resulting in the production of cytokines and inflammatory mediators (Moyes et al, 2015). Epithelial cells do not respond to commensal cells as much due to the no damage or low damage phenotype they exert (Naglik et al., 2019). Damage is associated with the adhesion, invasion, hyphal length and the production of Candidalysin; defects in those factors can result in no host cell damage. Active penetration of the host epithelial tissue can result in no damage unless Candidalysin is present. Hyphal switch and Candidalysin secretion are important for the damage-associated necrosis of epithelia (Allert et al., 2018).

During epithelial interactions, *C. albicans* have adhesion proteins that allow attachment on host surfaces. *C. albicans* attach and modulate their cell wall composition to ensure a successful interaction with the host cell (figure 1.10). *C. albicans* yeast initially attach to the host extracellular matrix due to the cell wall composition and the presence of adhesion protein Als3 (Gustafson et al., 1991, Tronchin et al., 1991). Once adhered to epithelia, *C. albicans* cells switch to the hyphal morphology where more adhesion proteins are secreted to the cell wall allowing for invasion and damage of the host cell (Moyes, Richardson & Naglik, 2015).

Cell surface proteins Hwp1 and Als3 are characterised as the main adhesion inducers. In a human study in Mexico the prevalence of adhesion gene expression by *C. albicans* during a vaginal infection was characterised from 50 patients. *Als4* was expressed in 100% of the patients, *Als1/2/3/5/7* were expressed in 87.5% of the patients and *Hwp1* is expressed in 75% of the patients. The findings highlight the importance of the genes for pathogenicity as they were expressed in human infection samples. The data also showed that more than one adhesion protein can be expressed at the same time, promoting *C. albicans* pathogenicity (Monroy-Perez et al., 2012).

C. albicans can either be endocytosed (promote non-invasive uptake by host cells) or actively penetrate epithelial cells (the hyphal stem produces enough force to penetrate and cause host cell damage) (Allert et al., 2018). The *Candida* adhesion proteins promote both endocytosis and active penetration of epithelial cells. Specifically, Als3 has an important role in binding host cell E-cadherin and allowing for the endocytosis of hyphal *C. albicans* by epithelial cells (Padovan et al., 2009, Naglik et al., 2017). During active penetration the adhesion proteins as well as the secreted aspartyl proteases (Saps) are also critical for the interaction and have an impact on the host for cell surface integrity and tissue damage (figure 1.15) (Staniszewska et al., 2015, Zhou et al., 2018). Saps are critical for active penetration as they degrade the tight junction protein E-cadherin (Moyes et al., 2015). The expression of adhesion proteins during host cell invasion is dependent on the ergosterol biosynthesis genes *ERG11* and *ERG3* as shown by previous studies using different *C. albicans* mutants for invasion assays (Zhou et al., 2018).

The tissue damage induced by *C. albicans* invasion, and the host immune responses can affect the availability of nutrients and increase the stress in the environment for *C. albicans*, this would promote adaptation of cells through the cell wall integrity pathways (figure 1.9) (Hebecker et al., 2016).

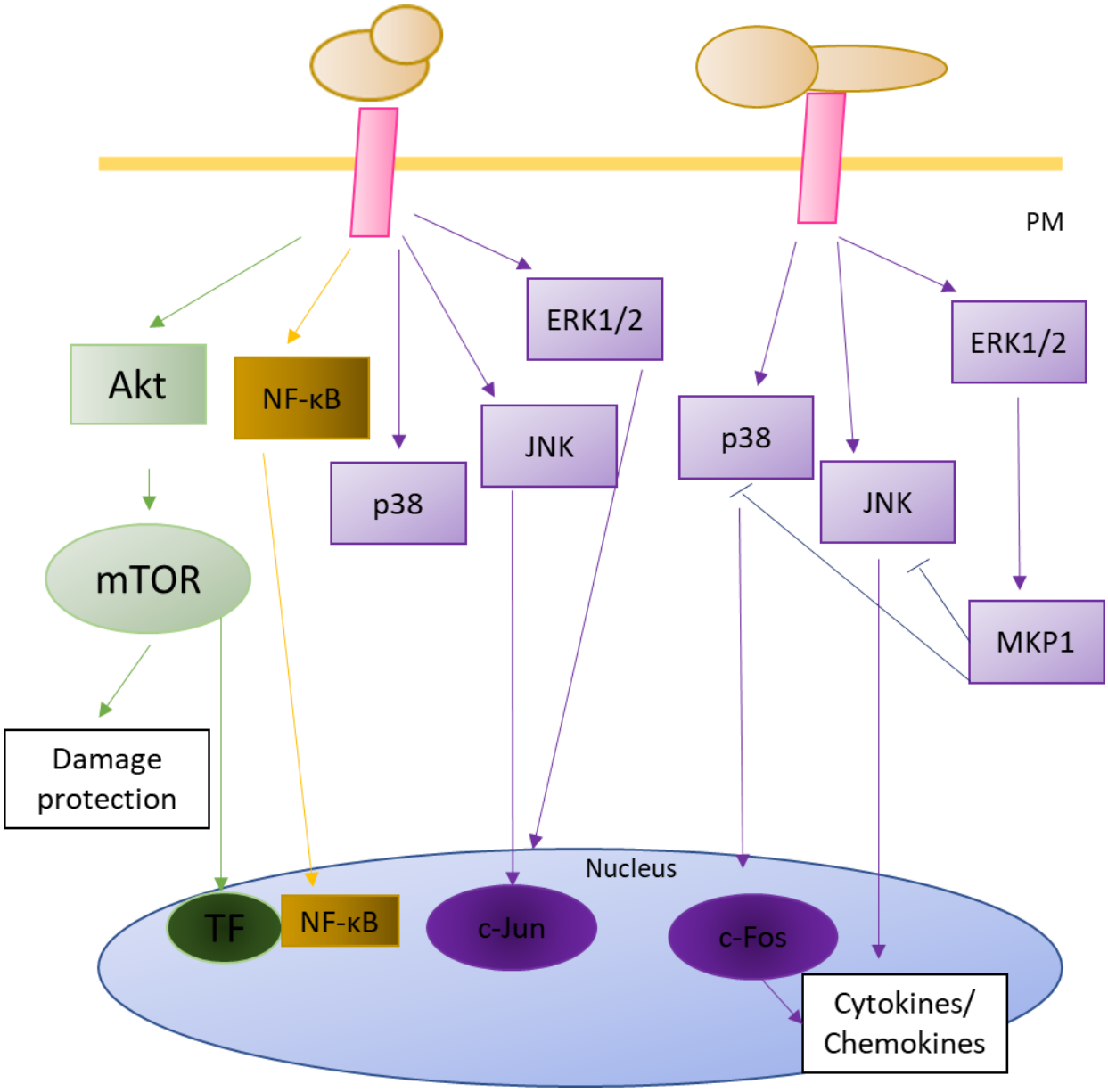

Figure 1.14: The activation of epithelial immune responses by Candida albicans yeast and hyphae. *The diagram illustrates the different responses stimulated during host epithelial interactions with C. albicans. When interacting with the yeast morphology the ERK1/2, JNK and p38 pathways are mildly activated and result in the transcription factor c-Jun activation, the response is not very strong. NFκB is also activated by the yeast morphology resulting in*

tissue repair and some recruitment of immune cells. Akt pathway is activated by C. albicans yeast which downstream induces a damage protection response via the mTOR pathway. During hyphal interactions p38, JNK and ERK1/2 are strongly activated resulting in the expression of genes encoded by the c-Fos transcription factor, downstream the response activates different cytokines and chemokines to respond to the host damage. ERK1/2 activates a MAPK response through MKP1 which modulates the p38 and JNK activities. The figure is adapted from (Naglik, Gaffen & Hube, 2019).

An important factor for host cell damage is the production of the fungal cytolytic protein Candidalysin which induces both host damage but also a host immune cell activation (Moyes et al., 2016). Candidalysin causes immune induction by stimulating proinflammatory cytokines, chemokines and antimicrobial peptides via the c-Fos activation (figure 1.14). Different immune responses have been shown to be stimulated by the recognition of Candidalysin by host cells. Macrophage and neutrophil cell recruitment was demonstrated to occur via the release of proinflammatory cytokine CXCL8 (Swidergall et al., 2019) as well as by the presence of interleukins, TNFα and NFκB (Naglik et al., 2017). T- helper 17 cells are also recruited for *C. albicans* clearance after Candidalysin recognition through the activities of IL-17 and antimicrobial peptides (Naglik et al., 2017, Verma et al., 2017, Ho et al., 2020). The immune interactions with Candidalysin are complex and still under investigation. The host immune responses are tissue specific.

Ho (2019) provided an understanding for how Candidalysin is recognised by host cells. Epidermal Growth Factor Receptor (EGFR) (responsible for host epithelial barrier maintenance and defence) is composed of a tyrosine kinase receptor and ErbB family subunits, involved in the recognition of Candidalysin by host cells. The recognition of Candidalysin occurs when there is shedding of molecules by Candidalysin, binding to ErbB ligands activating the EGFR receptor. The activation of EGFR is distinct in each host tissue interacting with *C. albicans*, EGFR stimulates an internal signalling response after the receptor is internalised. EGFR only influences the response against Candidalysin but has no effect on membrane permeabilization caused due to *C. albicans* invasion (Ho et al., 2019).

The activity of Candidalysin is not fully understood yet but there are key insights as to the role of the toxin in the *C. albicans* virulence. The damage caused by Candidalysin, and the immune responses elicited against the toxin influence the infection outcome. Candidalysin is not highly associated with commensalism as the toxin causes host damage and clearance however it could still be beneficial to the cells during polymicrobial interactions (Naglik et al., 2019). Commensal *C. albicans* could still be producing Candidalysin but at low levels which do not stimulate the immune response as the response against the toxin is dose dependent (Moyes et al., 2016).

The interactions with epithelial cells are important for the host pathogen interactions of *C. albicans* as there is a fine balance between a commensal and a pathogen.

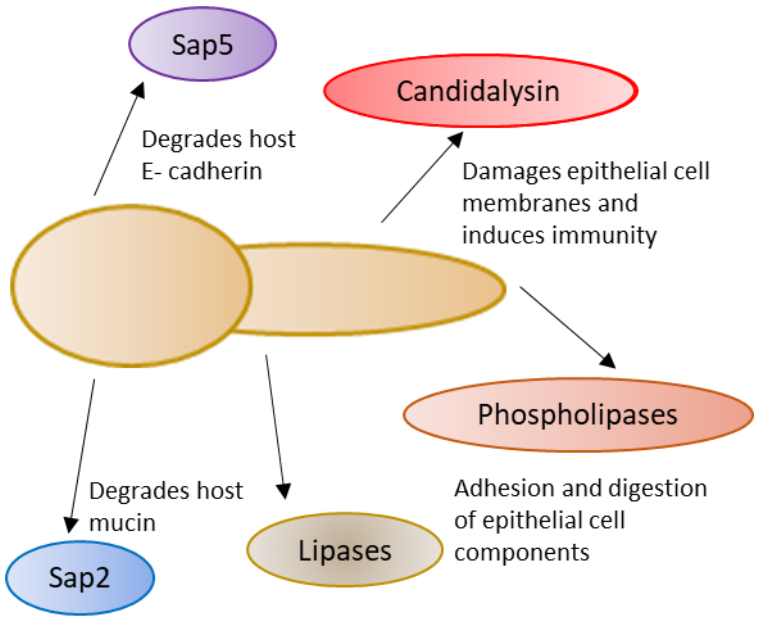

Figure 1.15: Candida albicans epithelial penetration responses. *The figure illustrates the C. albicans proteins that are most important for epithelial invasion and the impact of those proteins on the host. The figure is adapted from (Naglik et al., 2019).*

1.4 Models to study the *Candida albicans* host-pathogen interactions.

1.4.1 *In vitro* cell cultures

Through the years cell culture of murine and human cells has been established to understand the host pathogen interactions of *C. albicans*. The commensalism of the pathogen allows interactions with multiple cells from different tissue. Single cell or even more complex cultures combining different cell lines can be used for investigations. Epithelial cells can be used for invasion and adhesion assays as a monolayer for microscopy or for damage and permeability assays using the Trans-well model. Immune cells can be used to study the interactions of *C. albicans* with phagocytes. The cultures can be more complex and involve microfluidics and bioreactors or simple single cell culture of host cell to pathogen interactions (Tabatabaei et al., 2020).

Complex models such as the organ on chip technology, ex vivo tissue samples and commercial models can also be used. These more complex models increase the physiological relevance compared to the other *in vitro* approaches. *In vitro* cultures are key to understanding the host-pathogen interactions as they are relatively easy to grow and maintain; to image and to use in functional assays. The cultures are relatively cheap and are not under regulation. They can also provide preliminary data before animal models are used. The physiological relevance of *in vitro* models however is not as high as in *in vivo* approached, resulting in findings that might not occur *in vivo* where there are more complex cell to cell interactions. More physiologically relevant *in vitro* cultures are important to study the host-pathogen interactions (Tobin et al., 2012). New complex *in vitro* cultures such as the organ on chip cultures will keep becoming more physiologically relevant and cheaper to use. They could help make more accurate predictions of good drug targets as well as being used to study host-pathogen interactions. Recently researchers have been using the gut-on-a-chip model to study pathogenicity of bacteria and fungal pathogens (Grassart et al., 2019, Maurer et al., 2019). The aim is for complex *in vitro* models to replace as much animal testing as possible in the future.

1.4. *In vivo* infection models

In vivo models are biologically relevant and critical for the understanding of host-pathogen interactions. Multiple *in vivo* models have been established for Candidiasis. Good animal

models should be reproducible, relatively cheap, easy to set up and should reproduce some of the human symptoms (Maccallum, 2012). Different *in vivo* models have been used to study the host-pathogen interactions of *C. albicans*.

Galleria mellonella also known as wax moths have been used for survival assays as they are cheap, easy to handle and are genetically homogeneous. The immune cells of *G. mellonella* are relatively similar to the human immune cells. They have been used as a model to study virulence however they are not useful for imaging and are not as good as mammalian systems. *Caenorhabditis elegans* are multicellular eukaryotic organisms that are small, cheap and easy to handle. *C. elegans* are transparent and can even be frozen and still be alive. The problem however is that they are not able to grow at 37^{o}C and they do not have an adaptive immune response. They are useful for live imaging and survival experiments. *Drosophila melanogaster* are another relevant model recently developed. They are not mammalian organisms; however, they are cheap, easy to handle, easy for genetics and a high number of Drosophila can be used for experiments. They can be used for survival assays as well as for interactions with the immune system (Maccallum, 2012, Segal, Frenkel, 2018). Drosophila can be a good model to use before using rodents for experiments.

Rodents are the most well-established model for Candidiasis. Rodents can be injected through various routes and can recapitulate different forms of Candidiasis. The rodents can be used to establish disseminated candidiasis, dermal candidiasis, oropharyngeal candidiasis and vulvovaginal candidiasis. Mice and rats need to be stimulated with drugs or be immunocompromised to be used as models since *C. albicans* is not a commensal organism in rodents. The infection route does not recapitulate the human infection which is initiated from mucosal epithelial sites. The host-pathogen interactions in rodents are assessed through survival, organ fungal burden and histopathology. In comparison to other models mice are expensive and an animal licence is required. (Maccallum, 2012, Cassone & Sobel, 2016, Segal & Frenkel, 2018). Usually, a combination of models is used to understand the host-pathogen interactions further, but rodents are always required before anything is used for clinical studies.

Zebrafish are a more recent model to study host to pathogen interactions. Zebrafish (*Danio rerio*) are vertebrates originally from rivers and lakes in India. Zebrafish are a good model of

human disease as the tissue and organ systems are very similar. Zebrafish are small, transparent, easy to handle and relatively cheap to use in comparison to rodents. Zebrafish are the only vertebrate model that allows fluorescence microscopy of the live organism. They are easy to visualize throughout the infection progress without culling the animal (Tobin et al., 2012, Bojarczuk et al., 2016). Due to their size, investigations of both the host and the pathogen gene expression at the different stages of infection can be performed. This is a significant benefit in comparison to other models (Gratacap & Wheeler, 2014). Genetic modifications can be at a line level or at the embryo level. Genetic modifications on embryos using a morpholino approach can last several weeks. Transgenic zebrafish lines only need about 8 weeks to be adults and used in experiments (Tobin et al., 2012, Ruzicka et al., 2019). This is a big benefit as the Zebrafish tools available allow temporary disruption of neutrophils and macrophages. In the mouse model the disruption of genes is permanent (Tobin et al., 2012, Davis et al., 2016). The zebrafish immune system is highly comparable to humans, zebrafish embryos have many PRRs similar to humans, they do not have Dectins but they do have genetically and functionally comparable receptors to mammalian Toll-like-receptors (Li, et al. 2017). This means that studies for the interactions of zebrafish to fungal pathogens can be comparable to humans. The adaptive immune response does not develop until 4 weeks post fertilization, this is a benefit as it allows researchers to focus on the innate immune response during host-pathogen interactions. The anatomy of Zebrafish allows for multiple infection routes and different types of infection. The Caudal vein and the duct of Cuvier are used for bloodstream infections. The swimbladder is a localised epithelial infection model. The hindbrain, somites and the yolk can be used as infection sites to study pathogen dissemination (Tobin et al., 2012).

There are several disadvantages during fungal pathogen infections is that the Zebrafish cannot survive at relevant temperatures. The zebrafish develop between 25 to 28 ^{o}C while the human body temperature is 37 ^{o}C (Tobin et al., 2012). For other human pathogens such as for *Mycobacterium tuberculosis* an equivalent of the human pathogen existed for Zebrafish allowing further and more a physiologically relevant understanding of the host pathogen interactions. The aim is to find something similar for fungal pathogens (Gratacap & Wheeler, 2014).

Zebrafish have been used to study *Candida albicans* host-pathogen interactions, recently allowing clear identification of the roles of yeast and hyphal cells during Candidiasis. The yeast morphology is critical for dissemination through the host. *C. albicans* cells locked in the yeast morphology can disseminate however are not as virulent as the hyphal morphology which is important for tissue invasion (Seman et al., 2018). Zebrafish are a good model to study Candidiasis, they are simple and cheap to use and can produce an immune response similar to mammals. Zebrafish have similar PRRs and immune pathways to mammals and the immune cells present similar phenotypes, an example of that is the formation of granulomas and NETs by macrophages (Gratacap et al., 2013, Gratacap & Wheeler, 2014, Li, et al., 2017). Therefore zebrafish was chosen as the *in vivo* model used to study the host-pathogen interactions of *C. albicans*.

1.5 Aims and Objectives:

The aim of this study has been to elucidate the role of the AP-2 endocytic adaptor complex of *C. albicans* during host pathogen interactions using different models. The main objectives were the following:

- Study the impact of the AP-2 endocytic adaptor complex in *C. albicans* on the phagocytosis of *C. albicans* by murine macrophages.
- Study the significance of the AP-2 adaptor on macrophage interactions.
- Investigate hyphal switch of *C. albicans* in different host environments.
- Determine the impact of *C. albicans* AP-2 adaptor complex on virulence.
- To explore the impact of *C. albicans* AP-2 adaptor complex on epithelial invasion.

The key findings from this investigation are summarized here:

- The increased cell wall chitin levels, changes in mannan organization and cell size shown during dissociation of the AP-2 complex result in increased phagocytosis by host macrophages. The increase in phagocytosis is not linked to increased exposed β glucan levels.
- In the murine phagosome *C. albicans* with a dissociated AP-2 complex present a hyphal switch defect. The deficiency is linked to the mechanical properties of the *apm4* deletion *C. albicans* and the increased levels of chitin in the *C. albicans* cell wall.

- *C. albicans* cells that have hyphal switch deficiencies are not cleared by host immune cells but rather grow and form new buds in the phagosome environment.
- *C. albicans* cells with a dissociated AP-2 complex show reduced virulence during zebrafish embryo infections and increased survival of the host. The reduced *C. albicans* virulence during zebrafish embryo infections is not linked to pathogen clearance by host cells but with the ability of cells to switch to the hyphal morphology.
- The *C. albicans* with a dissociated AP-2 complex form microcolonies within the zebrafish host that are similar size to the wild type microcolonies even though they present a hyphal switch deficiency. These findings suggest that the mutant cells grow and proliferate inside the host. The results also suggest that there could be more dissemination by mutant cells compared to wild type cells.
- The zebrafish immune system is stimulated in a similar way for both the wild type and mutant *C. albicans* cells.
- The cell wall chitin of *C. albicans* has an impact on the virulence phenotype during zebrafish infections. A decrease of chitin levels partially restores the virulence phenotype. Suggesting that the chitin has a role in virulence, but other factors influenced by the AP-2 complex could also be involved.
- During epithelial interactions hyphal switch is reported by *C. albicans* with a dissociated AP-2 complex however there is a defect hyphal in elongation in the host tissue. This could support the decreased host invasion phenotype observed by the mutant *C. albicans*.
- The AP-2 complex, and the cell wall changes that occur after the deletion of *apm4* result in decreased epithelial adhesion. Suggesting a potential role for AP-2 in the recycling of adhesion proteins as well as an impact of increased chitin levels on adhesion.

Overall, the results suggest an important role of the AP-2 complex during host – pathogen interactions and hyphal switch during interactions in different environments. Dissociation of the AP-2 complex results in reduced virulence and in phenotypes that are more associated with commensalism.

Chapter 2: Materials and Methods

2.1 Cell culture techniques

2.1.1 *Candida albicans*

2.1.1.1 Overnight cultures

A colony of *Candida albicans* from a streaked YPD agar plate was collected using a sterile 1µL loop (Star Labs) and resuspended in 10mL of YPD broth (1% yeast extract, 2% glucose, 2% peptone) + 50 mg/mL uridine. The culture of YPD and *Candida* was suspended inside a 25mL Universal tube (Stardest) with the lid sealed enough to remain sterile and allow aerobic respiration. The culture is incubated at 30°C in a shaking incubator at 200 x g overnight.

2.1.1.2 Hyphal induction in vitro

YPD broth + 10% FBS (Gibco) + 80 µg/mL L- uridine were added to create the hyphal induction media in a sterile glass conical flask, covered with aluminum foil. *Candida albicans* cells from overnight cultures were used at a 1:20 ratio of cell volume to media (500 µL in 10 mL of media). The culture was incubated at 37°C 200 x g. The hyphal induction begins from about 30 minutes, so the cells were incubated for as long as desirable for the purposes of the experiment.

2.1.1.3 Candida albicans *stocks*

The stocks of *Candida albicans* contain a 1:1 ratio of overnight cultures to 50% glycerol. The stocks are stored in screw top vials which were sterile and safe to use in a -80°C freezer.

2.1.1.4 Streaking from stocks

A 1 µL sterile inoculation loop was dipped in the *Candida albicans* stock vials. The loop with the *Candida* sample was streaked on a dried YPD + 80 µg/mL L-uridine agar plate. The plate was then either placed in a 30°C incubator to grow overnight to be used the next day or placed on the bench to be used a few days later and to grow at room temperature.

2.1.2 J774 macrophages

2.1.2.1 Cell passage and culture

The J774 cells (Sigma) are a mouse macrophage cell line. Culturing media used for growth were DMEM media (Sigma) with 50 mL Fetal Bovine Serum (10% v/v) (Gibco), 5 mL L-Glutamine (1% v/v) (Fisher Scientific) and 5 mL Penicillin with Streptomycin (1% v/v) (Fisher Scientific). During experimental periods the cells were kept in serum-free DMEM media (DMEM + 1% L- Glutamine + 1% Penicillin and Streptomycin). When a tissue culture treated T-75 flask (Greiner lab biosciences) was 80% confluent the serum containing DMEM media were removed and fresh media were added, then a tissue culture sterile cell scraper was used to gently detach the cells. The detached cells were then used for passaging as a cell ratio to a new T-75 flask with fresh media. The detached cells were only centrifuged to collect the cells when they were used for a freeze down.

2.1.2.2 Seeding macrophages for experiments

Cells from an 80% confluent T-75 J774 flask were detached as previously described. A 10 µL volume of the detached cells was used to count the cell number using a hemocytometer. A $5x10^4$ cells/mL solution was prepared and the cells were seeded on either plastic 24-well plates or glass-bottom 96-well plates (Greiner lab biosciences). The cells were incubated at 37°C with 4% CO_2 for 24 hours so that the cells were attached and had adjusted to the environment.

2.1.3 CACO-2 gut epithelial cells

2.1.3.1 Passaging

The media from a 100% confluent T75 flask were removed and 5mL of sterile PBS was added to rinse the cells. PBS was removed and 2mL of 0.25% Trypsin/EDTA (Sigma) was added. The cells were incubated for 5 minutes at 37°C and were regularly checked to monitor how well they were detaching. The flask was gently tapped and checked under the microscope to monitor the detachment. When the cells were detached 8 mL of DMEM- Glutamax (Gibco) with 10% FBS and 1% Penicillin with streptomycin (P/S) (the cell culture media) was added at a 1:4 ratio to deactivate the trypsin. Cells were collected in a 15 mL centrifuge falcon (Star Labs) and collected after centrifugation at 1000 rpm for 3 minutes. The supernatant was then discarded, and the cells were resuspended in fresh cell culture media. The cells were

passaged as a ratio of cell suspension to media independent of cell numbers. The cells were cultured in T-75 flasks. Every 3 days the media from the flask were removed and fresh cell culture media were added until the cells reached confluency.

2.1.3.2 Freezing and thawing cells

100% confluent T-75 flasks were initially passaged to detach and wash the cells. When the cells were collected instead of resuspension in culture media Quick recovery freeze down media (Thermo Scientific) were added. 1 mL of Freeze down media was added for each flask used for the procedure. 1 mL of the cell and freeze down suspension was added to each cryovial (Thermo Scientific) and the cells were then either moved temporarily to -80^{o}C or to Cryostores were they were permanently stored in liquid Nitrogen.

The process of thawing cells involved collection of cryovials from the liquid nitrogen stores and warming the vial in a waterbath so that the liquid was thawed. The thawed cell suspension was added at a 1:10 ratio to fresh culture media to deactivate the DMSO present in the freeze down media it was important to do this quickly as it is a toxic solution. The cells were than collected, media were discarded, and cells were resuspended to 10 mL of culture media and kept in a tissue culture treated T-75 flask. The next day the media were discarded and replaced with fresh culture media to remove any DMSO that could have still been in culture. The cells were maintained, and once confluent they were passaged.

2.1.3.3 Seeding of a CACO-2 cells and monolayers

To seed CACO-2 cells (Sigma) in dishes, cells from a 100% confluent T-75 CACO-2 flask were detached and collected as in section **2.1.3.1**. A 10 µL volume of detached cells resuspended in fresh culture media was used on a hemocytometer to count the number of cells in the cell culture and was used to prepare a solution with 1x10^{5} cells/mL. The cells were then seeded either on a 96-well glass bottom plates or on a glass coverslip inside a 24-well plastic plate. The cells were cultured for about 10 days or until they appeared well attached to each other, the culture media were discarded and replaced by fresh media every 3 days.

Seeding a monolayer required cell priming for the CACO-2 cells to attach to the bottom of the well using Gelatin. Glass coverslips in 24-well plates and 8-well glass-bottom chamber slides (Thermo Scientific) were coated with 0.2% gelatin (Sigma) for 1 hour at 37^{o}C. The wells were washed twice with PBS and then incubated at room temperature for no more

than 30 minutes with 1% sterile glutaraldehyde (Sigma) dissolved in PBS for crosslinking. The wells were incubated with 1M sterile glycine (Sigma) for 20 minutes at room temperature after the wells were washed twice with PBS. After the incubation was over the wells were washed twice with PBS before $1x10^5$ cells/mL were seeded onto the wells. The cells were cultured for 18 days at 37°C with 4% CO_2. The media were carefully discarded and replaced with fresh media every 3 days. The cells were then used for infection experiments.

2.1.3.4 Seeding a gut-on-chip organoplate:

The process of seeding an OrganoPlate involved multiple steps like preparation of solutions, coating with collagen, detachment of cells and seeding. It is important to refer to the OrganoPlate format below to understand where each solution was added.

The coating steps required to mix a solution of 5 mg/mL collagen (Biotechne), 37 g/L of NaHCO3 and 1M of HEPES (Fisher Scientific) first thoroughly. The solution was used as the extracellular matrix mixture, 1.6 µL of the mix were inserted in the middle channel. To ensure that the mix was inserted well enough the plate can be observed from the bottom and it should have appeared as a single black line through the lane. It was important to keep the OrganoPlate (Mimetas) closed as much as possible to avoid the samples drying. Once the mixture was added to all the wells the plate was incubated for exactly 20 minutes in a 37°C static incubator, during this time cells from a confluent CACO-2 T-75 flask were detached as described in section **2.1.3.1** and an aliquot was diluted in equal volume of trypan blue. The stained cells were transferred to a hemocytometer and a solution of $2x10^7$ cells/mL was created. Once the incubation period of the matrix was complete, the plate was examined to ensure that the collagen was polymerized well, if the polymerization was not very good then the cells wouldn't have attached to the plate. Once the matrix was polymerized, 2 µL of the CACO-2 cell suspension were added to the upper inlet channel of each chip. 50 µL PBS were added to the observation window to ensure that the plate had some moisture. The plate was then incubated in a static incubator set to 37°C with 4%CO_2 for 45 minutes in a 75° angle. After the incubation 50 µL of the cell culture media were added to the top media inlet (same wells as the ones where the cells were inserted) and then the plate was incubated for 4-6 hours. Once the cells had attached to the matrix 50 µL of culture media were added to the top outlet as well as the bottom inlet and outlet. The

cells were then moved inside a 37°C incubator with 4% CO_2 and placed on a perfusion rocker set at a 7° angle changing sides at every 8 minutes interval. The OrganoPlate could be used between 4-8 days post seeding. The media of the OrganoPlate were removed and replaced with fresh culture media every 3 days.

2.2 *Candida albicans* assays

The following section describes assays used with *C. albicans* cells.

2.2.1 *Candida albicans* DNA assays

Methods to change the genetics of the *C. albicans* cells are described here.

2.2.1.1 Candida albicans transformations

2.2.1.1.1 Transformation cassettes

The cassettes were created by searching for the sequence in the Candida Genome website and then choosing the best position in the sequence to create the primers for (Eurofins). The primers need to be stable and annealed at a similar temperature. On the transformation tag primer sequence sticky ends of the plasmid that needs to be integrated were added. The transformation purpose was to tag the *Candida* cells with GFP or to delete a gene which required a forward and reverse tag as well as two external primers that would be used in PCR to ensure the correct integration of the transformation cassette to the gene (figures 2.2). The gene deletion cassettes used were from previous work in the lab, figure 2.2 represents the transformation of *eno1* to add a GFP tag. The transformation cassettes were produced through PCR, 4 PCR mixes were required. The PCR mix contained: 10x Buffer (Bioline), 50mM $MgCl_2$ (Bioline), the 5' transformation tag primer 150ng/µL, the 3' transformation tag primer 150ng/µL, di-nucleotides mix, the plasmid DNA template at a 1:10 ratio, hot-start Taq Polymerase (Bioline) and sterile distilled water. The plasmid DNA template used was different depending on the transformation that will be carried out. The PCR program was set as follows: 1) 93°C for 3 minutes 2) 92°C for 1 minute 3) 53°C for 1minute 4) 72°C for 4 minutes 5) steps 2-4 repeated 30 times 6) 72°C for 10 minutes 7) 4°C for 10 minutes. The success of the PCR was assessed through DNA gel electrophoresis, 1µL of the PCR product was mixed with 10µL of dye and run on a gel next to a 1kB DNA ladder. Once the PCR was successful the 4 PCR reactions were combined and a 1:10 volume of 3m NaOAc at pH 2 with 2 volumes of 96% ethanol were added to the mix and were incubated at

-20°C for 30 minutes. After the incubation the mix was centrifuged at maximum speed for 5 minutes to remove the supernatant and was washed with 750 µL of 70% ethanol. Ethanol was then removed, the mix was dried and resuspended in 150µL of distilled water.

2.2.1.1.2 The transformation process

Overnight cultures of the strains of interest were refreshed at a 1:200 ratio and incubated for 4 hours at 30°C 2000 x g. The cells were washed once with sterile di-ionised water and once with LiOAc (100mM lithium acetate, 10mM Tris-HCl, 1mM EDTA at pH 7.5-8). Cells were resuspended in 150µL of LiOAc. In a new Eppendorf the following ratios of components were added 13.3% cell suspension, 1.3% ssDNA (10mg/mL), 5.3% of PCR product of the transformation cassettes and 80% of 50% PEG_{400}. The cells were mixed well and grew overnight. The next day cells were heat shocked for 15 minutes at 44°C, were washed and resuspended in 100µL of di-ionized water. The cells were spread on selection plates with the appropriate selection markers (LEU^-, URA^-, ARG^- or HIS^-).

2.2.1.1.3 Colony PCR

The colonies that grew on the selection media after the transformation were collected and carefully streaked on a fresh selection media plate and grown overnight in a static 30°C incubator. The next day a small amount of the colonies was placed in an Eppendorf tube that contained 20µL of 0.02M sodium hydroxide. The Eppendorf tubes were clearly labelled so that it was easy to identify which colony the samples were from. The samples were mixed and placed in a 100°C heat block for 15 minutes. After the incubation a colony PCR mastermix was produced with the following: 2x Phusion master mix (Bioline), 100µg/mL 5' primer, 100µg/mL 3' primer and sterile distilled water. PCR tubes for each sample were clearly labelled and 17.5µL of the master mix was added to each with 2.5µL of the incubated colony in NaOH. Once the samples were prepared PCR was used to amplify the DNA, the PCR program was set as follows: 1) 98°C for 30 seconds 2) 98°C for 10 seconds 3) 65°C for 30 seconds 4) 72°C for 1 minute (30 sec/kB) 5) repeat steps 2-4 for 30 cycles 6) 72°C for 5 minutes 7) 4°C for 10 minutes. The samples were then used for DNA electrophoresis (Section **2.2.1.1.5**), 5µL of the PCR product with 10µL of DNA dye in each sample. The samples were running next to a 1kB DNA ladder. The positive transformants were used to run more diagnostic PCR using different primers to ensure that the cassette was fully

integrated. The controls for all the PCR steps are genomic DNA from Wt samples and other strains with a similar transformation.

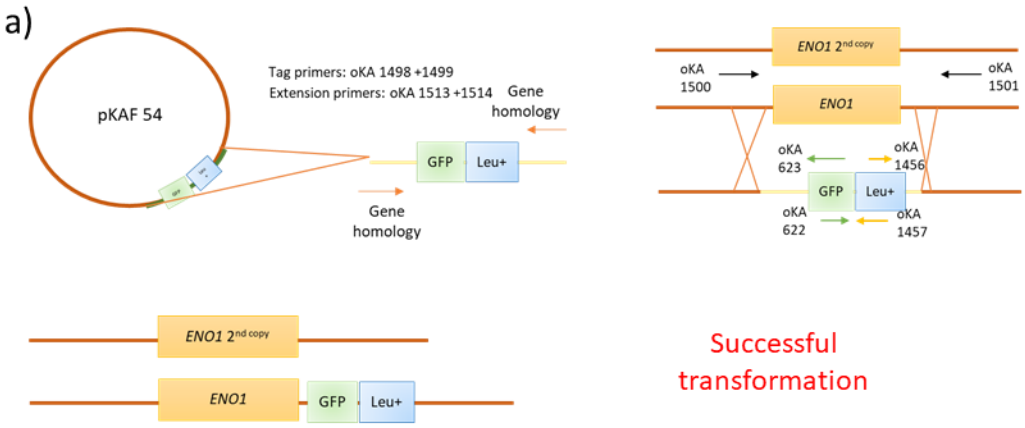

b) **Tag primer oKA 1498**
5'
TGAAAGATTGGCCAAATTGAACCAAATCTTGAGAATCGAAGAAGAATTAGGTTCTGAAGCTAT
CTACGCTGGTAAAGATTTCCAAAAGGCTTCTCAATTGggtgctggcgcaggtgcttc 3'
Tag primer oKA 1499
5'
AGATGGGTAAAAAATTATCATTTAATTAGTTCATATATTCAAGATGTTCCTATAAAAGAAAAA
AAAGCACCAGCTTTTTTTTATTTAATCAGAGG tctgatatcatcgatgaattcgag 3'
Extension primer oKA 1513
5'
TACTTTCATTGCTGACTTGTCAGTTGGTTTAAGATCTGGTCAAATCAAGACTGGTGCTCCAGCC
AGATCTGAAAGATTGGCCAAATTGAACCAAATCTTG 3'
Extension primer oKA 1514
5'
TCACCAGGTGCTGTATCCCTTTTTCTTTGACTGCAGCTCAGTGATTAAGAGTAAAGATGGGTAA
AAAATTATCATTTAATTAGTTCATATATTCAAGATG 3'
Diagnostic PCR primer oKA 1500
5' CCACAGATCCGGTGAAACCGAAG 3'
Diagnostic PCR primer oKA 1501
5' CCGTTCATCTCTTCACCAGGTGC 3'

Figure 2.1 : Eno1 GFP Candida albicans transformation. *C. albicans has two copies of the same gene and it is thus complicated to transform. The principal of homologous recombination is that a sequence is homologous on the transformation cassette and the gene of interest and as a result the full gene sequence is replaced by the cassette. a. The diagram represents the process of tagging DNA with GFP, the plasmid used for the transformation was oKAF 54 the gene of interest was Eno1 and the tag primers used are named on the figure and their sequence is in b. Extension primers were used in combination to the tag primers for a higher rate of successful transformations. The transformation cassette includes GFP and auxotrophic marker Leucine. Successful transformants contain the*

Eno1 followed by GFP and the Leucine marker. Successful transformants contain an untagged gene and the tagged gene which is much longer in base pairs. The diagnostic PCR primers were placed at the ends of the gene and of the key cassette components. b. The sequences of all the key primers used for this specific transformation are presented here. In red is the sequence of the tag primers that was correlating to the extension primers and in green are the sticky ends of the sequence that binds to the GFP cassette.

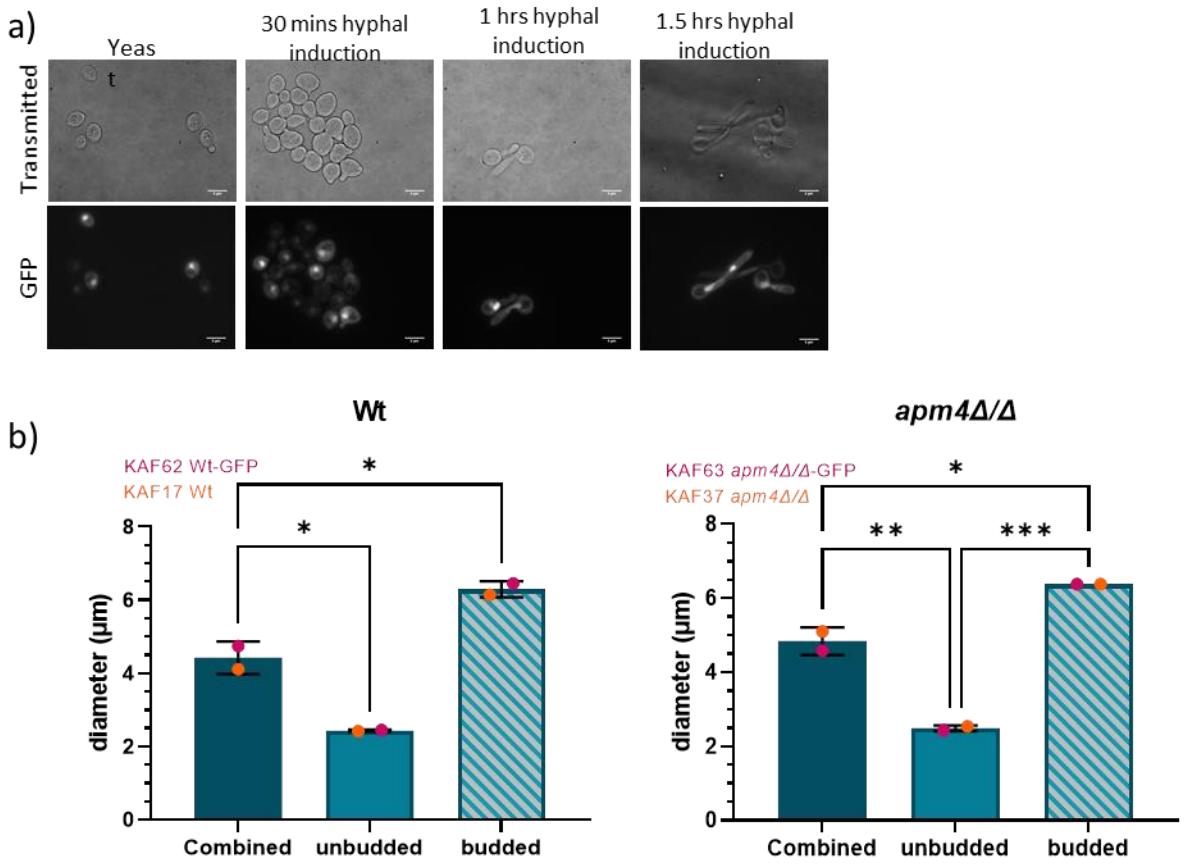

Figure 2.2: Validation of Eno1 GFP strains. *a) The images were captured at different stages of C. albicans growth. The GFP channel represents the expression of the GFP plasmid on the Eno-1 gene. The signal is localized in the cytoplasm but it is also strongly associated with the endoplasmic reticulum and the vacuoles. The signal was strong, so the cells were easily tracked during interactions with the host environment. b) The CASY counter was used to automatically count the cell size of overnight cultures refreshed for 30 minutes at 30°C b-c,*

the n =>200000. b) the mean diameter of Wt cells. c) the mean diameter of apm4Δ/Δ cells, the pink lines represent the GFP strains, and the orange strains represent the non-GFP strains used in previous investigations. There was no significant difference in the size of GFP and non-GFP strains suggesting that the mutation did not have an impact on the phenotype.

2.2.1.1.4 Genomic DNA isolation and DNA sequencing

The colony of interest was grown overnight in 5 mL of YPD + 50 mg/mL L-uridine, the cells were collected through centrifugation the next day and transferred to a 2 mL Eppendorf. The Eppendorf was span at maximum speed to remove the rest of the YPD media and then 200 µL of lysis buffer (2% Triton X-1000, 1% SDS, 100mM NaCl, 10mM Tris-HCl, 1mM EDTA at pH 8), 200 µL of phenol chloroform (Merck) and 3 g of glass beads were added to the washed overnight cells. The cells were vortexed for 3 minutes and then 200µL of TE buffer (1M Tris base at pH 8, 0.5M EDTA, double distilled water) were added and the mix was centrifuged at maximum speed for 5 minutes. The liquid phase or the top liquid that is clear after centrifugation was moved to a fresh 2 mL Eppendorf tube and 1 mL of cold 96% ethanol was added, this step was followed by another maximum speed centrifugation for 2 minutes. The supernatant was removed, and the pellet was resuspended in 400 µL of TE buffer with 3 µL of 10 mg/mL RNAse-a (Merck) and the sample was incubated for 30 minutes at 37^{o}C. 7.5M of ammonium acetate and 1 mL of cold 96% ethanol were then added to the samples, and this was followed by a 30 minute incubation in -20^{o}C. The samples were then centrifuged at maximum speed for 3 minutes and the supernatant was removed and replaced with 70% ethanol carefully to not resuspend or lose the pellet. The pellet was dried in an incubator and then resuspended in 200 µL of sterile distilled water.

Once the genomic DNA was isolated the samples were prepared then the concentration of DNA was measured on the nanodrop. The cells were diluted according to the instructions of the sequencing facility and appropriate primers were sent with the genomic DNA for sequencing. When the sequencing results were ready the cassette sequence was searched within the results to confirm a positive transformation.

2.2.1.1.5 DNA electrophoresis

The process of DNA electrophoresis involved a 1.5% agarose gel dissolved in TAE buffer (originally from a 50x stock prepared as follows: 242 g Tris base, 57.1 mL of glacial acetic

acid and 100 mL of 50OmM EDTA at pH 8.3) with 10 µg/mL of ethidium bromide. The agarose gel contains wells which were prepared by using combs when the mix was poured. Once the agarose gel the comb was removed and was placed in an electrophoresis chamber filled with TAE buffer, it was critical to have enough of the buffer solution to cover the agarose gel. When the DNA samples of interest were prepared, they were mixed with 5-10 µL of 10x DNA loading dye called Orange G prepared from 30% glycerol and 2 mg/mL Orange G. The samples were loaded inside the wells and the gel was run at 100V for approximately 30 minutes or until the loading dye ran to about 3/4ths of the gel. The DNA ladder used to determine the size of the bands was a 1 kB ladder.

2.2.2 *Cell wall staining*

2.2.2.1 Calcofluor white staining of Candida albicans

Cells from overnight cultures were added to fresh YPD + 80 µg/mL L-uridine media and incubated at 30^{o}C 200 x g for 4 hours or alternatively overnight cultures were used for the staining. After the incubation cells were collected and washed 3 times with PBS. The cells were resuspended in 1 mL of PBS and 1 µL of a stock 1 mg/mL of Calcofluor white (CFW) (Merck) was added to the suspension. The cells were incubated at room temperature for 5 minutes and then 2 µl of the stained cells were added to a slide and were sealed using a cover slip and nail paint. The samples were imaged at 150x on a fluorescent microscope for DIC and DAPI. The DAPI exposure was set to 100 ms. 100 cells from 3 independent experiments were analyzed for integrated intensity in FIJI. The cell periphery was hand drawn and the intensity was measured by the software. The results were then processed in Prism. Descriptions of the imaging and analysis of the cells are in section **2.5**.

2.2.2.2 Fc-Dectin staining for exposed β-glucan

Overnight cultures of *C. albicans* were inoculated at a 1:200 ratio in fresh YPD + 80 µg/mL L-uridine and incubated for 4 hours at 30^{o}C 200 x g. After the incubation the cultures were centrifuged at 1000 rpm for 3 minutes, the cells were resuspended in 1 mL of 4% PFA for 30 minutes and were kept on ice. After the fixation step cells were washed 3 times with PBS and resuspended in 5 µg/mL of Fc-Dectin from a stock of 2 mg/mL kindly donated by Prof. Gordon Brown's lab. The cells were incubated with the primary Fc-Dectin for 1 hour on ice. After the primary incubation cells were washed 3 times with freshly made FACs buffer (0.5%

bovine serum albumin, 5mM EDTA, 2Mm Na azide in PBS) and then resuspended in a 1:200 suspension of the secondary antibody anti-human IgG conjugated with Alexa-Fluor 488 (Jackson Immuno Research Laboratories) suspended in FACs buffer. The final concentration of the antibody was 1.25 µg/mL. The cells were incubated for 45 minutes on ice in the dark. Once the incubation step was over the cells were washed 3 times with FACs buffer before they were imaged on a glass slide on a fluorescent microscope. The microscope was set up at 150x magnification and the channels imaged were DIC and GFP. The GFP exposure was set to 100 ms per sample. The images from 3 independent experiments were analyzed for the Integrated intensity per cell on the GFP channel. The analysis was carried out using FIJI software, a line was drawn around the cell periphery and the integrated intensity was quantified by the software. Descriptions of the imaging and analysis methods are in section **2.5**.

2.2.3 Quantification of the phenotype

2.2.3.1 Quantification of the budding patterns

Observations from cultures

Overnight cultures of the cells were added to fresh YPD in a 1:100 ratio, the absorbance at 600nm was approximately 0.1 abs. Cells were incubated at 30^{o}C at 200 x g for 8 hours. Every hour 1 mL of culture was collected to measure the OD_{600} and for microscopy. Using a light microscope 1 µL of cells was assessed for the phenotype. The percentage of cells in yeast and budding morphology was calculated for each strain. Records of cells with more than 1 budding site and with a daughter cell of equal size as the mother cell were collected. The data were analysed as a proportion using the Prism software.

CASY^{TM} counter

The overnight cultures were diluted 1 in 10 in the CASYton (Roche), the cultures were sampled for the following sizes 0.75 to 15 µm to capture all the cells. Based on the histogram produced by the counter we took 2 more measurements 0.75 to 3.75 µm and 3.75 to 15µm. The number of cells in the budded site of the histogram was compared to the overall number of cells to estimate the percentage of cells budding.

2.2.3.2 Measurements of cell size

Yeast cells were prepared and imaged as described in section **2.2.1.2.1** and the images were then analyzed to determine the size of yeast cells. The FIJI software was used for analysis of the cell size. The microscope settings provided a scale for the image size which was input on the FIJI software. The cell size data were collected as follows, using the FIJI software lines were drawn across the entire cell vertically and diagonally, then vertical and diagonal lines were drawn for each bud of the cell. FIJI software calculated the lengths for these distances. The collected data were analyzed for overall cell width and length. The data were also analyzed for the size of the buds. There was a comparison between the size of mother cells and the size of the buds. The data are presented in the results section.

The CASY^{TM} counter was also used for measurements of cell size. The overnight cultures incubated in fresh YPD at 30^{o}C for 30 minutes and then were diluted 1 in 10 in the CASYton, the cultures were sampled for the following sizes 0.75 to 15 µm to capture all the cells. Based on the histogram produced by the counter we took 2 more measurements 0.75 to 3.75 µm and 3.75 to 15µm. The average diameter of cells overall and at the two peaks was measured by the counter.

2.2.3.3 Agar invasion assay

YPD agar at different percentages (1, 2 and 4%) was melted and cooled down to ensure the *C. albicans* cells that will be added to the agar would not burn. Overnight cultures of *C. albicans* were diluted 1 in 1000 using PBS. Cooling the agar involved pouring into 50 mL falcons 25 mL of agar and mixing it constantly until the agar was cool enough with no condensation and cool to the touch. Once the agar was cool 10 µL of the *Candida* dilution were added and the mix was poured in Petri dishes. The Petri dish was incubated for 48 hours at 30^{o}C. Images of colonies were captured using a stereomicroscope. The stereomicroscope captured Z stacks and then created maximum intensity projection of each colony.

2.2.4 Growth assays

2.2.4.1 Growth on media with different carbon sources

Media

The media used for these experiments were the following: lactate media (YNB without amino acids + 2% D/L lactate + 80 µg/mL L-arginine + 80 µg/mL L-uridine + 80 µg/mL L-histidine), amino acid rich media (YNB without amino acids + 80 µg/mL L-arginine + 80 µg/mL L-uridine + 80 µg/mL L-histidine), glycerol media (YNB without amino acids + 2% glycerol from a 100% stock + 80 µg/mL L-arginine + 80 µg/mL L-uridine + 50 mg/mL L-histidine), NGY media (0.1% peptone + 0.4% glucose + 0.1% yeast extract + 80 µg/mL L-arginine + 80 µg/mL L-uridine + 80 µg/mL L-histidine) and YPD (2% peptone + 2% glucose + 1% yeast extract + 80 µg/mL L-arginine + 80 µg/mL L-uridine + 80 µg/mL L-histidine). 1.5% agar of all the media was used for this experiment.

Growth on agar plates

Overnight cultures of KAF 17 and KAF 37 were refreshed in YPD + 80µg/mL L-uridine media and incubated at 30°C 200 x g for 3 hours. After the incubation OD_{600} was counted and the aim was for the absorbance to be approximately 0.5 abs so the cultures were diluted accordingly. The cultures were diluted 1:10 for 5 series of dilution. A volume of 5 µL per dilution per strain was spotted on the different media conditions. The plates were incubated for 24 hours at 30°C and 37°C, images of growth were then captured. The results are from 2 independent experiments.

2.2.4.2 Growth on different pH conditions

Medium 199 (Invitrogen) was prepared according to the manufacturer's instructions and the pH was altered to the following pH conditions pH 4, 5, 6 and 7. Overnight cultures of *Candida* cells were washed once with PBS and 200µL of cell culture was added into 50 mL falcons with 10 mL of medium 199 media. Cells were incubated for 24 hours at 30°C 200 x g. OD_{600} was measured at different time-points (0, 4, 8, 10 and 24 hours). The absorbance at each time point were plotted to determine the growth rate of each condition.

2.3 Infection of mammalian cells with *C. albicans*

2.3.1 Response to interactions with Macrophages

2.3.1.1 Phagocytosis of Candida albicans *by J774 macrophages*

An 80% confluent flask of J774 macrophages was detached from the flask, cells were counted and a cell suspension of $1x10^6$ cells/mL of J774 macrophages was created. 1mL of the cell suspension was added on a sterile glass coverslip inside a 24-well plate and incubated overnight in serum containing DMEM media (Gibco) (section 2.1.b). The next day *Candida* overnight cultures were inoculated in fresh YPD + 80µg/mL L-uridine media and incubated for 30 minutes at 30°C 200 x g. The cultures were then washed 3 times with PBS before the cell number was counted. A *Candida* cell suspension of $1x10^7$ cells/mL was created. The macrophages were washed and fresh, serum free DMEM media was added to each. The macrophages were incubated with the *Candida* cell suspension, the macrophage to *Candida* ratio of 1:10. Cells were incubated 30 minutes in a 37°C incubator with 4% CO_2. After the incubation the cells were washed with PBS and 1 mL of 4% PFA (Thermo Scientific) was added to each well. The culture with 4% PFA was incubated at room temperature for 10 minutes. At the end of the incubation cells were washed 3 times with PBS and 3 times with distilled water. The coverslip was removed from the 24-well plate and 6 µL of Mowoil oil was added before the coverslip was placed on a glass slide. The next day the slides were imaged on a widefield fluorescence microscope. The microscope was set at 60x magnification and was capturing a Z stack distance of 10 µm slicing at every 1 µm. The images were analysed to determine the percentage of macrophages that contained Candida and the number of *C. albicans* cells per macrophage, the process was manual and the NIS Elements software was used for visualization of the images.

2.3.1.2 Macrophage timelapse experiments for hyphal switch and proliferation

Cells from an 80% confluent J774 T-75 flask were detached the day before the experiment. The cells were counted and a cell suspension of $5x10^4$ cells/mL in serum containing DMEM was produced. 1 mL of cell suspension was added in each well of a plastic 24-well plate and incubated for 24 hours. On the day of the experiment 5 µL of cresyl violet dye was added to each well and incubated for 2 hours at 37°C with 4% CO_2. Overnight *Candida* cultures were incubated with fresh YPD + 80µg/mL L-uridine at 30°C 200 x g for 30 minutes and then washed twice with PBS. The *Candida* cells were counted and a cell suspension of $5x10^4$

cells/mL was prepared. At the end of the 2-hour incubation of macrophages with cresyl violet the cells were washed 3 times with serum-free DMEM. After the preparation of the macrophage and *Candida* cells the microscope was setup; the microscope chamber was warmed up to 37°C with 4% CO_2 and 80% air. The samples were imaged at Phase 20x on a widefield fluorescent microscope. Each condition was imaged at 4 different spots within the well and the perfect focus system was applied. The microscope was capturing images every 10 minutes for 18 hours. At the end of the timelapse experiments the data were analysed for different parameters as described in section **2.5**.

The timelapse experiments with yeast locked strains had some alterations in the overall methodology as the experiments with TT21 and NRG1^{oex} did not contain any cresyl violet staining but the rest of the protocol was unchanged. The increased temperature timelapse experiments had a small alteration as the microscope chamber was maintained at 38.5°C instead of 37°C.

2.3.1.3 Cell wall staining of Candida albicans *cells inside the phagosome*

J774 cells from an 80% confluent T-75 flask were seeded on a 96-well plate at the cell number 5x10^4 cells/mL and incubated for adherence overnight at 37°C with 4% CO_2. The plate media was discarded the next day and replaced with serum free DMEM. Cells from the overnight cultures of KAF 19 and KAF 59 were inoculated into fresh YPD + 80µg/mL L-uridine broth at a 1:200 ratio and incubated for 30 minutes at 30°C 200 x g. After the incubation the cells were washed 3 times with PBS and a cell suspension of 5x10^4 cells/mL was created. The macrophage cultures were infected with *Candida albicans* at a 1:1 ratio for different timepoint 30 minutes and then were fixed with 4% PFA for 10 minutes. The cells were permeabilized with 40 µL per well of 0.25% Triton X 1000 for 3 minutes. After the permeabilization step the cells were washed 3 times with PBS and then 40 µL of 5 µg/mL of Fc-Dectin (stock 2 mg/mL) suspended in PBS was added to each well. The cells were incubated on ice for 1 hour and then washed 3 times with freshly prepared FACS buffer (0.5% FBS, 5 mM EDTA, 2mM sodium azide in PBS). A volume of 40 µL of 1:200 AlexaFluor 488 suspended in FACS buffer to a final concentration of 1.25 µg/mL was added to each well. The plate was then incubated for 45 minutes in the dark on ice. At the end of the incubation the wells were washed twice with PBS and incubated on ice with 1:400 Phalloidin

conjugated with AlexaFluor 568 (Invitrogen) for 1 hour. The cells were washed before staining with 1 µg/mL of Calcofluor white for 5 minutes. The wells were washed with PBS and imaged using an automated fluorescent microscope. The images were captured at 40x magnification using the DAPI, Texas Red and GFP channels set to a constant exposure and laser power. The data from the images were then collected using the FIJI software by manually drawing around the *Candida* cell periphery to measure using the software the integrated intensity for each channel. The controls for these experiments were cells that were not incubated with macrophages and cells which were incubated with macrophages but not phagocytosed.

2.3.1.4 Prediction of the phagolysosomal pH using the Lysosensor Yellow/Blue stain

The lysosensor Yellow/ Blue (Invitrogen) predicts the pH of a phagosome based on the emission thus it was critical to calibrate the samples. J774 cells from a confluent flask were seeded as $5x10^4$ cells/mL in a glass bottom 96-well plate (Greiner Biolabs) the day before the experiment. The cells attached overnight to the wells. On the day of the experiment the cells were refreshed with serum free DMEM media and were prepared for the different conditions of the experiment.

The macrophages were infected with non-fluorescent *C. albicans* strains KAF 19 and KAF 59, the control for the experiment were macrophages in serum free media. Overnight cultures of Candida albicans were washed 3 times with PBS and counted. A cell suspension of $5x10^4$ cells/mL was created and the cells were used to infect cells at different time points (1 hour, 2 hours, 3 hours, 4 hours, 6 hours and 8 hours). Before the incubation was over the Lysosensor Yellow/Blue dye was thawed and centrifuged quickly to separate the DMSO (Sigma) from the dye. At the end of the incubation 1 µL of the dye was added to 200 µL of the media to a final concentration of 5 µg/mL. The cells with the dye were incubated in the 37^{o}C with 4% CO2 incubator for 5 minutes. At the end of the staining the media were removed and replaced with 4% PFA to fix the samples for 10 minutes. The cells were washed 3 times with PBS before being resuspended with PBS and imaged. If the imaging could not happen at the time the plates were stored at 2^{o}C in the dark.

Two different methods were used for imaging and analysis of these experiments. The experiments were either imaged manually using a widefield fluorescent microscope set at

20x or an automated fluorescent microscope at 20x. The imaging with both microscopes captured GFP and DAPI set at a constant exposure and laser power. The manual imaging data was collected by manual analysis of the images using FIJI software. The periphery of macrophages was manually traced and the software collected the integrated intensity values of cells. The data from the automated microscope were collected automatically by programming the ImageXpress software to recognize macrophages and tracing the periphery based on the stain and to finally collect the integrated intensity in each channel. The analysis of the data was the same for both imaging techniques. The average integrated fluorescence intensity from each replicate was plotted for each replicate to compare the groups.

2.3.2 Interactions with the CACO-2 monolayer

2.3.2.1 CACO-2 staining

CACO-2 cells from the infection experiments were fixed for 10 minutes with 4% PFA + 1:2000 Hoechst or 1:1000 DAPI at the end of the experiment. The volume of solutions depended on where the experiment was taking place for 96-well plate 40 µL per well was used, 24-well plate 200 µL per well and 384-well plate 50 µL per well. After the fixation step the PFA solution was removed and cells were permeabilized in 0.25% of Triton X 1000 for 3 minutes if the experiment was a monolayer and 5 minutes for the gut-on-chip infections. After the permeabilization cells were washed 3 times with PBS before 1:400 Phalloidin conjugated with AlexaFluor 568 (Invitrogen). The cells were incubated for 1 hour in the dark and were shaking for even suspension on a rocker. After the Phalloidin stain cells were washed 3 times and PBS and resuspended in PBS in the maximum volume for each well. The plates were stored in the dark at 2°C until they were imaged.

2.3.2.2 Monolayer infection for invasion

Once the cells from a seeded monolayer in a glass-bottom 96-well plate were confluent and adhered the experiment begun. The media of the monolayer were discarded and 100 µL DMEM-Glutamax (Gibco) without FBS (Gibco) and P/S (Fisher Scientific) were added to the cells. The cells were incubated at 37°C with 4% CO_2 for 2 hours before the experiment started to ensure that they adjusted to the new environment. A 1 mL volume of overnight cultures of KAF 62 and KAF 63 was added to Eppendorf tubes and washed 3 times with PBS.

The cells were then diluted 1:100 so that the counting using the hemocytometer was more reliable. The cells were prepared at varying cell concentrations so different solutions were made. Once the monolayer and the *Candida* were ready for the experiment, the monolayer was infected with the appropriate cell number. The plates were incubated at 37^{o}C with 4% CO_2 for 24 hours and 48 hours. At the end of the incubation cells were fixed and stained as described in section **2.3.2.1**. The cells were then imaged using the Nikon A1 confocal, the microscope was set up to 40x magnification capturing DAPI, GFP and AlexaFluor568. Z stack sections were captured according to NIS software recommendations. The stack's top and bottom were defined based on the phalloidin staining. The images were analyzed for invasion using the FIJI software.

The invasion was quantified based on the staining for transcellular and paracellular invasion. The percentage of cells from a Z slice that were through and on top of the monolayer were quantified for the percentage of cells invading.

2.3.2.3 Infection of the CACO-2 monolayer to assess adhesion

Once the cells from a seeded monolayer on glass coverslips inside a 24-well plate were confluent and adhered well the experiment begun. The media of the monolayer were discarded and 1 mL DMEM-Glutamax without FBS and P/S was added to the cells. The cells were incubated at 37^{o}C with 4% CO_2 for 2 hours before the experiment started to ensure that they adjusted to the new environment. A 1 mL volume of overnight cultures of KAF 62 and KAF 63 was added to Eppendorf tubes and washed 3 times with PBS. The cells were then diluted 1:100 so that the counting with the hemocytometer was more reliable. The cell solution prepared contained 1x10^{6} cells/mL. Once the monolayer and the *Candida* were ready for the experiment, the monolayer was infected with the appropriate cell number. The plates were incubated at 37^{o}C with 4% CO_2 for 1 hour. At the end of the incubation the monolayer media with *Candida* cells were removed and the wells were washed 3 times with PBS before being fixed and stained as described in Section **2.3.2.1**. At the end of the staining process the coverslips were removed carefully from the wells using tweezers and were placed on glass slides on top of 2 µL of Mowoil. The coverslips were gently pushed down to avoid bubbles and then kept at room temperature in the dark overnight before imagining. The slides were imaged on a widefield fluorescent microscope at 60x magnification

capturing GFP and Cy3, 100 randomized fields of view were captured per slide. The number of cells in each image was counted and recorded in a spreadsheet. For the analysis it was critical to know the area of the field of view which was 0.006 cm and the size of the coverslip 19.1 cm, these numbers indicated that there were about 2963.25 fields of view within each coverslip. It was also critical that the initial number of cells added was known. The calculations assumed that the slide had an even distribution of *Candida* cells, the number of cells from the 100 field of views per strain was averaged to estimate the average number of cells in a field of view. Assuming even distribution the average number of cells in a field of view was multiplied to the number of field of views that fit within the coverslip of these dimensions. These calculations provided an estimation of the number of cells adhered to the slide. The predicted number of cells was then calculated as a percentage to the initial number of cells added. The results were analyzed using the Prism software.

2.3.3 Interactions with the gut-on-chip model

2.3.3.1 Gut-on-chip leakage assay

Once the OrganoPlate was considered ready to use for experiments but before the infection occurred it was critical to test the integrity of the plate so a leakage assay was performed. A solution of 25 mg/mL of FITC-dextran (SLS) in culture media was prepared and the media from both inlets and outlets of the OrganoPlate were removed. The media were replaced with 20 µL of culture media in the bottom inlets and outlets and 40 µL of FITC-dextran solution on the top inlets and outlets. The plates were immediately imaged on the InCell microscope which was capturing automated images in the FITC channel every 5 minutes for an overall period of 20 minutes at a 4x magnification. If the culture was not leaky then experiments were performed. To remove the FITC-dextran from the OrganoPlate the media was discarded and replaced by infection media DMEM-Glutamax + 1% FBS + 1% P/S, the overall volume added per well was 50 µL.

2.3.3.2 Gut-on-chip invasion assay

Overnight cultures of KAF 62 and KAF 63 were washed 3 times with PBS and then the cell number in each culture was measured using a hemocytometer. Cell suspensions of different cell concentrations in the infection media were created. Once the gut-on-chip was not leaky and the gut-on-chip wells were in the infection media described in section **2.3.3.1**, *C.*

albicans cell suspensions of different concentrations replaced the media in the top inlet of the chip. The OrganoPlate was then incubated inside a 37°C incubator with 4%CO_2 and placed on a perfusion rocker set at a 7° angle with 8 minutes interval between each side for 24 hours. At the end of the experiments the cells were fixed and stained as described in section **2.3.2.1**. The plates were imaged using the A1 Nikon confocal at 40x magnification set to capture the DAPI (Sigma), AlexaFluor 568 (Invitrogen) and GFP channels. Z-stacks were captured slicing according to the NIS software recommendations. The images were then analyzed using the FIJI software for invasion.

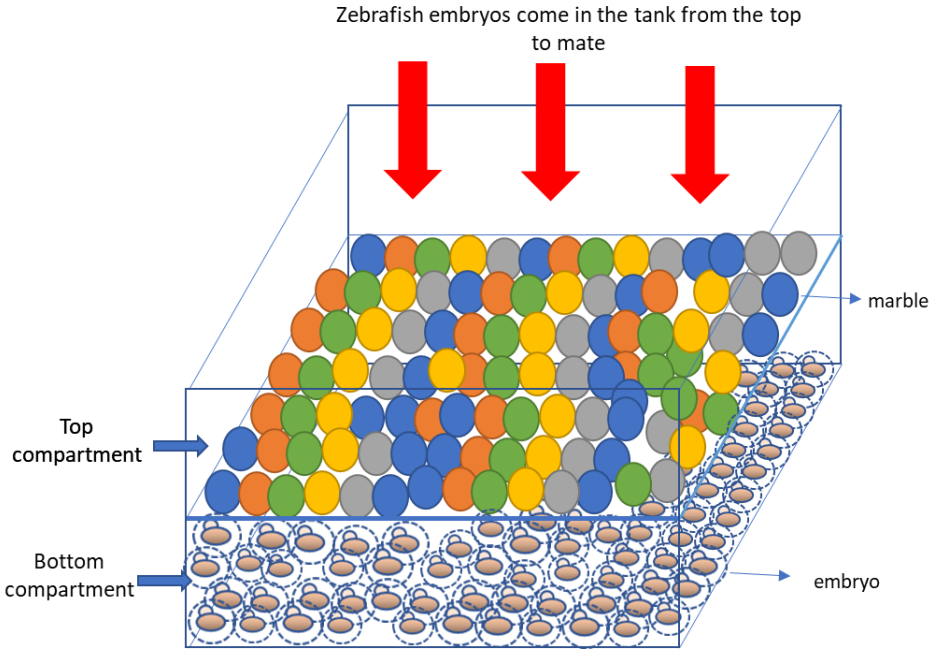

Figure 2.3: The zebrafish marbling tank. *The marbling tank is composed of two compartments separated by a stainless-steel net, the top compartment is composed of marbles. Zebrafish like the marbles and thus come into the tank to mate and release eggs which are fertilized. The zebrafish eggs go through the net into the bottom compartment which collects the embryos. The marbling tank bottom compartment protects the embryos from being eaten by adult dish. The marbling tank is placed in the zebrafish tanks in the aquarium and removed after the mating is complete.*

2.4 Zebrafish handling and infection experiments

2.4.1 Zebrafish breeding and handling

The zebrafish embryos used in the experiments were not allowed to reach further than 5.2 days post fertilization (dpf) when they come into production by the UK Animals in Scientific Procedures Act 1986. The zebrafish lines used in the experiments are Nacre embryos (do not have stripes and are transparent), embryos with fluorescent blood vessels *Tg(kdrl:mCherry)is5* referred to as KDRL from further on and embryos expressing fluorescent IL-1β *TgBAC(il1b:eGFP)sh445* referred to as IL-1β GFP.

2.4.1.1 Zebrafish marbling

A tank of adult zebrafish was selected for breeding. The tank selected should not have been used for breeding in the past two weeks. A marbling tank with two compartments, a top compartment covered in a full layer of marbles with a sieve so that the embryos will drop to the bottom compartment where embryos will be stored was added to the selected tank of adult zebrafish on the afternoon (figure 2.3). The early on the next day at the beginning of the zebrafish light cycle the marbling tank was removed from the zebrafish tank. The top compartment with the marbles was washed with aquarium water, at that point the bottom compartment contained all the embryos. A sieve was used to transfer the embryos from the bottom compartment of the marbling tank to a fresh petri dish which was filled with aquarium water. Before the transfer the embryo whilst in the sieve were washed with aquarium water to remove any dirt. The zebrafish were then ready to use and were incubated at 28.5^{o}C in an incubator with an automatic light cycle for 14 hours and a dark cycle for 10 hours.

2.4.1.2 Zebrafish embryo sorting according to the developmental stage

The embryos that were collected after breeding needed sorting into fresh petri dishes with 60 zebrafish embryos each in 1x E3 water (5 mM NaCl, 0.17 mM KCl, 0.33 mM $CaCl_2$, 0.33 mM $MgSO_4$ and in uninfected embryos 10^{-5}% Methylene Blue). All the zebrafish that were used in each experiment needed to be of a similar developmental stage, so the most prevalent developmental stage of the breeding was selected. Using a Pasteur pipette under a dissecting microscope the zebrafish were collected from the breeding plate and placed into fresh petri dishes with E3 water. The embryos were then incubated at 28.5^{o}C in an

incubator with an automatic light cycle for 14 hours and a dark cycle for 10 hours. The embryos were incubated until there was a need to be used for experiments.

Figure 2.4: Zebrafish embryo developmental stages. *The image includes the different developmental stages of zebrafish embryos before the 1dpf stage. The sorting of embryos was executed in reference of this diagram from* BioRender.

2.4.1.3 Zebrafish embryo dechorionation

Zebrafish embryos naturally dechorionate between 2-3 dpf but most of the experiments took place before that developmental stage. Early in the morning of the experiment and after 1 dpf the chorions were manually removed using dechorionation forceps which were very thin and sharp. Once the dechorionation was complete for a plate the chorion debris

and damaged zebrafish were removed. The embryos were then incubated at 28.5°C for at least 3 hours before the experiment started.

2.4.2 Zebrafish infections to monitor the virulence

2.4.2.1 Zebrafish injections in the caudal vein and the duct of Cuvier

2.4.2.1.1 Materials

E3 agar plates, dechorionated zebrafish, washed overnight cultures of *C. albicans*, pulled needles (World Precision Instruments) pulled using an electrode puller (heat 380, pull 200, velocity 199, time 200, pressure 500), forceps for needle breaking, PVP + 20% Phenol Red (Sigma), Tricaine, petri dishes, needle loading tips, E3 water without Methylene Blue, dissecting microscope and an injection rig.

2.4.2.1.2 *Candida albicans* preparation

Overnight cultures of *C. albicans* of the desired strain were used for the injections. 1 mL of the overnight culture was transferred to a sterile 1.5mL Eppendorf tube and washed 3 times with PBS. The cell number was then counted using a hemocytometer, a calculation was used to estimate the volume of PBS that would be required to get the culture to have 1000 colony forming units (cfu). The washed cells were collected by centrifugation and resuspended in the calculated volume of PBS. Through proportion calculations the cfu was adjusted to the desired cfu that was for example 500 cfu for survival assays. The cfu was adjusted using the PVP + 20% Phenol red solution, the solution was important as it ensures that cells wouldn't be very sticky and that a successful injection would have been easy to identify.

2.4.2.1.3 Injections in the Caudal vein and the Duct of Cuvier

A prewarmed E3 agar plate was required, the zebrafish needed to develop enough for the injection. The caudal vein and the duct of Cuvier injections are both injections into the bloodstream, the caudal vein was easier to inject 1 dpf and the duct of Cuvier was easier to inject at 2 dpf. The *C. albicans* cultures prepared were thoroughly mixed and 7 µL were loaded into a needle using the loading tips. The needle was then loaded to the injection rig and with the dissecting microscope. The tip of the needle was the point of focus using forceps the tip of the needle was broken so that it had an angle on one side and was sharp. The needle needed to be small enough to inject into the zebrafish but not too small that the

Candida cells would not be injected. Once the needle was broken the droplet size was measured using a 10 mm graticule and adjusted to fit within 2 lines of the graticule. The number of cells in each droplet was counted. The zebrafish plates were anesthetized using tricaine for at least 2 minutes before being used. The E3 agar plate was used to load anesthetized embryos using a Pasteur pipette, when adding the zebrafish to the plate it was important to remove any excess moisture and to ensure that the zebrafish were on their side with their tail flat for both types of injections. Before injecting the zebrafish, the number of cells in each droplet was counted again on the agar plate and adjusted accordingly. The area of the zebrafish that was the injection point was focused on (figure 2.5) using the dissecting microscope and was injected with the cfu that was required for the experiment. The number of cells that was in each droplet was counted every 2-4 zebrafish. The successful injections were easily identified as the dye was not in the bloodstream, those zebrafish were marked on their yolk and removed later from the samples. When the zebrafish on the plate were injected E3 water without Methylene Blue from a fresh petri dish was used to transfer the embryos into the dish. The embryos were then sorted and the unsuccessful injections and the damaged zebrafish were removed. Once the number of zebrafish per group was the one required by the experiment and the power calculations, the next injection group was injected. The control for the injections was clear PVP + 20% Phenol red.

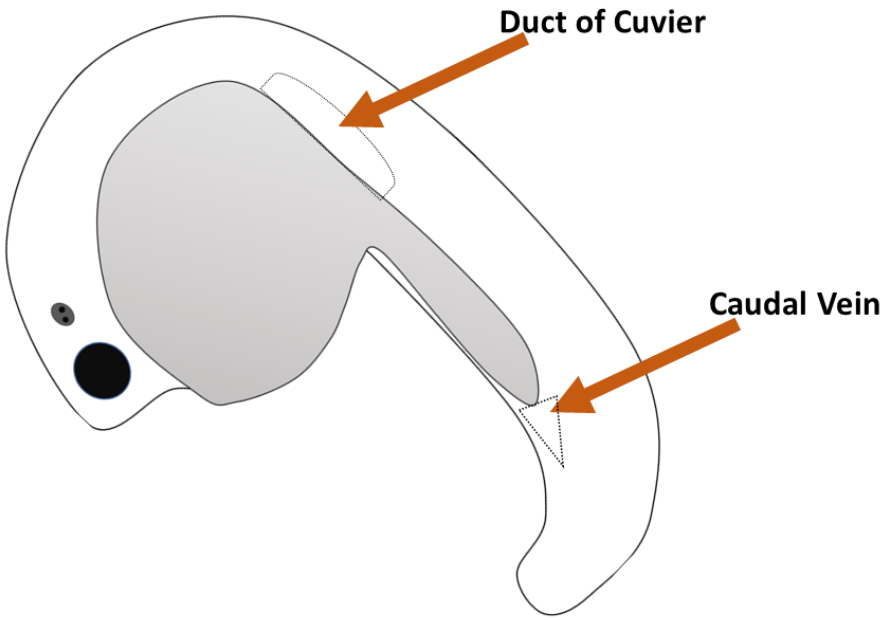

Figure 2.5: The zebrafish injection sites. *The diagram illustrates a zebrafish embryo, and the arrows point onwards the two major injection sites used in this study.*

2.4.2.2 The zebrafish survival curves

The zebrafish for survival curves were injected as described in section **2.4.2.1**. The zebrafish embryos were injected at 1 dpf in the caudal vein with 500 cfu of *C. albicans*. The n number for each injection group was 30 embryos per replicate, the number of biological replicates was 3. The zebrafish survival was monitored up to 4 dpi and the number of deaths was recorded every 24 hours. The death of a zebrafish was determined by cessation of heartbeat. The survival data were imported in Prism and survival curves were created for each replicate; the statistical test used was the Mantel-Cox survival test. At the end of all the experiments the data from each replicate were compared and if there was no statistical difference between the replicates the results of all the replicates for individual zebrafish were integrated for a survival curve where the n number for each group was n= >90.

2.4.b.c Survival studies of zebrafish with depleted macrophages

Zebrafish embryos sorted and dechorionated as described in sections **2.4.1**. The zebrafish were injected into the caudal vein at 1 dpf with the methodology described previously however instead of injections with *C. albicans* zebrafish were injected with the clodronate liposome. The clodronate depletes macrophages and the PBS liposome was used as the control. A volume of 3 µL of well mixed clodronate solution or PBS liposome was loaded onto a needle and using a graticule it was calculated so that 1 nL of the solution was injected in each embryo through the caudal vein. There was no phenol red solution added in these injections, but it was obvious whether the injection was successful due to the dark color of the solution. Successfully injected zebrafish embryos were incubated overnight at 28.5^{o}C. The next day early in the morning 2 dpf embryos were injected with 200 cfu of KAF 62 and KAF63 through the duct of Cuvier, the zebrafish were then used to monitor survival and burden. The processes of injection, monitoring survival and studies for fungal burden through microscopy used were like the ones described in sections **2.4.3** and **2.5**.

2.4.3 Assays with infected zebrafish embryos

2.4.3.1 Zebrafish embryo mounting

The embryos used for imaging were positioned onto the imaging plate in a process called mounting. 1% of low melting agarose (Sigma) was melted with E3 water without Methylene Blue and incubated so that it is warm enough to not set but not too warm to harm the embryos. The zebrafish were anesthetised using tricaine, the excess water was removed, and a few drops of low melting agarose were added before the agarose was set the zebrafish embryos were positioned in the imaging plate using a loop or a needle loading tip. Once the zebrafish were in position and the agarose set the zebrafish embryos were imaged.

2.4.3.1 Studies for the zebrafish fungal burden

2.4.3.1.1 Method of burden quantification using fluorescent pixels

Zebrafish injected with 100 cfu of KAF 62 and KAF 63 were used for imaging. The zebrafish were placed in a 96 well plate and were imaged daily up to 3 dpi, it was important to label and know the zebrafish as the burden in each zebrafish was monitored over time. The zebrafish embryos were mounted so that they had the appropriate position in the 96 well

plate. A glass bottom 96 well plate was used for 10x imaging of embryos and a plastic 96 well plate was used for 2x imaging of the embryos. The microscope settings for laser power and exposure were constant through each experiment. The microscope was capturing at the DIC and DAPI channels, Z stacks were captured for the zebrafish imaged at 10x. The maximum intensity projections of the Z stacks and the images of zebrafish were analysed using the FIJI software after a threshold was set for the GFP channel. Analysis was carried out by drawing around the perimeter of the zebrafish and quantifying the integrated intensity. The results were normalised to uninfected zebrafish from the same experiment. The results were analysed in the Prism software using a one-way ANOVA statistical test.

2.4.3.2.2 Method of fungal burden quantification by counting the number of colonies

Zebrafish infected with 100 cfu of KAF 62 and KAF 63 and were used to study the fungal burden. Zebrafish were lysed using Liberase enzyme at 0, 1, 2 and 3 dpi. The zebrafish were anesthetised and transferred to 1.5 mL Eppendorf tubes individually. In the individual tubes a final volume of 98.5 µL of ice-cold PBS was added with 1.5 µL of Liberase enzyme (Roche – SLS) (2.5mg/mL). The tubes were incubated for 15 minutes on a heat-block at 37^{o}C. At the end of the incubation the embryo solution was mixed using a 1000 µL pipette tip and then a 200 µL pipette tip. The embryo solution was placed on the heat-block for another 15-minute incubation and then mixed again; the process is repeated until the embryos are fully lysed. Once the embryos are lysed the Eppendorfs were placed on ice and 100 µL of FBS, this made a 1:2 dilution of the solution. The embryo solution was diluted accordingly and then 20 µL were added onto dry YPD plates with antibiotics. The YPD plates contained 40 mg/mL Gentamycin (Fisher Scientific), 135 µg/mL Penicillin G (Merck) and 10 mg/mL Penicillin/ Streptomycin (Thermo Scientific). The plates were incubated at 30^{o}C for 2 days before the number of colonies was counted to estimate the fungal burden of the embryos.

2.4.3.3 Injection of IL1-β GFP zebrafish

Zebrafish confirmed for the expression of IL1-β GFP were breed and infected with 100 cfu of KAF 19 and KAF 59. The zebrafish were mounted and imaged on a glass bottom 96 well plate. The embryos were imaged at 10x using a Z stack, for DIC and GFP. The microscope settings were constant for each experiment. There were 3 biological replicates with the n=10 per experiment. The maximum intensity projections of the Z stacks images were

analysed using the FIJI software. The analysis was manual, the zebrafish perimeter was outlined, and the software was quantifying the integrated intensity. The results were normalised to uninfected zebrafish from the same experiment. The results were analysed in the Prism software using a one-way ANOVA statistical test.

2.4.3.4 Injection of KDRL-mCherry zebrafish and dissemination timelapse experiments

Adult zebrafish confirmed for KDRL-mCherry expression were mated and the embryos were injected at 1 dpf with 100 cfu of KAF 62 and KAF 63. The infected zebrafish embryos were allowed 1-2 hours of recovery before being mounted on 96 well plates in 1% low melting agarose and prepared for microscopy as in section **2.4.3.1**. The embryos were then screened using the widefield fluorescent microscope to choose the brightest zebrafish for both the mCherry channel which stained the zebrafish blood vessels and the GFP channel for the *C. albicans* cells. The head to mid-body of the embryos were imaged using a Z-stack slicing every 3 µm and covering the distance of the entire embryo. The timelapse was capturing images every 7 minutes for up to 18 hours of interaction.

2.4.3.5 α-Nitrotyrosine staining of zebrafish embryos

Nacre Zebrafish embryos at 1 dpf were injected with 500 cfu of KAF 62 and KAF 63, as a control zebrafish were injected with PVP + 20% Phenol red. At 1 dpi about 10 zebrafish embryos per group were fixed in an Eppendorf tube with 4% PFA (Thermo Scientific) overnight at 4^{o}C. The next day PFA was removed, and the embryos were washed twice for 2 minutes with PBS-Tween (Sigma) (1:200 dilution of 20% Tween20), this step was followed by 4 washes of 5 minutes with 1 mL of PBS-0.4% Triton X. The samples were washed using a rocker. The washing steps were followed by a 30-minute incubation of the samples with 1 mL of 10 µg/mL Proteinase K (Sigma) diluted in PBS-0.4% Triton X (Sigma), the incubation was on a rocker at room temperature and then the samples were washed 4 times for 10 minutes using PBS- 0.4% Triton X. The embryos were blocked for 2 hours on a rocker using 1 mL of 5% Sheep Serum (Stratech) diluted in PBS-0.4% Triton X. After the blocking step 100-200 µL of the 1:250 dilution of the α-nitrotyrosine antibody (Millipore) in 5% Sheep Serum diluted in PBS-0.4% Triton X were added. The samples were incubated overnight at 4^{o}C on an orbital shaker. The next day the primary antibody was washed 4 times every 10 minutes in 1 mL of PBS-0.4% Triton X before blocking for 1 hour at room temperature with 5% Sheep

Serum diluted in PBS-0.4% Triton X. After the blocking 200 µL of 1:500 GAR secondary antibody (Molecular Probes) in 5% Sheep Serum diluted in PBS-0.4% Triton X were added to the samples and then they were incubated for 2 hours at room temperature in the dark. When the incubation with the secondary antibody was complete the samples were washed 4 times every 20 minutes with PBS-0.4% Triton X and then fixed again with 4% PFA in 0.4% Triton X for 20 minutes at room temperature. At the end of the second fixation step the samples were rinsed with PBS-0.4% Triton X and then were kept in the dark suspended to PBS-0.4% Triton X until imaging. For the imaging step the fixed embryos were mounted on imaging plates and were imaged using the 40x water lens of the confocal. The microscope was set up for the GFP and the Far-Red channels with the focus of the image being a 3 µm Z stack of the caudal vein area. At least 6 zebrafish per group were imaged. FIJI software was used to quantify the intensity of the α-nitrotyrosine staining of each group. To prevent bias the 6 brightest spots per image were selected from the maximum intensity projections of the Z in each area imaged. The results were analysed using the Microsoft Excel and the Prism software for calculated fluorescence.

2.5 Imaging and analysis techniques.

2.5.1 Microscopy

2.5.1.1 Fluorescence Microscopy

The fluorescent microscopy in these studies included two microscopes the Olympus inverted microscope and the Nikon widefield microscope. The Olympus microscope was used for imaging *C. albicans* cells and the widefield microscope was used for imaging the infected mammalian cells, for timelapse experiments and imaging of zebrafish embryos. The microscope settings were changed according to the experimental needs. In some experiments the automated microscope ImageExpress was used to image the samples, the setup of the microscope was different depending on the experiment. The automated microscope was set up to autofocus on each well of a multi-well plate and capture multiple images quickly for different channels.

2.5.1.2 Confocal Microscopy

The Nikon A1 microscope was used for confocal microscopy. The lens used for the imaging was the 40x and 60x oil lens and the confocal channels used were based on the staining of

the samples. The resolution was increased by reducing the size of the field of view. The intensity of the samples was either increased by scanning the samples more times or by increasing the resolution. It was critical to maintain the laser power and the HV as low as possible to avoid bleaching of the samples. Depending on the sample Z stacks or images of a single point were acquired. The Z stack slice size used was recommended by the NIS software as the recommendation would have provided the best resolution. The images from the confocal microscope were analysed using FIJI.

2.5.1.3 Scanning Electron Microscopy

The samples used for SEM were mammalian cell cultures of J774 macrophages and CACO-2 cells seeded on a glass coverslip inside a 24-well plate and infected with *C. albicans*. The samples were fixed initially with 4% PFA for 10 minutes and washed 3 times with PBS before a second fixative 2.5% Glutaraldehyde in 0.1M of Sodium phosphate was added overnight at 2^{o}C. The fixed samples could be stored after washing the fixative in PBS for up to 2 months. The samples were washed 3 times for 10 minutes with PBS-0.1M sodium cacodylate. The sodium cacodylate solution was then removed, 1 mL of 2% aqueous osmium tetroxide was added and the samples were incubated for an hour at room temperature. The incubation was followed by 3 washes of 10 minutes each with PBS-0.1M sodium cacodylate. The samples were dehydrated using the following steps: 15 minutes incubation with 75% ethanol, 15 minutes incubation with 95% ethanol, 15 minutes incubation with 100% ethanol and this step was repeated before the final dehydration step which was 15 minutes incubation using 100% dried ethanol. After the dehydration step the coverslips were removed from the 24-well plates and dried with 100% ethanol using an automated drier machine. Once the drying process was complete the samples were removed and placed on carbon tabs with aluminium stabs, the samples were facing up the aluminium stabs not towards them. The next step was to coat the samples with gold particles and then imaged on the SEM microscope. The microscope was set to 10kV HV, 5mm WD to Z and the beam intensity of 8. The samples were then analysed using software. The procedure was carried out with the help of Dr Jaime Canedo.

2.5.1.4 Light sheet microscopy

Live zebrafish embryos were anesthetised using tricaine and mounted into capillaries using 1.5% low melting agarose. Once the agarose was set the embryos were loaded into the LightSheet imaging chamber filled with PBS. The zebrafish embryos were focused on using the camera and then the embryo points were selected for setting up a Z stack and using a Zen program for the number of tiles needed to image the entire embryo. The number of tiles depended on how well the embryos awere mounted and the overlap needed to then put together the images. The channels used for imaging the embryos depended on what was the interest and the zebrafish line used.

Live imaging of embryos was also achieved using the LightSheet microscope, the area of interest was selected and as the microscope is fast, timepoints were chosen to observe dissemination using the KDRL zebrafish embryo line.

After the imaging process the Arrivis 4D imaging software was used to attach the different imaging tiles. The program allowed a reconstruction of the entire embryo. The reconstruction was used for analysis of the interactions of the embryo and the *C. albicans*. The images were further exported into tiffs to allow for analysis of the samples using FIJI.

2.5.1.5 Atomic Force Microscopy

Overnight cultures of *C. albicans* were induced to the hyphal morphology as described in **Section 2.1.1.2**. The hyphal cells were washed three times in acetate buffer pH5. After the wash cells were transferred on a 100% ethanol cleaned glass slides, another slide was added on top to allow cell adherence to the surface. The cells were allowed 15 minutes for adherence before the slides were separated and the slide with the highest cell density was used for AFM.

During AFM the slide was washed three times with acetate buffer to remove any non-adherent cells. The sample was images in acetate buffer using the Cantelivier nominal spring constant 0.2 N/m (NanoWorld Switzerland). The experiments were done using Quantitative Imaging (QI) mode using the JPK Nanowizard3 system, with trigger force set as 2 nN, loading speed 150 um/s and mapping resolution (in x-y) 50 nm/pixel. The n number for the experiment was a minimum of 14 cells per group. During analysis the Young's modulus for each cell was separated in the mother region and the hyphal stem region. Frequency

distributions of the data are presented. The AFM and data analysis was done with the kind help of Dr Xinyue Chen (Hobbs lab) from the Department of Physics and Astronomy at the University of Sheffield.

2.5.2 Analysis methods

2.5.2.1 Quantification of single cell observations

The proliferation timelapse experiments were analysed by observations of every macrophage and the *Candida* cells inside it throughout the course of the timelapse. Observations about how the *Candida* cells looked before uptake and the changes that occurred during the interaction were recorded. The timepoints of those changes were also recorded. The results were then processed and presented as proportions using the Prism software. It was a critical rule that only changes inside the phagolysosome were recorded and if for example a cell appeared budded before the uptake and then there was a hyphal switch then this was not a change inside the phagolysosome as the process of hyphal switch occurred before the uptake. The proportions were based on the number of cells taken up plus the number of cells that divided inside the phagolysosome. These results reflect what can be observed inside a phagolysosome with the different strains. The data collected were analysed for hyphal switch inside the phagolysosome, for proliferation inside the phagolysosome and for the different morphological changes inside a phagolysosome.

2.5.2.2 Quantification of fluorescence intensity

The FIJI software was used for the quantification of fluorescence in this study. The FIJI software has the Measure function which could be adjusted to measure different aspects in an image such as the area, mean intensity and threshold. The measure function was set to capture the Name of the image, the area of the objects, the mean intensity within an object and the integrated intensity. The process was manual as shapes were drawn around the periphery of the sample to create a closed object and then the measure function was used. Some samples required thresholding before they were processed. The results collected were analysed using Microsoft Excel and exported into the Prism software, the measurements for intensity used were Area x Mean Intensity and the Integrated Intensity.

2.5.2.3 Quantification of the microcolony sizes and behaviour during zebrafish infections

The FIJI and NIS elements analysis software were used to analyse the size of all microcolonies from both the LightSheet imaging and the zebrafish widefield fluorescent microscope timelapses. The microcolonies were manually tracked using the GFP channel and then using the analysis software, the surface of the microcolony was traced and the area per microcolony was calculated. The results were plotted in Prism using the SuperPlot function.

Microcolony behaviour was also manually tracked using NIS elements software. The microcolonies were observed, if the microcolony did not move from its position for 10 frames before and after the timepoint of interest then the microcolony was classified as adherent. If the microcolony was observed outside of the vessels for 10 frames before and after the timepoint of interest in the timelapse then the microcolony was classified as disseminated. The proportions of adherent and disseminated microcolonies were calculated and plotted using Prism.

2.5.3 Statistics

The statistical tests used in this study were a Mann-Whitney test, Fisher's exact test, One-way ANOVA and a Mantel-Cox survival test, unless otherwise stated. The stars in figures represented the significance values with a confidence interval of 95%. No significance was illustrated by ns and a p value of more than 0.05. One star (*) signified a significance with a p value of ≤0.05. Two stars (**) also indicated significance with a p value of ≤0.01 while the three stars (***) indicate a p value of ≤0.001. The highest level of significance with the lowest p value boundary was indicated by four stars (****) and the p value is less or equal to 0.0001. The GraphPad Prism version 9 was used for all the results presented.

Table 2.1: Buffers

Name	Composition
Acetate buffer	18 mM Sodium acetate, 1 mM Calcium chloride, 1 mM Manganese chloride. Solution pH 5.2
Phosphate buffered saline (PBS)	0.8% (w/v) Sodium chloride, 0.02% (w/v) Potassium chloride, 0.144% (w/v) Disodium phosphate, 0.024% (w/v) Monopotassium phosphate. Solution pH 7.4
Tris EDTA (TE) buffer	10 mM Tris Hydrocholoride, 1 mM EDTA. Solution pH 8.0
Tris acetate EDTA (TAE) buffer	40 mM Tris, 20 mM acetic acid, 1mM EDTA. Solution pH 8.3

Table 2.2: Candida albicans strains

Strain name	Genotype	Origin
SN76 (KAF17)	*ura3Δ::imm^{434} / ura3Δ::imm^{434}, iro1Δ::imm^{434} / iro1Δ::imm^{434}, his1Δ / his1Δ, arg4Δ / arg4Δ*	(Noble, Johnson, 2005)
SN148 (KAF19)	*ura3Δ::imm^{434} / ura3Δ::imm^{434}, iro1Δ::imm^{434} / iro1Δ::imm^{434}, his1Δ / his1Δ, arg4Δ / arg4Δ, leu2Δ / leu2Δ*	(Noble, Johnson, 2005)
KAF 37	SN76 *apm4Δ::HIS1/ apm4Δ::ARG4*	Dr Iwona Smaczynska de-Rooij (Ayscough lab)
KAF 52	SN76 *apm4Δ::HIS1/ apm4Δ::ARG4, CHS3/chs3Δ::SAT1*	Dr Harriet Knafler (Ayscough lab)
KAF 56	SN76 *apm4Δ::ARG4/ apm4$^{1-454}$::HIS1*	Dr Harriet Knafler (Ayscough lab)
KAF 59	SN148 *apm4Δ::HIS1/ apm4Δ::ARG4*	Stella Christou (this study)
KAF 62	SN148 ENO1/ENO1-GFP::LEU2	Stella Christou (this study)
KAF 63	SN148 ENO1/ENO1-GFP::LEU2, *apm4Δ::HIS1/ apm4Δ::ARG4*	Stella Christou (this study)
TT21	*ade2::hisG/ade2::hisG ura3::imm^{434}/ura3::imm^{434}::URA3-tetO-ENO1/eno1::ENO1-tetR-ScHAP4AD-3XHA-ADE2*	(Johnston et al., 2013)
NRG1^{OEX}	*ade2::hisG/ade2::hisG ura3::imm^{434}/ura3::imm^{434}::URA3-tet-O-NRG1 ENO1/eno1::ENO1-tetR-ScHAP4AD-3XHA-ADE2*	(Peters et al., 2014)

Chapter 3: *Investigating the impact of Candida albicans apm4 deletion on the interactions with macrophages*.

3.1 Introduction:

In mammals, macrophages are the first line of defense against microbes and *C. albicans* cells can be recognized and taken up by macrophages. This step is critical for pathogen clearance by the immune system (Newman, Holly, 2001, Hernandez-Chavez et al., 2017, Scherer et al., 2020). The *C. albicans* cell wall which is the outer-most structure is critical for recognition and uptake by macrophages. Specifically, β glucan is recognized and bound by the major pathogen recognition receptors Dectin-1 (Herre et al., 2004, Gow, N. A. et al., 2007, Mansour et al., 2013, Hasim et al., 2016). The levels of chitin have been identified as important for β glucan recognition as increased levels of chitin are proposed to mask recognition and binding by Dectin-1 and consequently reduce uptake by host macrophages (Mora-Montes et al., 2011).

Deletion of *apm4* in *C. albicans* has been shown to inhibit endocytosis of the major chitin synthase, Chs3 from the cell surface resulting in increased levels of chitin. As well as an increase in chitin there are change in morphology described by Knafler (2019). It was also noted that a heterozygous deletion of *chs3* in the *apm4Δ/Δ* results in a reduction of chitin on the cell surface and a partial rescue of the *apm4* deletion phenotype (Knafler et al., 2019).

In this chapter the interactions of *C. albicans* wild type and mutant cells with murine macrophages were investigated. The aim was to determine whether *apm4Δ/Δ* phenotypes, particularly those affecting the cell wall, impacted the uptake, virulence and phagosome responses.

Chapter 3 results

3.2 Impact of the *apm4* deletion on uptake by murine macrophages

Deletion of *apm4* has been shown to result in an increase in the cell wall chitin levels (Knafler et al., 2019). In order to determine whether this cell wall change influenced uptake by murine macrophages, adhered murine J774 macrophages were infected with Wt and

apm4Δ/Δ C. albicans. Cells were allowed to interact for 30 minutes at 37°C (Section 2.3.1.1), these conditions were chosen based on timepoints used in other investigations (Newman & Holly, 2001, Evans et al., 2017, Westman et al., 2018, Evans et al., 2019). It is enough time to allow for phagocytosis while the *C. albicans* cells are in the yeast morphology and not growing as hyphae.

To assess whether deletion of *apm4* impacted phagocytosis two measurements were made. First, the proportion of macrophages that phagocytose *Candida* cells was assessed. Second, the number of *Candida* cells in the phagosome of individual macrophages were counted.

The macrophages from 30 images captured during 5 independent experiments were recorded and all macrophages on these images recorded in the field of view were studied as to whether they contained a visible *C. albicans* cell. At least 20 macrophages were counted for each repeat. Representative images of macrophages infected with *C. albicans* are presented on figure 3.1.a. It was observed that cells from both populations were phagocytosed. The white arrows illustrated *Candida* cells inside the macrophages. The images were analyzed for the percentage of macrophages that take up *C. albicans* (figure 3.1.b). Unexpectedly, the analysis showed that there was a significant difference in the percentage of macrophages that uptake Wt compared to *apm4Δ/Δ* cells with a higher proportion of macrophages phagocytosing *apm4Δ/Δ* cells compared to Wt cells.

The second measurement made was to count the number of *C. albicans* cells inside a macrophage. As shown in figure 3.1.c. approximately two Wt cells were taken up in this frame. The outcome for the *apm4Δ/Δ* cells again reflected a higher level of uptake with more than two cells being phagocytosed per macrophage.

The data reveal the unexpected outcome that despite the increased level of cell wall chitin associated with the deletion of *apm4* there was increased phagocytosis by host macrophages of this mutant strain. Both the proportion of macrophages taking up the mutant and the number of *apm4Δ/Δ* cells per macrophage showed a significant increase.

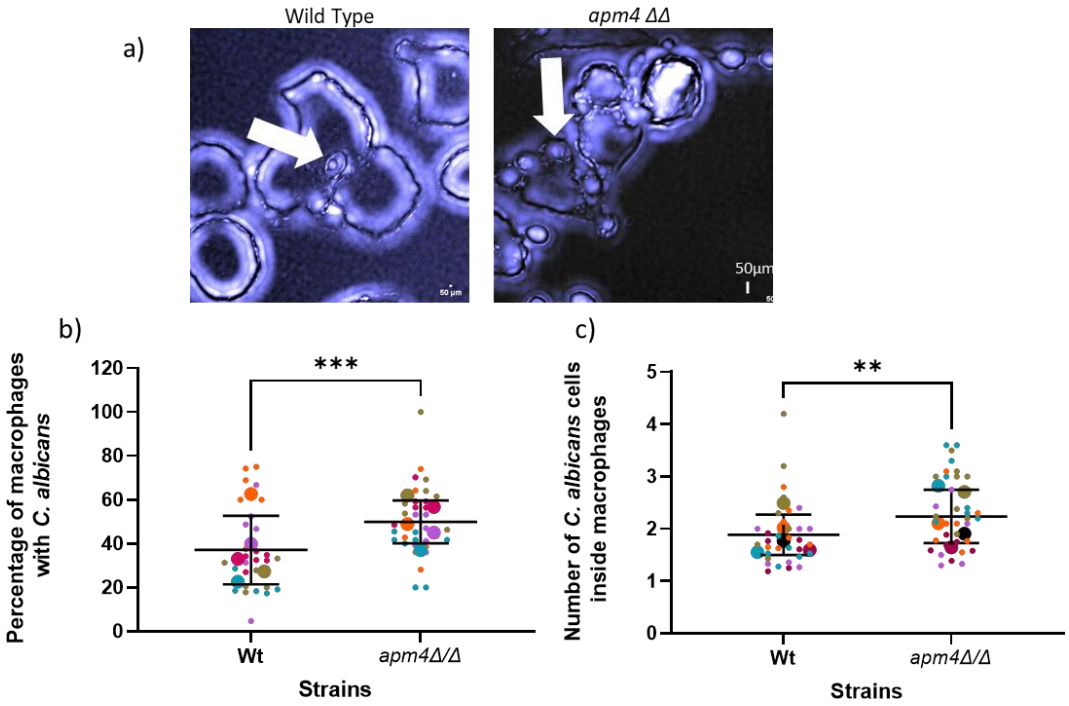

Figure 3.1: Deletion of apm4 in Candida albicans results in increased levels of phagocytosis. *C. albicans and J774 macrophages were co-incubated at 1:10 ratio for 30 minutes at 37°C, then fixed and imaged. a) Maximum intensity projection images of Wild type and apm4Δ/Δ infected macrophages. The white arrows illustrate phagocytosed C. albicans, the scale bar is equal to 50µm. b) The proportion of macrophages in a field of view that phagocytose C. albicans were quantified. 5 independent replicates with 9 images per replicate containing more than 30 macrophages each. The larger circles represent the average of each replicate, and the small circles represent the values for each image analyzed. The Mann-Whitney statistical tests show a significance with a p value 0.008 of ***. c)The number of Candida albicans per macrophage. 5 independent replicates with 9 images per replicate containing more than 30 macrophages each. The larger circles represent the average of each replicate, and the small circles represent the values for each image analyzed. The Mann-Whitney statistical tests show a significance with a p value 0.0072 of **.*

3.3 Impact of exposed β glucan on the *apm4Δ/Δ* phagocytosis phenotype

B glucan levels and exposure are important for uptake and recognition of *C. albicans* cells by macrophages (Munro, 2013, Bain et al., 2014). The levels of β glucan in *apm4Δ/Δ* cells have

been previously studied and there was no overall change compared to the Wt cells (Knafler et al., 2019). The levels of exposed β glucan however are important for uptake and recognition by immune cells (Gow, N. A. et al., 2007, Galan-Diez et al., 2010, Mora-Montes et al., 2011, Davis et al., 2014, Hasim et al., 2016). This experiment aimed to address the hypothesis that despite elevated chitin, the cell wall perturbations could result in more exposed β glucan in *apm4Δ/Δ* cells and this could contribute to the increased uptake by macrophages that was observed.

Immunofluorescence microscopy was used to investigate the levels of exposed β glucan. Cells were stained with Fc-Dectin which binds only to exposed β glucan and allows levels of exposed β-glucan to be quantified (Graham et al., 2006, Bain et al., 2014). Overnight cultures were incubated in fresh media for 3 hours at 30^{o}C before fixation and staining with Fc-Dectin as a primary antibody. Anti-human IgG with Alexafluor-488 was used as a secondary antibody before imaging (Section 2.2.2.2). 300 cells from 3 independent experiments were imaged at the same exposure settings. Representative images of the staining demonstrated that exposed β glucan was in patches around the cell surface (figure 3.2.a). In both the Wt and *apm4Δ/Δ* populations the exposed β glucan localized in large patches near the bud neck regions. Figure 3.2.b shows quantified overall levels of exposed β glucan per cell. There was no significant difference in the exposed β glucan levels between the two populations. The results indicate that the changes in the cell wall composition of *apm4Δ/Δ* cells do not result in a change of the exposed β glucan levels and that the increased phagocytosis observed during murine interactions was not linked to the β glucan recognition.

An additional approach was used to analyze β glucan exposure as it was hypothesized that β glucan could potentially become more exposed on incubation with mammalian cell media or in the presence of macrophages. The analysis above was conducted with cells grown in normal yeast growth media. The levels of exposed β glucan were investigated during interactions with macrophages using an immunofluorescence imaging approach. In a 96 well plate, adherent J774 macrophages were infected with *C. albicans* for 30 minutes at 37^{o}C. The cultures were fixed, stained as previously described and imaged using Image Xpress automated microscope (Sections 2.3.1.3 and 2.5.1.1). The images were analyzed using the

FIJI software similar to the analysis in figure 3.2.b. In this analysis differences of β glucan exposure between Wt and *apm4Δ/Δ* were suggested. In all cases the levels of exposed β glucan were lower in the *apm4Δ/Δ* strain with this reduction being significant when cells were in media alone or non-phagocytosed in the presence of macrophages. However, there was no significant difference for either Wt or *apm4Δ/Δ* when compared across conditions (figure 3.2.c). The results from this analysis indicate that there was a difference in the levels of exposed β glucan between the Wt and *apm4Δ/Δ* cells in different conditions. This result suggests that the increased levels of *apm4Δ/Δ* cell uptake by macrophages cannot be explained by a higher level of exposed glucan. It also suggests that as expected the increased chitin in the *apm4Δ/Δ* mutant correlate with decreased exposure of β glucan.

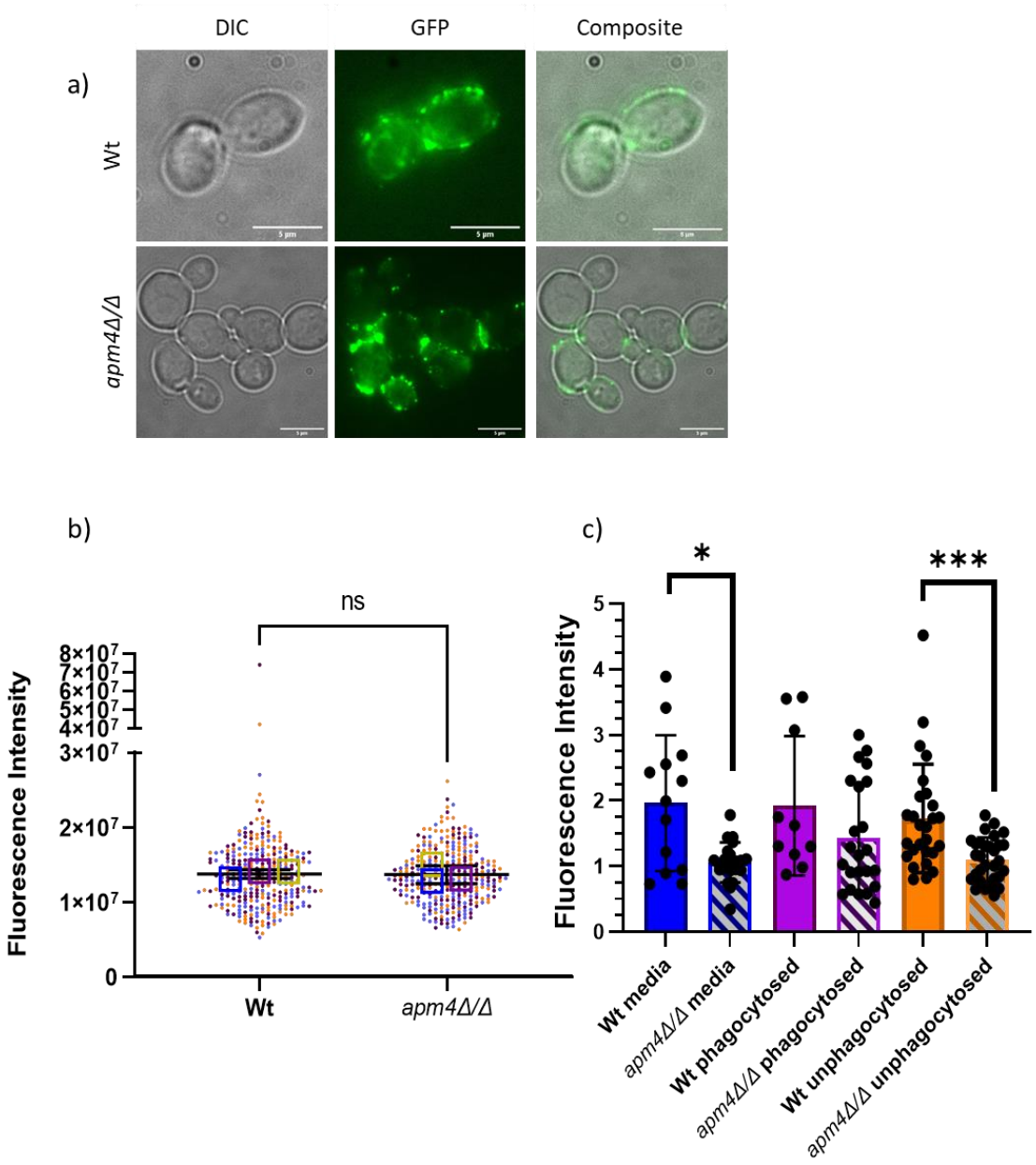

Figure 3.2 : Exposed cell wall β glucan levels of apm4Δ/Δ cells. *The levels of exposed β-glucan were investigated through immunofluorescence. Overnight cultures of C. albicans were incubated with fresh media for 3 hours before fixing with PFA and staining using Fc-Dectin as a primary and anti-human IgG conjugated to Alexafluor-488. The cells were imaged using a fluorescence microscope and the fluorescence intensity of the staining was quantified. a) Representative images of the staining b) Fluorescence intensity SuperPlot of exposed β glucan from 3 biological replicates, the statistical analysis indicated no significant difference p= >0.05. c) C. albicans were used for infection of macrophages then fixed and*

*stained after 30 minutes of interaction. The data represent the fluorescence intensity of the cells. * p = 0.0321, *** p = 0.0004*

3.4 Impact of the *apm4* deletion on cell size

Previous work in the Ayscough lab using the *apm4Δ/Δ* strain showed that the mutant cells are larger than Wt cells (Knafler et al., 2019). Size is a factor that could influence uptake by macrophages as it could be a limiting factor if the pathogen is too big or it could enhance uptake, as bigger structures might be detected faster by host immune surveillance cells. A suitable condition chosen was to refresh the overnight cultures in YPD media for 30 minutes before using the *C. albicans* cells for macrophage interactions, this would allow for a similar morphology for both populations. The size of cells after growing in fresh media for 30 minutes was investigated and compared to the findings in previous investigations, the Wt width was 4 µm and the mutant diameter was 6 µm (Knafler et al., 2019). Images of cells were captured and the cell size from different lengths and widths of the mother cells were analysed using FIJI.

The length and width of mother cells were measured at the points illustrated in the diagram on figure 3.3.a. The graph shows all the values counted for both length and width of mother cells. It was observed that the length and width of the mother cell are relatively similar values in both populations. Overall, the analysis demonstrated that the *apm4* deletion cells were larger than the Wt population as both the length and width of mother cells are approximately 1 µm greater.

The previous investigation showed that *apm4Δ/Δ* mother cells are bigger but did not provide any understanding of the overall size of cells and the changes in volume. A Schärfe Systems CASY™ counter was used to investigate the size and volume of cells. Overnight cultures of cells were incubated in fresh YPD media for 30 minutes before being used for measurements (Section 2.2.3.2). The CASY™ counter measured the volume of cells and then predicted the radius based on the volume assuming that cells are spheres.

The raw results as well as images of the histograms drawn by the counter are presented in **Supplementary material 1**. One observation from the histograms was that there were two peaks of measurements one considered most likely to represent budded and one for un-

budded cells. The mutant cells have a higher cell number on the second peak than Wt cells. Wt cells have a higher cell number on the first peak.

The results suggested that the average diameter of *apm4Δ/Δ* cells including both budded and unbudded populations is 1 µm greater than Wt cells while the average diameter of unbudded and budded cells show no significant differences (figure 3.3 b). The CASY™ counter also provided measurements of volume where significant differences are observed. The volume of *apm4Δ/Δ* cells is larger than Wt cells.

The length and volume of the average *apm4Δ/Δ* cell was larger than that of a Wt cell, this could mean that the macrophages encounter larger cells allowing more interactions with the macrophage pathogen recognition receptors and leading to the observed higher level of uptake. The data from the CASY™ counter also suggest that the proportion of un-budded and budded cells are different in the two populations.

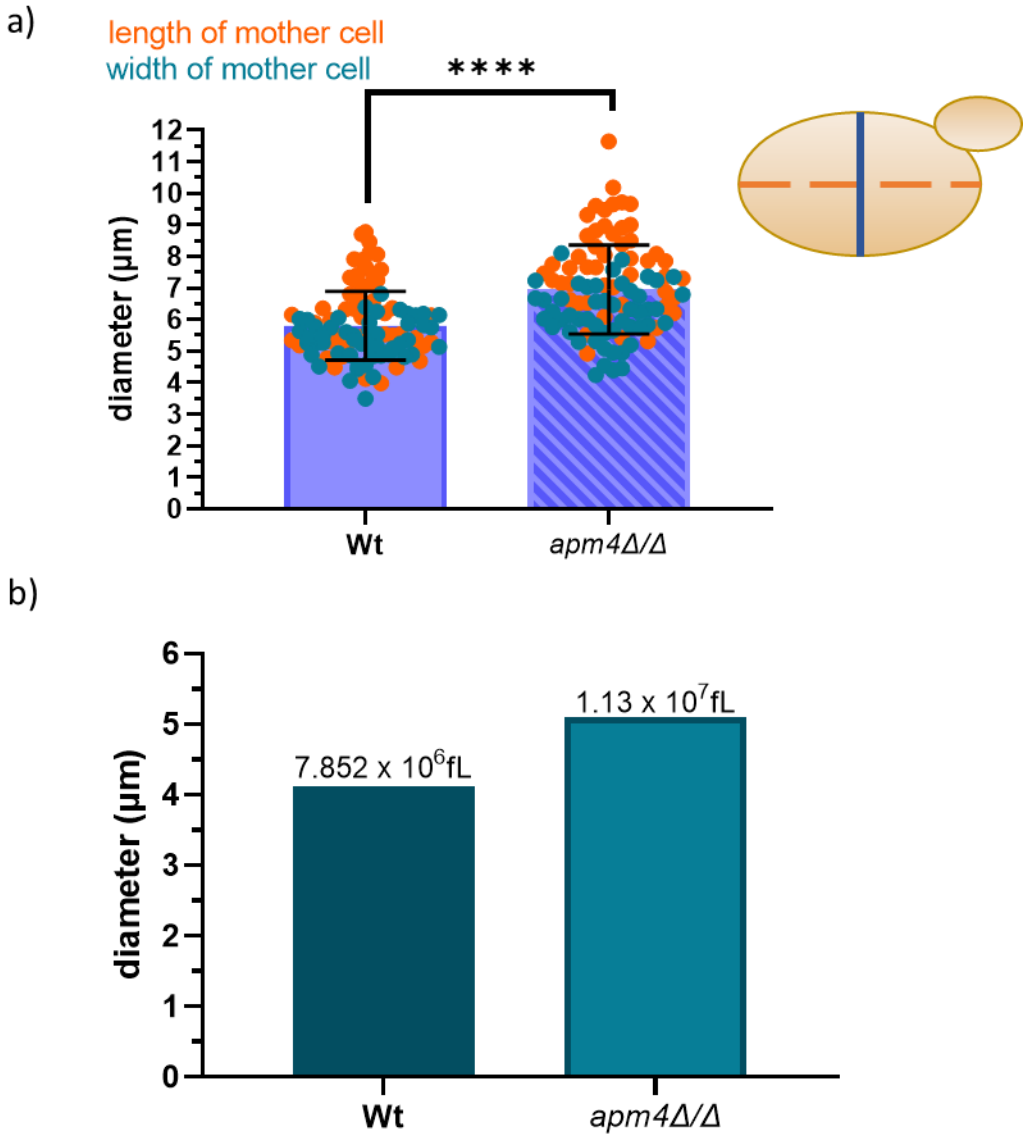

Figure 3.3: The size of cells with an apm4 deletion. *a) Overnight cultures of C. albicans were refreshed with YPD media for 30 minutes and then images of cells were captured and analyzed for cell size. The n for these experiments is n=50 cells per group. The bar chart illustrates the size in µm for the length (orange) and width (blue) of mother cells from both populations. The small circles are the values measured for each individual cell in the experiment, p=<0.0001 ****. The diagram next to the graph illustrates where each measurement was taken. b) The CASY counter was used to automatically count the cell size and volume of overnight cultures refreshed for 30 minutes at 30°C the n =>200000. The graph presents the mean diameter of cells, the numbers represent the average volume of cells in fL.*

3.5 Impact of budding on the cell size of *apm4Δ/Δ* cells

As shown above the *apm4Δ/Δ* mutant cells were larger in length and volume compared to Wt cells. These findings lead to the hypothesis that the budding could be different. Investigation of the differences in budding patterns between the two strains was then analyzed. Differences could indicate a reason contributing to the increased surface area that the macrophage cells would encounter during an infection.

The budding patterns of the cells were investigated by refreshing overnight cultures in fresh YPD media and observing the percentage of budding cells in the population (Section 2.2.3.1). Cells were studied for 8 hours, sampling cells for measurements every hour. It was observed that at the initial time point the Wt cells were primarily unbudded (>85%) which was expected for cells after an overnight incubation. Following inoculation into fresh media the cell cycle can restart and budding resumes such that by three hours more than 90% of cells are budding. The proportion of budded cells reduced as cells divided and entered G1, unbudded phase relatively asynchronously (figure 3.4.). The *apm4Δ/Δ* cells however had a much higher proportion of budded cells at the first timepoint with over 40% budded cells, showing that the cells do not all arrest in an unbudded state. Following inoculation into fresh media budding was stimulated in the unbudded cells and increased to a similar level (>90%) by three hours. The proportion of budded cells remains higher in the mutant strain possibly suggesting a slower overall cell cycle.

The increased cell size observed in mutant cells is likely to be largely due to the high percentage of the population in the budded state. More budding means that there is increased surface area, and this can potentially influence uptake and recognition by macrophages.

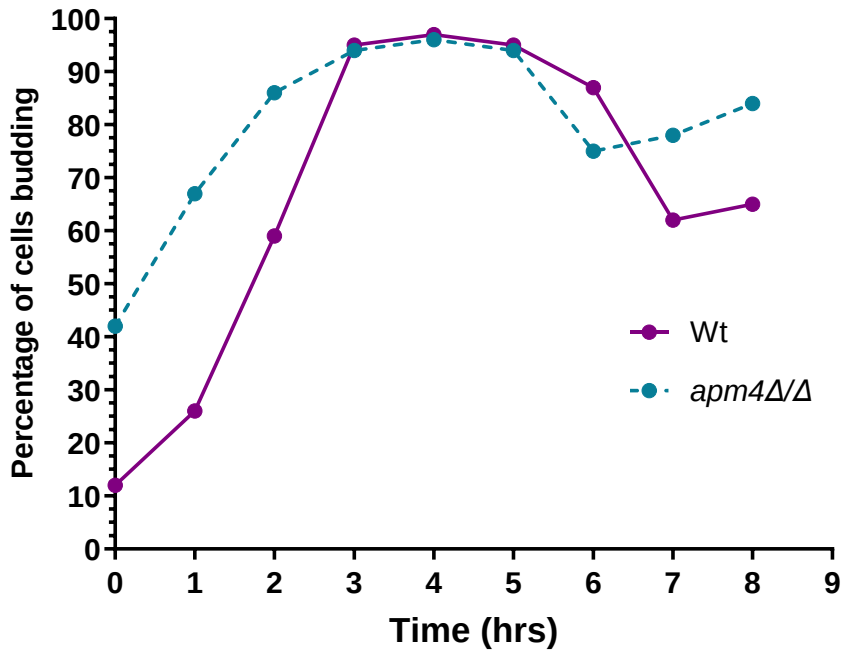

Figure 3.4: apm4Δ/Δ cells present differential budding patterns. *Overnight cultures of C. albicans were refreshed in YPD, the cultures were monitored every hour for the percentage of budding cells over time. The cells were placed onto glass slides and classified percentage budded and un-budded through observations.*

3.6 Impact of *apm4* deletion on macrophage death during infections

Having shown that both Wt and *apm4Δ/Δ* cells are effectively phagocytosed by murine macrophages it was of interest to determine how the cells behaved following uptake. It has been reported by many labs that following uptake, *C. albicans* cells are able to switch morphology to a hyphal form causing macrophage death from lysis due to hyphal penetration of the plasma membrane (El-Kirat-Chatel & Dufrene, 2012, Hernandez-Chavez et al., 2017, Westman et al., 2018, Westman et al., 2020). In this study the proportion of macrophage death due to *C. albicans* infection was investigated

Overnight cultures of *C. albicans* cells were incubated for 30 minutes in fresh media. The cells were then used to infect adhered J774 macrophages on a 1:1 ratio for 18 hours of interaction. The interaction was monitored through time-lapse, capturing images every 10 minutes (Section 2.3.1.2). The results were analyzed through observation of *C. albicans* behavior inside the phagolysosome. The proportion of macrophage death due to a *C. albicans* infection was analyzed the number of macrophages observed overall was 75 per group from overall 3 biological replicates. The macrophage death observed was lysis through the timelapse.

The results suggest that a Wt infection resulted in an increase in macrophage death (figure 3.5.a). The statistical analysis indicated no significant difference between the two populations. However, the analysis only included a small proportion of cells that could be tracked throughout the timelapse and may not be representative of the whole population.

During this investigation it was observed that *C. albicans* cells formed microcolonies containing macrophages. This made it difficult to discern individual cells but some macrophages that were within the microcolonies could be observed to be lysed and *C. albicans* growth was recorded. The last timepoint of the time-lapses was analyzed to count the number of microcolonies in each field of view, assuming that microcolonies were related to *C. albicans* virulence. The number of fields of view counted was eight per infection group from two independent experiments. The overall microcolony number of each field of view is presented on figure 3.5.b by the circles while the average for each group is represented with the bars. The results of this analysis showed a significant difference in the number of microcolonies formed by each infection, suggesting that the Wt cells were more virulent

than the *apm4Δ/Δ* cells. Representative images of the microcolonies are presented on figure 3.5.c, besides the overall number of Wt microcolonies being higher than the mutant it can also be observed that the microcolonies can be larger and contain elongated hyphae.

The data suggest that there are differences in macrophage death due to infections by Wt and mutant *Candida* cells. Cells with *apm4* deletion result in a reduced level of macrophage mortality than Wt cells.

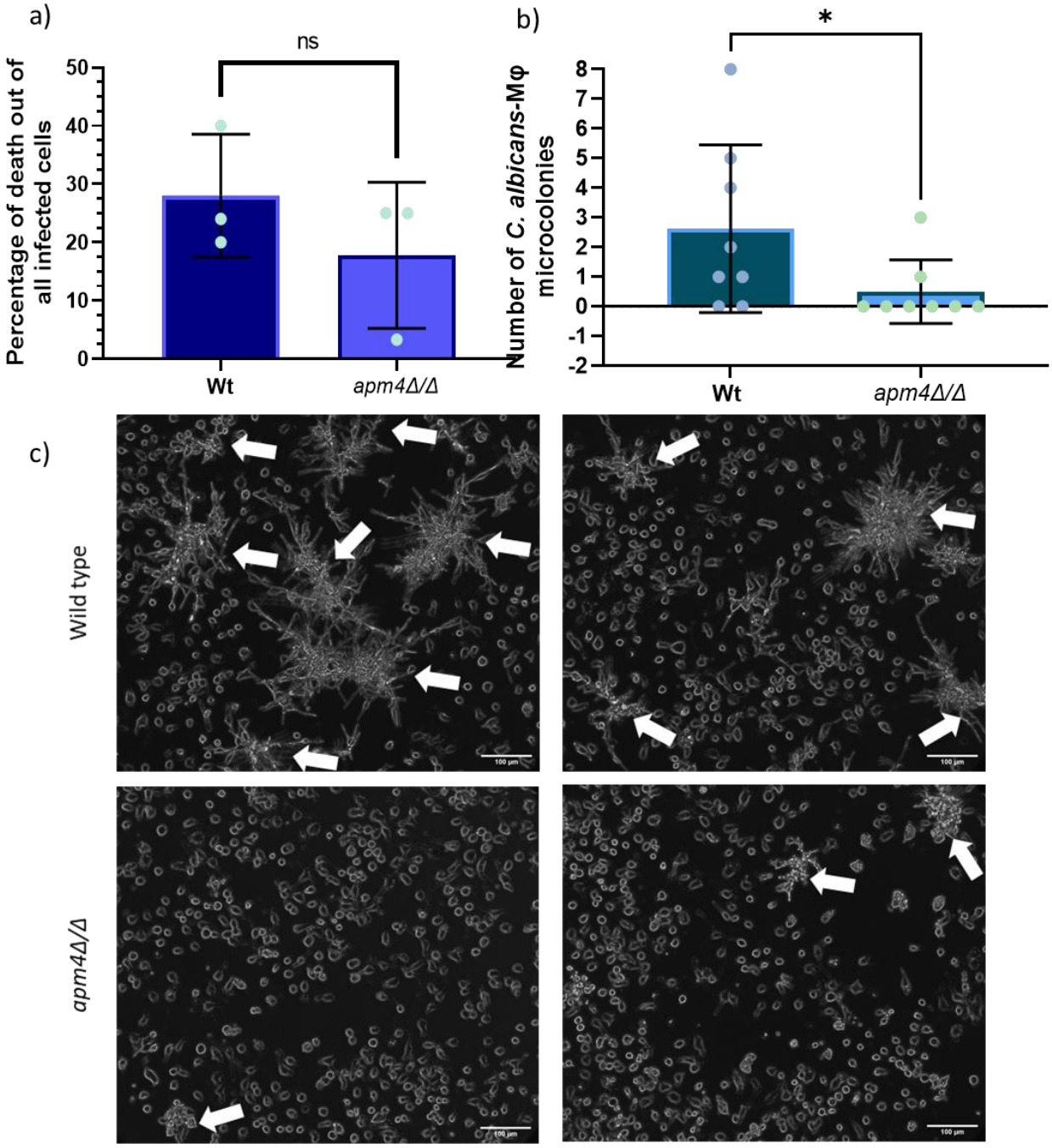

Figure 3.5: Candida albicans cells with an AP-2 deletion lead to reduced macrophage death. *C. albicans and J774 macrophages at 1:1 ratio were co-incubated for 18 hrs. The interaction was monitored by time-lapse microscopy at Phase 20x, the results were then analyzed by single cell observations and the changes inside the phagolysosome were recorded. a) The percentage of macrophage death from a C. albicans infection was calculated from the overall number of infected macrophages studied. The statistical analysis indicated no significant difference p = >0.05. b) The number of microcolonies (C. albicans and*

*macrophages) counted in each field of view. Each circle represents the number of microcolonies in the field of view while the bar represents the average number of microcolonies. The p value from the Mann-Whitney statistical test is 0.0493 *. c) Capture of the last timepoint, the white arrows point at macrophage to C. albicans microcolonies. The scale bars are equal to 100µm.*

3.7 Impact of the *apm4* deletion on hyphal switch inside the phagosome.

During the interactions between murine macrophages and *apm4Δ/Δ* it was concluded that the *apm4Δ/Δ* cells were phagocytosed more than Wt cells but that *apm4Δ/Δ* cells were less virulent. To understand why the greater level of uptake was not causing more death, later time points after infection were studied further.

Adherent J774 macrophages on glass coverslips were infected with Wt and *apm4Δ/Δ* cells at a 1:1 ratio for 18 hours at 37°C. The cultures were fixed, prepared and imaged for SEM by Dr Jaime Canedo (Johnston lab, University of Sheffield) (Section 2.5.1.3). SEM images are shown in figure 3.6. Using SEM allowed observations of the consequences of *C. albicans* cell uptake on macrophage morphology at higher resolution than with standard light microscopy approaches though is likely limited to analysis of the cell surface. Macrophages infected with Wt cells appeared to have more extensions indicative of *C. albicans* switch to hyphal morphology within the macrophages (grey arrows). In *apm4Δ/Δ* infections only one hyphal cell penetrating the macrophage was observed out of all the SEM images presented. Out of 10 SEM images per group only the ones included on figure 3.6 showed clear signs of infection.

While SEM allowed for observations of the impact of *C. albicans* uptake on overall macrophage morphology and supported the observations that the mutant *apm4Δ/Δ* cells have low levels of hyphal formation inside macrophages. It is relatively a slow procedure and was not suitable for furthering understanding of the mechanism underlying the differences in cells.

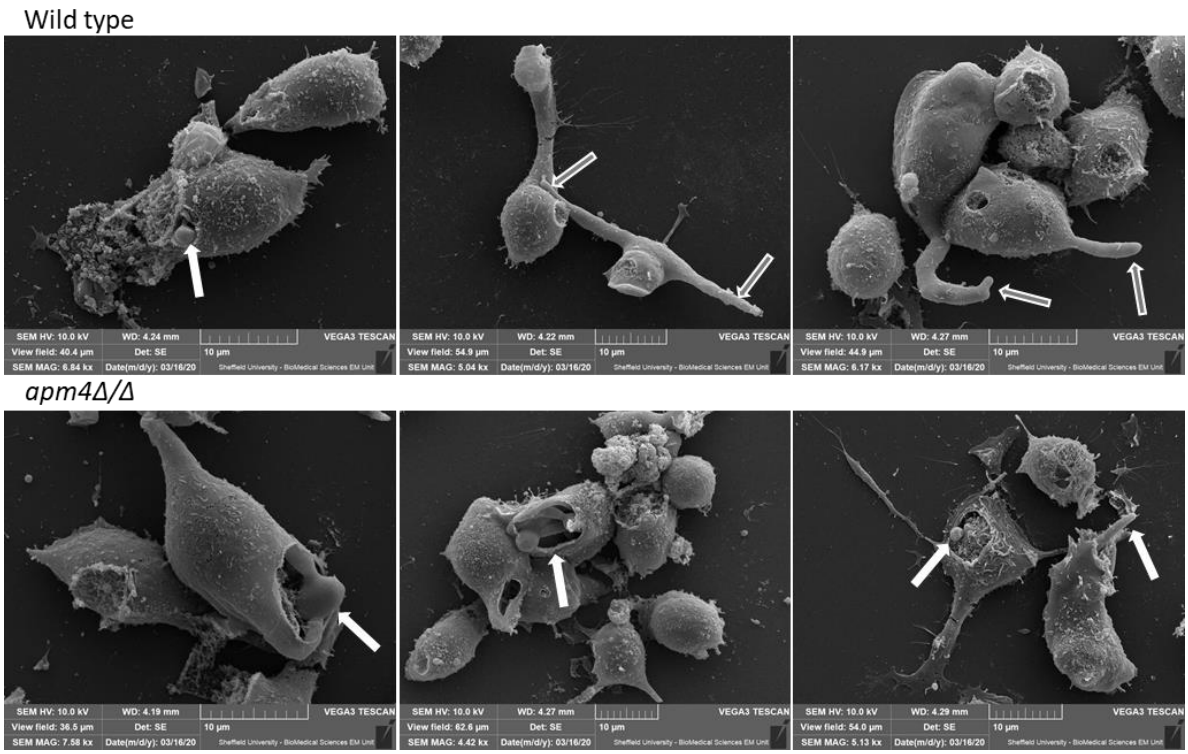

Figure 3.6: Candida albicans interaction with macrophages. *C. albicans and J774 macrophages at 1:1 ratio were co-incubated for 18 hours. The cultures were fixed and prepared for SEM imaging. Representative SEM images are presented here, white arrows point at C. albicans while gray arrows represent extended macrophages containing elongated hyphae.*

Hyphal switch is used by *Candida albicans* as an escape mechanism from macrophages, and it facilitates survival in a range of environmental conditions (Brothers et al., 2011, Vylkova & Lorenz, 2014, Wagener et al., 2017, Westman et al., 2018). The SEM provided data at a fixed time point only allowing external observations of the interaction. It was of interest to observe the interactions inside the phagosome as they allowed further understanding of the infection phenotype during real-time interactions.

The *C. albicans* tools used so far were difficult to use during live infections as the *C. albicans* cells were difficult to follow after uptake into a host cell. A strain was therefore constructed that expressed GFP on a single copy of the cytoplasmic protein Eno1 (Figure 2.2). The GFP expression of the protein and the validation of the strains can be found in the figure 2.3. The

Eno-1 GFP expressing strains allowed for the observation of *C. albicans* cell behaviour inside the phagosome during time-lapse experiments.

Overnight cultures of *C. albicans* were incubated for 30 minutes in fresh media. The cells were then used to infect adhered macrophages at a 1:1 ratio for 18 hours of interaction. The interaction was monitored by a time-lapse, capturing images every 10 minutes (Section 2.3.1.2). Through observations the number of cells switching to the hyphal morphology inside the phagosome out of all the population of cells observed were quantified. The quantification categorized cells in two groups (1) Yeast form (including yeast and budding yeast) (2) Hyphae (including hyphae and pseudohyphae).

The images in figure 3.7.a show that cells from both Wt and *apm4Δ/Δ* populations were phagocytosed by macrophages at the 10-hour post infection timepoint shown. On the left panel the murine macrophages were infected with Wt cells. The majority of Wt cells (>80%) had switched to the hyphal morphology. The macrophage in the higher magnification panel had been penetrated by the hypha. The rest of the macrophages in the field of view were also penetrated by elongated hyphae. The macrophages appeared more elongated during the infection; a phenotype supported by the SEM in figure 3.6. On the right panel murine macrophages were infected with *apm4Δ/Δ* cells. In the higher magnification panel *C. albicans* can be observed primarily in the yeast form. Hyphal-like cells could also be observed (a morphology between a short hypha and an elongated bud). No elongated hyphae or penetration of macrophages were observed in the mutant infections. The macrophages infected by *apm4Δ/Δ* appeared more rounded rather than elongated.

The *C. albicans* cells in each macrophage were monitored for *C. albicans* morphology switch from the beginning of the interaction until the end of the time-lapse. Phenotypic changes only occurring within the phagolysosome are presented in figure 3.7.b. The cell morphology at the beginning of the interaction was not included in the analysis. The results include the analysis from 3 biological replicates and observations of more than 60 macrophages per group. The findings support the observations from figure 3.7.a. There was approximately a twofold reduction in hyphal switch of *apm4* deletion cells compared to Wt cells suggesting a hyphal switch deficiency.

Cells with an *apm4* deletion have a hyphal switch deficiency as supported by the data. This phenotype could potentially impact the virulence as hyphal switch is one of the major *C. albicans* virulence factors. The mutant hyphal switch inside the phagosome was different compared to the switch in liquid media (figure 3.7.c.). In liquid media 61% of the *apm4Δ/Δ* cells switch to the hyphal morphology while 35% switch to the hyphal morphology in the phagosome.

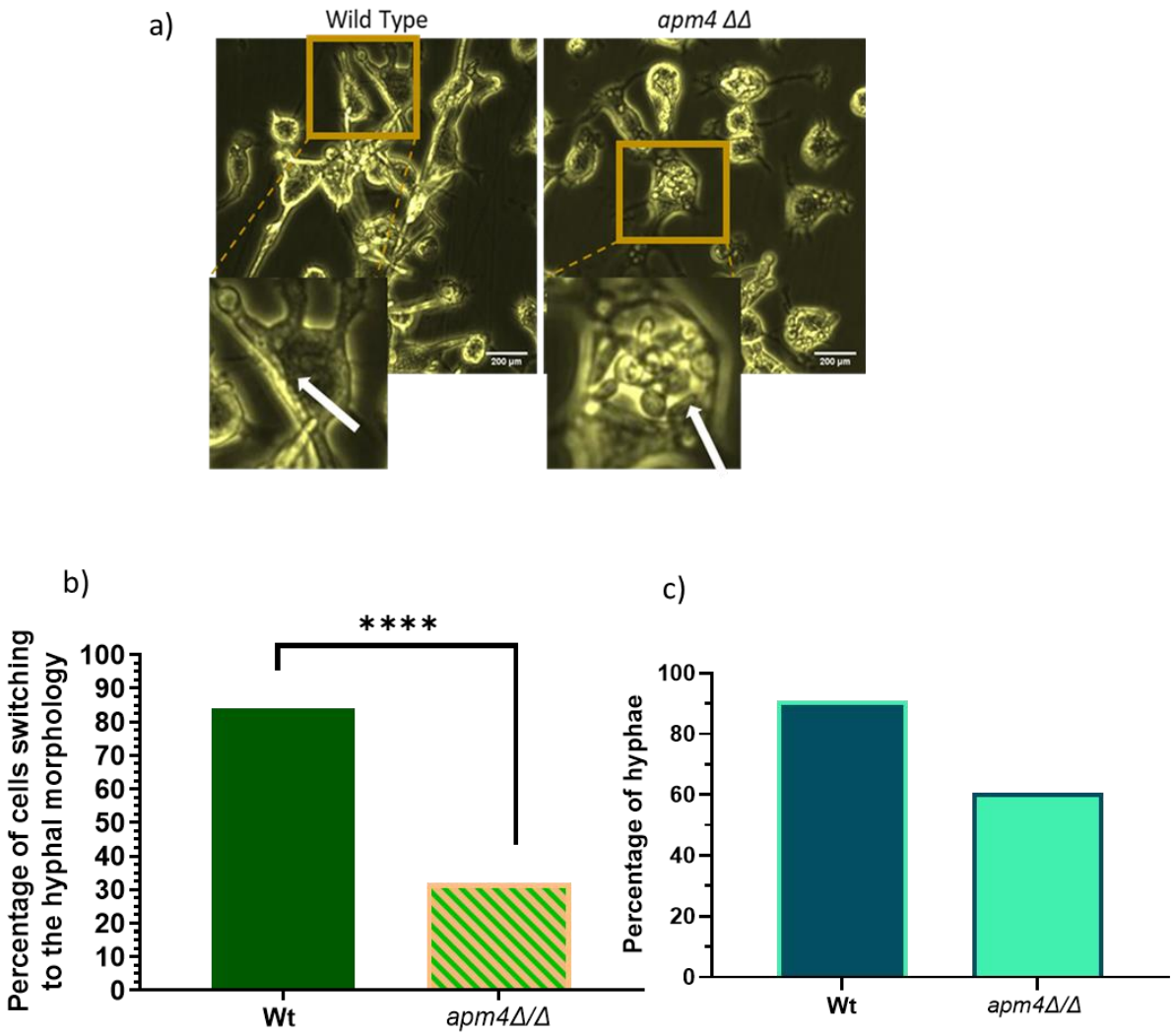

Figure 3.7: apm4 deletion in Candida albicans impacts hyphal switch. *C. albicans and J774 macrophages at 1:1 ratio were co-incubated for 18 hours. The interaction was monitored by time-lapse microscopy, the results were then analyzed by single cell observations for hyphal switch in the phagosome from 75 infected macrophages. a) The images are time-lapse captures at 10 hours post interaction. The panels focus on individual macrophage cells, the white arrow illustrate phagocytosed C. albicans. b) Quantification of hyphal switch inside the phagolysosome. Cell morphology changes that occurred only inside the phagolysosome were recorded. Stats: Fishers exact test, p = <0.0001 ****. c) The percentage of hyphal switch after a 90-minute induction at 37^{o}C in YPD + 10% FBS media was quantified using observation. Cells from the culture were transferred to slides and using observations were categorized as hyphae (including both hyphae and pseudohyphae) or as yeast (including yeast and budding yeast) using a compound microscope. The percentage of hyphae was*

plotted using GraphPad Prism. The n number for the experiment was >105 cells per group from one biological replicate.

3.8 The impact of cell wall chitin levels on phagosomal hyphal switch

In the study of Knafler (2019) it was shown that a strain with a heterozygous deletion of *chs3* in the *apm4Δ/Δ* background reduced cell wall chitin levels and also partially rescued the capacity of cells to form true hyphae. It was of interest to study this strain and determine whether decreasing the chitin levels also rescued the hyphal switch deficiency phenotype of *apm4Δ/Δ* cells during interactions with the phagosome.

The Eno1-GFP expressing Wt and *apm4Δ/Δ* cells were stained with Calcofluor white to ensure that the reduction of chitin reported previously was reproduced in these strains. As shown in figure 3.8.a and similar to the outcome described by Knafler (2019), there was an increase in the chitin levels of *apm4Δ/Δ* compared to the Wt and this level was partially rescued in the *apm4Δ/Δ,chs3Δ* cells.

Infection experiments of macrophages with *C. albicans* for time-lapse microscopy were then used to understand the role of chitin in the phagosomal hyphal switch deficiency phenotype of *apm4Δ/Δ* cells. Overnight cultures of *C. albicans* were incubated for 30 minutes in fresh media. The cells were then used to infect adhered macrophages on a 1:1 ratio for 18 hours of interaction. The interaction was monitored through a timelapse, capturing images every 10 minutes. The proportion of cells switching to the hyphal morphology inside the phagosome out of the population investigated was quantified.

Reducing the chitin levels resulted in cells with the *apm4Δ/Δ* background and an increase in hyphal switching, demonstrating an important role for chitin in the hyphal switch deficiency phenotype observed in cells with an *apm4* deletion.

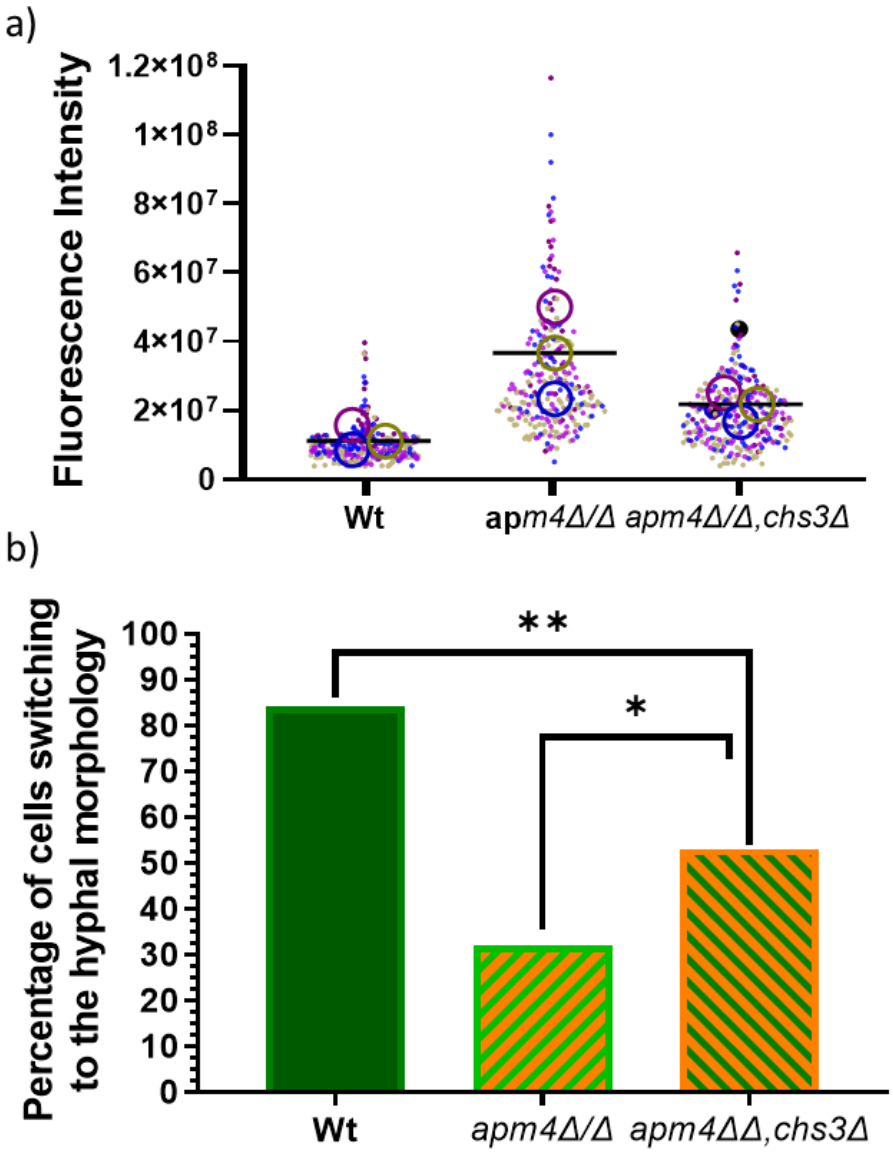

Figure 3.8 The Candida albicans cell wall composition impacts hyphal switch in the phagosome. *a) C. albicans overnight cultures were incubated with fresh media for 3 hours before staining with Calcofluor white and imaging with a fluorescent microscope. The dataset from 3 biological replicates was represented using a SuperPlot. The integrated intensity of Calcofluor white staining was plotted. b) C. albicans and J774 macrophages at 1:1 ratio were co-incubated for 18 hours. The interaction was monitored by time-lapse microscopy at Phase 20x, the results were then analyzed by single cell observations and recording hyphal switch that occurred inside the phagolysosome from 75 infected macrophages. * p of ≤0.05 ** p ≤0.01.*

3.9 The impact of environmental stiffness on *C. albicans* hyphal switch

The environments tested during previous investigations for hyphal switch were liquid media and growth on agar. Under these conditions, successful hyphal switching was observed for *apm4Δ/Δ* for mutant cells from 30 colonies per condition, the hyphae formed however were often morphologically altered (Knafler et al., 2019). The data shown so far (figure 3.7) indicated that there was a significant reduction in the level of switching inside the phagosome to only about 30%. The phagosome presents a distinct environment from those previously tested and the phagocytosed *C. albicans* cells will be exposed to different chemical and physical challenges inside this organelle.

Because the *apm4Δ/Δ* cells have wider hyphae and have some polarization deficiencies, we considered whether the mutant cells could have a deficiency in producing sufficient force during hyphal growth to penetrate the macrophage phagosome membrane (Knafler et al., 2019). Assessing force production inside the phagosome was attempted but the results were inconclusive. An alternative approach investigated whether the mutant cells were defective in their ability to penetrate agar during growth in the hyphal form.

Overnight cultures of *C. albicans* were mixed with cooled YPD agar at different percentages (1,2 and 4%). The cells would evade the agar to produce colonies. The colonies were incubated at 30^{o}C for 48 hours before imaging using a dissecting microscope (Brown et al., 1999). The dissecting microscope was used for imaging, the colonies were not removed from the agar and as it allowed better observations of the colony morphology and invasion. The percentages of agar selected were sufficient to mimic soft tissue stiffness (Alonso & Goldmann, 2003, Manickam et al., 2014). Representative images are shown in figure 3.9. A switch to hyphal growth at all the different conditions tested for both Wt and mutant strains. The white arrows point to hyphae of a range of lengths growing out of the colonies. The black arrows represent the growing microcolonies composed of yeast and hyphae. The images were processed for brightness and saturation to ensure that the hyphae are visible.

All the conditions tested in this study showed that mutant cells can successfully switch to the hyphal morphology. The results suggest that environmental stiffness similar to the conditions of soft tissue tested is not a limiting factor in hyphal switch.

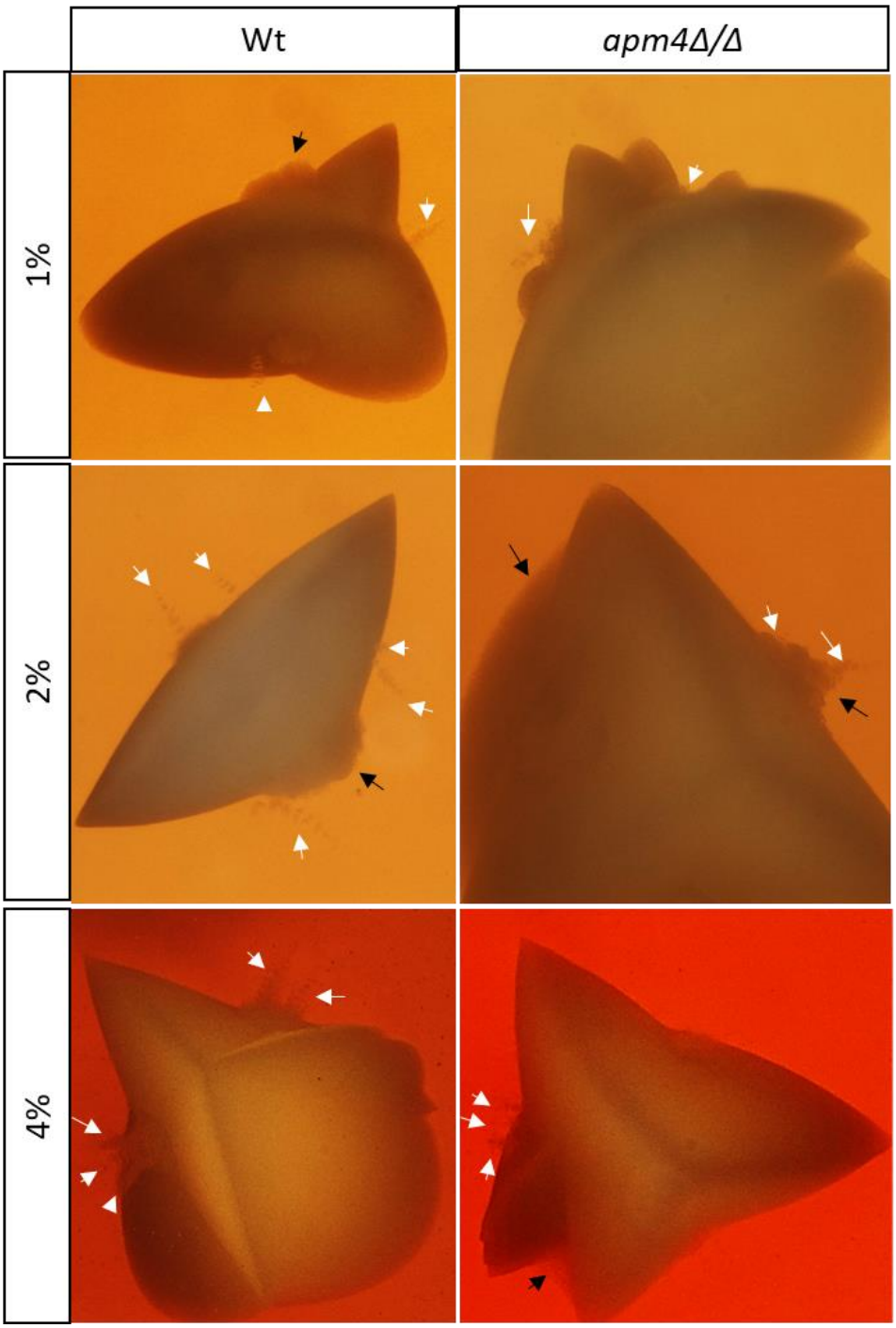

Figure 3.9: Candida albicans with an apm4 deletion interaction with different percentages of agar. *YPD agar at different percentages (1, 2 and 4%) was used to embed overnight cultures of C. albicans diluted 1 in 1000 using PBS, 10 µL of the Candida dilution were added in 25mL of agar and poured in Petri dishes. The Petri dishes were incubated for 48 hours at 30°C. Images of colonies were captured using a stereomicroscope. The images represent colonies for each strain at the different agar stiffness conditions. White arrows illustrate*

hyphae growing out of the colony and black arrows illustrate a microcolony of yeast mixed with hyphae growing out of the colony.

3.10 The mechanical properties of *C. albicans*

The changes in the *C. albicans* cell wall after the deletion of *apm4* as reported by Knafler (2019) could impact the mechanical properties of the cells. The increased chitin levels can result in increased cell rigidity while the changes in the mannan organization could impact the flexibility (Gow et al., 2017, Knafler et al., 2019). To study the differences in the stiffness of the *C. albicans* hyphae and whether this can impact the host pathogen interactions, Atomic Force Microscopy (AFM) was used to count the Young's modulus of hyphal cells (Section 2.5.1.5). The Young's modulus is a measurement of the ability of the cell wall to bend reform and stretch after an amount of force is exhibited to the cell wall. Overnight cultures of *C. albicans* were induced in the hyphal morphology using YPD + 10% FBS media for 90 minutes. The hyphal cells were washed using acetate buffer and adhered to glass slides. The AFM and data analysis was carried out in collaboration with Dr Xinyue Chen (Hobbs lab, University of Sheffield).

During AFM analysis Young's modulus of the hyphal mother and hyphal tube were separated to observe the differences in the distribution of cell stiffness. It was hypothesized that the *C. albicans* hyphal cells would have a difference in the distribution of cell wall stiffness with the hyphal tube (site of active growth) being stiffer than the mother.

The graph on figure 3.10 illustrates the distribution of the Young's modulus for the two strains. There is a widespread of the data however for the Wt the results show that the Young's modulus of the hyphal tube was higher than the mother cell (3.10.a). The *apm4Δ/Δ* hyphae however present a different phenotype, the Young's modulus of the hypha is similar for both the mother and the hyphal tube (3.10.b). The *apm4Δ/Δ* hyphae have an overall lower Young's modulus compared to Wt cells suggesting that the *apm4Δ/Δ* hyphae are softer than Wt hyphae.

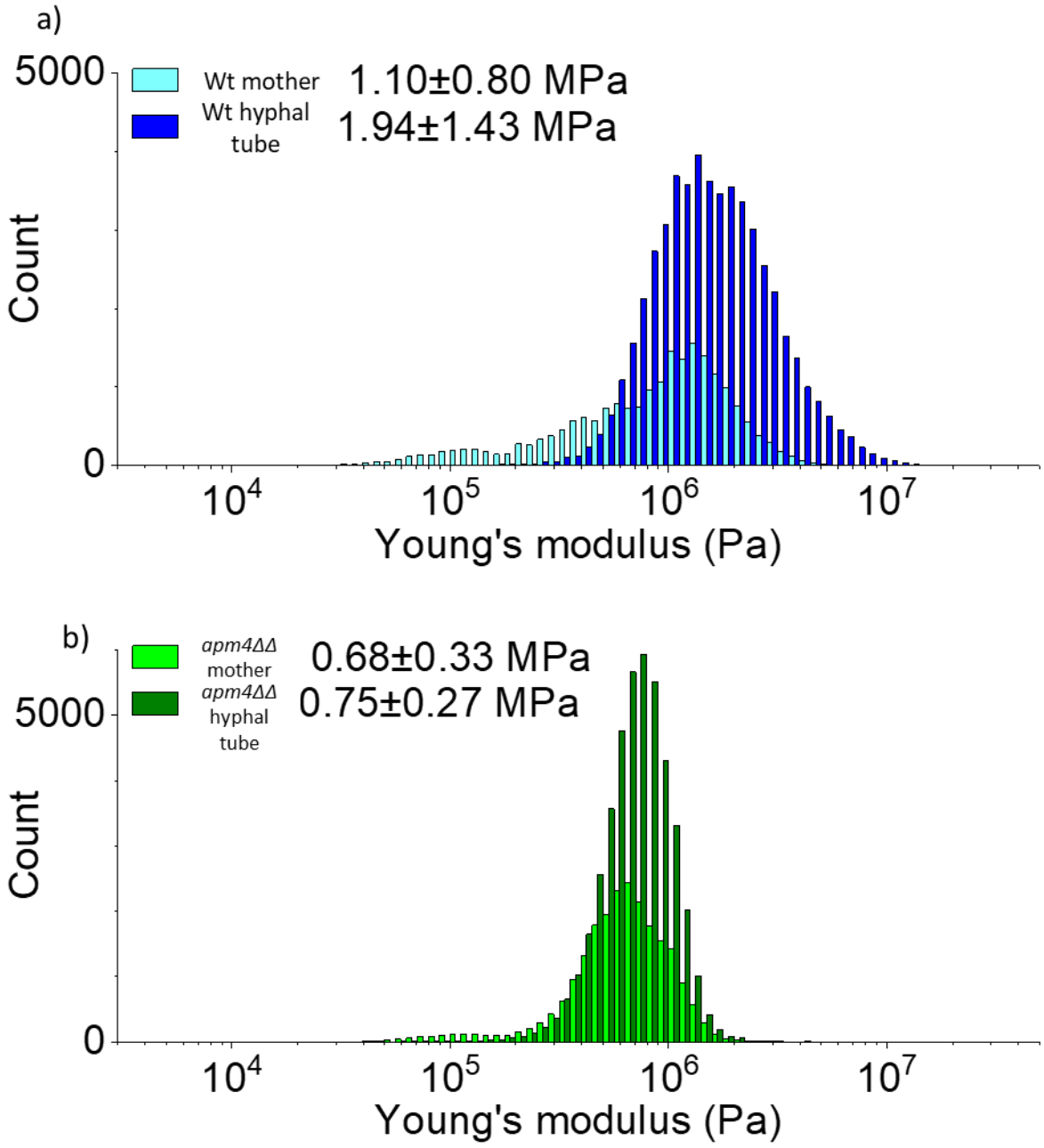

Figure 3.10: There are differences in the mechanical properties of the wild type and apm4Δ/Δ Candida albicans. *Atomic force microscopy was used to determine the Young's modulus of hyphal cells. Overnight cultures were induced to the hyphal morphology in YPD + 10% FBS for 90 minutes before preparation for AFM on glass slides. The graphs represent the distribution of the Young's modulus in Wt and apm4Δ/Δ cells for the hyphal mother and hyphal tube. The lighter colors represent the mother, and the darker colors represent the stem a) C. albicans Wt distribution is presented from an n of 14 cells from 3 independent*

experiments. b) C. albicans apm4Δ/Δ distribution is presented from an n of 17 cells from 2 independent experiments.

3.11 Impact of carbon source during growth of *C. albicans*.

The phagolysosome is a harsh environment for cells to survive as there is nutrient deprivation, low pH, hypoxia and antimicrobial peptides involved in clearance (May & Casadevall, 2018). Interactions with the phagosome environment are considered to influence the signaling for hyphal stimulation and morphology switch (Brown et al., 1999, Lorenz, 2013, Brown, A. J. et al., 2014, Ene et al., 2014, Danhof et al., 2016, Sherrington et al., 2017). In order to determine whether aspects of signaling and metabolism might underlie the differences in hyphal switching, this part of the study aimed to investigate whether different carbon sources impact the growth of Wt and *apm4Δ/Δ* cells.

Different agar media were used in these experiments; YPD and NGY representing high and low glucose concentrations, Lactate media, Glycerol media and Amino acid only media. Overnight cultures were used for spot assays on agar plates of different carbon resources. The agar plates were incubated for 48 hours at 30 and 37^{o}C.

Images of the spot assay are presented on figure 3.11. Overall, there was no condition where growth was largely absent in one strain compared to another as expected, the cells grew less well on amino acid media compared to other carbon source media. At both 30 and 37^{o}C the cells were growing in the hyphal morphology for both populations.

These data suggest that nutrient starvation do not appear to underlie the difference in the hyphal switch deficiency of the *apm4Δ/Δ* cells.

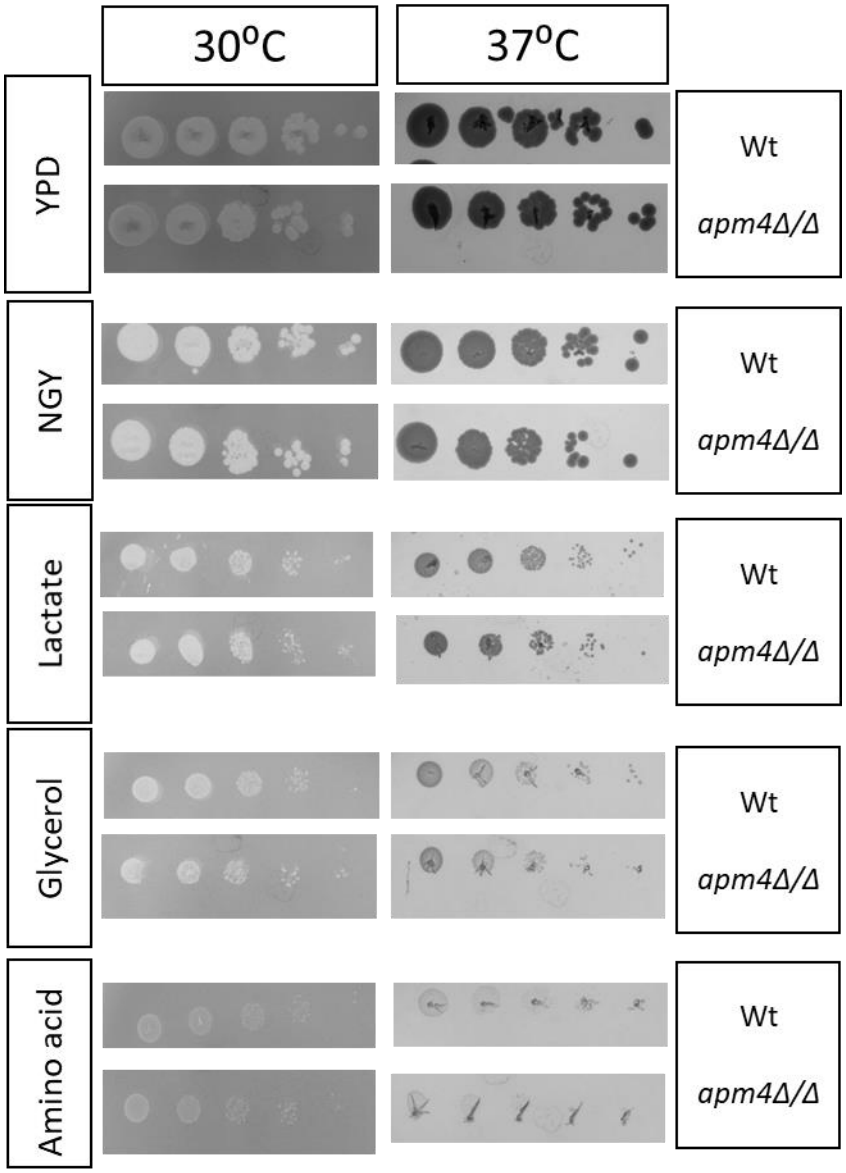

Figure 3.11 : Growth of apm4Δ/ Δ cells in different carbon sources. *Overnight cultures of Candida albicans were used to make a serial dilution of 1 in 10 for overall 4 dilutions. The C. albicans were plated on agar plates with the following carbon sources: Glucose (YPD with high concentration and NGY with low concentration), Lactose, Glycerol, and amino acids only. The plates were incubated at 30 and 37°C for 2 days before imaging.*

3.12 Impact of different pH media on *C. albicans* growth

The pH inside the phagosome is acidic, *C. albicans* cells have mechanisms to respond to the environment. The growth at different pH values was investigated *in vitro* to understand the impact of low pH on cell growth.

Overnight cultures of *C. albicans* cells were incubated in Medium 199 adjusted to different pH values (pH 4, 5, 6 and 7). The cells were incubated at 30^{o}C in a shaking incubator and growth was measured (based on OD600 nm light scattering) at different timepoints (Section 2.2.4.2). Using the absorbance, a predicted cell number was calculated (figure 3.12).

The growth curve of cells incubated at pH 4,5,6 and 7 are in figures 3.12.a-d at these conditions both populations grew at a similar rate. The results showed no significant difference between the Wt and *apm4Δ/Δ* growth at the different pH values. The results were further compared for each strain to assess differences in growth between pH values. At pH 7 the Wt cells initially grew slower compared to other pH values investigated however the growth plateaus at the same cell number for all values tested at the 24-hour timepoint assuming steady state growth was reached by that timepoint (figure 3.12.e). The *apm4Δ/Δ* cells grow at a similar rate at all the pH values investigated (figure 3.12.f). The results from this investigation show that both Wt and *apm4Δ/Δ* cells grow equally well at all the pH values tested and thus the low pH inside the phagosome is unlikely to underlie the difference in hyphal switching observed as the cells are live and growing in these conditions.

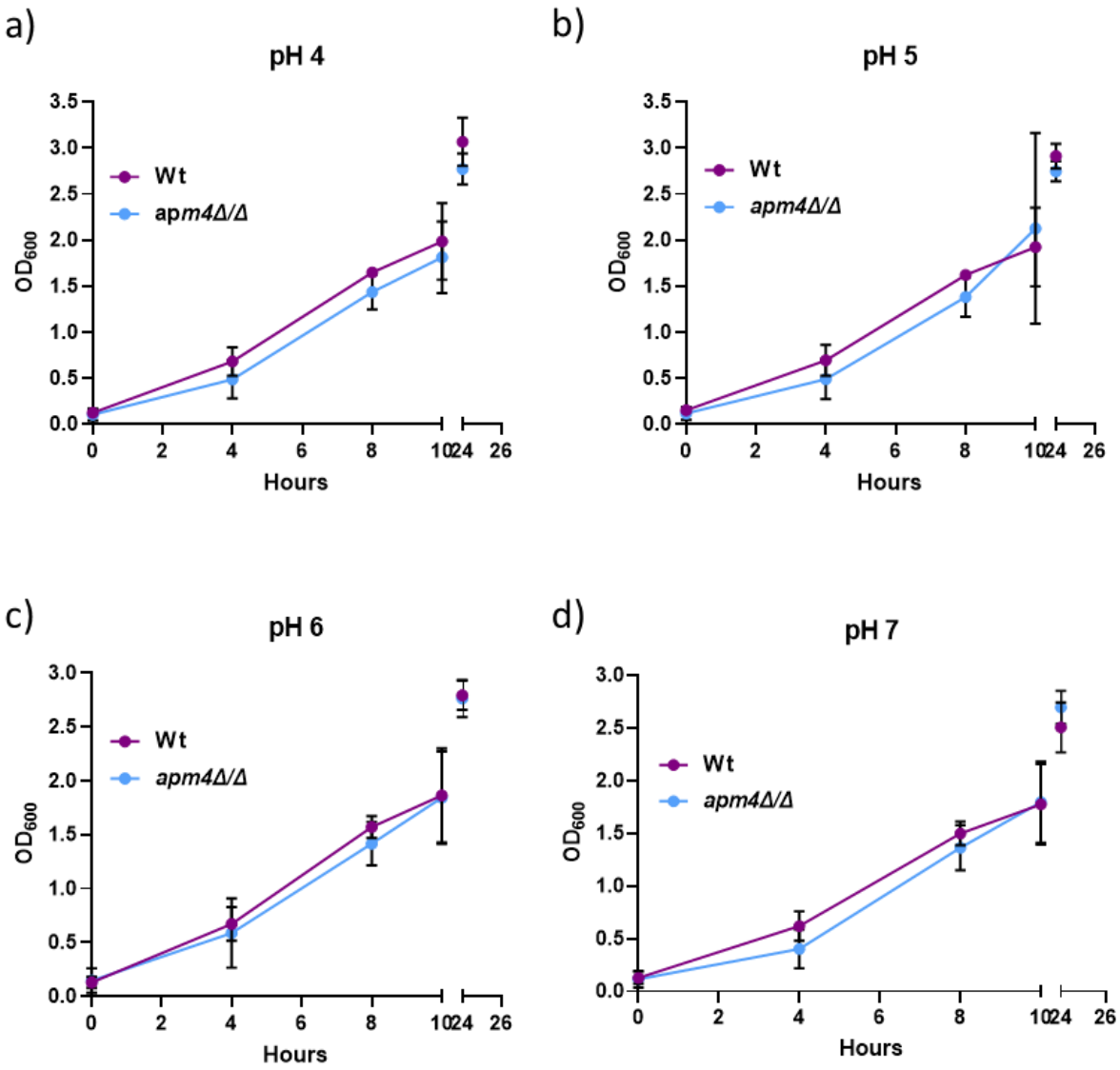

Figure 3.12: Growth of C. albicans at different pH values. *Overnight cultures of C. albicans were used for growth curves using medium 199 at different pH levels. The experiment was for 24 hours at 30°C. At different timepoints (0, 4, 8, 12 and 24 hours) the absorbance of the culture at OD600 was measured. The absorbance was then used to calculate an estimated cell number. The results are from 3 independent biological replicates, the error bars on the plots represent standard deviation. a) pH 4 b) pH 5 c) pH 6 d) pH 7.*

3.13 Investigation of the phagosome alkalinization response of *C. albicans*.

During interactions of *C. albicans* with the phagosome the pH changes from an acidic pH to alkaline. This alkalinization response is linked to *C. albicans* hyphal switch. There have been multiple reports on this response suggesting that the hyphal switch of *C. albicans* drives the alkalinization but also that alkalinization is important for the hyphal switch signaling (Vylkova & Lorenz, 2014, Wagener et al., 2017, Westman et al., 2018). *apm4Δ/Δ* cells show reduced switching to the hyphal morphology in macrophages so, it was hypothesized that *apm4Δ/Δ* cells might be reduced in their capacity to alkalinize and this inability could be coupled to reduced hyphal switching.

Phagolysosomal pH dye Lysosensor Yellow/ Blue was used to estimate the pH during infections. The emission of the dye from both GFP and DAPI channels can be used as a prediction of the phagosome pH. Adherent J774 macrophages were infected with *C. albicans* for 3 hours before being stained, fixed, and imaged. The representative images from the experiment are presented on figure 3.13.a. The differences were not easy to observe so the data were analyzed for the fluorescence emitted per cell for each channel. The values measured were used to predict the phagosomal pH.

The mean fluorescence intensity from 5 biological replicates is presented on figure 3.13.b. The mean intensity per channel for a 3 hour infection is illustrated in the graph. The 3-hour timepoint was where the alkalinization phenotype has been previously reported (Westman et al., 2018). The results showed that the mean intensity of the *apm4Δ/Δ* infected cells is similar to the uninfected acidic control macrophages for both the GFP and DAPI channels. The Wt infected macrophages had a higher fluorescence intensity than the control and *apm4Δ/Δ* infected phagosomes.

The results from this investigation highlight that the phagolysosome response is different during *apm4Δ/Δ* infections compared to Wt infections. The data suggested that mutant cells do not respond similarly to Wt cells in the phagosome environment and suggest that the hyphal deficiency phenotype could be linked to this phenotype.

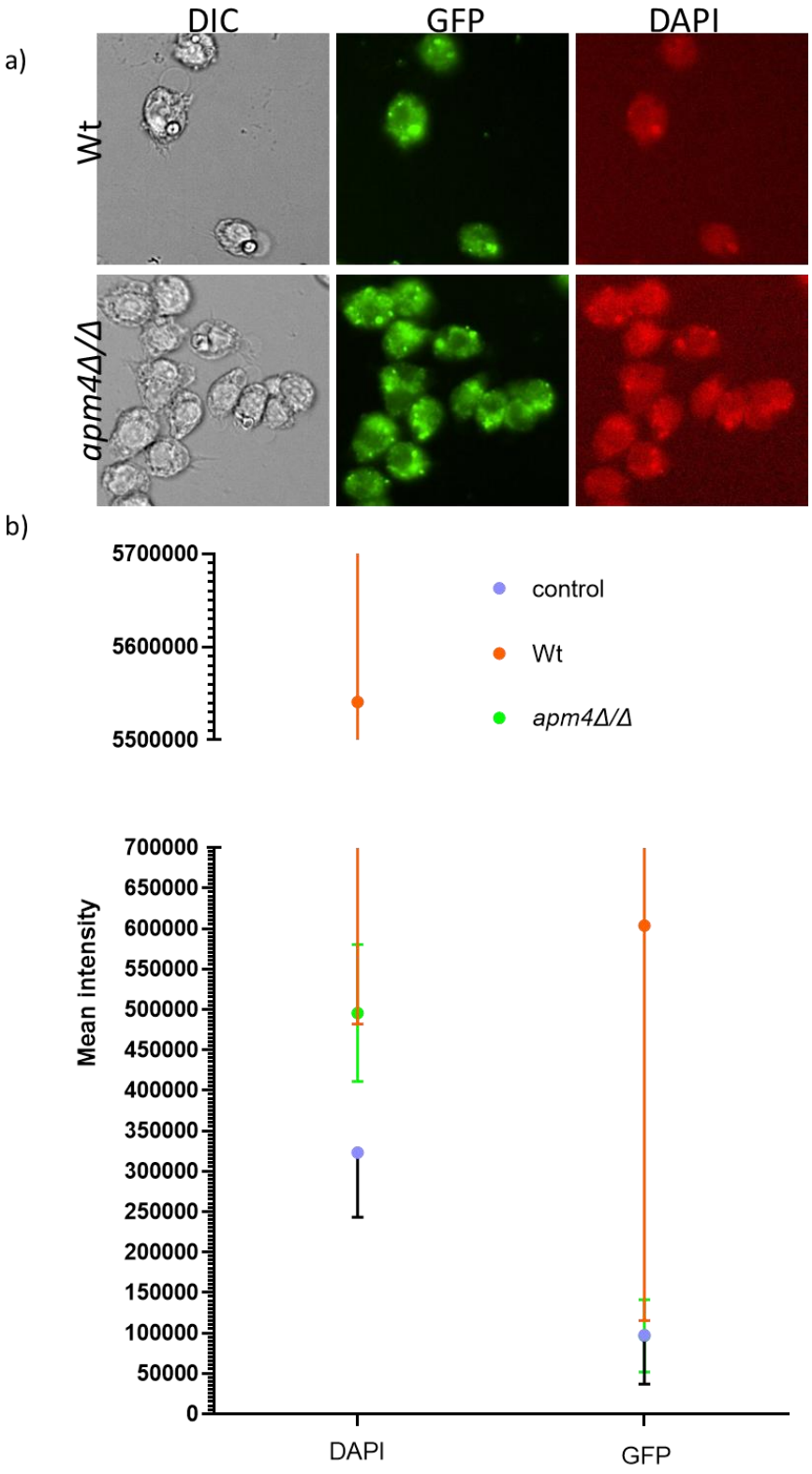

Figure 3.13 : The phagosomal pH after Candida albicans infections. *C. albicans and J774 macrophages at 1:1 ratio interacted for 3 hours. Changes in the phagolysosomal pH were monitored using Lysosensor Yellow/Blue. a) Representative images of the staining for Wt and*

apm4Δ/Δ infections. b)The graph illustrates the mean fluorescence intensity for each infection from 5 biological replicates.

3.14 Impact of the *apm4* deletion on budding inside the phagosome.

The majority of *C. albicans* cells with an *apm4* deletion do not switch to the hyphal morphology inside the phagosome. However, it was also observed that the cells are not killed by the macrophages and can induce some host cell death during murine macrophage infections. It was hypothesized that while *apm4Δ/Δ* cells do not get cleared by the host macrophages and cannot switch to the hyphal morphology, they are able to continue to grow inside the phagolysosome as yeast. Such growth has been reported recently by another group (Scherer et al., 2020). Examples of continued yeast growth can be seen in figures 3.5 and 3.7.a where the mutant cells were in the yeast morphology and continued to be able to grow vegetatively.

Overnight cultures of cells were incubated for 30 minutes in fresh media. The cells were then used to infect adhered J774 macrophages on a 1:1 ratio for 18 hours of interaction. The interaction was monitored through time-lapse microscopy, capturing images every 10 minutes (Section 2.3.1.2). The cells forming buds inside the phagosome were quantified using observations from 75 macrophages. A quantification of budding that occurred only during the phagosome interactions was recorded.

As seen in previous experiments the *apm4Δ/Δ* cells were inside macrophages (figures 3.5, 3.6 and 3.7), the cells were growing and forming new buds in the phagolysosomal environment (figure 3.14). Specifically, 40% of the *apm4* cells which were phagocytosed proliferate inside the phagosome while less than 10% of the Wt population exhibited the same behavior. a*pm4Δ/Δ* cells with one copy of *chs3* deleted were also able to proliferate with 30% of the population formed buds during the time course.

Here, it was demonstrated that *C. albicans* cells with an *apm4* deletion do not only survive interactions with the phagosome but also grow in those conditions. It suggests that *C. albicans* cells that have hyphal switch deficiencies use alternative mechanisms to promote survival and growth.

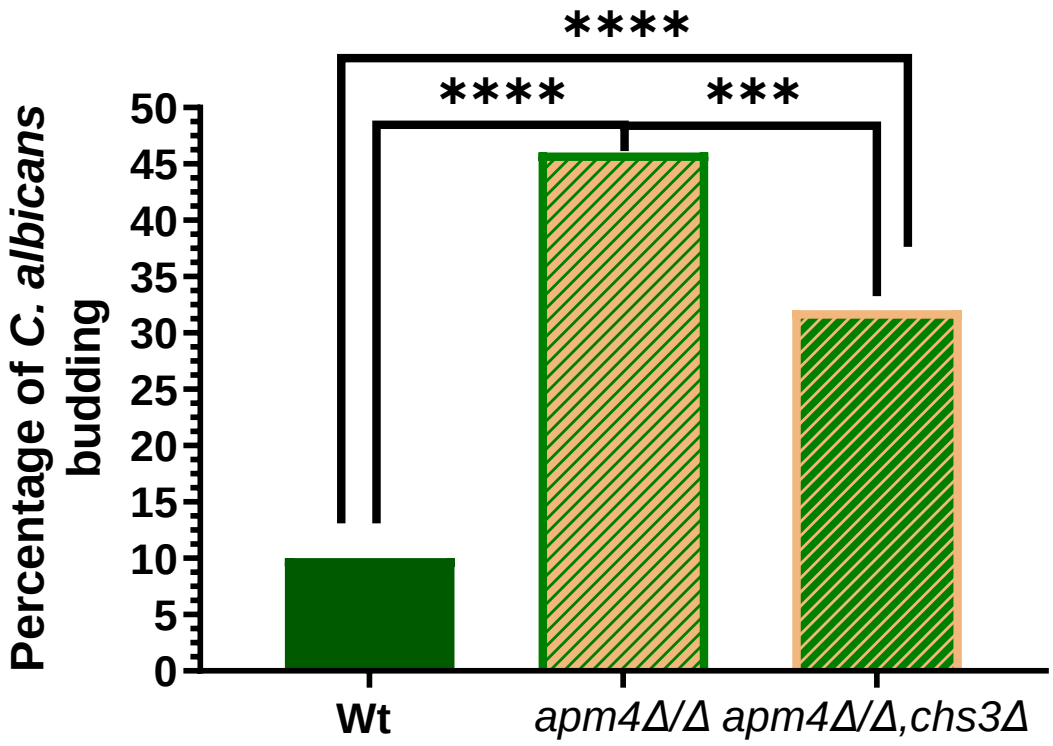

Figure 3.14: Candida albicans cells with an apm4 deletion grow inside the phagolysosome.

*C. albicans and J774 macrophages at 1:1 ratio were co-incubated for 18 hours. The interaction was monitored by time-lapse microscopy, the results were then analyzed by single cell observations and recording the percentage of cells out of the population forming buds inside the phagosome. *** indicate a p value of ≤0.001, **** indicate a p value of ≤0.0001.*

3.15 Study of phagosome proliferation in yeast locked cells.

The data above suggest that *apm4Δ/Δ* cells that have hyphal switch deficiencies proliferate inside the phagosome. This led to the following question, do other cells with an inability to switch to the hyphal morphology exhibit a similar behavior?

To address this NRG1^{oex} (yeast-locked cells) and the parental TT21 strains were used for a time-lapse experiment. *Nrg1* is a hyphal switch repressor, when the gene is expressed, cells cannot switch to the hyphal morphology. The overexpression TET ON system for *nrg1* represses hyphal switch as the gene is expressed, so the cells are genetically modified to remain in the yeast morphology (Johnston et al., 2013, Seman et al., 2018). Overnight yeast cultures of Wt (TT21) parental strain and the characterized yeast-locked strain NRG1oex were incubated with fresh media for 30 minutes and used to infect adhered J774 macrophages at a 1:1 ratio. The cells were co-incubated with macrophages for 18 hours. Time-lapse microscopy was used to monitor the interaction, capturing images every 10 minutes (2.3.1.2). The cells forming buds inside the phagosome were quantified using observations from 60 macrophages. A quantification of budding that occurred only during phagolysosome interactions and no changes in budding was recorded.

The hyphal forming TT21 cells did not form any buds inside the phagolysosome whilst 70% of the yeast locked NRG1oex cells did form new buds in the phagolysosomal environment (figure 3.15). The results here were similar to cells with an *apm4* deletion, suggesting that proliferation occurs due to a disruption in the hyphal signaling or hyphal signaling maintenance.

The results suggest that cells who cannot switch to the hyphal morphology are not cleared by macrophages, instead the cells proliferate in the environment. It is currently not understood how this phenotype contributes to virulence during interactions with the full host environment and its impact on dissemination.

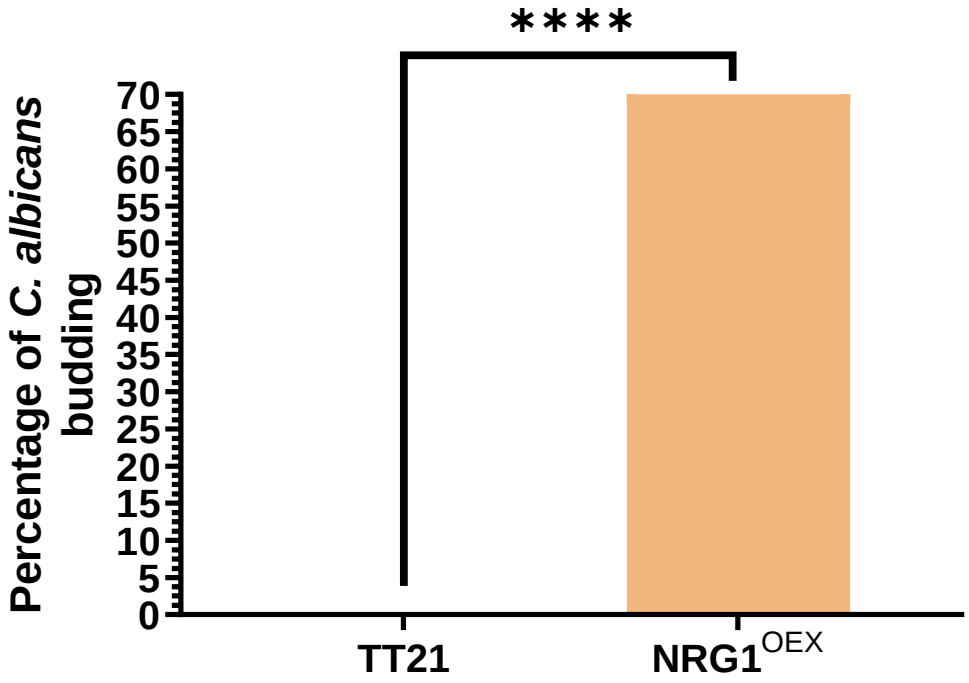

Figure 3.15: Candida albicans yeast-locked cells are budding inside the phagosome. *C. albicans and J774 macrophages at 1:1 ratio were co-incubated for 18 hours. The interaction was monitored by time-lapse microscopy, the results were then analyzed by single cell observations and recording the percentage of cells out of the population forming buds inside the phagosome. **** indicate a p value of ≤0.001.*

3.16 Phagocytosis of *C. albicans* with an *apm4* deletion by murine macrophages.

Phagocytosis is a critical step for pathogen clearance (Newman, Holly, 2001, Case, Samuel, 2016). The results from the investigation of *C. albicans* phagocytosis by murine macrophages concluded that *apm4Δ/Δ* cells are phagocytosed more than Wt cells. The phenotype could be due to multiple reasons including the cell wall composition and the cell size. The increased phagocytosis of cells by macrophages can have an impact on the *C. albicans* virulence as the cells could be recognized and cleared faster by host immune cells.

3.16.1 Cell wall

The exposed β glucan levels were the first to be investigated for their role on phagocytosis. During growth in YPD media no changes in the exposed β glucan levels were observed for either Wt or *apm4Δ/Δ* populations. During interactions with macrophages however the exposed β-glucan levels of *apm4Δ/Δ* cells were lower than Wt which was in agreement with previous reports. Exposed β glucan has been demonstrated to be critical for phagocytosis as it is the main component involved in pathogen recognition (Mora-Montes et al., 2012, Bain et al., 2014b). Here, it was shown that eventhough the exposed β-glucan levels are lower, there was more phagocytosis of the mutant cells (figure 3.2). Interestingly, work in other labs suggested that under some conditions exposed β glucan and chitin can result in increased phagocytosis (Duvenage et al., 2019). This can be used to postulate that chitin recognition can be important for the phenotype. Recognition can be through a chitin specific PRR (so far none identified) or through co-recognition with other cell wall components like glucans and mannans.

A different PRR could be responsible for the phenotype instead of Dectin-1 and the PAMP recognition might be β glucan independent. The mannan organization is different in the *apm4Δ/Δ* mutant, from TEM the mannans appear longer but more disperse around the surface (Knafler et al., 2019). Mannans have multiple pathogen recognition receptors involved in the recognition. There are also some receptors that bind to both mannans and chitin for recognition (Netea et al., 2008, Snarr et al., 2017). Mannans can be of interest as they could possibly be responsible for the increased *apm4Δ/Δ* phagocytosis observed on figure 3.1.

The assay used in this study is different compared to previous investigations. Phagocytosis assays of cells by macrophages were previously used as an indication of exposed β glucan levels while here, β glucan exposure was investigated via staining and immunofluorescence (Gow, N. A. et al., 2007, Bain et al., 2014). Phagocytosis is an indirect measurement, influenced by more than one factor and thus could change the findings resulting in different conclusions.

3.16.2 Size

A different factor that could be influencing phagocytosis is the size of cells. The size of a *C. albicans* cells is between 3 - 8 µm depending on the budding state (Wiles, C.M & Mackenzie, D.W.R, 1987, Aryal Sagar, 2018). Larger cells have more surface area and thus can be potentially recognized and phagocytosed more. Increased surface area could result in a bigger site for attachment of the host cells leading to more phagocytosis. The results from two independent investigations showed that the *apm4Δ/Δ* mutant cells are larger than Wt (figure 3.3).

The budding of cells influences cell size. The budding after overnight cultures is different between the two populations as most of the *apm4Δ/Δ* cells are budding while the Wt cells are not budding (figure 3.4). The budding state become more similar between 3 - 6 hours after incubation in fresh media. It was hypothesized that the phenotypic changes observed are due to changes in the growth signals caused by the mutation as AP-2 is important for the endocytosis of cargoes from the cell surface and for cell polarity (Knafler et al., 2019). The imbalance between secretion and endocytosis could results in changes in the cell budding state (Jones & Sudbery, 2010, Chapa-y-Lazo et al., 2014, Bassilana et al., 2020). This signaling deficiency could influence the ability of cells to switch and result in the phenotypes observed by this study and the one by Knafler (2019).

The volume of *apm4Δ/Δ* cells is larger which indicates a higher surface area. It is hypothesized that there is increased phagocytosis because of the size of cells (figure 3.3). Recent investigations on phagocytosis using different-sized beads concluded that there is no significant difference in the phagocytosis of cells with a similar diameter of beads to Wt and *apm4Δ/Δ* cells. Smaller sizes of cells are phagocytosed more by murine macrophages (Unpublished work from Dr Jaime Canedo's thesis, Johnston lab, University of Sheffield).

These findings suggest that eventhough the mutant cells are larger this does not influence phagocytosis as hypothesized. The cell shape is important however, recent investigations suggested that the ellipsoid shape of pathogens (yeast shape) is phagocytosed slower than spheroids (Paul et al., 2013). This could mean that the phagocytosis rate could be slower for the Wt cells compared to *apm4Δ/Δ* cells but currently no experiments have been performed to understand this. The cell wall is demonstrated to be more important for the phenotype.

3.17 *C. albicans apm4Δ/Δ cell* virulence during macrophage infections.

An important phenotype during host to pathogen interactions is the virulence. The *C. albicans* cells switch to the hyphal morphology and lyse host macrophage (El-Kirat-Chatel & Dufrene, 2012, Hernandez-Chavez et al., 2017, Westman et al., 2018, Westman et al., 2020). The results from single cell observations showed no significant difference in macrophage lysis between the Wt and *apm4Δ/Δ* groups (figure 3.5.a). There were some limitations to the analysis such as that some macrophages were in *Candida* to macrophage microcolonies, and it was hard to quantify lysis as the macrophages could not be observed individually (figure 3.5.c). To ensure that the data were analyzed appropriately the number of microcolonies in each field of view at the end of the time-lapse was quantified (figure 3.5.b). This analysis was with the assumption that macrophages which are part of the microcolony were not live and the microcolonies were a measurement of virulence.

The analysis of microcolonies showed that the Wt cells are significantly more virulent that the mutant. The reduced virulence phenotype observed for *apm4Δ/Δ* cells can be linked to the ability of cells to switch to the hyphal morphology and possibly the expression of other virulence phenotypes such as adhesion, damage, and the production of Candidalysin which are all linked to hyphal morphology switch (Moyes et al, 2015).

3.18 Hyphal switch inside the phagosome and the impact of the environment.

The results from time-lapse observations concluded that *apm4Δ/Δ* cells have a hyphal switch deficiency inside the phagosome (figure 3.7). The macrophages from both SEM and fluorescence images appear less extended during the *apm4Δ/Δ* mutant infections contrary to Wt infected macrophages (figures 3.6 and 3.7.a). Previous investigations suggested that the macrophages infected with hyphae are more stretched due to the hyphae penetrating the membranes, this could suggest that *apm4Δ/Δ* cells do not switch to the hyphal

morphology (El-Kirat-Chatel & Dufrene, 2012). These results are different to the *in vitro* phenotypes previously investigated in the Ayscough lab (figure 3.7.c). In *in vitro* liquid and agar media there was successful hyphal switch, however the *apm4Δ/Δ* mutant hyphae appear shorter and wider than Wt hypha. The differences in hyphal switching in the phagosome are possibly due to the differences in the environment and cell wall composition, some of these factors will be discussed here.

3.18.1 Impact of chitin

The structure of the cell wall can influence hyphal switch as it could introduce less flexibility impacting the cell shape (Garcia-Rubio et al., 2020, Liu et al., 2020). The impact of increased cell wall chitin for the hyphal switching of *apm4Δ/Δ* cells inside the phagosome was investigated using the *apm4ΔΔ,chs3Δ* strain. The results show a partial rescue of the hyphal switch phenotype in *apm4ΔΔ,chs3Δ* indicating a role of increased chitin in the hyphal switch deficiency phenotype. There is an important role of the cell wall composition in the response of hyphal switch in that environment however this does not fully rescue the phenotype. In future studies it would be interesting to understand the other aspects of the *apm4* deletion that result in reduced hyphal switch. There is not a good understanding currently as to how the cell wall composition impacts hyphal induction. It can be postulated that the organization of the cell wall possibly impacts the cell shape but it is not well understood how the mechanism then impacts polarized growth.

3.18.2 Mechanical forces

The environment can influence the *C. albicans* interactions. The mechanical properties of *C. albicans* cells can impact the hyphal switch phenotype. In this study two experiments were used to understand the mechanical properties of cells: 1) invasion assays 2) AFM measuring the cell surface stiffness.

During invasion assays agar of different percentages was used as an indication of invasion potential, this was a preliminary experiment. The results of the assay showed that both Wt and *apm4Δ/Δ* cells can switch to the hyphal morphology at all the agar percentages. An observation from the experiment however was that the *apm4Δ/Δ* cells form shorter hyphae than Wt cells at 4%. This could suggest that *apm4Δ/Δ* cells have hyphal switch deficiencies in stiffer environments, however this was not investigated further or quantified in this

study. In the future the experimental conditions could be improved to mimic the physical conditions of a phagosome using more complex polymers and measure the invasion potential of cells using mathematical calculations, such methodology has been recently developed (Puerner et al., 2020).

The cell wall elasticity of hyphae was measured using AFM. The analysis on figure 3.10 separates the mother from the hyphal tube to study any differences in the mechanical properties of those areas. Wt hyphae show differences in stiffness between the mother and the hyphal tube of the hyphae. The hyphal tube is stiffer than the mother region. The *apm4Δ/Δ* hyphae present no changes in stiffness between the mother and the hyphal tube. The *apm4Δ/Δ* hyphae are also overall softer than Wt. The Wt phenotype can complement previous work on *C. albicans* hyphal cells demonstrating that the active growth site is the hyphal tube and has more trafficking at the tip while the mother is vacuolated, this could possibly be reflected on the cell surface properties of cells (Weiner et al., 2019). The increased stiffness at the tip could suggest that cells have a focused polarized growth and possibly a host invasion potential. The *apm4Δ/Δ* hyphae do not show differences in stiffness between mother and hyphal tube like Wt cells, this could be due to the endocytosis defects previously described by Knafler (2019) the new cell wall material is deposited across the *apm4Δ/Δ* cells rather than on active growth sites. The differences in cell wall elasticity reported for Wt and *apm4Δ/Δ* hyphae provide an indication of the differences in the cell wall of the cells complementing previous work in the Ayscough lab (Knafler et al., 2019). *apm4Δ/Δ* hyphal surface being softer than Wt hyphae could propose that the mutant hyphae have hyphal switch deficiencies in some environments because of the cell wall elasticity. It is currently unknown if there is a link but the cell wall properties of *apm4Δ/Δ* cells could have an impact in the invasion potential at the tip. More experiments on *C. albicans* invasion could provide an insight into the phenotype and show if there is a correlation between the hyphal cell surface stiffness and host invasion.

Further understanding of the mechanical properties of *C. albicans* cells is of interest as it could provide a deeper understanding of the host-pathogen interactions.

3.18.3 Environment

The phagosome environment is harsh and there are different stimuli that can affect survival and growth. Nutrient depletion as well as the harsh environmental pH can be limiting factors to survival and growth of cells (Case & Samuel, 2016, May & Casadevall, 2018). The findings from *in vitro* experiments inducing growth at a range of pH values as well as growth on different carbon sources suggested no significant differences between the Wt and *apm4Δ/Δ* mutant populations (figures 3.11 and 3.12). The cells did not grow as well as on full media however there was still growth in all conditions tested *in vitro*. The results show that cells can potentially grow inside the phagolysosome, the decreasing pH and carbon source do not stop growth.

3.18.4 Phagosome pH supporting the phenotype

To understand further the hyphal switch deficiency phenotype the phagosomal pH was estimated using the Lysosensor Yellow/Blue dye. The methodology used to investigate the phagolysosomal pH was optimised during the study. The mean fluorescence intensity of macrophages was measured at the different conditions. The results indicate a difference in the fluorescence intensity in Wt infected cells compared to *apm4Δ/Δ* infected cells suggesting differences in phagosomal pH. The *apm4Δ/Δ* infected phagosomes are stained similarly to acidic control macrophages suggesting that the phagosomes are not alkalinized.

The phagosome pH has been shown to alkalinize during a *C. albicans* infection, this phenotype is linked to hyphal switch. The evidence so far do not provide a clear understanding of which phenotype drives the other (Vylkova & Lorenz, 2014, Vylkova et al., 2011, Vylkova & Lorenz, 2017, Westman et al., 2018). The results concluded that Wt cells alkalinize the phagosome while *apm4Δ/Δ* cells do not. The *apm4Δ/Δ* phagosome has a similar pH to the control group (figure 3.13). The *apm4Δ/Δ* cells have a mutation on the AP-2 protein which is important for endocytosis. The receptors on the cell surface involved in the alkalinization response can be impacted by the AP-2 mutation and do not respond to the environment in a similar way to Wt cells.

The results could reflect the hyphal switch status of cells in the phagosome. Based on recent investigations, the hyphal switch deficiency of *apm4Δ/Δ* cells results in insufficient force to penetrate the phagosome membrane, resulting in no membrane rupture and leakage of

phagosome components. If the membrane is not leaky then the phagosome pH does not alkalinize (Westman et al., 2018). The data from this investigation could complement the observational analysis data that *apm4Δ/Δ* cells do not switch to the hyphal morphology (figure 3.7).

3.18.5 Section conclusion

Overall, it is concluded that the mutant cells do not switch to the hyphal morphology, these results can be supported by the SEM imaging, single cell observation analysis as well as the phagosomal pH experiment. The results from *in vitro* investigations suggested that the environmental factors inside the phagosome do not result in growth defects when the Wt and *apm4Δ/Δ* cells are compared. The cell wall composition and trafficking could be the main factors contributing to the hyphal switch deficiency phenotype inside the phagosome.

3.19 Discussion: Phagosome proliferation

During the investigation for the interactions between *C. albicans* and the macrophage phagosome it was observed that the *apm4Δ/Δ* cells were not switching to the hyphal morphology but were forming buds instead (figure 3.14). The percentage of the population growing new buds inside the phagosome was quantified and the results matched the observations. There were no previous investigations suggesting of such a phenotype, recently however the Scherer's (2020) investigation described a similar phenotype during infections of zebrafish embryos with yeast-locked *C. albicans* (Scherer et al., 2020). These findings suggest that the phenotype observed is not an *in vitro* artifact. The data from this study also showed that proliferation phenotype is present in cells with hyphal switch deficiencies (figure 3.15). NRG1^{oex} cells (yeast-locked) were also budding inside the phagosome, this does not happen in the parental TT21 cells.

It can be concluded that inside the phagolysosome *C. albicans* cells have two choices; to switch to the hyphal morphology and invade host tissue or to remain as yeast and grow intracellularly. The studies in the zebrafish and mouse models revealed that cells locked in the yeast morphology are avirulent (Lo et al., 1997, Seman et al., 2018). The intracellular growth could be linked to host mortality which might not be significant enough to be observed during *in vivo* experiments.

The mechanism could be interest as the increased growth could be resulting in enough force onto the phagosomal membrane causing leakage and eventually macrophage death. The phenotype can also be of interest during *C. glabrata* studies as the cells also do not switch to the hyphal morphology, *C. glabrata* cells could be using a similar proliferation mechanism in combination with other factors to be virulent during interactions with the host.

It is currently not well understood whether this phenotype is beneficial to cells for virulence and dissemination *in vivo*. The proliferation could be a phenotype of commensalism.

3.20 Chapter 3 Conclusion

The results of this study conclude that *apm4Δ/Δ* cells are recognised and taken up more by host macrophages which is not linked to β glucan exposure but rather the cell surface area and other cell wall components. Overall, it is a complex phenotype which might be due to the exposure of mannans and chitin rather than the traditional β glucan pathogen recognition pathway. Eventhough, the cells are taken up more by murine macrophages the cells are not cleared and can result in host cell death and proliferate in the environment.

The *apm4Δ/Δ* mutation results in decreased virulence linked to the hyphal switch deficiency phenotype presented inside the phagosome. The hyphal switch deficiency phenotype is linked to the increased chitin levels of *apm4Δ/Δ* cells. It is hypothesised that increased chitin influences the cell shape. There is a link between the cell wall composition and hyphal switch. Cells with morphology switch deficiencies grow inside the phagosome, this phenotype could be relevant for the studies of virulence and dissemination of other *Candida spp.* such as *C. glabrata*.

Chapter 4: *Investigating the impact of Candida albicans apm4 deletion on virulence during zebrafish infections*.

4.1 Chapter 4 Introduction

A deficiency to switch to the hyphal morphology is associated with decreased virulence during host interactions (Lo et al., 1997, Seman et al., 2018). As previously described, *Candida apm4Δ/Δ* cells which are unable to assemble the AP-2 endocytic adaptor, and which have resulting changes in their cell wall, form morphologically aberrant (shorter and wider) hyphae *in vitro* (Knafler et al., 2019). Interestingly, and as shown in Chapter 3, following uptake by macrophages *apm4Δ/Δ* cells show reduced switching to the hyphal morphology, though the mutant *Candida* do appear to continue to proliferate within the phagosome environment. To understand the impact of the defect in the AP-2 adaptor on *C. albicans* pathogenesis, an *in vivo* model was used.

A recently developed *in vivo* model that allows the observation of host-pathogen interactions in real time is the zebrafish embryo infection model. Zebrafish *Danio rerio* are proving to be a useful and complementary model of human disease as they demonstrate a good conservation of function from the level of genes to whole organs. They are small, transparent in the embryo stage which facilitates live cell imaging, easy to handle and relatively cheap to use in comparison to rodents. The generation and availability of many genetically modified fish strains, harbouring mutations or fusion tags, also facilitates analysis at multiple developmental stages (Maccallum, 2012, Tobin et al., 2012, Ruzicka et al., 2019).

The zebrafish immune system shows similarities to that in humans (Renshaw & Trede, 2012). The zebrafish adaptive immune response does not develop until 4 weeks post fertilization. This timing is beneficial as it allows researchers to focus on the innate immune response during host-pathogen interactions in the embryo. The anatomy of zebrafish allows for multiple infection routes and different types of infection; disseminated and different tissue specific infections are possible, making it a good model to use for infections (Tobin et al., 2012).

Zebrafish have been used by several labs to study *Candida albicans* host-pathogen interactions. Previous studies have described that the fungal burden can be used as a prediction of whether the infection will be cleared by the host. Increased fungal burden is an indication of no clearance and results in reduced host survival (Brothers et al., 2011, Gratacap et al., 2017). The transparent nature of zebrafish in early embryos allowed clear visualization of the impact of yeast and hyphal cells during Candidiasis. In mammals, the yeast morphology is critical for dissemination through the host. *C. albicans* that are unable to undergo hyphal switch are locked to the yeast morphology and disseminate. However, they are not as virulent as the hyphal morphology which is important for tissue invasion (Seman et al., 2018). It was recently reported that *Candida* cells in yeast form proliferate inside zebrafish phagolysosomes over time, and they utilise macrophages for their dissemination (Scherer et al., 2020).

In this study, it was concluded that inside the phagosome environment the *apm4Δ/Δ* cells do not switch to the hyphal morphology but instead grow in the phagosome. It was hypothesised that these phenotypes would have an impact on the pathogenicity of the fungus during *in vivo* interactions as hyphal-deficient *C. albicans* have been reported to be avirulent (Lo et al., 1997, Seman et al., 2018). In this chapter the zebrafish model of infection was used to address the findings from the previous chapters and investigate whether *Candida* cells with defects in endocytic recycling caused by the *apm4* deletion alter host survival, fungal burden, dissemination in the host, and host immune responses.

Chapter 4 Results

4.2 Impact of the *apm4* deletion on virulence in zebrafish.

In vitro apm4Δ/Δ cells can switch to form hyphae, but the hyphae are shorter and wider than those formed by wild type cells. During interactions with macrophages the *apm4Δ/Δ* cells were less able to switch to the hyphal morphology and caused a lower level of reduced macrophage lysis and death compared to Wt *Candida* (Chapter 3). Many other studies have shown that reduced hyphal switching is linked to lower virulence in mouse models (Lo et al., 1997, Seman et al., 2018). Here we hypothesized that the inability to effectively switch to morphologically normal hyphae would reduce killing in a zebrafish model. Therefore, overnight cultures of *C. albicans* were used to infect zebrafish 1 day post fertilisation (dpf).

The virulence was evaluated by the survival of embryos and death was assessed by cessation of heartbeat. The survival was monitored for up to 4 days post infection (dpi) as previously established to be sufficient to see virulence (Bojarczuk et al., 2016) (Section 2.4.2.2). The injection control group showed the highest level of survival (figure 4.1). Zebrafish infected with Wt *Candida* showed only about 30% survival after 4 days post infection, with a dramatic reduction in survival between two and three days. The *apm4Δ/Δ* infection was less virulent with more than 80% of zebrafish still viable after four days.

Zebrafish embryos were also visually inspected for the appearance of hyphae at the surface of the organism. The emergence of hyphae was only seen in the case of the embryos infected with Wt *C. albicans* (figure 4.2) and not in *apm4Δ/Δ* infected embryos (figure 4.3). The *apm4Δ/Δ* infected embryos did not have any visible hyphae however heart oedemas were a common phenotype of the infection.

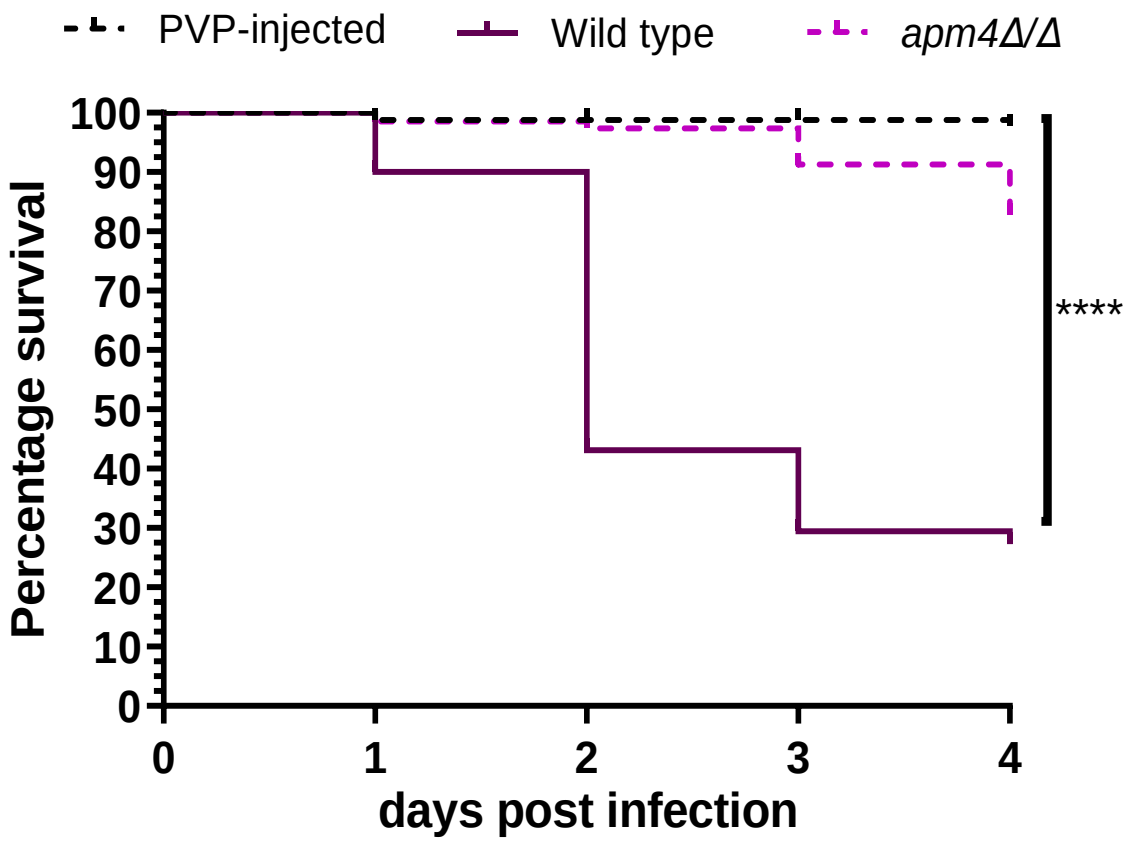

Figure 4.1: Deletion of apm4 in C. albicans results in increased zebrafish survival. *Nacre zebrafish embryos at 1 dpf were injected with 500 cfu of C. albicans in the caudal vein. The embryos were monitored for survival up to 5 dpf. Survival was assessed by cessation of heartbeat. The number of surviving embryos was counted every day until 4 dpi. The graph represents survival from 3 biological replicates. The zebrafish were infected the Wt (solid purple line), apm4Δ/Δ (pink dotted line) and the PVP control (purple dotted line). Kaplan-Meier survival analysis concluded a p = <0.0001 from an n=90 embryos/group signified using ****.*

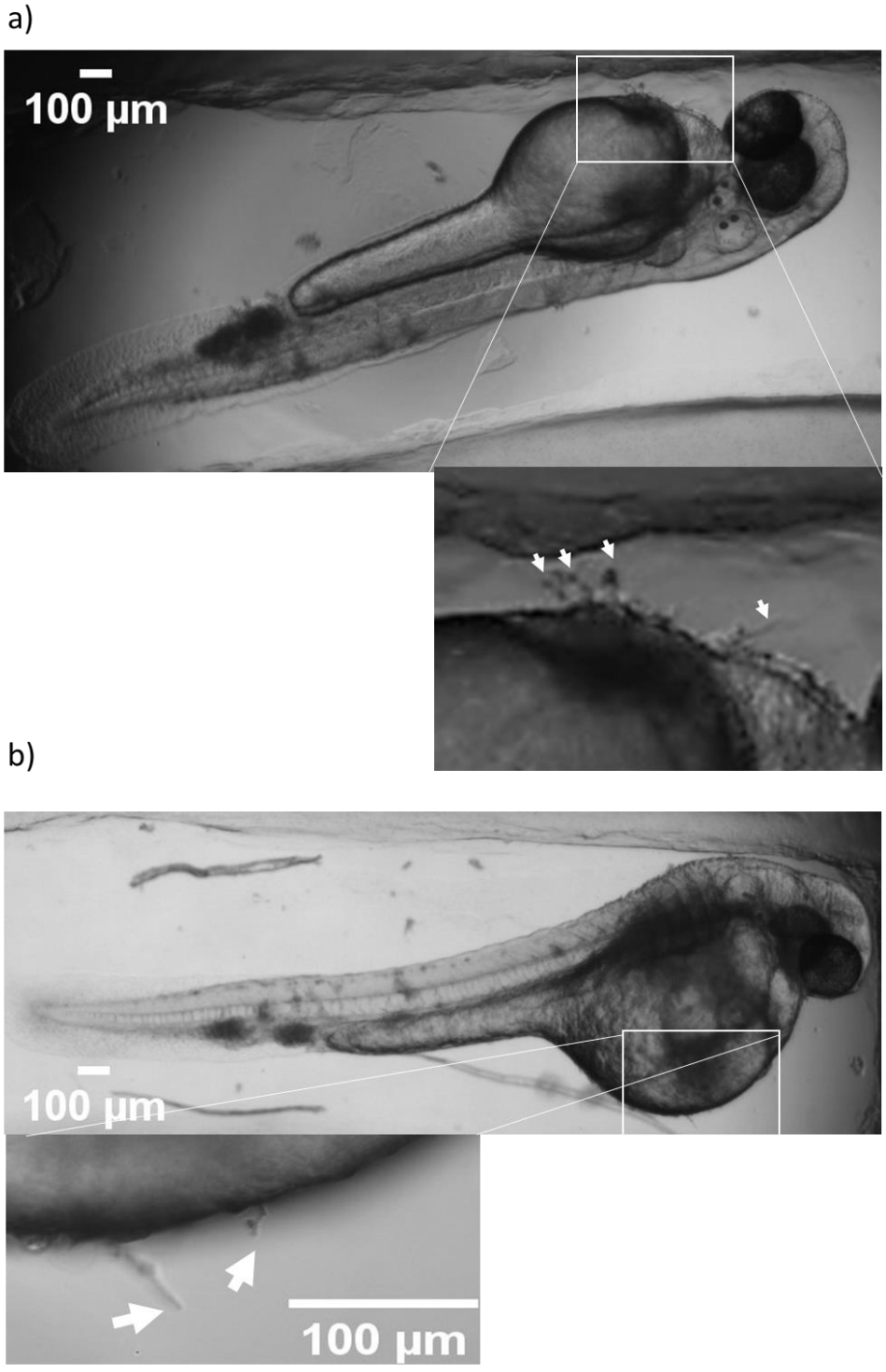

Figure 4.2: Zebrafish infected with wild type C. albicans phenotypes. *Nacre zebrafish embryos at 1 dpf were injected with 500 cfu of C. albicans in the caudal vein. Images of the infected embryos at 1 dpi were captured to observe pathogenicity. Embryos a and b show signs of Wt cells infection with C. albicans cells in the vessels and hyphae penetrating the*

embryo tissue. The zoomed panels focus on areas with hyphal growth, white arrows point to hyphal cells.

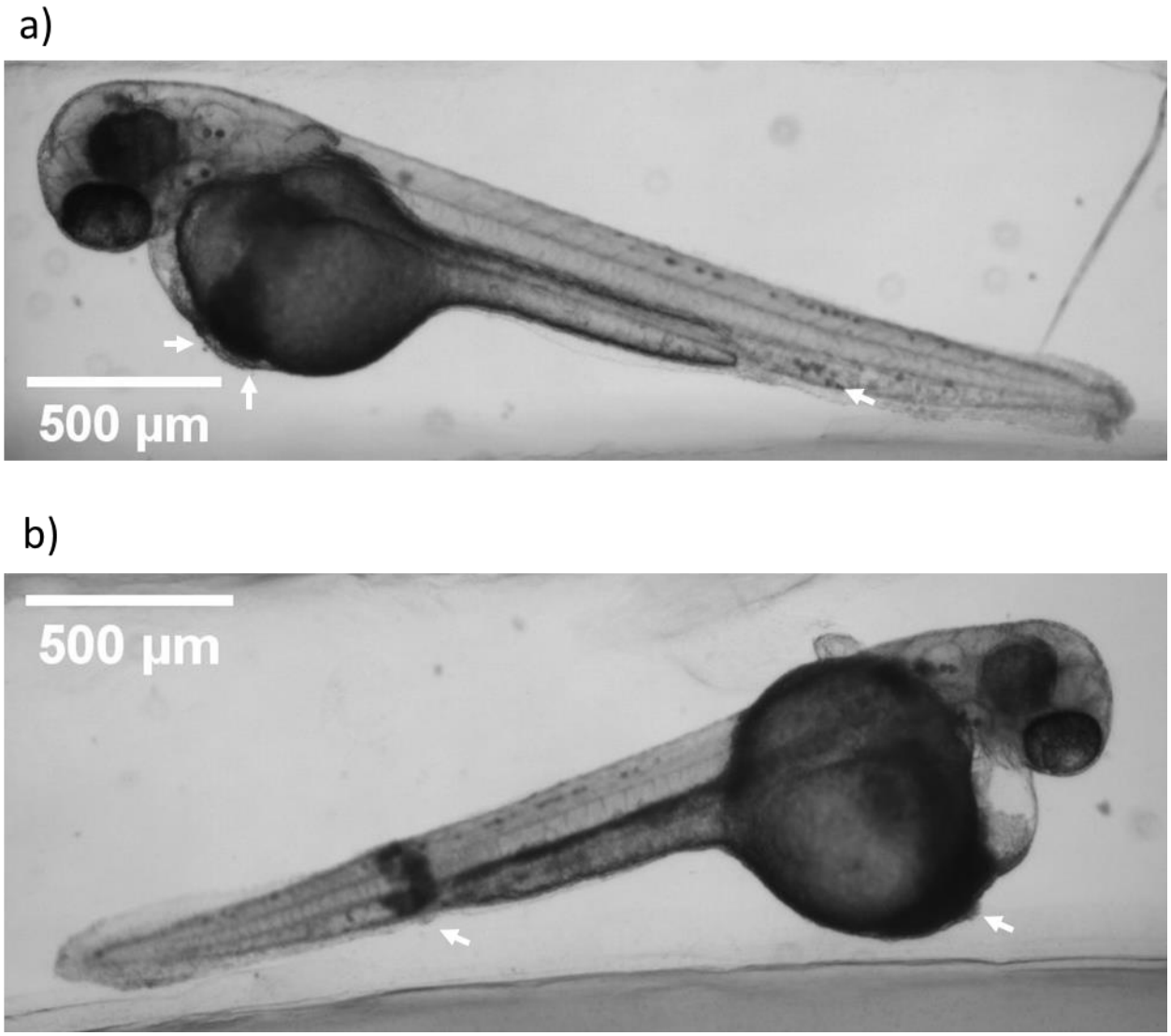

Figure 4.3: Zebrafish infected with apm4Δ/Δ C. albicans phenotypes. *Nacre zebrafish embryos at 1 dpf were injected with 500 cfu of C. albicans in the caudal vein. Images of the infected embryos at 1 dpi were captured to observe pathogenicity. Embryos a and b show signs of apm4ΔΔ/ infection with C. albicans cells in the vessels, no hyphal cells were observed penetrating the embryo were observed. White arrows point towards sites of infection visible where no hyphal switch was observed.*

4.3 Impact of the *apm4* mutation on fungal burden

In order to determine whether the decreased virulence phenotype of *apm4Δ/Δ* cells was due to clearance of the *Candida* infection by the zebrafish, the total fungal burden of infected embryos was investigated. To facilitate visualisation of the *C. albicans*, the cells that were injected into the embryo were the strains that expressed GFP (Figure 2.2). Nacre embryos were injected at 1 dpf with 500 cfu of *C. albicans*. This is the same number of cells that were used for survival analysis described in the previous section. The fungal burden per embryo was measured using fluorescence microscopy with the fluorescence intensity per embryo being used to indicate the level of *C. albicans* in the embryo. The burden was measured over three days for zebrafish infected with both Wt and *apm4Δ/Δ* GFP tagged strains (Section 2.4.3.2.1). As shown, the fungal burden increases over time in both infection groups (figure 4.4.a). The level of increase is also similar. Through the course of the experiment the n number for Wt infected embryos decreases as the embryos did not survive the infection. Statistically there is a significant increase in the fungal burden for each group between days post infection but no statistical significance between the Wt and *apm4Δ/Δ* infection groups was observed. While the increase in fungal burden with the Wt *Candida* was expected, the data indicated that even in the zebrafish infected with the *apm4Δ/Δ* strain the fungal burden continues to increase despite the lack of visible hyphae forming and without impacting greatly on survival.

A complementary assay was then used to study the fungal burden. This used an approach commonly used in other animal models where fluorescence measurements are not possible and is based on the principle that the entire fungal burden within an organism can be extracted and can give rise to a measurable number of colonies. When 500 cfu of *C. albicans* were injected into zebrafish embryos there was a high mortality during Wt infections (figure 4.1). In the fungal burden experiments the goal was to keep the embryos live and not inject them with a high burden, this would allow for measurements of burden from live embryos and would allow for the zebrafish immune system to possibly respond and clear the infection. To allow for this a lower fungal burden was used in the experiment. Nacre embryos were infected at 1 dpf with 100 cfu of *C. albicans* in the Caudal vein. The infected zebrafish embryos from 1-3 dpi were dissociated with liberase enzymes, dead embryos were not included in the experiment (Section 2.4.3.2.2). The dissociated embryos were plated on

YPD plates with appropriate antibiotics. The number of colonies was counted after growth and the fungal burden was estimated based on serial dilutions. The fungal burden from this assay is presented on figure 4.4.b. As in the previous assay the fungal burden range appears broadly similar for both infection groups. In some cases, there was some clearance, this was based on the cfu which is below the number of cells used for the infection, but this is similar for Wt and *apm4Δ/Δ* infected embryos. For both infections the burden was overall higher at 3 dpi. An increased burden is often associated with host death but in this experiment both Wt and *apm4Δ/Δ* infections, this was not the case presumably because of the lower level of infecting cells injected and because the time course is limited to 3 dpi.

Overall, the findings from both investigations demonstrate that both Wt and the *apm4Δ/Δ* strains grew inside the host and despite being less virulent (figure 4.1) *apm4Δ/Δ* cells were not cleared more effectively than Wt cells by the host.

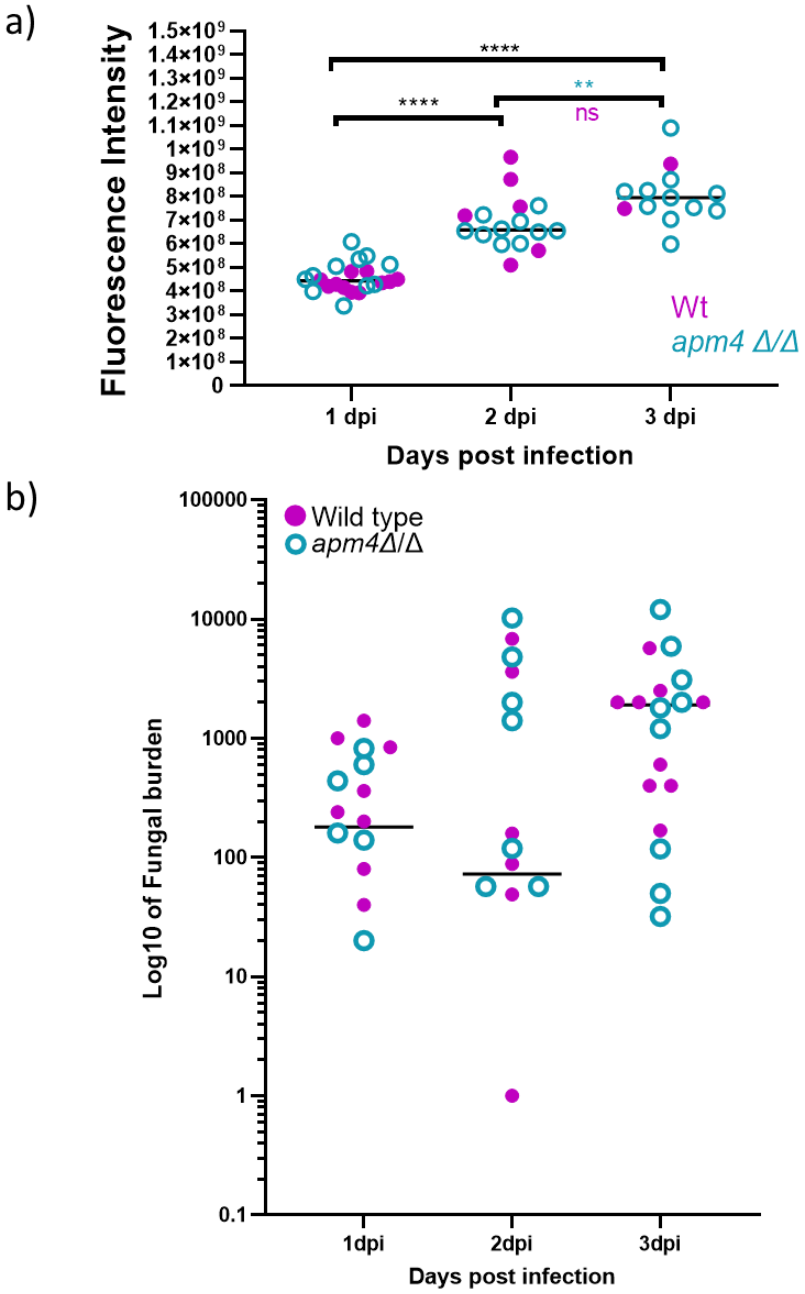

Figure 4.4: C. albicans with a deletion of apm4 are not cleared by the host. *Nacre zebrafish embryos at 1 dpf were injected with C. albicans in the caudal vein. There were 3 biological replicates per experiment. The purple dots represent Wt injected embryo burden, and the turquoise dots represent the burden from apm4Δ/Δ injected embryos. a) The fungal burden of embryos infected with 500 cfu was assessed using fluorescence. Embryos were imaged at 1,2 and 3 dpi. Candida cells injected into embryos expressed cytoplasmic GFP and thus the fluorescence emitted during microscopy represented Candida cells. A Z-stack was captured for each embryo and the fluorescence intensity analysis was conducted using the Maximum*

Projection of the images. The statistical significance analysis revealed a p value of of ≤0.01 for ** and >0.0001 for ****. *b) The fungal burden from embryos with 100 cfu was quantified by lysing the embryos and plating them on YPD with antibiotics. 2 days post plating the number of colonies was counted and an estimated fungal burden for each embryo was calculated.*

4.4 Microcolony sizes and morphology during zebrafish infections

The previous analysis was focused on the overall fungal burden which was shown to increase over the infection time course for both the Wt and *apm4Δ/Δ* infections. It was then of interest to observe the fate of single cells within the host following the infection. During microscopy analysis microcolonies made up of fluorescent *C. albicans* interacting with zebrafish host immune cells could be observed as bright spots in the bloodstream (figure 4.5). Qualitative visual inspection suggested that the size of microcolonies appeared to be different between the two infection groups with the *apm4Δ/Δ* microcolonies appearing larger. To investigate further a KDRL zebrafish line was used. Embryos of this fish line have fluorescent blood vessels and were injected with 100 cfu of *C. albicans* into the caudal vein. A low burden was used to ensure that the embryos would survive the infection and to also allow for the possibility of clearance. The infected embryos were then imaged live using the Light Sheet microscopy at 1 and 2 dpi (Sections 2.4.3.4 and 2.5.1.4). The images were reconstructed and analysed manually to measure the size of microcolonies and to observe the microcolony morphologies. In figure 4.6 images of the infected embryos and the microcolonies in blood vessels are presented. Images were captured to present the morphology of the microcolonies over a 180^{o} view. The Wt microcolonies overall appeared less smooth than the *apm4Δ/Δ* microcolonies. It was considered that roughness of the microcolonies could be a sign of hyphal morphology and smoothness could indicate an overall yeast morphology (figure 4.6 panels i-iv). The appearance of microcolonies suggests differences between the two infections. The Wt microcolonies appeared to contain more hyphal cells (figures 4.6.i and 4.6.ii) while the *apm4Δ/Δ* microcolonies contained more yeast cells (figures 4.6.iii and 4.6.iv). At 1 dpi *apm4Δ/Δ* microcolonies were significantly larger than the Wt microcolonies however there was no significant difference in the microcolony

size at 2 dpi (figure 4.7). The Wt microcolonies significantly increased in size between 1 and 2 dpi.

The results from the investigation showed that the greatest difference in microcolony sizes between the Wt and the *apm4Δ/Δ* mutant was observed within 1 dpi. Time-lapse microscopy of infected KDRL embryos was then used to investigate the interactions between 2 and 18 hours post infection to look at differences in microcolony sizes. The embryos were allowed recovery post injection for approximately 1 hour before being used for imaging. The microcolony sizes at different timepoints were counted manually and are presented on figure 4.8.a. The relative size of Wt and *apm4Δ/Δ* microcolonies did not significantly change over time but the distribution of sizes did change. Over time the percentage of larger microcolonies increased for both strains (figure 4.8.b). There were fewer microcolonies with area between 0-200 μm^2 and an increasing number of microcolonies between 200-400 μm^2. The distribution of microcolony sizes was similar at 18 hpi however as observed by the full dataset (figure 4.8.a) some of the *apm4Δ/Δ* microcolonies were larger in size compared to Wt microcolonies.

As demonstrated in the previous sections the *apm4Δ/Δ* cells are not simply cleared by the host. In fact, the microcolonies of yeast and immune cells were larger when the *apm4Δ/Δ* mutant *C. albicans* were injected compared to Wt microcolonies. It was observed that *apm4Δ/Δ* microcolonies were not hyphal but had a similar size as hyphal Wt microcolonies.

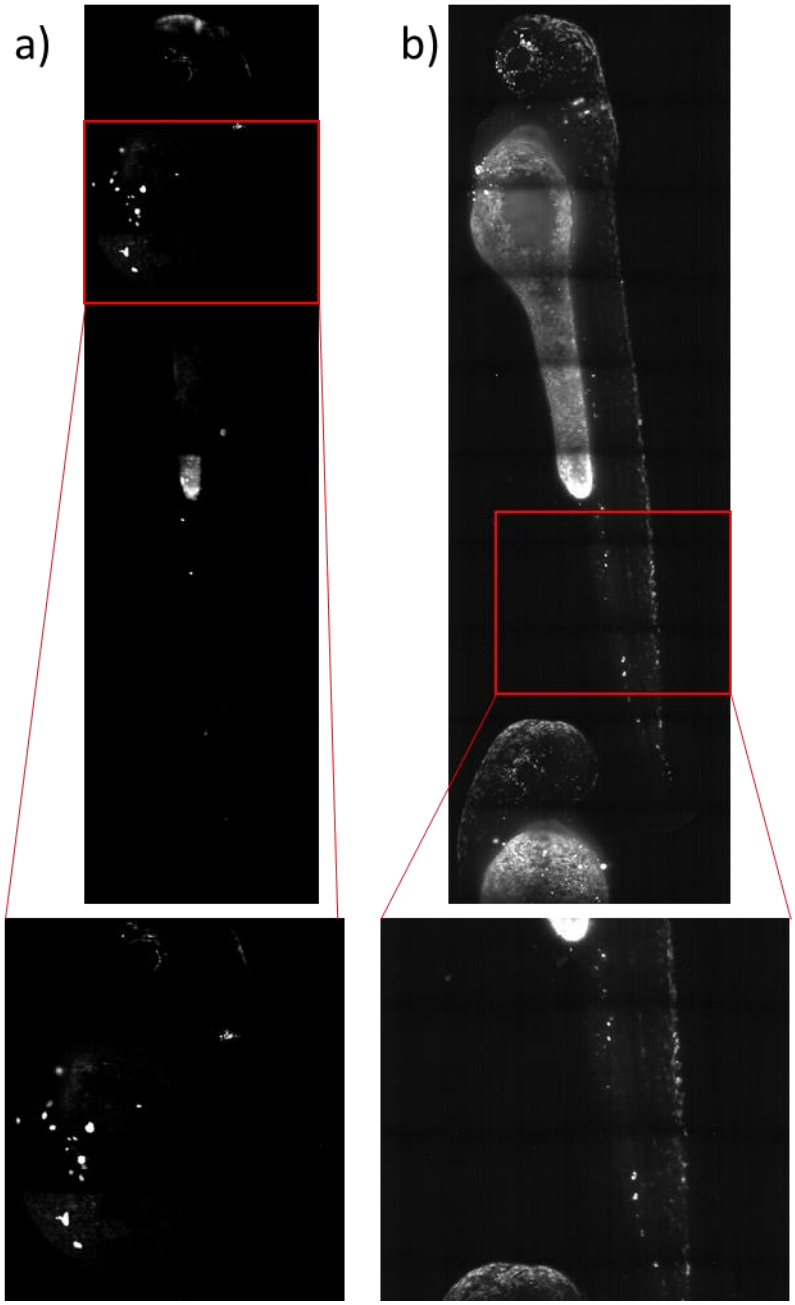

Figure 4.5: Microcolonies during zebrafish infections are different between infection groups. *Zebrafish embryos with fluorescent blood vessels at 1 dpf were injected with 100 cfu of C. albicans in the caudal vein. The embryos were allowed injection recovery before imaging at 1 dpi. The embryos were imaged using the Light Sheet microscopy. Images of zebrafish embryos captured by the Light Sheet microscopy are presented. The C. albicans microcolonies are presented in the Z project of the embryos. The zoomed panels show the areas with a high number of microcolonies. a) apm4Δ/Δ infected embryo b) Wt infected embryo.*

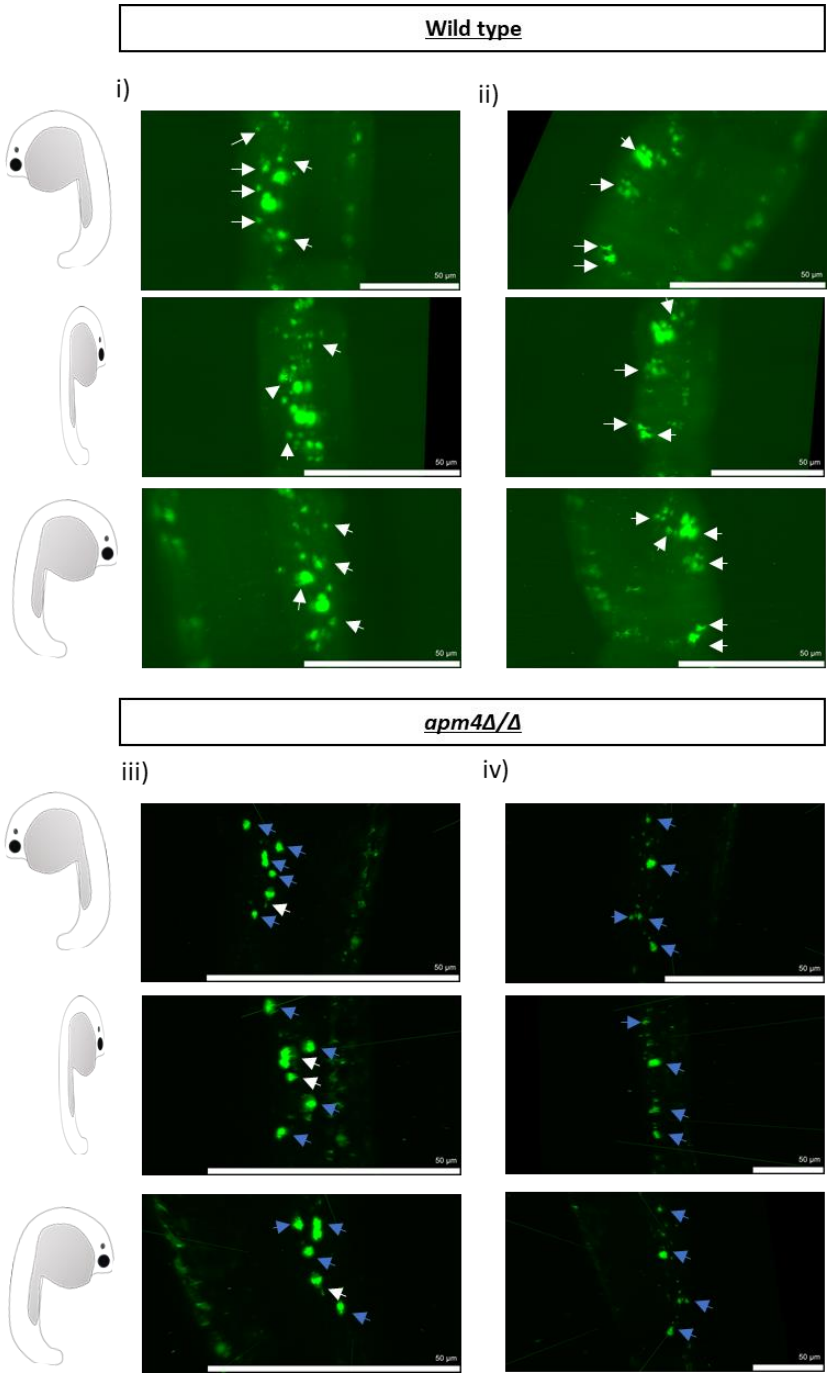

Figure 4.6: The morphology of microcolonies is different between Wild type and apm4Δ/Δ during zebrafish infections. *Zebrafish with fluorescent blood vessels at 1 dpf were injected with 100 cfu of C. albicans in the caudal vein. The embryos were allowed injection recovery before imaging. The embryos were imaged using the Light Sheet microscope at 1 dpi. Images from the experiment showing the microcolony morphologies as a 180^{o} view. Panels i and ii present Wt microcolonies while iii and iv present apm4Δ/Δ microcolonies. The white arrows*

point to not smooth microcolony regions that look like hyphae and blue arrows show smooth microcolonies that appear to have more yeast cells. The scale bars represent 50 µm.

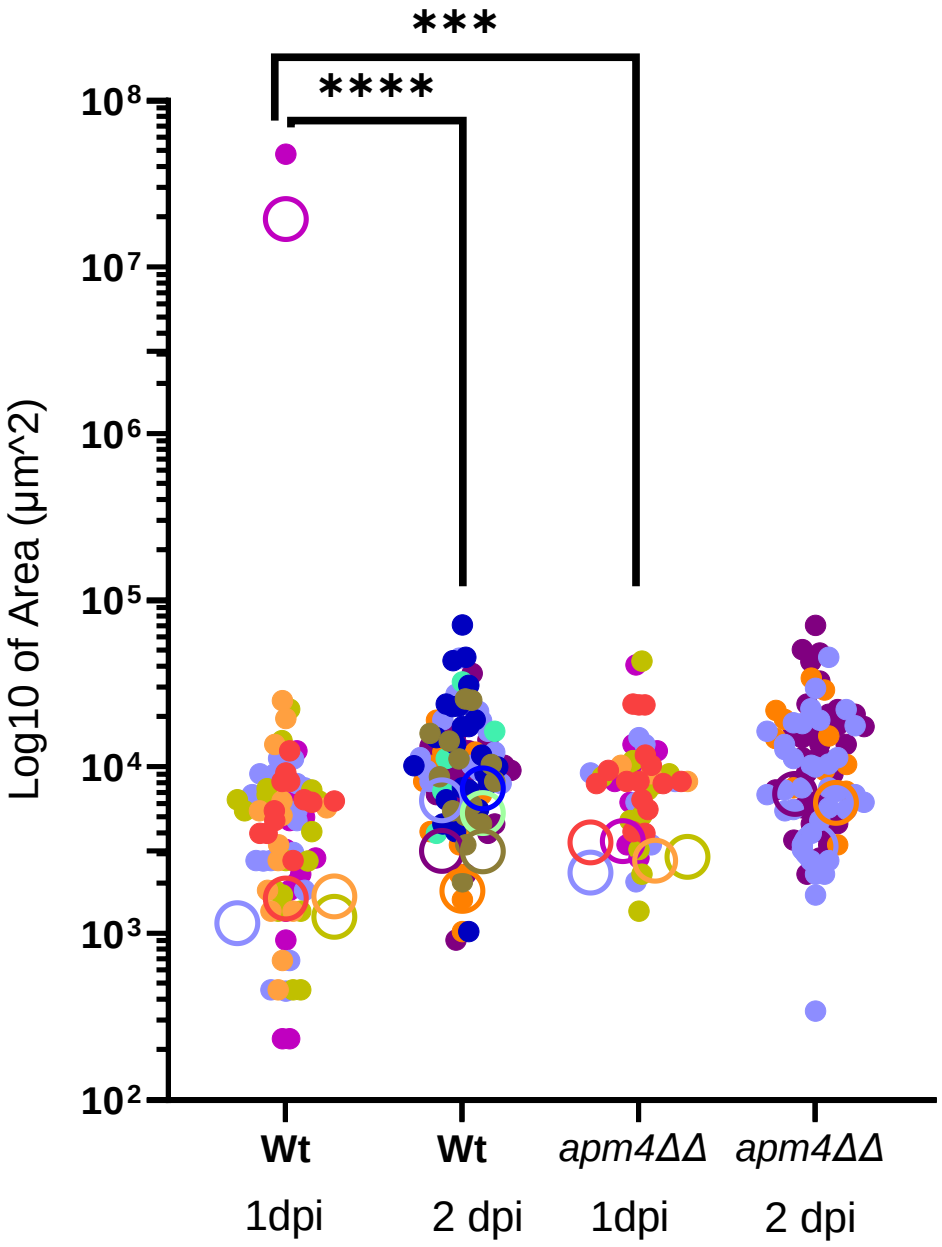

Figure 4.7: The size of microcolonies during zebrafish infections is different between infection groups. *Zebrafish embryos with fluorescent blood vessels at 1 dpf were injected with 100 cfu of C. albicans in the caudal vein. The embryos were allowed injection recovery before imaging at 1 dpi and 2 dpi. The embryos were imaged using the Light Sheet microscopy. The images were reconstructed and converted. The sizes of microcolonies were*

*manually analyzed through the drawing and measurement tools in FIJI. The n ≤ 5 per group. The results are presented in scatter plots each color represents microcolonies from a different zebrafish embryo. The larger circles represent the average microcolony size for each embryo. The Log10 of the microcolonies area from embryos imaged at 1 and 2 dpi for both infections are presented in the Scatter Plot. The size of microcolonies is defined as the area. The black line represents the average area from all the microcolonies analyzed, each color represents a different embryo n<5. The statistical analysis used was non-parametric multiple comparisons One-way ANOVA. *** p=0.0007 and **** p=<0.0001.*

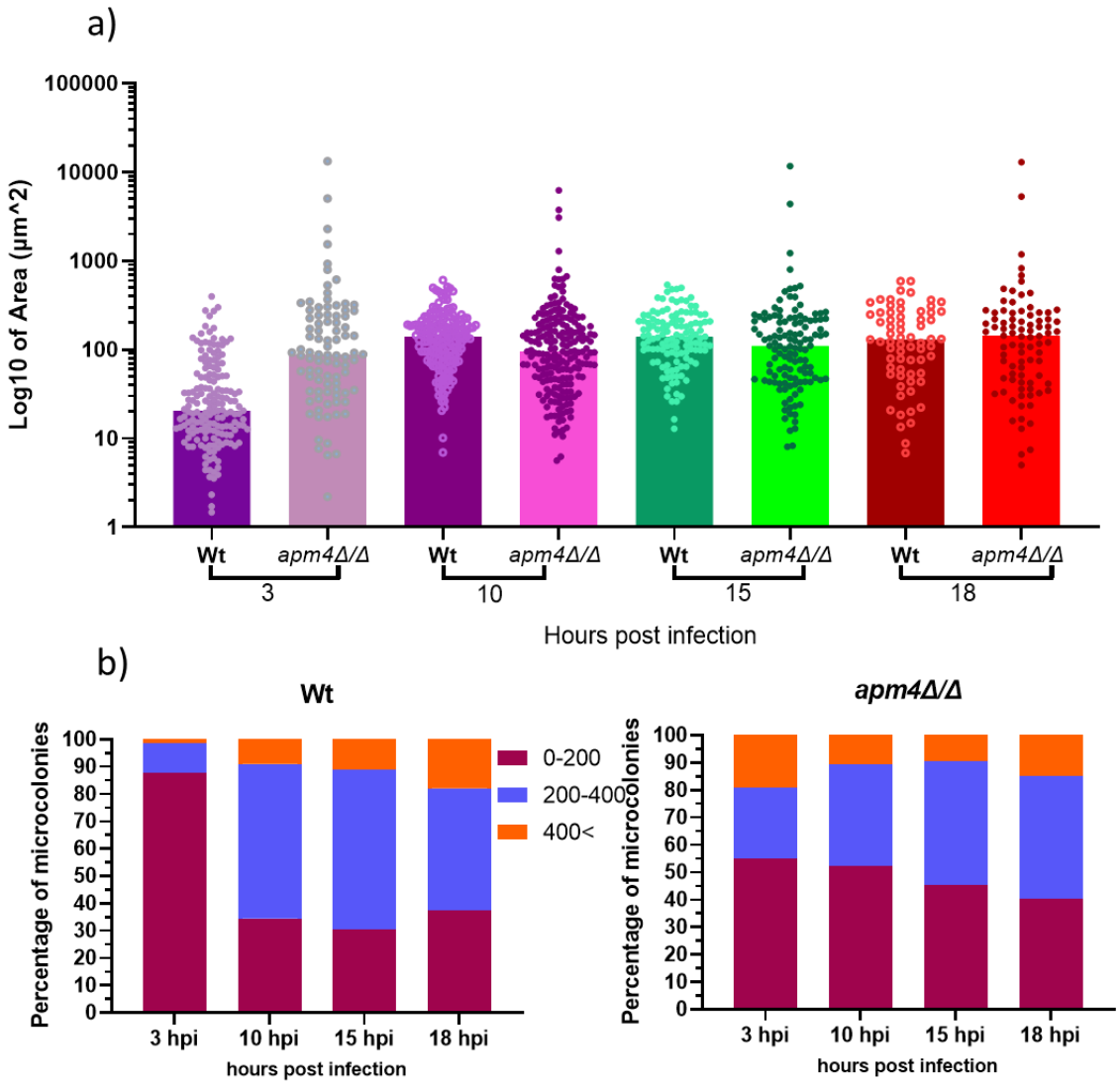

Figure 4.8: Microcolony size changes through the infection. *Zebrafish embryos with fluorescent blood vessels were injected with 100 cfu of C. albicans in the caudal vein at 1 dpf. The embryos were allowed injection recovery for 1 hour before time-lapse imaging. The*

embryos were mounted and imaged every 7 minutes for a maximum of 18 hours post infection. Z stacks of the whole embryo were captured at each timepoint. The time-lapses were analyzed for microcolony sizes over different timepoints, counting the microcolony area. a) The results are presented as a Scatter plot of all the individual values and a bar chart for the median, the area is presented as a Log10. There was no statistical significance between the groups p = ≥ 0.05. b) Using histograms binned for 0-200, 200-400 and 400< µm^2 the proportion of microcolonies at different sizes was calculated for each infection group. The results are presented in bar charts.

4.5 Impact of the *apm4* mutation on IL1-β expression.

The data above demonstrate that *apm4Δ/Δ* cells were not cleared by the host as there was an increase in fungal burden and the microcolony sizes increase. It was of interest to investigate the immune signals and their expression to understand if there was a difference between infections with Wt and *apm4Δ/Δ* cells. During interactions with pathogens, host immune cells are stimulated by the Pathogen Associated Molecular Patterns (PAMPs) on the pathogen cell surface and internally trigger downstream responses to fight against the infection. The presence of *C. albicans* can trigger various signals such as IL-1β, IL-6, 10 and 17 as well as TNF-α and other inflammation signals (Whiley et al., 2012, Wagener et al., 2014, Munawara et al., 2017).

The inflammatory signal IL-1β was investigated. IL-1β and Reactive Oxygen Species are important for the clearance of phagocytosed pathogens (Benmoussa et al., 2017). The cytokine is stimulated further by the production of Candidalysin (Kasper et al., 2018). In addition, IL-1β is an important signal for macrophage pyroptosis. A recent publication suggested that expression of the gene *CHS3* could be responsible for pyroptosis (O'Meara et al., 2018). It was shown previously that *apm4Δ/Δ* cells had increased levels of Chs3 on the cell surface (Knafler et al., 2019). It was therefore hypothesized that this could trigger increased levels of IL-1β expression, pyroptosis and possibly lead to the lack of clearance phenotype observed for the *Candida* mutant.

Zebrafish embryos producing GFP under the promoter IL-1β (meaning that GFP is produced only when IL-1β is expressed) were infected with 100 cfu *C. albicans* and the fluorescence

expression was quantified over time as a measure of IL-1β induction (Section 2.4.3.3). The fungal burden was low to allow for zebrafish survival and for the induction of an immune response over time. The fluorescence signal was from IL-1β expression and the results were normalised to the control injection group (n>30 embryos per condition). The data indicate that there was no statistically significant change in IL-1β levels over the time course of the experiment for either Wt or mutant (figure 4.9). Thus IL-1β expression a factor influencing the lack of clearance phenotype in zebrafish embryos infected with the *apm4Δ/Δ* mutant as the immune stimulation is similar during both *C. albicans* infections.

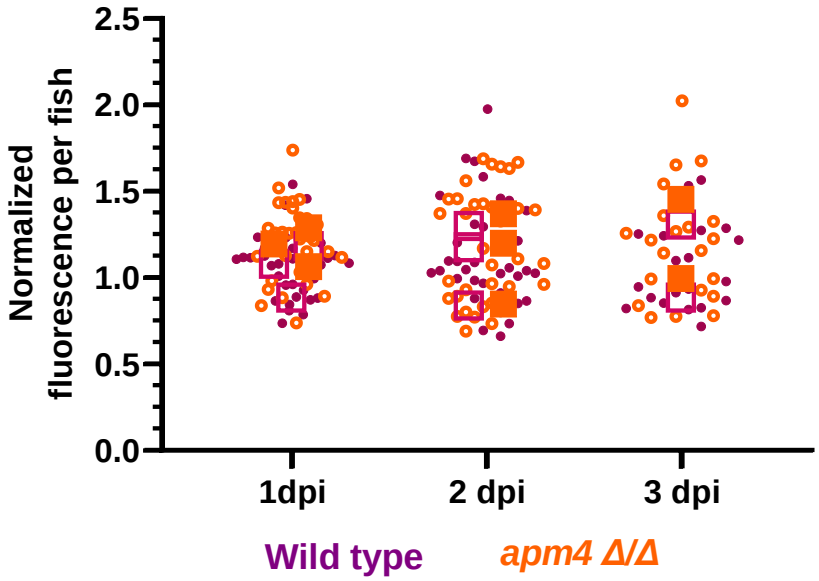

Figure 4.9 : The IL1-ϐ expression in infected zebrafish embryos shows no relative difference between the infection groups. *IL-1ϐ GFP expressing zebrafish embryos at 1 dpf were injected with 100 cfu of C. albicans in the caudal vein. The embryos were monitored for IL-1ϐ induction at 1,2 and 3 dpi through fluorescence microscopy. The expression was quantified using fluorescence intensity per fish and the results were normalized using the control injected embryos. The data were collected from 3 biological replicates and were statistically analyzed using a one-way ANOVA indicating no significant difference between the groups p = ≥ 0.05. The SuperPlot presents the IL-1ϐ expression of embryos infected with Wild type (purple) and apm4Δ/Δ (orange) C. albicans. Each small circle represents an*

individual embryo, the larger squares are the average expression intensity of each biological replicate (n>30 per condition).

4.6 Impact of the *apm4* deletion on the α-nitrotyrosine expression.

Recent investigations suggested that increased chitin levels have an impact on the levels of nitric oxide production resulting in reduced clearance. Specifically increased levels of chitin influence iNOS (inducible nitric oxide synthase) production resulting in reduction of NO levels (Wagener et al., 2017). The role of NO levels in the zebrafish model was investigated through immunostaining for α-nitrotyrosine induction, to test the hypothesis that the increased level of chitin in *apm4Δ/Δ* cells could lead to reduced NO production and facilitate its continued infection of the host. This experiment was undertaken in collaboration with Dr Ffion Hammond (Elks lab, University of Sheffield). Nacre embryos at 1 dpf were infected with 500 cfu of *C. albicans* allowed recovery for 1 day before being fixed and immunostained for α-nitrotyrosine (Section 2.4.3.5). The embryos were infected with a high fungal burden as the experiment was not for a long period of time and the mortality of embryos up until 1 dpi was not very high (figure 4.1). The embryos were imaged using confocal microscopy and the expression was quantified from the fluorescence. Images from the immunostaining are presented on figure 4.10.a, the α-nitrotyrosine appears reduced during a *C. albicans* infection. As expected, based on previous experiments, more hyphal cells were observed in the Wt infection images compared to *apm4Δ/Δ* infection images. The results for α-nitrotyrosine levels from the infection of 3 biological replicates are presented on figure 4.10.b. The overall response of the infection is similar to the characterised phenotype where immune cells infected with *C. albicans* express less α-nitrotyrosine (Wagener et al., 2017). There was no significant difference between a Wt and an *apm4Δ/Δ* infection.

The immune response was similar for both infection groups at the conditions tested. At 1 dpi when the embryos were fixed, it was the timepoint before the sudden zebrafish embryo death caused by a Wt infection. The immune responses were expected to be different as the Wt infected embryos were undergoing an infection leading to high mortality while the *apm4Δ/Δ* embryos even though they were infected there was low mortality. The results could also show that the α-nitrotyrosine response is independent of host mortality.

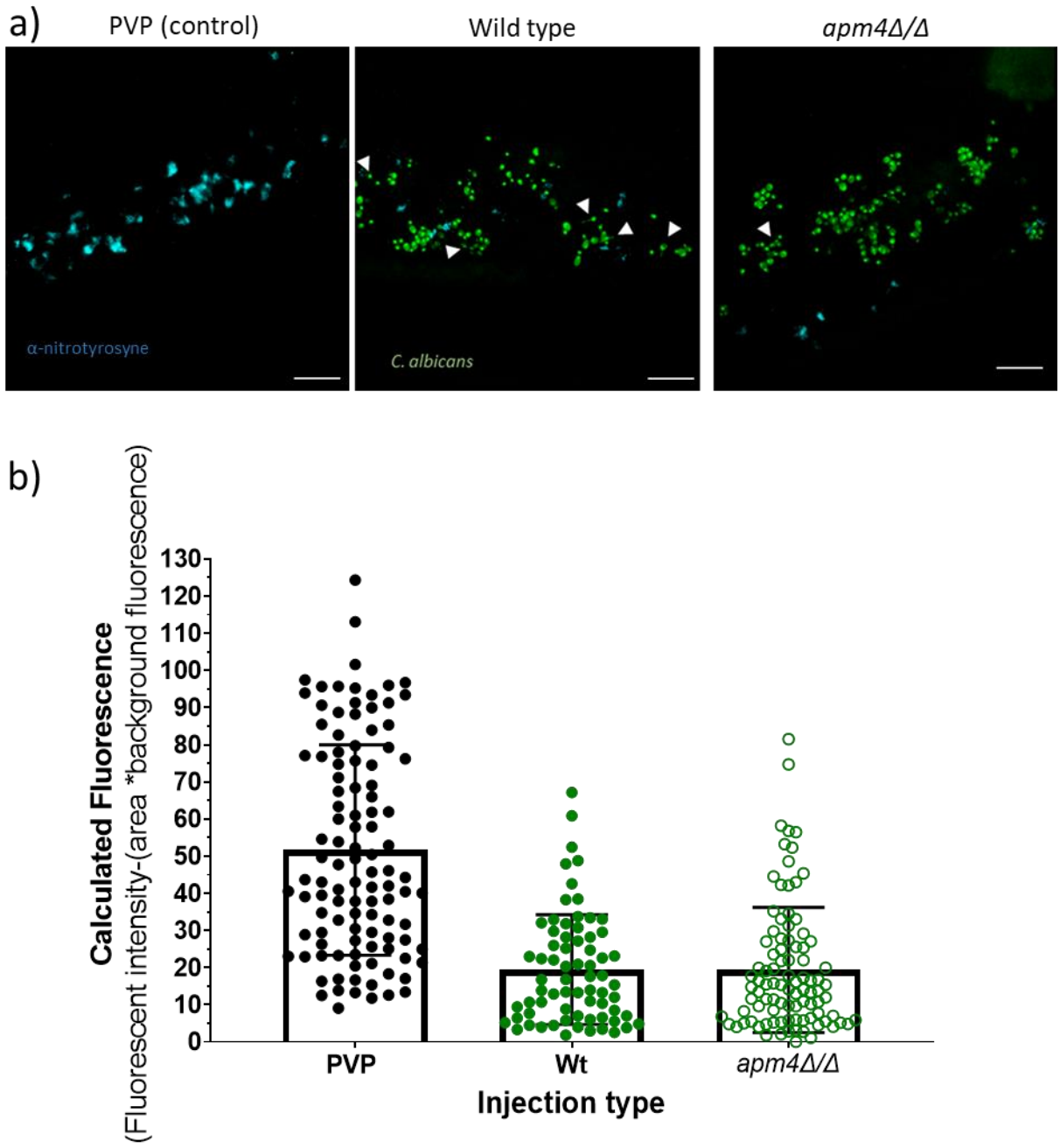

Figure 4.10: The α-nitrotyrosine expression in infected zebrafish embryos was similar in both infection groups. *Nacre zebrafish embryos at 1 dpf were injected with 500 cfu of C. albicans in the caudal vein. The embryos were fixed in 4% PFA, permeabilized and stained with α-nitrotyrosine antibody at 1 dpi. Embryos were imaged using confocal microscopy for the α-nitrotyrosine expression. a) Representative images of the experiment, in turquoise is α-nitrotyrosine and in green are the C. albicans cells (scale bar: 25µm). The white arrowheads point at hyphal cells. b) The data were collected from 3 biological replicates, normalized to background fluorescence per image. 6 cells per image were analysed for α-*

nitrotyrosine expression for a total of 6 images captured per replicate. The graph represents α-nitrotyrosine levels, each dot is an individual cell analyzed and the bars represent the average expression, statistical analysis indicated no significant difference p = ≥ 0.05.

4.7 Impact of cell wall chitin on virulence during zebrafish infections

The *apm4Δ/Δ* cells have increased chitin levels in the cell wall compared to Wt cells. In both *in vitro* (Knafler et al., 2019) and murine macrophage experiments (Section 3.8) a reduction in chitin levels achieved by deletion of one copy of *CHS3* increased the ability of *apm4Δ/Δ* cells to switch to the hyphal morphology. Given the demonstrated importance of the cell wall in host pathogen interactions (Mora-Montes et al., 2011, Bain et al., 2014, Hall, 2015, Shen et al., 2015, da Silva Dantas et al., 2016, Hernandez-Chavez et al., 2017, Wagener et al., 2017, Swidergall, 2019, Davis et al., 2014), it was of interest to understand the impact of restoring the chitin levels on the virulence phenotype shown on figure 4.1. To test this, *apm4Δ/Δ,chs3Δ* cells were used to inject Nacre zebrafish at 1 dpf in the caudal vein. The survival of embryos was monitored and presented in figure 4.11. This experiment was conducted alongside those in Figure 4.1 but shown here, as this strain was used to investigate impact of this additional mutation. As shown the deletion of one copy of *chs3* in the *apm4Δ/Δ* background partially rescues the ability of the *Candida* to kill zebrafish embryos. The zebrafish survival by the end of the investigation was 30% for the Wt infected embryos, 85% for the *apm4Δ/Δ* infected embryos and 54% for *apm4Δ/Δ,chs3Δ* infected embryos. The results from the investigation show that chitin levels are an important factor contributing to virulence, this could be linked to the ability of *apm4Δ/Δ,chs3Δ* cells to switch to the hyphal morphology. It was previously demonstrated that reverting the levels of chitin to the physiological levels in the *apm4Δ/Δ* cells increases the ability of cells to switch to the hyphal morphology, partially rescuing the hyphal switch deficiency phenotype of *apm4Δ/Δ* cells. It is also clear that this is not the only factor responsible for the phenotype however as the deletion only resulted in a partial rescue of the virulence phenotype. This indicates the importance of other factors impacted by AP-2 in *C. albicans* which influence pathogenicity.

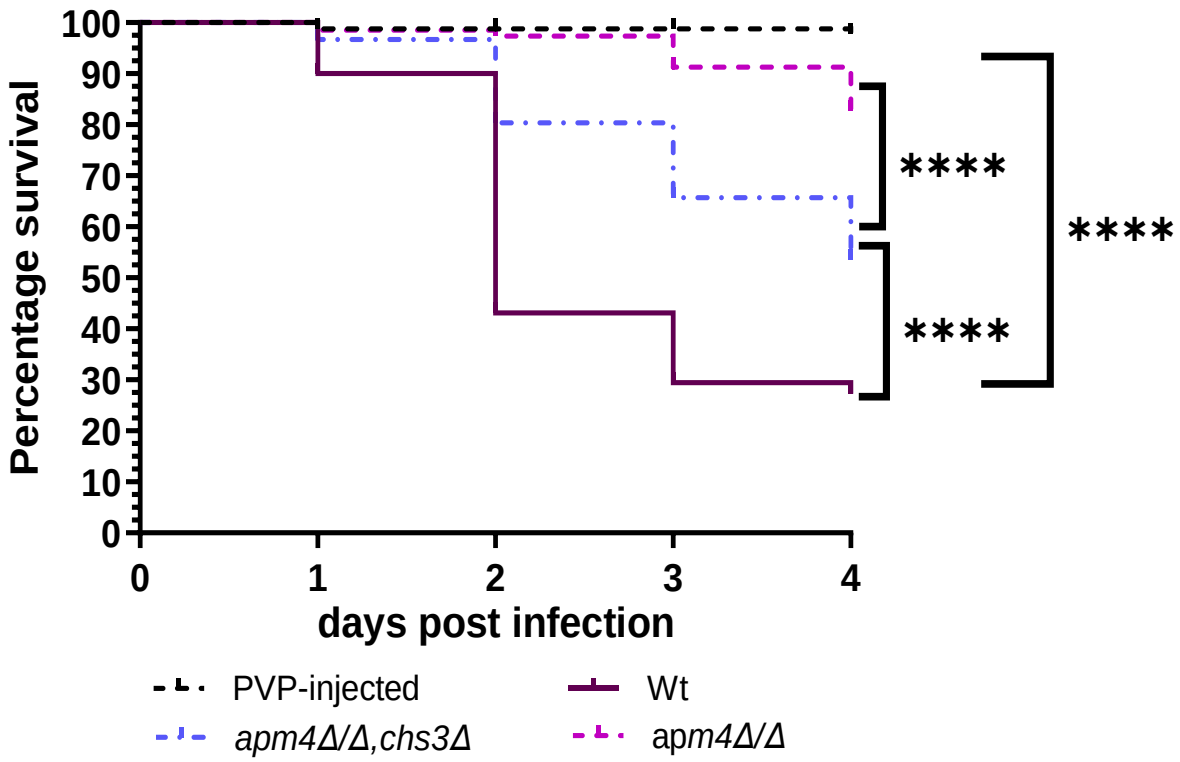

Figure 4.11: Chitin levels are important for the Candida albicans virulence phenotype.

*Nacre zebrafish embryos at 1 dpf were injected with 500 cfu of C. albicans in the caudal vein. The embryos were monitored for survival up to 5 dpf. Survival was assessed by cessation of heartbeat. The number of surviving embryos was counted every day until 4 dpi. The graph represents survival from 3 biological replicates. The zebrafish were infected with the Wt (solid purple line), apm4Δ/Δ (pink dotted line), apm4Δ/Δ,chs3Δ (blue dotted line) and the PVP control (purple dotted line). Survival statistical analysis concluded a **** p = <0.0001 from an n=90 embryos/group.*

4.8 Contribution of macrophages to the fungal burden in Wild type and *apm4Δ/Δ* infected zebrafish.

In Chapter 3 it was reported that the *apm4Δ/Δ* cells appeared to be able to proliferate inside the murine macrophages being studied. Such a phenotype could be beneficial for dissemination once inside a host organism. Investigations published at the time that these experiments were being conducted described the activity of *C. albicans* cells during host

interactions and how macrophages are used as 'Trojan horses' for dissemination in zebrafish (Scherer et al., 2020).

To determine the contribution of macrophages to the total fungal burden in embryos infected with Wt and *apm4Δ/Δ* cells, zebrafish embryos were injected with clodronate, a macrophage liposome that induces macrophage apoptosis, or a negative control PBS liposome at 1 dpf. At 2 dpf the embryos were infected with 200 cfu of *C. albicans* (Section 2.4.2.3). To confirm the activities of the clodronate on macrophage depletion, zebrafish embryos with fluorescent macrophages were injected with the clodronate and then used for macrophage counts (data not shown). The data from this optimization showed depletion of macrophages during Clodronate injections and high numbers of macrophages present during PBS liposome infections. The fungal burden used for the survival assay was high enough to induce zebrafish death but not too high where differences between the different conditions would not be observed. As shown in figure 4.12.a the fungal burden at 3 dpi was not altered in the presence or absence of clodronate to deplete macrophages, nor was there a difference between the burden in Wt or *apm4Δ/Δ* cells. The results from the survival curves on figures 4.12.b and 4.12.c show that macrophages were not essential for the *C. albicans* infection clearance in zebrafish as depletion of macrophages resulted in approximately 10% less viability of embryos in both Wt and *apm4Δ/Δ* infections.

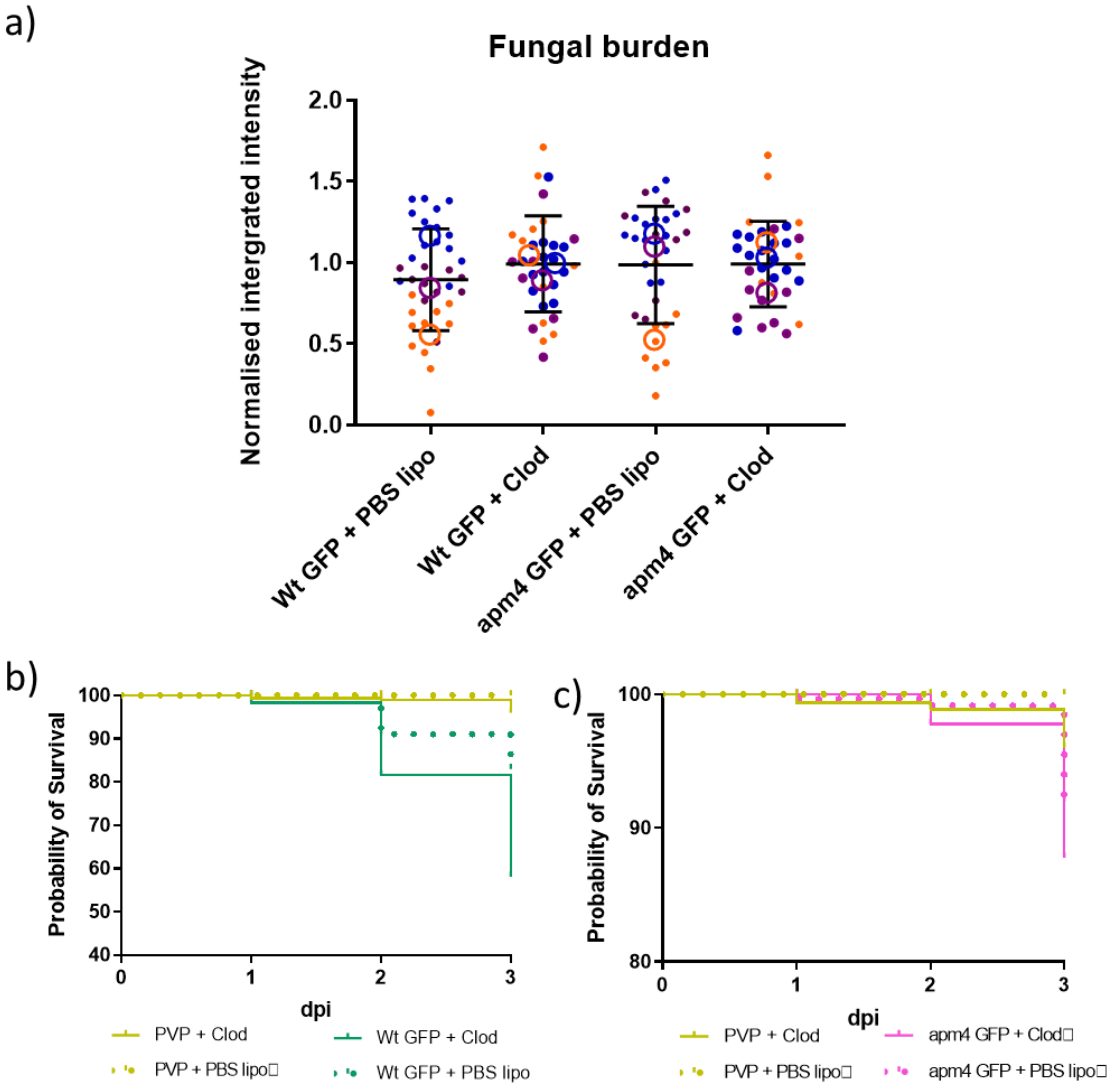

Figure 4.12: Depletion of macrophages in zebrafish embryos decreases zebrafish survival when infected with Candida albicans but results in no changes in the fungal burden. *Nacre zebrafish embryos at 1 dpf were injected with Clodronate a macrophage detergent or PBS liposome as a control in the caudal vein. At 2 dpf the emrbyos were injected with 200 cfu of C. albicans in the duct of Cuveir. The embryos were monitored for survival and fungal burden up to 5 dpf. a) The fungal burden of infected embryos was assessed using fluorescence. Embryos were imaged at 3 dpi using a fluorescence. The results were normalized to control injected embryos. The results from the integrated intensity of each embryo were plotted on a SuperPlot colored differently for each replicate, large circles represent the average burden per replicate and large circles represent the burden of individual embryos. The results were analyzed using a one-way ANOVA statistical test, indicating no significant difference p =*

>0.05. Survival of zebrafish embryos post fungal infection was assessed by cessation of heartbeat. The number of surviving embryos was counted every day until 3 dpi. The graph represents survival from 3 biological replicates. Solid survival lines represents the macrophage depleted embryos injected with Clodronate and the dotted lines represent embryos with macrophages and the mock injection with PBS liposome. b) Survival of embryos infected with PVP (yellow) and Wild type (green) is presented. c) Survival of embryos infected with PVP (yellow) and apm4Δ/Δ (green) is presented.

4.9 Impact of *apm4Δ/Δ* on dissemination of *Candida albicans* within zebrafish embryos

Time-lapse microscopy of infected zebrafish embryos with fluorescent blood vessels was used to study dissemination of *C. albicans* through the host. Dissemination of a microcolony was counted as a microcolony that is not within the fluorescent blood vessel limits. At 1 dpf KDRL embryos were injected with 100 cfu in the Caudal vein, were allowed recovery for 1 hour and then were used for imaging (Section 2.4.3.4). The time-lapses were quantified for the number of microcolonies that can be visualised at sites away from the fluorescent blood vessels. The number of microcolonies disseminating at 3 and 10 hpi is presented on figure 4.13.

The microcolony dissemination is low for the Wt at the 3-hour timepoint but the *apm4Δ/Δ* microcolonies disseminated more. The results are similar at the 10-hour timepoint with more *apm4Δ/Δ* microcolony dissemination. Overall, the results show that *C. albicans apm4Δ/Δ* mutant cells disseminate from the bloodstream more than Wt cells during zebrafish infections.

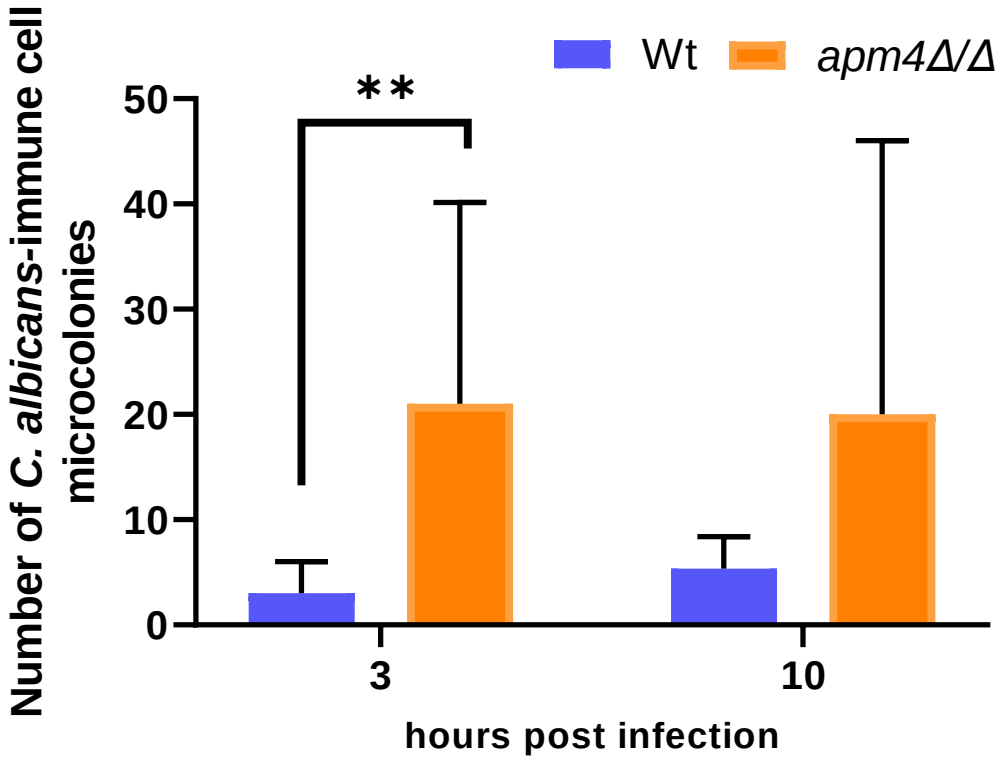

Figure 4.13: Candida albicans microcolonies disseminate from blood vessels over time during in zebrafish embryos infections. *Zebrafish embryos with fluorescent blood vessels were injected with 100 cfu of C. albicans in the caudal vein at 1 dpf. The embryos were allowed injection recovery for 1 hour before time-lapse imaging. The embryos were mounted and imaged every 7 minutes for a maximum of 18 hours post infection, for 3 biological replicates. Z stacks of the whole embryo were captured. The time-lapses were analyzed and microcolonies not in blood vessels were counted over time. The number of microcolonies out of the fluorescent vessels at 3 and 10 hours post infection were calculated. The results are presented as a bar chart for the average value from all three replicates. The error bars represent Standard deviation, Fisher's exact test was used for Statistical analysis for multiple comparisons ** = p 0.0033, ns = p 0.0698 - 0.2337.*

Chapter 4 Discussion

In this chapter it was demonstrated that there is a reduced zebrafish embryo mortality during infections with *apm4Δ/Δ* cells. The reduction of *C. albicans* virulence is linked to the ability of cells to switch to the hyphal morphology and not because the cells are cleared by the host immune cells. The *apm4Δ/Δ* cells are not cleared but rather grow in the host environment. The data presented here suggested that the *apm4Δ/Δ* cells disseminate more from the infection site than Wt cells. These findings will be discussed here.

4.10 Virulence of *apm4Δ/Δ* cells in zebrafish infections

The virulence of *C. albicans* cells during a zebrafish infection was assessed through survival. The results show that *C. albicans* cells with an *apm4* deletion are less virulent than Wt cells. *apm4Δ/Δ* infected embryos do not have hyphal cells growing out of the embryos like Wt infected embryos (figures 4.2 and 4.3). The results suggest a hyphal switch deficiency of *apm4Δ/Δ* cells during infection. Work in other research labs concluded that *C. albicans* cells unable to switch to the hyphal morphology are not virulent as the cells are unable to cause damage and death during host interactions (Lo et al., 1997, Seman et al., 2018). It was expected that the hyphal switch deficiency observed during *apm4Δ/Δ* infections was one of the major factors impacting the pathogenicity.

The reduced virulence could be due to multiple factors: host clearance, differential host immune stimulation and response and hyphal switch deficiency. These factors were investigated through this study.

4.11 *C. albicans* with an *apm4* deletion are not cleared by the host

It was hypothesized that the increased zebrafish survival showed during *apm4Δ/Δ* infection could be a result of increased host clearance. The hyphal switch deficiency could lead to a reduced ability of cells to escape immune cells resulting in increased clearance. The clearance of *C. albicans* by the host was initially investigated through fungal burden assays. It was shown that the *apm4Δ/Δ* cells are not cleared by the host but rather have a fungal burden similar to Wt infected embryos. It was also shown that during zebrafish infections larger microcolonies are formed by *apm4Δ/Δ* cells compared to Wt cells.

The fungal burden was studied using two different methods: 1) using the intensity of fluorescence pixels emitted by the GFP tagged pathogen as a prediction of burden 2)

embryo lysis and plating for colony counts. The findings on fungal burden from both assays show that *apm4Δ/Δ* was not cleared by the host cell (figure 4.4). The methodology of the experiments was not sensitive enough to allow for the understanding of any differences between the Wt and *apm4Δ/Δ* infections.

High resolution microscopy was used to investigate the difference between Wt and *apm4Δ/Δ* infections. During fixed timepoint imaging of the microcolonies at 1 and 2 dpi it was observed that the *apm4Δ/Δ* microcolonies were larger than Wt microcolonies at 1 dpi and by 2 dpi both the Wt and *apm4Δ/Δ* microcolonies were larger (figures 4.5- 4.6). The *apm4Δ/Δ* microcolonies might be larger than Wt microcolonies at 1 dpi because overall the *apm4Δ/Δ* cell size is larger than Wt cells size (figure 3.3). Another possibility is that *apm4Δ/Δ* cells grow faster than Wt cells in the host environment and leading to an increased burden. On figure 4.6 the Wt microcolonies have more uneven morphologies than *apm4Δ/Δ* microcolonies suggesting that Wt microcolonies are composed of hyphae. The microcolony size of Wt cells could be due to the hyphal morphology cells elongating and growing the microcolony size and not a cell number increase while the *apm4Δ/Δ* cells grow more in numbers.

Timelapse microscopy of the early stages of infection was used to complement the microcolony size findings from later timepoints of interaction. Embryos were imaged from 1 to 18 hpi (figure 4.8). The findings show overall larger microcolonies during *apm4Δ/Δ* infections but when the data were analysed for the proportions of microcolonies at the different sizes, the proportions of cells at the different binning values used was similar for both groups.

The results from the 3 different assays highlight that *apm4Δ/Δ* cells were not cleared by the host more than Wt cells are. The *apm4Δ/Δ* cells grow inside the host and possibly have a higher fungal burden than Wt infected embryos. The increasing microcolony sizes reported here can complement the findings in figure 3.14 showing that *C. albicans* proliferate inside the host phagosome growing in burden and possibly disseminating further into the host. Clearance by the host is not responsible for the decreased virulence observed in *apm4Δ/Δ* infected embryos.

4.12 The host immune responses are similar for both Wild type and *apm4Δ/Δ* infections

The host immune system controls infections and could result in the decreased virulence observed during *apm4Δ/Δ* infections. Immune responses to *C. albicans* available in the Johnston lab were used. The IL-1β and the Nitric oxide production responses were investigated. The results from the investigations of the immune activation showed that the immune system is active in a similar way for both Wt and *apm4Δ/Δ* infections.

IL-1β is a proinflammatory cytokine and the production is critical for host activation. IL-1β is also expressed during macrophage pyroptosis. A recent report linked the expression of *CHS3* to increased levels of macrophage pyroptosis (O'Meara et al., 2018). The *apm4Δ/Δ* cells have higher levels of Chs3 on the cell surface due to the defect in endocytosis. The expression of IL-1β in zebrafish embryos infected with *C. albicans* was investigated, interestingly not a big response was elicited by zebrafish after infection with *C. albicans*. The IL-1β expression was assessed through fluorescence emitted by zebrafish embryos. The results in this investigation suggest no change in the expression levels between Wt and *apm4Δ/Δ* cells or even no IL-1β expression of zebrafish embryos at all (figure 4.9).

The results show that the immune response was not differentially stimulated in *apm4Δ/Δ* infections compared to Wt infections. This suggests that increased cell surface Chs3 does not result in increased overall IL-1β expression (O'Meara et al., 2018). The findings could indicate that eventhough there is more Chs3 in the cell surface of *apm4Δ/Δ* cells it does not mean that all the Chs3 is active and functional. It is possible that over time Chs3 either through damage or deactivation mechanisms might not be active on the cell surface.

The nitric oxide response for *C. albicans* clearance was investigated. The *C. albicans* cells respond to the nitric oxide production by producing arginases that utilise the available L-arginine in the immune cell environment. The L-arginine is critical for nitric oxide production. The cell wall chitin levels are suggested to increase the arginase response by *C. albicans* and thus resulting in decreased nitric oxide production (Wagener et al., 2017). The *apm4Δ/Δ* cells have more chitin on their cell wall so it was of interest to study this response. The results from the investigation and the 3 biological replicates show that both Wt and *apm4Δ/Δ* cells resulted in reduced nitric oxide production by host cells (figure 4.10). The

results suggest that the increase in the chitin levels of *apm4Δ/Δ* cells is not enough to stimulate the response described by previous reports.

Overall, the results from both immune investigations concluded that the immune stimulation is similar in Wt and *apm4Δ/Δ* infected embryos. The immune response was not responsible for the differences in virulence and clearance observed during *apm4Δ/Δ* infections. In addition, during the *apm4Δ/Δ* infections eventhough there is a hyphal deficiency, the immune system responds similarly to hyphal producing Wt infections.

4.13 The role of cell wall chitin and hyphal switch on infection

The influence of chitin on virulence was investigated. The *apm4Δ/Δ* cells have been previously described to present a hyphal switch deficiency under different conditions, it was thus of interest to study hyphal switch during the infection (figure 3.7). The *apm4Δ/Δ,chs3Δ* cells were used in this investigation to understand the role of increased chitin on virulence. The *apm4Δ/Δ,chs3Δ* cells were used for survival assays, the results showed a partial rescue of the virulence phenotype. These findings suggest that the levels of chitin are important for the reduced virulence phenotype. *apm4Δ/Δ,chs3Δ* cells were reported previously to partially rescue the hyphal switch phenotype during phagosome interactions (figure 3.8). It is currently unknown however how the levels of chitin have an impact on hyphal morphology. It can be hypothesised that there is a correlation between the cell wall composition and hyphal switch which in turn impacted virulence.

It is concluded that the reduction in virulence is not linked to the host reactions such as immune stimulation and clearance but because of the *C. albicans* biology. It is linked to the hyphal switch deficiency of *apm4Δ/Δ* cells, evidence for this were shown in figures 4.2, 4.3, 4.5, 4.6, 4.10 and 4.11. The hyphal morphology is essential for virulence as the fungal toxin Candidalysin is only produced by cells that switch to the hyphal morphology (Moyes et al., 2016, Richardson et al., 2018). The hyphal morphology is linked to host damage. A deficiency in hyphal switch results in less host tissue damage and thus a decrease in virulence. It could be that the *apm4* deletion in *C. albicans* results in a more commensal phenotype where there is a mixed population of yeast and hyphae that does not result in uncontrollable host damage and virulence (Jouault et al., 2009, Chairatana et al., 2017,

Burgain et al., 2019, Cottier & Hall, 2020, Romo & Kumamoto, 2020). It would be an interesting topic to study during future investigations with the strain.

4.14 Host dissemination

The dissemination of pathogens during infection is important. *C. albicans* is known to adhere onto the host and invade the tissue and was recently characterised for using macrophages as a "Trojan Horse" of dissemination. *C. albicans* is phagocytosed by immune cells and uses the immune cells to disseminate further than the infection site before the *C. albicans* can escape the macrophages promoting the infection phenotype (Scherer et al., 2020). The findings from this investigation show that macrophages were not critical for *C. albicans* clearance, and do not promote *apm4Δ/Δ* cell dissemination more than Wt dissemination, however overall *apm4Δ/Δ* cells disseminated from the bloodstream more than Wt cells. The data on microcolony sizes suggest that *apm4Δ/Δ* cells proliferated during interactions with immune cells (figure 4.7) so it is possible that the assay used to study the fungal burden of macrophage-depleted embryos was not sensitive enough to capture this growth.

It was previously showed that *apm4Δ/Δ* cells grow in murine macrophages, this phenotype was not reflected during zebrafish infections (figure 4.12) as the fungal burden of *apm4Δ/Δ* and Wt cells is similar in the presence and absence of macrophages.

Dissemination from the bloodstream of zebrafish embryos was also investigated (figure 4.13). The *apm4Δ/Δ* microcolonies disseminated more than Wt microcolonies at the infection timepoints studied. The cells move from the infection site, possibly adhere to different sites and row. The results suggest that eventhough the *apm4Δ/Δ* cells have hyphal switch deficiencies they survived and possibly presented other infection phenotypes.

The results overall suggest, that the *apm4Δ/Δ* microcolonies can disseminate more than Wt microcolonies in the host. The *apm4Δ/Δ* cells present virulence phenotypes however the virulence of *C. albicans* is reduced, based on the data here the reduced virulence can be attributed to the hyphal switch deficiency of the mutant cells.

4.15 Chapter 4 Conclusion

The data in this study suggest that the *apm4Δ/Δ* cells are not virulent *in vivo*. The data here conclude that the loss of function of AP-2 in *C. albicans* results in a hyphal switch deficiency reducing the virulence of the cells during zebrafish infections. Instead of switching to the hyphal morphology the *apm4Δ/Δ* cells present a vegetative growth and are not cleared by the host immune cells. This suggests that the *C. albicans apm4Δ/Δ* cells are more commensal during *in vivo* interactions. The cells grow in burden however, they do not switch to the hyphal morphology or trigger the host damage response, so they co-exist with the host. The similarities in the immune responses that are reported for Wt and *apm4Δ/Δ* infections were possibly because IL-1β was responding to the increased *C. albicans* growth in the host and the α-nitrotyrosine response occurs independently of the hyphal morphology and damage.

Chapter 5: *Investigating the impact of Candida albicans apm4 deletion during interactions with epithelial cells.*

5.1 Introduction to Chapter 5

C. albicans reside on mucosa and interact with oral, gut and vaginal epithelia resulting in Candidiasis. The epithelia at the different sites respond differentially to stress resulting in upregulation of distinct combinations of cytokines and chemokines (Whiley et al., 2012). During interactions with epithelial and endothelial cells *C. albicans* adhesion proteins bind to the host and interact with the extracellular components and surface expressed receptors. These interactions allow attachment and recognition by the epithelial cells (Moyes et al., 2015).

Epithelial damage and cytokine induction are independent of the *Candida* adhesion molecules expressed but they are dependent on production of Candidalysin (Naglik et al., 2017). Epithelia respond to *C. albicans* interactions through pathways involving AP-1, c-Fos and MKP1. This results in release of IL-1α/β, IL-6 and IL-17 to recruit immune cells (Zhou et al., 2018). *C. albicans* invasion of tissue becomes deeper over time with damage and loss of host cell integrity later in the infection process (Allert et al., 2018). Host damage includes apoptosis (self sacrifice) and necrosis (damage of cells by external factors) of cells. The host cells respond to *C. albicans* using a damage protection response to survive the pathogen stimuli (Moyes et al., 2015). The damage phenotypes are associated with the adhesion, invasion and hyphal length of infecting *Candida.* Defects in those factors can result in a lack of damage pathway induction (Allert et al., 2018). *C. albicans* need to express damage inducing genes to cause host cell damage. The hyphal morphology is important to cause damage but not all hyphal cells can induce damage (Moyes et al., 2015). During infection *C. albicans* can either be phagocytosed by epithelia or it can actively penetrate host tissue. Active penetration does not result in measurable tissue damage (judged by release of certain cytokines) unless Candidalysin is present. Both the hyphal switch and Candidalysin secretion are important for the damage associated necrosis of epithelia (Allert et al., 2018).

Adhesion and invasion are very important contributing factors in the pathogenicity of *C. albicans* and defects in these can lead to reduced virulence and result in a commensalism phenotype. The interaction Wild type and *apm4Δ/Δ* cells with epithelial gut cells were investigated as there is growing evidence of the importance of the gut as the major entry route of disseminated *C. albicans* in systemic Candidiasis.

Chapter 5 Results

5.2 Scanning Electron Microscopy analysis of the morphology of *C. albicans* during epithelial interactions

C. albicans can grow as commensal cells on the surface of the gut epithelium but it is thought that epithelial damage, induction of immune responses and changes, in the gut microflora can trigger changes in *C. albicans* which allow it to switch to a virulent invasive form (Kennedy & Volz, 1985, Vautier et al., 2015, Graf et al., 2019, Witchley et al., 2019).

The morphology of *C. albicans* cells on gut cells was investigated. Caco-2 cells were seeded on glass slides until confluency, the cells were infected with *C. albicans* for 24 hours, fixed, prepared, and imaged through SEM (Section 2.5.1.3). The SEM preparation and imaging was undertaken in collaboration with Dr Jaime Canedo (Johnston lab, University of Sheffield). The *C. albicans* phenotypes on Caco-2 cells are shown in figure 5.1. As shown, Wt cells switch to the hyphal morphology and are relatively uniform in both morphology and size (panels 1-4). The Wt hyphae often overlay and clump together during invasion (panels 4-7). Higher resolution images (panels 7,8) show that there are surface projections on the outer cell wall. These appear to be uniformly distributed along the hyphae and on the mother cells. The *apm4Δ/Δ* hyphae were less uniform in morphology and although hyphal switch was observed budding yeast cells were present (panels 12,13 and 16). The surface of *apm4Δ/Δ* cells show larger surface projections compared to those on Wt cells. These projections were more varying in size and less uniformly distributed (panels 15-16). Overall, the *apm4Δ/Δ* hyphae are not as long as Wt hypha, in agreement with findings from previous *in vitro* investigations (Knafler et al., 2019).

The SEM provided a good understanding of the interactions on the surface of epithelial cells however it was of interest to observe the invasion beyond the surface of the epithelium during deeper host interactions.

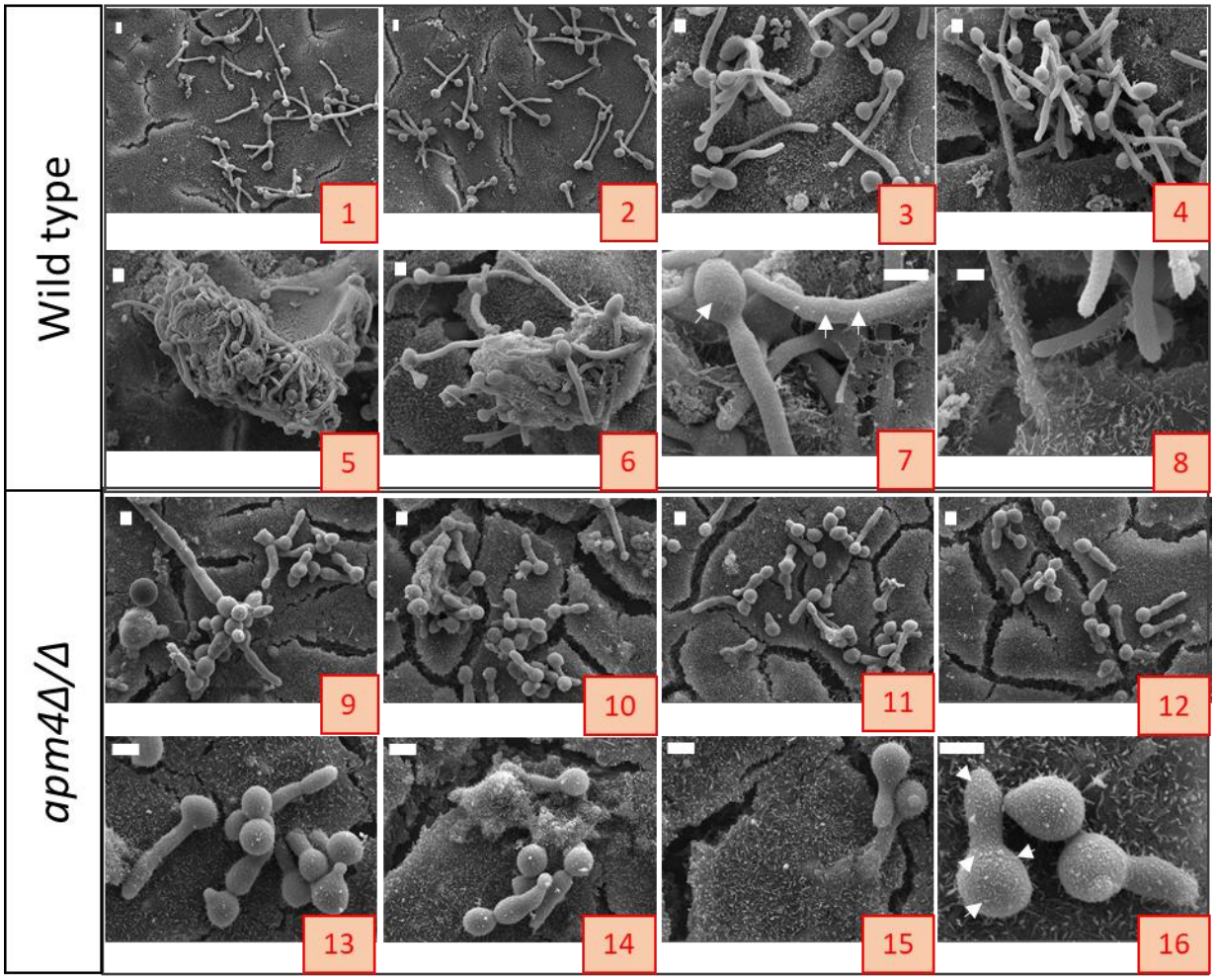

Figure 5.1: Candida albicans with a deletion of apm4 switch to the hyphal morphology during epithelial cell infections . *Caco-2 cells were seeded on glass coverslips in a 24-well plate for 3 days and then infected with Wt and apm4Δ/Δ cells for 24 hours. The cells were fixed, washed and prepared for SEM. The samples were imaged, the figure is composed of representative SEM images of each infection group, 20 images per condition were captured. Panel 7 is a higher magnification of panel 6 and panel 9 is a higher magnification of panel 13. The white arrows point towards examples of surface projections on C. albicans cell wall surface.*

5.3 Impact of the *apm4* deletion on epithelial adhesion.

In *C. albicans* there are proteins expressed which increase the adhesion to host cells. These proteins are secreted from the cell and localize to the cell wall. Key adhesion proteins are the Als family proteins and Hwp1. Post translational modifications of the proteins are important for the adherence on different tissue (Tronchin et al., 1991, Liu & Filler, 2011, Monroy-Perez et al., 2012, Fan et al., 2013, Moyes et al., 2015, Ho, V. et al., 2019). The main cell wall components: chitin, β glucan and mannans, are also important for adhesion as the structure, composition and arrangement can result in masking of adhesion proteins. The morphology of the cells during the interaction can also be critical as the hyphal cells are reported to adhere more than yeast on host epithelia during increased rates of fluid flow. The mother cell is the site where most of the adhesion occurs in hyphae, suggesting that the availability of adhesion sites is different across the same cell (Grubb et al., 2009). The *apm4Δ/Δ* cells have increased levels of chitin and changes in the mannan density and length (Knafler et al., 2019). It was of interest to study the influence of the mutation on adhesion to host epithelial cells.

Caco-2 cells were seeded on glass coverslips of known size, 4 days post seeding the cells (Section 2.1.3.3) were infected with $1x10^6$ cells/mL *C. albicans* for 1 hour while the culture was on a rocker to ensure even spread of the *C. albicans* cells (Section 2.3.2.3). The cultures were washed, fixed, and imaged for analysis. The average number of cells per field of view was calculated to estimate the percentage of cells adhering in the entire area of the coverslip. The experiment was repeated twice, the results from the first replicate are presented on figure 5.2. The results showed that *apm4Δ/Δ* cells are less adhesive under these conditions than Wt cells.

The results suggested that the cell wall changes in the *apm4Δ/Δ* cells led to decreased adhesion of *C. albicans* to host epithelial cells. The surface projections observed using SEM (figure 5.1) and their organisation could impact the adhesion. It could also suggest a role for AP-2 or its downstream effectors on adhesion protein localisation. The findings could impact the interactions of cells with the host for both commensalism and invasion.

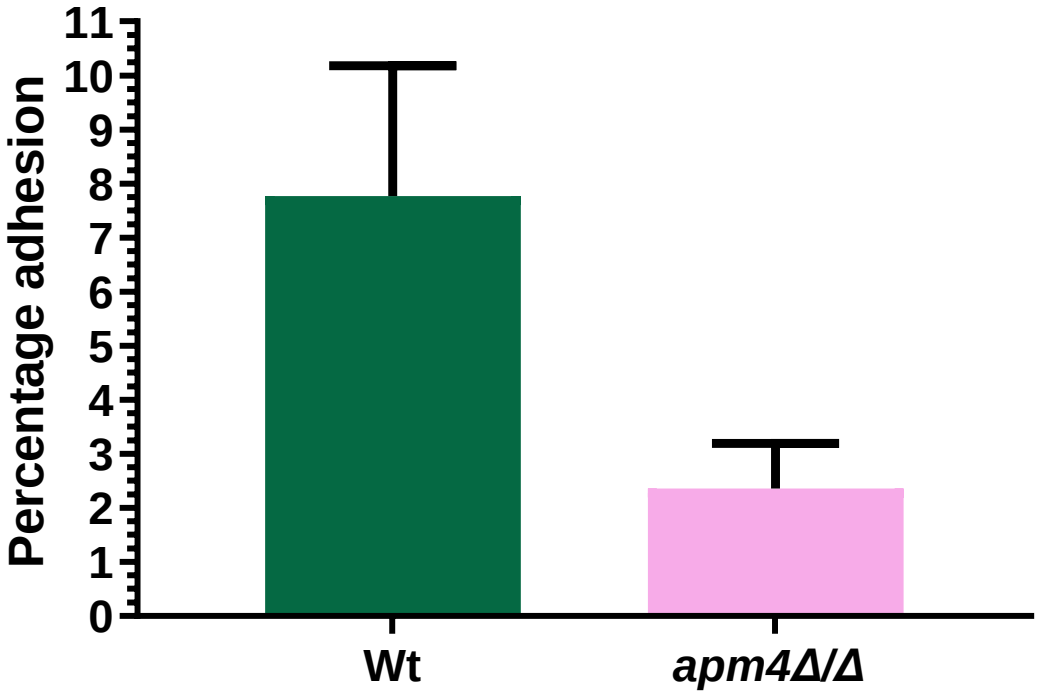

Figure 5.2: apm4Δ/Δ cells adhere less than Wild type cells on Caco-2 cells. *Caco-2 cells were seeded in glass coverslips were infected with 1x10^{6} cells/mL for 1 hour. During the 1 hour of infection the cells were in the 37^{o}C incubator on a rocker for even infection. After the infection, the cell cultures were washed 3x with PBS to remove any non-adhered C. albicans cells before being fixed for imaging. Images from 100 fields of view were used to estimate the number of cells adhering in each coverslip. The results from 2 adhesion experiment replicates are shown on the graph. The error bars represent the standard deviation, there is no statistical significance between the groups p= ≥0.05.*

5.4 Impact of the *apm4* deletion on the invasion method.

The *C. albicans* cells have two epithelial invasion mechanisms: endocytosis and active penetration. Endocytosis of *C. albicans* by host epithelial cells is not thought to be very common in the gut (Moreno-Ruiz et al., 2009, Moyes et al., 2015). Active penetration is the most common invasion method used by *C. albicans* and is subdivided into two types: paracellular when the invasion is between cells in the epithelium and transcellular when the hypha penetrates the cell. In this part of the study, observations were made to determine whether the Wt and mutant *C. albicans* cells invaded the epithelium and if they did, then what penetration method was used.

Caco-2 monolayers were analysed after 24 and 48-hours infections with *C. albicans*. The cultures were fixed, stained and imaged using confocal microscopy (Section 2.3.2). The images were analysed for invasion: paracellular (between cells) and transcellular (through cells). Examples of paracellular and transcellular invasion are presented on figure 5.3.a. Paracellular invasion was categorized as invasion at tight junctions (defined as the brightly stained phalloidin area on the cell periphery) while transcellular invasion was anywhere within the cell. The images in figure 5.3.a highlight the method used to differentiate the type of invasion. The percentage of invading cells in a transcellular fashion as a proportion of all the invading cells in the field of view was quantified. The percentage was quantified from 3 independent replicates investigating a minimum of 5 images per replicate, the minimum number of cells included in the analysis was 15. The results for the percentage of transcellular invasion after 24 hours of the interaction are presented on figure 5.3.b. After 24 hours of interaction the percentage of transcellularly invading cells is similar for both infection groups (>75%), transcellular invasion after 48 hours of interaction is similar for both Wt and *apm4Δ/Δ* infections (>75%) (figure 5.3.c).

The *C. albicans* hyphae invaded host epithelia mostly through transcellular penetration. No endocytosis of *C. albicans* was observed which was expected as the assay was not optimised for detecting endocytic uptake. The data suggest that Wt and mutant cells use similar invasion mechanisms. The mutation of *apm4* and the hyphal morphology changes observed, do not impact the invasion mechanism the cells use during epithelial interactions.

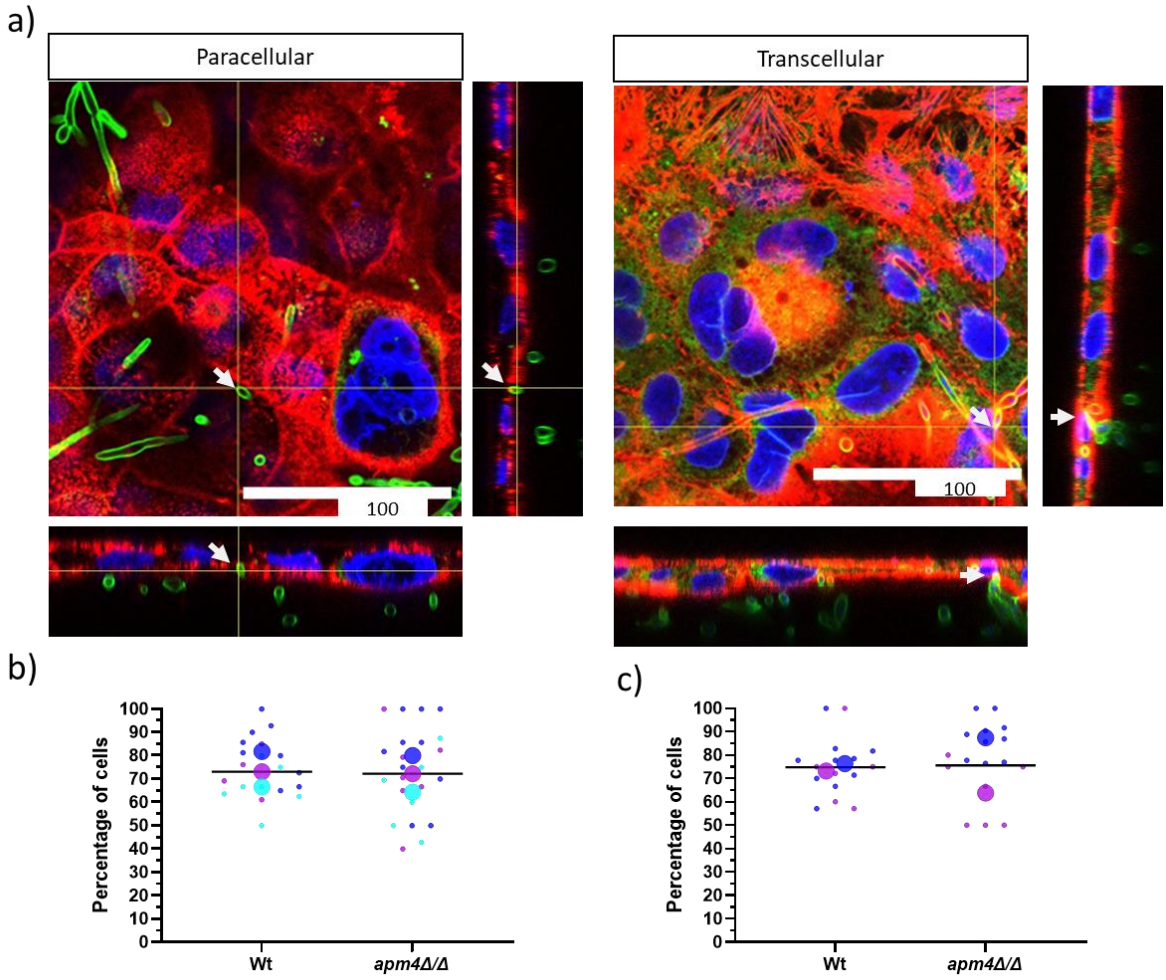

Figure 5.3: Candida albicans with a deletion of apm4 invade Caco-2 monolayers similarly to Wild type cells. *Caco-2 cells were seeded on squared dishes coated with gelatin. The cultures were incubated for 17 days in the 37^{o}C incubator to develop into monolayers. The Caco-2 monolayers were infected with 1x 10^{6} cells/mL for 24 and 48 hours before being fixed, permeabilized and stained with phalloidin (actin = red), Hoechst (nuclei = blue) and Concavalin a – 488 (C. albicans = green). The scale bar is equal to 100 µm. The monolayers were imaged using confocal microscopy. The images captured were analyzed for invasion, there are 3 independent experiments for the assay, >15 images with a minimum of 3 C. albicans cells in the field of view were analyzed. a) Representative images of the two types of invasion: paracellular and transcellular are presented, the white arrows point towards the invading C. albicans cells. The images are of XY slices with an XZ slice and a YZ slice through*

the Z stack. b) The graph represents the results for the percentage of transcellular invasion after 24 hours of infection, there is no statistical significance between the groups p= ≥0.05. c) The graph represents the results for the percentage of transcellular invasion after 48 hours of infection, there is no statistical significance between the groups p= ≥0.05.

5.5 Impact of *apm4* mutation on invasion

The analysis above indicated that both Wt and *apm4Δ/Δ* cells can form hyphae and invade the Caco-2 gut epithelium by active penetration. However, it did not consider whether the two strains were able to form hyphae and penetrate to a similar degree. The level of epithelial invasion was assessed using the same Caco-2 monolayer infections with *C. albicans*. The infected monolayers were fixed, stained and imaged before the analysis for invasion (Sections 2.1.3.3 and 2.3.2). The images were used to assess the percentage of invading cells in a field of view. The diagram on figure 5.4.a shows what was considered as an invading (through the monolayer) and what was considered as a non-invading cell (outside of the monolayer). Three independent experiments were analysed, 5 images of which 5 random fields of view were studied, the total number of fields of view analysed per infection group was equal to and more than 20. The results collected were analysed in two ways 1) average the percentage of invasion per image (figure 5.4.b) 2) percentage of invasion per field of view (figure 5.4.c). The results from the average percentage of invasion per image suggested that at 24 hours post infection the proportion of invading cells in each strain is similar. However, at 48 hours the Wt cells were significantly more invasive than *apm4Δ/Δ* cells (figure 5.4.b) with *apm4Δ/Δ* cells in fact showing lower levels of invasion by later time points compared to at 24 hours. In the second method of analysis the percentage of invading cells in each field of view is presented. Here, the variability between the different fields of view can be observed (figure 5.4.c). At 24 hours there was no significant difference in the percentage of Wt and *apm4Δ/Δ* invasive cells. At 48 hours there was a higher percentage of Wt invading cells compared to *apm4Δ/Δ* cells. Similarly, to figure 5.4.b the Wt cells became more invasive over time while the *apm4Δ/Δ* cells showed a slight decrease in the percentage of invasion over time. The findings suggest that the overall trend

from both analysis methods is similar and thus both approaches were appropriate for analysis.

The results here showed that the *apm4* mutation results in a reduction in host invasion and possibly virulence. This could be linked to multiple factors such as hyphal extension, toxin production, an inability to produce enough force for invasion or that *apm4Δ/Δ* hyphae are overall softer than the Wt.

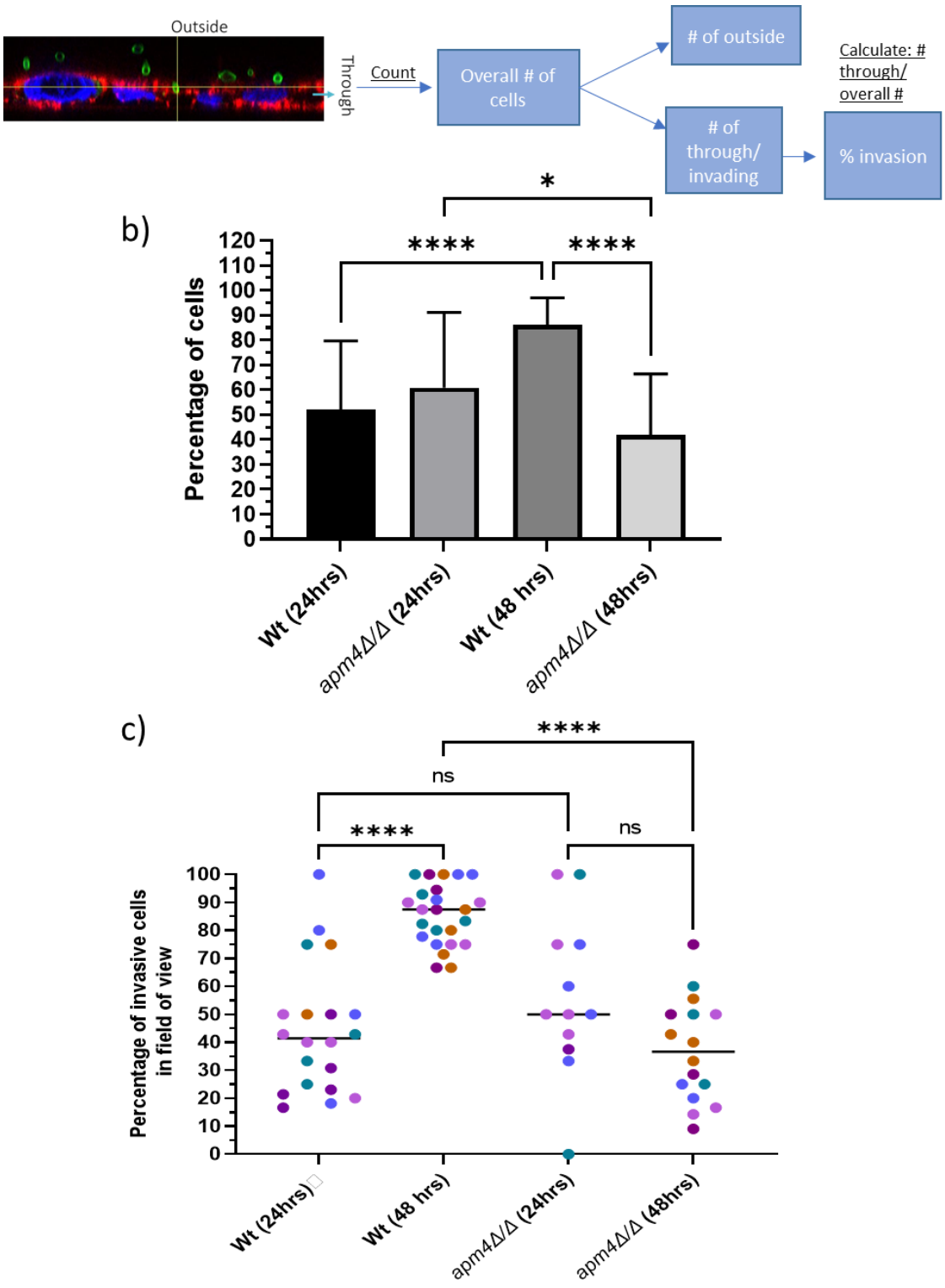

Figure 5.4: Candida albicans with a deletion of apm4 are less invasive than Wild type cells.

Caco-2 cells were seeded on squared dishes coated with gelatin. The cultures were incubated for 17 days in the 37^{o}C incubator to develop into monolayers. The Caco-2 monolayers were infected with 1x 10^{6} cells/mL for 24 and 48 hours before being fixed, permeabilized and

*stained with phalloidin (actin = red), Hoechst (nuclei = blue) and Concavalin a – 488 (C. albicans = green). The monolayers were imaged using confocal microscopy. The images captured were analyzed for invasion, there are 3 independent experiments for the assay, >15 images with a minimum of 3 C. albicans cells in the field of view were analyzed. a) Illustration of the analysis for invasion. The number of cells through the monolayer or on top of the monolayer was quantified in 3-5 random fields of view per image from an overall of 5 images per condition. b) The graph represents the percentage of cells as an average from each image. The error bars represent the standard deviation, the results were analyzed using a One-way ANOVA statistical test * p = 0.0345, ** p = 0.0025 and **** p = <0.0001. c) The graph represents the percentage of invasive cells in a field of view. The line represents the average number of invasive cells from all the replicates. The dots represent individual fields of view colored based on the image the field of view is part of. The results were analyzed wit a One-way ANOVA statistical test ns p = ≥0.05, *** p = 0.0005 and **** = <0.0001.*

5.6 Impact of hyphal morphology during invasion

The deletion of *apm4* in *C. albicans* resulted in decreased percentage of invasive cells. The results from previous investigations suggested that *apm4Δ/Δ* cells were able to switch to the hyphal morphology during epithelial interactions so it was of interest to understand the difference between the two groups in terms of invasion.

Caco-2 monolayers were infected with *C. albicans* for 24 and 48 hours post infection, the cells were fixed, stained and imaged using confocal microscopy (Sections 2.1.3.3 and 2.3.2). During analysis of the images it was observed that a difference between Wt and *apm4Δ/Δ* cells was the form of the hyphal extension. Quantifying the length of hyphae was challenging given the growth in three dimensions and the limited time remaining for the study. Instead, observations of the interactions after 24 hours of infection were undertaken and presented in figure 5.5. Three images per infection group are shown. It was observed that Wt hypha are extending into and along the monolayer, invading and forming new long hyphal branches. The *apm4Δ/Δ* hyphae had a different morphology, the hyphae were shorter but often had more branches than the Wt. These branches often appeared as elongated buds along the length of the hypha. Invasion was observed with both

populations. At the 48 hour timepoint the Wt cells appear long and branched fully invading the monolayer and growing into and along the monolayer while the *apm4Δ/Δ* hyphae are shorter (figure 5.6). Both Wt and *apm4Δ/Δ* hyphae invade the monolayer but due to the elongation and long hyphal branches observed in Wt cells there seems to be more invasion. While not quantified here, hyphal elongation or expansion does appear to be different between the two populations and could contribute to the differences in effective invasion.

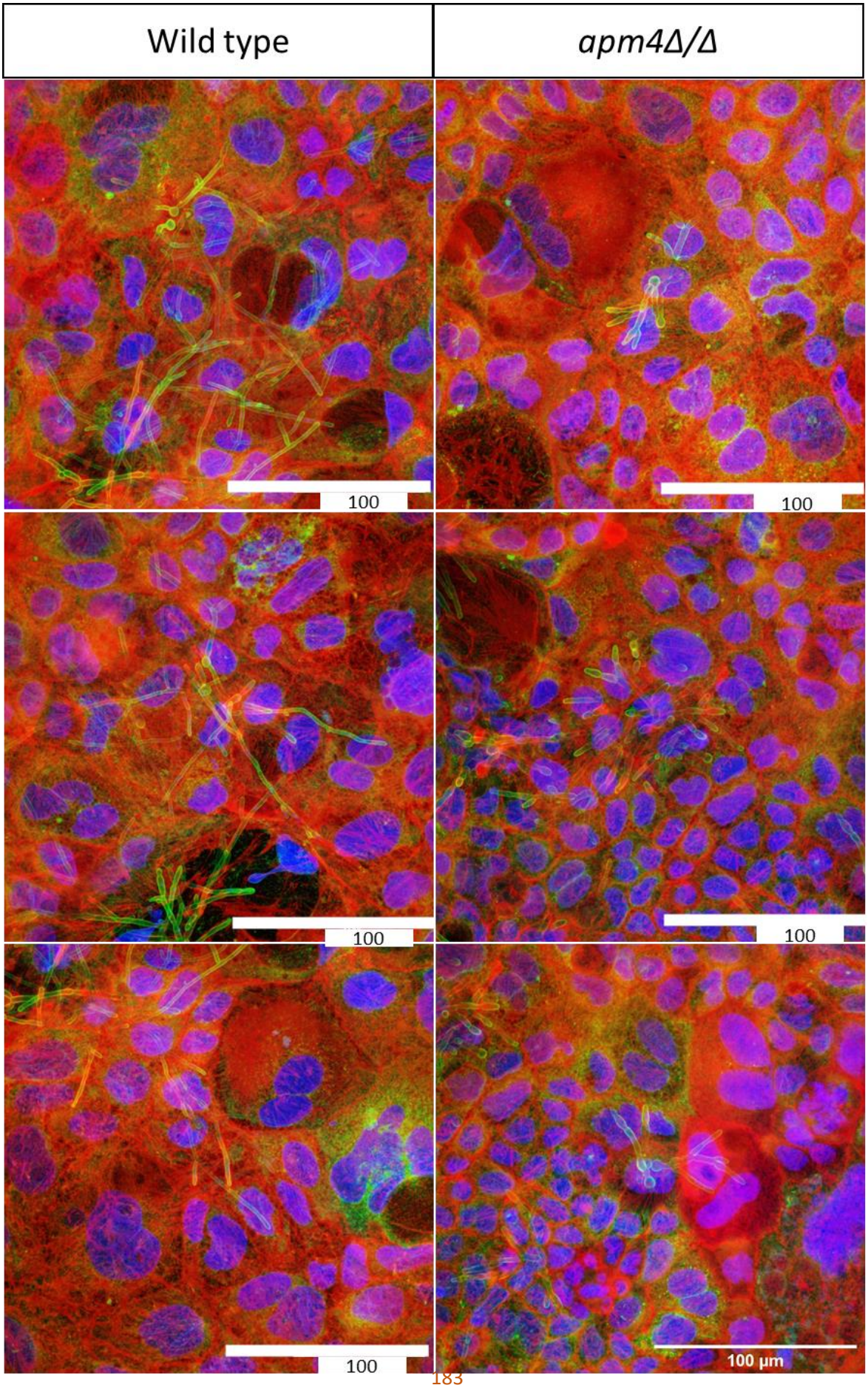
Wild type
apm4Δ/Δ
100
100
100
100
100
100 µm

Figure 5.5: Candida albicans morphology on epithelial monolayers 24 hours post infection.

Caco-2 cells were seeded on squared dishes coated with gelatin. The cultures were incubated for 17 days in the 37^{o}C incubator to develop into monolayers. The Caco-2 monolayers were infected with 1x 10^{6} cells/mL for 24 hours before being fixed, permeabilized and stained with phalloidin (actin = red), Hoechst (nuclei = blue) and Concavalin a – 488 (C. albicans = green). The scale bar is equal to 100 µm. The monolayers were imaged using confocal microscopy. The morphology of C. albicans cells on the monolayer is observed using Z stack projections.

Figure 5.6: Candida albicans morphology on epithelial monolayers 48 hours post infection.

Caco-2 cells were seeded on squared dishes coated with gelatin. The cultures were incubated for 17 days in the 37^{o}C incubator to develop into monolayers. The Caco-2 monolayers were infected with 1x 10^{6} cells/mL for 48 hours before being fixed, permeabilized and stained with phalloidin (actin = red), Hoechst (nuclei = blue) and Concavalin a – 488 (C. albicans = green). The scale bar is equal to 100 µm. The monolayers were imaged using confocal microscopy. The morphology of C. albicans cells on the monolayer is observed using Z stack projections.

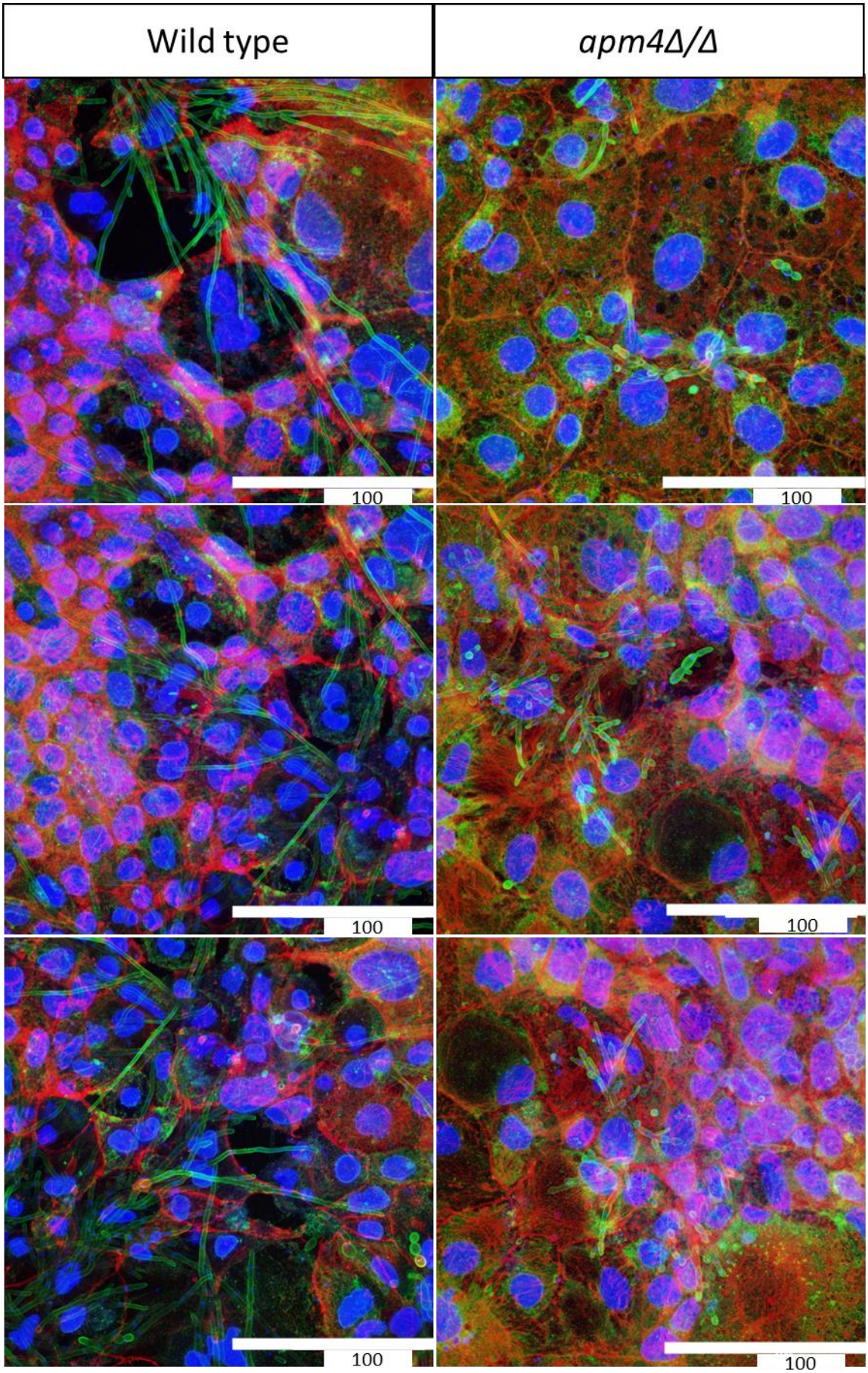
Wild type
apm4Δ/Δ
100
100
100
100
100
100

5.7 Use of an OrganoPlate gut-on-a-chip to investigate *C. albicans* infections

Because of the long time to incubate cells to achieve a confluent epithelium and because of variability in growth, we sought an alternative system to investigate *C. albicans* interactions with gut epithelium. Local developing expertise allowed preliminary experiments to be undertaken using a gut on chip approach.

The Caco-2 cells were seeded into OrganoPlates for 4 days until the gut-on-chip was developed before infection with *C. albicans* cells (Section 2.1.3.4). A schematic of the gut-on-a-chip is shown on figure 5.7. The gut-on-chip was fixed 24 hours post interaction, permeabilised, stained and imaged using confocal microscopy (Section 2.3.3). The images captured are presented on figure 5.7. The images from the interactions of *C. albicans* with the gut-on-a-chip model show that both Wt and *apm4Δ/Δ* cells switch to the hyphal morphology in the environment (figure 5.7). The Wt cells all switched to the hyphal morphology while *apm4Δ/Δ* cells showed a lower level of switching to the hyphal morphology and many *apm4Δ/Δ* cells continued to have a more yeast-like morphology. The findings support those from the SEM where the Wt hyphae are uniform in size and morphology while the *apm4Δ/Δ* hyphae were variable.

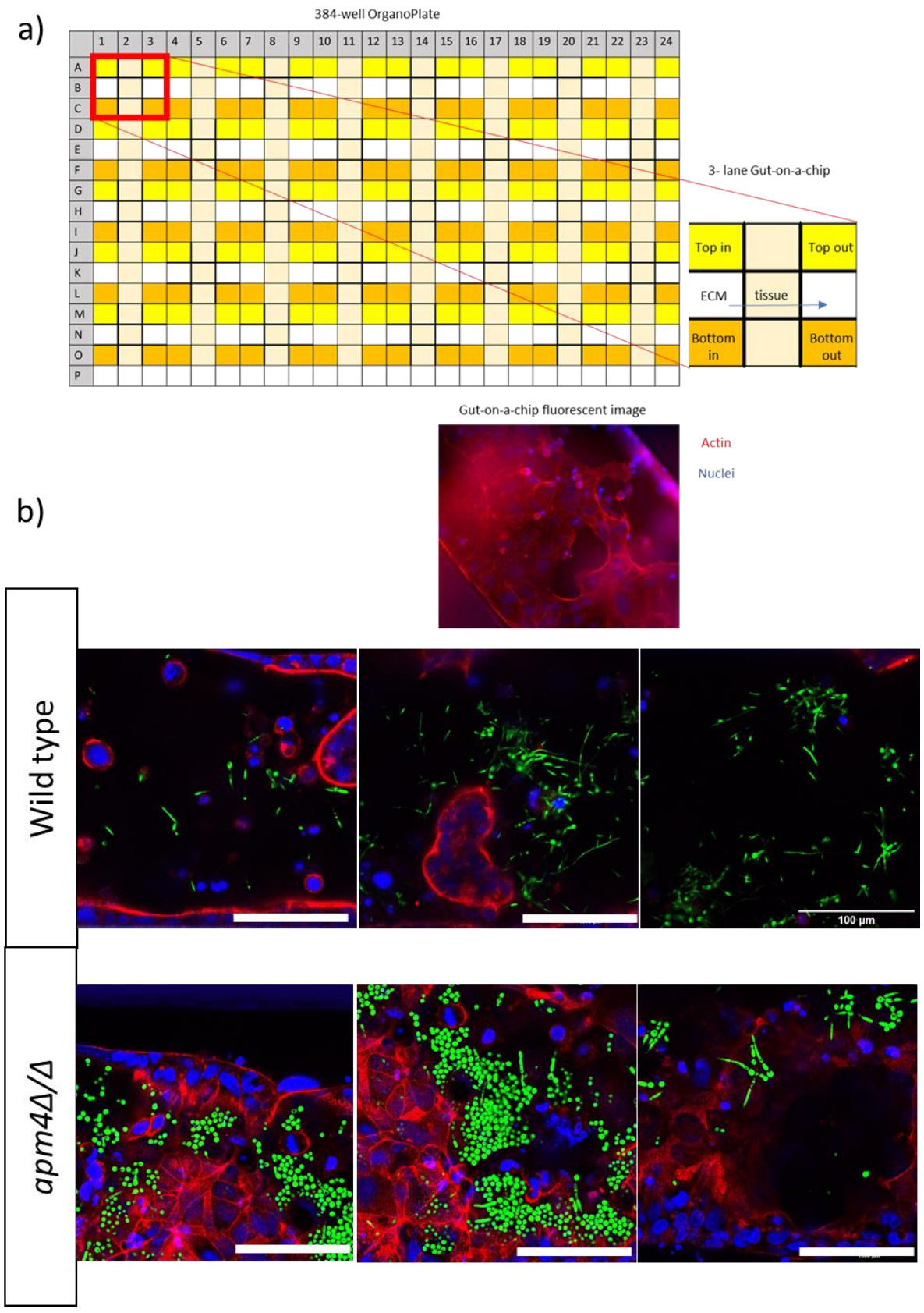

Figure 5.7: Candida albicans with a deletion of apm4 switch to the hyphal morphology during epithelial gut-on-a-chip infections. *Caco-2 cells were seeded on OrganoPlates for 4*

days for the gut-on-chip to develop and then infected with Wt and apm4Δ/Δ cells for 24 hours. The cells were fixed, washed and stained before confocal microscopy. In red is the actin stained with phalloidin conjugated with an Alexafluor 568, in blue are the nuclei stained with Hoechst and in green are the C. albicans cells. a) A schematic of the gut-on-a-chip OrganoPlate is illustrated. b) The gut-on-chip cultures were infected with different cell concentrations. The images are representative of the experiment. The images are from 2 independent experiment and representative of the 10 images per condition captured. The scale bar represents 100 µm.

Chapter 5 Discussion

5.8 Hyphal morphology and invasion

The *apm4Δ/Δ* cells were previously concluded to not switch to the hyphal morphology during interactions in some environments (Chapter 3). It was of interest to study the effect of the mutation during interactions with other host environments. In this Chapter however, it was demonstrated that *apm4Δ/Δ* cells switch to the hyphal morphology during interactions with epithelial cells. The data also showed that *apm4Δ/Δ* cells are less invasive than Wt cells.

In the SEM images on figure 5.1 hyphal switch was observed by both strains. The *apm4Δ/Δ* cell morphology observed is similar to the *in vitro* observations in liquid media and agar assays; the *apm4Δ/Δ* hyphae were shorter and wider than Wt cells (Knafler et al., 2019). The Wt population was uniform in morphology while *apm4Δ/Δ* cells have septa, multiple budding sites and some cells were more yeast-like than hyphal (figure 5.1). The hyphal tip of cells was different; Wt tips were skinny while the *apm4Δ/Δ* tips were wide, consistent with results from previous investigations. The findings support immunofluorescence data on cell morphology. No differences were observed compared to *in vitro* growth, previously showed by the Ayscough lab (Knafler et al., 2019). The SEM showed differences between the Wt and *apm4Δ/Δ* cell surface possibly linked to the cell wall composition of the cells.

Host invasion is critical for virulence, it results in the production of lytic enzymes in the host as well as Candidalysin production. *C. albicans* invade host tissue through active penetration (Allert et al., 2018, Ho, J. et al., 2020). The invasion method was similar for both Wt and

apm4Δ/Δ cells however the percentage of invasion is different. The *apm4Δ/Δ* mutation resulted in decreased host invasion compared to Wt cells at 48 hours and was similar in to Wt invasion at 24 hours (figure 5.4). The Wt invasion increased over time while *apm4Δ/Δ* invasion did not. During previous investigations it was observed that *apm4Δ/Δ* cells were not as uniform in morphology as Wt cells, with cells appearing more yeast-like. It was hypothesized that the hyphal elongation could thus have an impact on the invasion phenotype as *apm4Δ/Δ* hyphae imaged so far appeared shorter (figure 5.1). The Wt hyphae appeared longer than *apm4Δ/Δ* hyphae at both 24 and 48 hours (figures 5.5 – 5.6). The Wt hyphae increased in length and branching, invading into and though the monolayer as they grew in the culture. The *apm4Δ/Δ* hyphae were short and highly branched, the length of the hyphae doesn't increase over time. Quantifications of the hyphal length during monolayer invasions could not be achieved due to the *C. albicans* growth. *C. albicans* have multiple branches, grow through the monolayer and out of the monolayer which makes it very difficult to quantify for length.

Single cell cultures are not as complex and do not fully recapitulate the physiological environment. The recently developed gut-on-a-chip model is more physiological to the host environment than cell monolayers. The gut-on-a-chip model is made up of a layer of Collagen IV and CACO-2 cells. The OrganoPlate is incubated under flow conditions that mimic peristalsis of the gut. Incubation with flow and sheer stress allows quick cell polarization (Kim et al., 2012, Kim & Ingber, 2013). The findings from the infection of the gut-on-a-chip suggested that both Wt and *apm4Δ/Δ* cells invade the host (figure 5.7). There was hyphal switch but some of the *apm4Δ/Δ* cells were yeast-like. The gut-on-chip model would be a good model to use in future studies for *C. albicans* interactions. The model can become increasingly complex through the addition of other cell types. The format of the OrganoPlates also allows for different experiments to occur simultaneously increasing the number of experimental repeats and assays that can be run using the same biological repeat.

The results showed that the decrease in host invasion observed by *apm4Δ/Δ* hyphae can be associated with the elongation/ extension of hyphae. Hyphal extension has a role on invasion, possibly linked to the hyphal penetration force and polarity maintenance. A

decrease in invasion results in decreased host damage and virulence. The host damage and virulence would be an interesting area for future work with *apm4Δ/Δ* cells.

5.9 Host adhesion

Adhesion is an important virulence factor and commensal attribute for *C. albicans*. The *C. albicans* cells attach to the host and to each other to promote colonisation. The cell wall is critical for this phenotype as the adhesion proteins are secreted and transported to the cell wall for attachment. The *apm4Δ/Δ* cell wall has changes in structure and composition such as increased chitin levels and changes in mannan architecture with no changes in β glucan, those changes have an impact on adhesion (Knafler et al., 2019).

The percentage of adhesion to CACO-2 cells was investigated and it was shown that the *apm4Δ/Δ* cells are less adhesive to host epithelial cells than Wt cells (figure 5.2). The changes of the *apm4Δ/Δ* cell wall influence adhesion possibly due to the cell wall "masking" of adhesion proteins. The localisation of adhesion proteins in *apm4Δ/Δ* cells have not been previously investigated.

It is not understood which factor influences adhesion however the decreased adhesion of cells can influence virulence, invasion as well as commensalism. As a commensal adhesion is critical for binding to the host cell and grow in biofilms without causing host damage or at least uncontrolled host damage (Vautier et al., 2015, Noble et al., 2017, Witchley et al., 2019, Romo & Kumamoto, 2020). During invasion, the *C. albicans* cells require adhesion to the host tissue to promote the hyphal morphology switch. Decreased adhesion of *apm4Δ/Δ* cells can have an important effect on virulence and host survival.

5.10 Conclusions for Chapter 5

The results from this investigation showed that the *apm4Δ/Δ* cells can switch to the hyphal morphology during interactions with epithelial cells. The increased cell wall chitin levels and changes in the mannan organization can result in a reduced adhesion. The *apm4* mutation results in decreased host invasion, possibly due to a hyphal extension deficiency and insufficient generation of invasion force. The results suggest a reduced virulence of *apm4Δ/Δ* cells compared to Wt cells. It would be of interest to study the interaction with epithelia further for host cell damage after infection and Candidalysin expression to increase the understanding of the role of AP-2 in host – pathogen interactions.

Chapter 6: Discussion

Throughout this investigation different aspects of the host – pathogen interactions have been studied using three different models (macrophage infections, zebrafish embryo infections and epithelial infections). Results relating to individual models have been discussed in individual chapters. The aim of this Chapter is to review and discuss findings brought together from all three infection models to highlight similarities and differences in the host – pathogen interactions of wild type and endocytic recycling defective *C. albicans* cells.

The *in vitro* infections of macrophages and epithelial cells showed aspects of the interaction with individual cells, stimulating different responses. During macrophage phagosome interactions *C. albicans* cells adapted to survive harsh environmental conditions such as: low pH, hypoxia and nutrient depletion (El-Kirat-Chatel et al., 2012, Hernandez-Chavez et al., 2017, Westman et al., 2018, Westman et al., 2020). The phagosomal membrane surrounds the *C. albicans* cells imposing mechanical tension and the *C. albicans* can only escape the phagosome via phagosomal membrane penetration resulting in host cell lysis (Westman et al., 2018). The phagosome environment is very different in comparison to the epithelial environment which has more nutrients and the *C. albicans* cells are not surrounded by a membrane. In epithelial interactions adhesion to the host is important as well as invasion. Invasion can cause host cell damage and thus is mostly observed during *C. albicans* pathogenicity and not commensalism (Moyes et al., 2015). The two *in vitro* environments used in this study are very different in terms of *C. albicans* response and adaptation during the interactions. It was important to use both models to study the host-pathogen interactions of *C. albicans* cells during different environmental stimulations.

The *in vivo* infection model used in this study were zebrafish embryos. Using an *in vivo* model was important as it provides a better understanding of virulence when *C. albicans* cells are interacting with multiple host cell types. During *C. albicans* interactions with zebrafish embryos both macrophages and neutrophils are present in the bloodstream promoting pathogen clearance and activating immune signals against the pathogen. The *C. albicans* are also interacting with more than one epithelial cell type during host invasion (Gratacap et al., 2014). The *in vivo* model was key for this study as it shows more complex

interactions with the host that cannot be recapitulated with the more simple *in vitro* cultures.

The key findings from this study show that *C. albicans* with an *apm4* deletion are less effective in hyphal switching and this impacts on the outcomes with all three infection models. The hyphal switch deficiency results in decreased host cell invasion and *C. albicans* virulence. The data suggest that there is a link between the cell wall composition and virulence.

The chapter is separated based on the key concepts of the study: impact of the cell wall on host pathogen interactions, impact of hyphal morphology switch of *C. albicans* during host interactions and the overall impact of the *apm4* mutation on *C. albicans* virulence. At the end of the Chapter future directions for the project will be considered.

6.1 Impact of the cell wall changes caused by *apm4* deletion in *Candida albicans* on the interactions with the host.

The cell wall composition of *C. albicans* cells with an *apm4* deletion is different to the Wt cell wall. The *apm4Δ/Δ* cell wall contains elevated levels of chitin and has changes in the mannan organization (Knafler et al., 2019). Increased cell wall chitin levels have been previously shown to "mask" β glucan impacting phagocytosis (Mora-Montes et al., 2011). In this study the cell wall changes caused by the mutation were further investigated to assess the levels of exposed β glucan. It was shown that the exposed β glucan levels of *apm4Δ/Δ* are similar to Wt levels (after growth in fresh YPD media) but in some environments the levels of exposed β glucan were lower for *apm4Δ/Δ* cells compared to the Wt (during interactions with macrophages) (figure 3.2).

Different imaging techniques were used here and in the study by Knafler (2019) suggesting that the cell wall organization is different as a result of the mutation. The TEM images in the published work by Knafler and colleagues showed that the cell wall of *apm4Δ/Δ* cells is thicker due to the increased chitin levels and the mannans on the outer cell wall are organized differently (Knafler et al., 2019). In this study SEM images (figure 5.1) from *C. albicans* hyphae invading epithelial cells showed cell surface projections on the hyphal surface that are uniformly distributed in Wt hyphae and non-uniformly distributed in

apm4Δ/Δ hyphae. The findings support that there are changes in cell wall organization that could affect phagocytosis and other host interaction phenotypes.

The cell wall changes observed during deletion of *apm4* in *C. albicans* showed an unexpected result during phagocytosis studies. According to work by other research labs increased chitin levels reduce recognition of *C. albicans* through the Dectin-1 receptor (major recognition receptor) by "masking" β glucan (Lenardon et al., 2010, Mora-Montes et al., 2012, Bain et al., 2014). Findings during phagocytosis experiments showed that *apm4Δ/Δ* cells are taken up more by macrophages compared to Wt cells (figure 3.1). The findings were different than expected as the levels of exposed β glucan are reduced or similar to the Wt cells. The phagocytosis is possibly Dectin-1 independent and linked to the recognition of chitin and/or mannans instead of β glucan. No PRRs have been identified for chitin but there are receptors that co-recognize chitin and mannans like TLR6 and Dectin-2 (Netea et al., 2008). The differences in mannan organization observed in *apm4Δ/Δ* cells suggest that mannans could be mainly responsible for the increased phagocytosis observed, there are many PRRs for mannans such as Galectin 3, TLR3 and TLR6 (Netea et al., 2008).

Another host interaction response influenced by the cell wall organization is adhesion. The cell wall changes of *apm4Δ/Δ* cells influenced host cell adhesion. It was demonstrated that *apm4Δ/Δ* cells were less adhesive to host epithelial cells (figure 5.2). During interactions with epithelia *C. albicans* secrete adhesion proteins such as Als family proteins and Hwp1 to promote host cell adhesion (Liu, Y., Filler, 2011, Moyes et al., 2015, Vautier et al., 2015, Ho et al., 2019). The deletion of *apm4* has an impact on the cell surface composition and organization. The findings from the adhesion experiment suggest that the increased chitin levels and changes in mannan organization "mask" the adhesion proteins and stop the initial interactions with the host surface. The phenotype could also be linked to the polarization deficiency of the *apm4Δ/Δ* cells. The cells are unable to maintain polarization and deposit new cell wall material on the whole cell rather than at the active growth sites (Knafler et al., 2019). The adhesion proteins might be inappropriately localized at the cell surface impacting adhesion.

The mechanical properties of the cell wall were also investigated. The Young's modulus of *C. albicans* hyphae is a measurement of the cell wall elasticity (figure 3.10). The data show

two important findings. The first finding was that the Young's modulus of *apm4Δ/Δ* hyphae is uniform at the mother and hyphal tube regions while the Wt hyphae have a stiffer stem than the mother region. Firstly, the small variation between the mother and hyphal tube in the Young's modulus of *apm4Δ/Δ* cells can be supported by data from Knafler (2019) showing that the cells do not have a focused growth and there is new cell wall material deposited around the cell surface and not just at polarized growth sites like the hyphal tip (Knafler et al., 2019). The Young's modulus changes between the mother and hyphal tube regions of the Wt hyphae could be an indication of active growth. Work by Weiner (2018) showed that during hyphal growth a large number of vesicles and the ER are present at the tip to generate new cell wall material. The increase in cell wall stiffness at the hyphal tube could be a reflection of growth (Weiner et al., 2018). The second finding is that the *apm4Δ/Δ* hyphal cell wall is softer than the Wt cell wall. This suggests that the cell wall organization of *apm4Δ/Δ* hyphae is different compared to the Wt cells. The Young's modulus of Wt cells is larger than the mutant cell Young's modulus, suggesting some changes in the mechanical properties of the cell wall. The methodology used for AFM acquisition here and the analysis was different compared to the ones used in other studies measuring the yeast and hyphal Young's modulus so the data are not comparable (Ene et al., 2012, Colak et al., 2020). Previous work seeded *C. albicans* on Polydimethylsiloxane or FBS which can ultimately change the environment and the mechanical properties as the hyphae respond to different surfaces.

The results highlight the role of the cell wall composition and organization during host – pathogen interactions and demonstrate that the AP-2 cell wall changes can be critical for both adhesion and phagocytosis.

6.2 Impact of hyphal morphology switch on the host – pathogen interactions of *Candida albicans*.

One of the main findings of the study has been that the *apm4Δ/Δ* cells have hyphal switch deficiencies. These deficiencies were reported in all three infection models. In this section the hyphal morphology of *apm4Δ/Δ* cells as well as the impact of hyphal switch deficiencies to host – pathogen interactions will be discussed.

During interactions with macrophages (figure 3.7) the *apm4Δ/Δ* cells did not switch to the hyphal morphology at similar levels to Wt cells and mostly remained yeast-locked. The

phenotype was further confirmed by the differences reported for the phagosomal pH. *C. albicans* cells that switch to the hyphal morphology alkalinize the host phagosome (Vylkova et al., 2014, Wagener et al., 2017, Westman et al., 2018). The phagosomal pH during *apm4Δ/Δ* infections was similar to the control group and the pH during Wt infections was different according to the fluorescence intensity findings reported during Lysosensor Yellow/Blue staining (figure 3.13). These data could support the findings from figure 3.7 that the *apm4Δ/Δ* cells do not successfully switch to the hyphal morphology inside the phagosome.

During zebrafish infections some hyphal switch was observed by *apm4Δ/Δ* cells as shown in figures 4.6 and 4.10. The *apm4Δ/Δ* cells are mostly yeast-like as observed by the smooth microcolonies on figure 4.6. During zebrafish infections Wt cells switch to the hyphal morphology and possibly result in invasion and damage (figures 4.2, 4.6 and 4.10). In epithelial infections different phenotypes are observed, the hyphal switch deficiency might not be as severe.

During single cell and monolayer infections (figures 5.1, 5.5 and 5.6) hyphal switch is observed by both Wt and *apm4Δ/Δ* cells however the mutant hyphae are not uniform in size and some appear more yeast-like. The *apm4Δ/Δ* hyphae have an elongation deficiency compared to Wt hyphae. The hyphae are shorter, this phenotype was characterized previously during work in *in vitro* media cultures (Knafler et al., 2019). During the preliminary experiments using the gut-on-a-chip model for interactions with *C. albicans* (figure 5.7) it was observed that a high proportion of *apm4Δ/Δ* cells were in the hyphal morphology while the Wt cells were hyphal. Combined the results from the three models all show that there is a hyphal switch deficiency during *apm4* deletion in *C. albicans* cells with the most severe phenotype occurring during macrophage infections.

An important question here is why do *apm4Δ/Δ* cells have a hyphal switch deficiency in the phagosome environment? During macrophage interactions with *C. albicans*, the *Candida* cells have been characterized to induce lytic “escape” from the environment by switching to the hyphal morphology and penetrating the phagosome membrane (Scherer et al. 2020, Westman et al., 2020). The Wt cells present this phenotype however *apm4Δ/Δ* cells do not switch to the hyphal morphology and instead revert to the yeast morphology proliferating in

the environment (figure 3.14). The phenotype can be supported by the size of microcolonies (*Candida*-phagocytes) during zebrafish infections (figures 4.5, 4.7 and 4.8). Hyphal switching Wt microcolonies have a similar size to hyphal switch deficient *apm4Δ/Δ* microcolonies. One hypothesis is that this mechanism can be linked to the mechanical properties of cells suggesting that the *apm4Δ/Δ* hyphae are not producing enough invasion force at the tip to penetrate the membrane. A second hypothesis for the phenotype is that *apm4Δ/Δ* cells appear to be switching to the hyphal morphology but the cells "abort" the response due to signaling. It is hypothesized that there is an important step in the hyphal switch response where the cell "fate" is determined. Glory (2017) was studying the hyphal induction response compared to the cell cycle. The study showed that the cells express hyphal specific genes via the regulation of Ume6 however in some cases the *C. albicans* can look like elongated hyphae but do not express hyphal genes. Those cells appear like hyphae due to a mitotic block through a cell cycle cyclin (Cdc5) depletion (Glory et al., 2017). The findings from Glory (2017) in combination with the observations in this study can suggest that the hyphal switch associated genes need to be expressed before a cell is "committed" to becoming a hypha. The *apm4Δ/Δ* cells might not be expressing and localizing the hyphal associated proteins appropriately resulting in elongated buds that appear hyphal-like but the cells are still in the yeast morphology and proliferate in the phagosome environment.

The cell wall composition has an impact on hyphal switch. Chitin is important for maintenance of the cell shape, increased chitin levels such as the ones observed in *apm4Δ/Δ* cells impact the mechanical properties and could result in a hyphal switch deficiency (Garcia-Rubio et al., 2020, Liu, N. N. et al., 2020). The AFM data suggested that there is a change in the cell wall organization/ structure due to the mutation possibly linked to the increased chitin. Using the *apm4Δ/Δ,chs3Δ* strain (homozygous *apm4* deletion and heterozygous *chs3* deletion resulting in physiological levels of cell wall chitin), the overall levels of chitin were reduced but the localization of Chs3 and thus the chitin growth sites are still affected by the *apm4* mutation. During macrophage infections with *apm4Δ/Δ,chs3Δ* cells a partial rescue of the hyphal switch phenotype. We are currently unsure how the cell wall composition impacts hyphal morphology.

The cell wall chitin levels impact hyphal switch but restoring the chitin levels results in a partial rescue and not a full rescue suggesting that there are more factors involved in the observed phenotype. A modelling study of *S. cerevisiae* by Trogdon (2018) demonstrated the impact of cell geometry on the polarization of Cdc42. Cdc42 is a part of the polarisome at the hyphal tip. It is involved in vesicle docking and maintenance of polarized growth (figure 1.3). Using mathematical simulations, they concluded that the wider tip geometry (similar to the *apm4Δ/Δ* hyphae phenotype) results in Cdc42 drifting away from the tip over time impacting the stability of the polarisome. They showed that polarization of Cdc42 is more stable at spherical and elongated geometries similar to a yeast and a Wt hyphal morphology (Trogdon et al., 2018). Previous work in the Ayscough lab showed that there is some mis-localization of Cdc42 in *apm4Δ/Δ* cells. It is possible that the geometry of the cells and the mis-localization of Cdc42, are factors influencing hyphal morphology switch and maintenance. Unpublished work using *apm4Δ/Δ* cells in the Ayscough lab showed that proteins that localize at the tip marking polarity such as exocyst components Sec3 and Sec8 as well as Spa2 and Mlc1 are not localized appropriately. These suggest that during initial hyphal switch there could be markers that promote more polarized growth but the proteins are not localized at the appropriate sites and the process of hyphal switch is stopped. These findings could indicate that AP-2 has downstream effectors with a role in trafficking of exocyst and polarity components at the cell surface for active growth. Dissociating the AP-2 complex could thus influence hyphal switch and possibly the induction of host damage. Chs3 is a major cargo of AP-2 however we can postulate that it is not the only important cargo of the complex. These suggest that other changes caused by the *apm4* mutation in *C. albicans* such as polarization and geometry could have an impact on hyphal switch.

Overall, the data here show that AP-2 has a role in hyphal morphology switch during host-pathogen interactions. An inability to switch to the hyphal morphology results in vegetative growth inside the macrophage phagosome. The hyphal switch deficiency observed in *apm4Δ/Δ* cells is linked to the cell wall chitin levels and the trafficking at polarized growth sites. It is currently not well understood how the cell wall composition can influence the hyphal switch response.

6.3 Overall impact of the *apm4* deletion in *Candida albicans* virulence.

Through the different infection models, it was shown that *apm4Δ/Δ* cells are less virulent than Wt cells. The reduced virulence is attributed to the hyphal switch deficiency phenotype that the *apm4Δ/Δ* cells present during host interactions.

During zebrafish infection experiments the *apm4Δ/Δ* infected embryos showed increased survival after infection compared to Wt infected embryos (figure 4.1). The decreased virulence of *apm4Δ/Δ* cells is not linked to clearance or a differential activation of the immune cells but rather a hyphal switch deficiency (figures 4.2 - 4.3). Zebrafish infections with *apm4Δ/Δ,chs3Δ* cells showed a partial rescue of virulence compared to *apm4Δ/Δ* infections. This is due to either the cell wall composition or the increased hyphal switch of cells (figure 3.8). The reduced *apm4Δ/Δ* virulence can be further supported by the macrophage lysis data on figure 3.5 where less macrophage death is reported due to *apm4Δ/Δ* infections compared to Wt infections. The findings suggest an impact of the AP-2 complex on host virulence due to the deficiency of cells to successfully switch to the hyphal morphology.

During epithelial infections decreased invasion is reported during *apm4Δ/Δ* infections (figure 5.4). Reduced invasion can mean reduced virulence as the *C. albicans* cells do not cause host cell damage which is associated with the hyphal morphology. It can be hypothesized that *apm4Δ/Δ* cells do not result in host damage or at least uncontrolled high levels host damage in some environments as the cells are more yeast-like. According to a recent study by Allert and colleagues it is possible for *C. albicans* hyphae to invade but not induce any host damage. In this study the induction of Candidalysin by *apm4Δ/Δ* cells was not investigated but based on the hyphal switch deficiency phenotype findings, it can be postulated that the *apm4Δ/Δ* cells secrete less Candidalysin than Wt cells (Moyes et al., 2016, Allert et al., 2018). Candidalysin secretion and damage would be interesting avenues to explore in future studies to observed whether there is a link between Candidalysin secretion and damage to the increased survival reported during *apm4Δ/Δ* infections of zebrafish embryos.

To our knowledge this is the first study to identify vegetative growth of *C. albicans* inside the host macrophage phagosome. Recent work by Scherer (2020) mentioned that the yeast-

locked cells used in their study grew inside a macrophage, but this was not investigated further. In Chapter 3 the results showed that a high proportion of cells with hyphal switch deficiencies grew in the phagosome instead of switching to the hyphal morphology (figures 3.14 -3.15). Proliferation inside the host phagosome could be used as a dissemination mechanism, *C. albicans* have been shown to use phagocytes as a dissemination vessel during infection (Scherer et al., 2020). *apm4Δ/Δ* cells grow inside macrophages and as shown in figure 4.13 they disseminated more than Wt cells. Phagosome proliferation was also reported for yeast-locked cells (figure 3.15). Increased *C. albicans* growth inside the host phagosome can potentially induce physical damage to host cells. Findings in this study showed that *apm4Δ/Δ* cells as well as yeast-locked cells (**Supplementary 2**) can induce non-hyphal associated macrophage lysis. The data showed that 50% of macrophage lysis recorded in yeast-locked infections was not associated with hyphal switch. Based on work by Westman (2018 & 2020), it can be hypothesized that increase growth inside the phagosome can lead to phagosomal membrane rupture similar to the rupture caused by hyphal cells leading to macrophage death (Westman et al., 2018, Westman et al., 2020). There is not enough evidence to support this, however it would be of interest to study this phenotype further and investigate non-hyphal induced host cell death and the prevalence of the phenotype in non-hyphal switching *Candida spps*.

Overall, in this thesis it is concluded that the role of AP-2 endocytic adaptor complex is critical for *C. albicans* virulence. The complex has a role in cell surface remodeling and can influence both uptake and adhesion by the host. AP-2 influences the organization of the cell wall and the trafficking of components at the active growth sites. Loss of function of the complex results in a hyphal switch deficiency and reduced virulence in the host. This results in a more commensal lifestyle for *C. albicans* as the cells grow and adapt to the host environment without interference from the host immune cells as they do not induce a lot of host damage (Witchley et al., 2019, Romo & Kumamoto, 2020). These findings are important as *C. albicans* cells that only exhibit a commensal lifestyle and have deficiencies in virulence factors are not pathogenic. Keeping *C. albicans* cells commensal could be an important goal in future diagnostics as they would not be inducing any harmful infections. AP-2 or its downstream effectors can be targeted by future treatments to ensure that *C. albicans* remain as commensals and are not pathogenic to the host.

6.4 Future directions for this project

This thesis provided some insights in the role of the AP-2 complex for cell surface remodeling and hyphal morphology switch during host interactions. In this discussion Chapter the main findings were reviewed, and some interesting questions were raised. If there was more time to expand on this work there are some key experiments to address these questions. This would have increased our understanding of the *C. albicans* and host interactions as well as further strengthen our comprehension of the results presented in this thesis. Those experiments are outlined here:

- It was concluded that the hyphal switch deficiency observed for *apm4Δ/Δ* cells is linked to a polarization deficiency by not maintaining the polarisome and the Spitzenkorper at the active growth sites. To address this question, different *C. albicans* cells tagged with GFP for Spitzenkorper markers (such as Mlc1) and polarisome markers (such as Cdc42) can be used to run an *in vitro* invasion assay like the one described by Puerner (2020) from the Arkowitz lab. The set-up of this assay allows for measurements of the invasion forces through complex polymers in combination with the real-time fluorescent imaging that allows visualization of the GFP tagged proteins during the hyphal switch response.
- Different experiments in this study showed that the *apm4* deletion in *C. albicans* results in changes in the cell wall composition and structure which influence the host-pathogen interactions. Given more time it would be of interest to complement the Knafler (2019) data and repeat the TEM imaging including the *apm4Δ/Δ,chs3Δ* cells to have a better understanding of the impact of the *chs3* heterozygous deletion on the cell wall structure. Repeating SEM imaging of *C. albicans* cells during infections of different host cells would also be of interest as the organization of the cell surface can be observed. More AFM measurements in the yeast morphology and

using a different Cantilever would be needed to study the cell surface properties in more detail and to differentiate the properties of the hyphal and yeast cell wall.

- The findings suggested that the localization and exposure of adhesion proteins can be influenced by the cell wall organization. Immunofluorescence of *C. albicans* adhesion proteins would allow an understanding of the localization of proteins and if the staining is based on a receptor ligand model (similar to the Fc Dectin staining used in this study) it would be possible to investigate the level of exposure for different adhesion proteins.
- The results concluded that there is increased phagocytosis of *apm4Δ/Δ* cells compared to Wt cells. To investigate the impact of chitin on this phenotype, the experiment should be repeated to include *apm4Δ/Δ,chs3Δ* cells. To determine which receptors are involved in the interaction macrophages with knockdowns of different receptors such as Dectin-1.
- To assess more complex host-pathogen interactions, the response of damage and Candidalysin, it would be of interest to develop assays using the gut-on-a-chip model. The complexity of the model can be increased by adding different cell types to other channels such as macrophages in the bottom channel. This would allow for dissemination studies from macrophages to epithelia and vice versa. The OrganoPlates have multiple chips and can be used to run multiple assays simultaneously. Host cell damage can be assessed using assays such as β-galactosidase induction. The secretion of Candidalysin can also be investigated by running qPCR of the infection media.
- The zebrafish data in this thesis are from work during disseminated Candidiasis, it would be of important to study more localized infections of Candidiasis. It would be of interest to further develop the zebrafish feeding infection method (not included in this study) to recapitulate the commensal environment of *C. albicans*. Using this method, the zebrafish are infected with no invasion. The successfully infected embryos could then be used to study the interactions of *C. albicans* with the gut. Biofilms could be allowed to develop and possibly the embryos can be stained, imaged and studied for invasion. The biggest issue with the development of this assay was that the experiment requires an animal license. It would also be of interest

to use the Swimbladder infection phenotype developed by the Wheeler lab to study the localized epithelial infection and image for invasion using high resolution LightSheet and Spinning disk microscopy. Host damage during infection can be quantified using immunostaining assays such as TUNNEL staining, the results can then be compared to *in vitro* assays.

- It would be of interest to explore the non-hyphal associated cell death of macrophages showed in this study. To investigate the response other *Candida spp.* which do not switch to the hyphal morphology should be included in the study. The phagosome integrity needs to be assessed using different staining dyes and high-resolution microscopy. A staining method would also be important to use for assessing macrophage death, this can be done using microscopy as well as using FACs.

It is hoped that this work could provide further awareness into the interactions of *C. albicans* cells with different host environments as well as insights into new therapeutics avenues.

Chapter 7: References

Allert, S., Forster, T.M., Svensson, C.M., Richardson, J.P., Pawlik, T., Hebecker, B., Rudolphi, S., Juraschitz, M., Schaller, M., Blagojevic, M., Morschhauser, J., Figge, M.T., Jacobsen, I.D., Naglik, J.R., Kasper, L., Mogavero, S. & Hube, B. 2018, "Candida albicans-Induced Epithelial Damage Mediates Translocation through Intestinal Barriers", *mBio,* vol. 9, no. 3, pp. 10.1128/mBio.00915-18.

Alonso, J.L. & Goldmann, W.H. 2003, "Feeling the forces: atomic force microscopy in cell biology", *Life Sciences,* vol. 72, no. 23, pp. 2553-2560.

Alves de Lima, N.C., Ratti, B.A., Souza Bonfim Mendonca, P., Murata, G., Araujo Pereira, R.R., Nakamura, C.V., Lopes Consolaro, M.E., Estivalet Svidzinski, T.I., Hatanaka, E., Bruschi, M.L. & Oliveira Silva, S. 2018, "Propolis increases neutrophils response against Candida albicans through the increase of reactive oxygen species", *Future microbiology,* vol. 13, pp. 221-230.

Anton, C., Taubas, J.V. & Roncero, C. 2018, "The Functional Specialization of Exomer as a Cargo Adaptor During the Evolution of Fungi", *Genetics,* vol. 208, no. 4, pp. 1483-1498.

Arkowitz, R.A. & Bassilana, M. 2019, "Recent advances in understanding Candida albicans hyphal growth", *F1000Research,* vol. 8, pp. 10.12688/f1000research.18546.1. eCollection 2019.

Aryal Sagar 2018, 15/04/2018-last update, ***Candida albicans- An Overview*** [Homepage of Microbes and Notes], [Online]. Available: https://microbenotes.com/candida-albicans/ [2021, 20/10/21].

Bain, J.M., Louw, J., Lewis, L.E., Okai, B., Walls, C.A., Ballou, E.R., Walker, L.A., Reid, D., Munro, C.A., Brown, A.J., Brown, G.D., Gow, N.A. & Erwig, L.P. 2014, "Candida albicans hypha formation and mannan masking of beta-glucan inhibit macrophage phagosome maturation", *mBio,* vol. 5, no. 6, pp. e01874-14.

Balashov, S.V., Park, S. & Perlin, D.S. 2006, "Assessing resistance to the echinocandin antifungal drug caspofungin in Candida albicans by profiling mutations in FKS1", *Antimicrobial Agents and Chemotherapy,* vol. 50, no. 6, pp. 2058-2063.

Barnett, J.A. 2008, "A history of research on yeasts 12: medical yeasts part 1, Candida albicans", *Yeast (Chichester, England),* vol. 25, no. 6, pp. 385-417.

Bassilana, M., Puerner, C. & Arkowitz, R.A. 2020, "External signal-mediated polarized growth in fungi", *Current opinion in cell biology,* vol. 62, pp. 150-158.

Bates, S., Hall, R.A., Cheetham, J., Netea, M.G., MacCallum, D.M., Brown, A.J., Odds, F.C. & Gow, N.A. 2013, "Role of the Candida albicans MNN1 gene family in cell wall structure and virulence", *BMC research notes,* vol. 6, pp. 294-0500-6-294.

Benmoussa, K., Authier, H., Prat, M., AlaEddine, M., Lefevre, L., Rahabi, M.C., Bernad, J., Aubouy, A., Bonnafe, E., Leprince, J., Pipy, B., Treilhou, M. & Coste, A. 2017, "P17, an Original Host Defense Peptide from Ant Venom, Promotes Antifungal Activities of Macrophages through the Induction of C-Type Lectin Receptors Dependent on LTB4-Mediated PPARgamma Activation", *Frontiers in immunology,* vol. 8, pp. 1650.

Bhattacharya, S., Sae-Tia, S. & Fries, B.C. 2020, "Candidiasis and Mechanisms of Antifungal Resistance", *Antibiotics (Basel, Switzerland),* vol. 9, no. 6, pp. 10.3390/antibiotics9060312.

Bojarczuk, A., Miller, K.A., Hotham, R., Lewis, A., Ogryzko, N.V., Kamuyango, A.A., Frost, H., Gibson, R.H., Stillman, E., May, R.C., Renshaw, S.A. & Johnston, S.A. 2016, "Cryptococcus neoformans Intracellular Proliferation and Capsule Size Determines Early Macrophage Control of Infection", *Scientific reports,* vol. 6, pp. 21489.

Bowen, A.R., Chen-Wu, J.L., Momany, M., Young, R., Szaniszlo, P.J. & Robbins, P.W. 1992, "Classification of fungal chitin synthases", *Proceedings of the National Academy of Sciences of the United States of America,* vol. 89, no. 2, pp. 519-523.

Brand, A., Shanks, S., Duncan, V.M., Yang, M., Mackenzie, K. & Gow, N.A. 2007, "Hyphal orientation of Candida albicans is regulated by a calcium-dependent mechanism", *Current biology : CB,* vol. 17, no. 4, pp. 347-352.

Brothers, K.M., Newman, Z.R. & Wheeler, R.T. 2011, "Live imaging of disseminated candidiasis in zebrafish reveals role of phagocyte oxidase in limiting filamentous growth", *Eukaryotic cell,* vol. 10, no. 7, pp. 932-944.

Brown, A.J., Brown, G.D., Netea, M.G. & Gow, N.A. 2014, "Metabolism impacts upon Candida immunogenicity and pathogenicity at multiple levels", *Trends in microbiology,* vol. 22, no. 11, pp. 614-622.

Brown, D.H.,Jr, Giusani, A.D., Chen, X. & Kumamoto, C.A. 1999, "Filamentous growth of Candida albicans in response to physical environmental cues and its regulation by the unique CZF1 gene", *Molecular microbiology,* vol. 34, no. 4, pp. 651-662.

Brown, G.D., Denning, D.W., Gow, N.A., Levitz, S.M., Netea, M.G. & White, T.C. 2012, "Hidden killers: human fungal infections", *Science translational medicine,* vol. 4, no. 165, pp. 165rv13.

Brown, G.D. & May, R.C. 2017, "Editorial overview: Host-microbe interactions: fungi", *Current opinion in microbiology,* vol. 40, pp. v-vii.

Bulawa, C.E., Miller, D.W., Henry, L.K. & Becker, J.M. 1995, "Attenuated virulence of chitin-deficient mutants of Candida albicans", *Proceedings of the National Academy of Sciences of the United States of America,* vol. 92, no. 23, pp. 10570-10574.

Burgain, A., Pic, E., Markey, L., Tebbji, F., Kumamoto, C.A. & Sellam, A. 2019, "A novel genetic circuitry governing hypoxic metabolic flexibility, commensalism and virulence in the fungal pathogen Candida albicans", *PLoS pathogens,* vol. 15, no. 12, pp. e1007823.

Byrd, A.S., O'Brien, X.M., Johnson, C.M., Lavigne, L.M. & Reichner, J.S. 2013, "An extracellular matrix-based mechanism of rapid neutrophil extracellular trap formation in response to Candida albicans", *Journal of immunology (Baltimore, Md.: 1950),* vol. 190, no. 8, pp. 4136-4148.

Case, E.D.R. & Samuel, J.E. 2016, "Contrasting Lifestyles Within the Host Cell", *Microbiology spectrum,* vol. 4, no. 1, pp. 10.1128/microbiolspec.VMBF-0014-2015.

Cassone, A. & Sobel, J.D. 2016, "Experimental Models of Vaginal Candidiasis and Their Relevance to Human Candidiasis", *Infection and immunity,* vol. 84, no. 5, pp. 1255-1261.

Chairatana, P., Chiang, I.L. & Nolan, E.M. 2017, "Human alpha-Defensin 6 Self-Assembly Prevents Adhesion and Suppresses Virulence Traits of Candida albicans", *Biochemistry,* vol. 56, no. 8, pp. 1033-1041.

Chapa-y-Lazo, B., Allwood, E.G., Smaczynska-de, R.,II, Snape, M.L. & Ayscough, K.R. 2014, "Yeast endocytic adaptor AP-2 binds the stress sensor Mid2 and functions in polarized cell responses", *Traffic (Copenhagen, Denmark),* vol. 15, no. 5, pp. 546-557.

Chapa-Y-Lazo, B. & Ayscough, K.R. 2014, "Apm4, the mu subunit of yeast AP-2 interacts with Pkc1, and mutation of the Pkc1 consensus phosphorylation site Thr176 inhibits AP-2 recruitment to endocytic sites", *Communicative & integrative biology,* vol. 7, pp. e28522.

Chattaway, F.W., Holmes, M.R. & Barlow, A.J. 1968, "Cell wall composition of the mycelial and blastospore forms of Candida albicans", *Journal of general microbiology,* vol. 51, no. 3, pp. 367-376.

Chen, H., Zhou, X., Ren, B. & Cheng, L. 2020, "The regulation of hyphae growth in Candida albicans", *Virulence,* vol. 11, no. 1, pp. 337-348.

Chen-Wu, J.L., Zwicker, J., Bowen, A.R. & Robbins, P.W. 1992, "Expression of chitin synthase genes during yeast and hyphal growth phases of Candida albicans", *Molecular microbiology,* vol. 6, no. 4, pp. 497-502.

Cleary, I.A., Reinhard, S.M., Lazzell, A.L., Monteagudo, C., Thomas, D.P., Lopez-Ribot, J.L. & Saville, S.P. 2016, "Examination of the pathogenic potential of Candida albicans filamentous cells in an animal model of haematogenously disseminated candidiasis", *FEMS yeast research,* vol. 16, no. 2, pp. fow011.

Colak, A., Ikeh, M.A.C., Nobile, C.J. & Baykara, M.Z. 2020, "In Situ Imaging of Candida albicans Hyphal Growth via Atomic Force Microscopy", mSphere, vol. 5, no. 6, pp. 10.1128/mSphere.00946-20.

Correia, I., Alonso-Monge, R. & Pla, J. 2017, "The Hog1 MAP Kinase Promotes the Recovery from Cell Cycle Arrest Induced by Hydrogen Peroxide in Candida albicans", *Frontiers in microbiology,* vol. 7, pp. 2133.

Cota, E. & Hoyer, L.L. 2015, "The Candida albicans agglutinin-like sequence family of adhesins: functional insights gained from structural analysis", *Future microbiology,* vol. 10, no. 10, pp. 1635-1548.

Cottier, F. & Hall, R.A. 2020, "Face/Off: The Interchangeable Side of Candida Albicans", *Frontiers in cellular and infection microbiology,* vol. 9, pp. 471.

Cottier, F., Sherrington, S., Cockerill, S., Del Olmo Toledo, V., Kissane, S., Tournu, H., Orsini, L., Palmer, G.E., Perez, J.C. & Hall, R.A. 2019, "Remasking of Candida albicans beta-Glucan in Response to Environmental pH Is Regulated by Quorum Sensing", *mBio,* vol. 10, no. 5, pp. 10.1128/mBio.02347-19.

Crampin, H., Finley, K., Gerami-Nejad, M., Court, H., Gale, C., Berman, J. & Sudbery, P. 2005, "Candida albicans hyphae have a Spitzenkorper that is distinct from the polarisome found in yeast and pseudohyphae", *Journal of cell science,* vol. 118, no. Pt 13, pp. 2935-2947.

da Silva Dantas, A., Lee, K.K., Raziunaite, I., Schaefer, K., Wagener, J., Yadav, B. & Gow, N.A. 2016, "Cell biology of Candida albicans-host interactions", *Current opinion in microbiology,* vol. 34, pp. 111-118.

Danhof, H.A., Vylkova, S., Vesely, E.M., Ford, A.E., Gonzalez-Garay, M. & Lorenz, M.C. 2016, "Robust Extracellular pH Modulation by Candida albicans during Growth in Carboxylic Acids", *mBio,* vol. 7, no. 6, pp. 10.1128/mBio.01646-16.

Davis, J.M., Huang, M., Botts, M.R., Hull, C.M. & Huttenlocher, A. 2016, "A Zebrafish Model of Cryptococcal Infection Reveals Roles for Macrophages, Endothelial Cells, and Neutrophils in the Establishment and Control of Sustained Fungemia", *Infection and immunity,* vol. 84, no. 10, pp. 3047-3062.

Davis, S.E., Hopke, A., Minkin, S.C.,Jr, Montedonico, A.E., Wheeler, R.T. & Reynolds, T.B. 2014, "Masking of beta(1-3)-glucan in the cell wall of Candida albicans from detection by innate immune cells depends on phosphatidylserine", *Infection and immunity,* vol. 82, no. 10, pp. 4405-4413.

Deresinski, S.C. & Stevens, D.A. 2003, "Caspofungin", *Clinical infectious diseases : an official publication of the Infectious Diseases Society of America,* vol. 36, no. 11, pp. 1445-1457.

Desai, J.V. & Lionakis, M.S. 2019, "Setting Up Home: Fungal Rules of Commensalism in the Mammalian Gut", *Cell host & microbe,* vol. 25, no. 3, pp. 347-349.

Desnos-Ollivier, M., Bretagne, S., Raoux, D., Hoinard, D., Dromer, F., Dannaoui, E. & European Committee on Antibiotic Susceptibility Testing 2008, "Mutations in the fks1 gene in Candida albicans, C. tropicalis, and C. krusei correlate with elevated caspofungin MICs uncovered in AM3 medium using the method of the European Committee on Antibiotic Susceptibility Testing", *Antimicrobial Agents and Chemotherapy,* vol. 52, no. 9, pp. 3092-3098.

Dichtl, K., Samantaray, S. & Wagener, J. 2016, "Cell wall integrity signalling in human pathogenic fungi", *Cellular microbiology,* vol. 18, no. 9, pp. 1228-1238.

Duggan, S., Leonhardt, I., Hunniger, K. & Kurzai, O. 2015, "Host response to Candida albicans bloodstream infection and sepsis", *Virulence,* vol. 6, no. 4, pp. 316-326.

Duvenage, L., Walker, L.A., Bojarczuk, A., Johnston, S.A., MacCallum, D.M., Munro, C.A. & Gourlay, C.W. 2019, "Inhibition of Classical and Alternative Modes of Respiration in Candida albicans Leads to Cell Wall Remodeling and Increased Macrophage Recognition", *mBio,* vol. 10, no. 1, pp. 10.1128/mBio.02535-18.

El-Kirat-Chatel, S. & Dufrene, Y.F. 2012, "Nanoscale imaging of the Candida-macrophage interaction using correlated fluorescence-atomic force microscopy", *ACS nano,* vol. 6, no. 12, pp. 10792-10799.

Ene, I.V., Adya, A.K., Wehmeier, S., Brand, A.C., MacCallum, D.M., Gow, N.A. & Brown, A.J. 2012, "Host carbon sources modulate cell wall architecture, drug resistance and virulence in a fungal pathogen", Cellular microbiology, vol. 14, no. 9, pp. 1319-1335.

Ene, I.V., Brunke, S., Brown, A.J. & Hube, B. 2014, "Metabolism in fungal pathogenesis", *Cold Spring Harbor perspectives in medicine,* vol. 4, no. 12, pp. a019695.

Epp, E., Walther, A., Lepine, G., Leon, Z., Mullick, A., Raymond, M., Wendland, J. & Whiteway, M. 2010, "Forward genetics in Candida albicans that reveals the Arp2/3 complex is required for hyphal formation, but not endocytosis", *Molecular microbiology,* vol. 75, no. 5, pp. 1182-1198.

Evans, R.J., Pline, K., Loynes, C.A., Needs, S., Aldrovandi, M., Tiefenbach, J., Bielska, E., Rubino, R.E., Nicol, C.J., May, R.C., Krause, H.M., O'Donnell, V.B., Renshaw, S.A. & Johnston, S.A. 2019, "15-keto-prostaglandin E2 activates host peroxisome proliferator-activated receptor gamma (PPAR-gamma) to promote Cryptococcus neoformans growth during infection", *PLoS pathogens,* vol. 15, no. 3, pp. e1007597.

Evans, R.J., Voelz, K., Johnston, S.A. & May, R.C. 2017, "Using Flow Cytometry to Analyze Cryptococcus Infection of Macrophages", *Methods in molecular biology (Clifton, N.J.),* vol. 1519, pp. 349-357.

Fan, Y., He, H., Dong, Y. & Pan, H. 2013, "Hyphae-specific genes HGC1, ALS3, HWP1, and ECE1 and relevant signaling pathways in Candida albicans", *Mycopathologia,* vol. 176, no. 5-6, pp. 329-335.

Galan-Diez, M., Arana, D.M., Serrano-Gomez, D., Kremer, L., Casasnovas, J.M., Ortega, M., Cuesta-Dominguez, A., Corbi, A.L., Pla, J. & Fernandez-Ruiz, E. 2010, "Candida albicans beta-glucan exposure is controlled by the fungal CEK1-mediated mitogen-activated protein kinase pathway that modulates immune responses triggered through dectin-1", *Infection and immunity,* vol. 78, no. 4, pp. 1426-1436.

Garcia-Rubio, R., de Oliveira, H.C., Rivera, J. & Trevijano-Contador, N. 2020, "The Fungal Cell Wall: Candida, Cryptococcus, and Aspergillus Species", *Frontiers in microbiology,* vol. 10, pp. 2993.

Gazendam, R.P., van de Geer, A., Roos, D., van den Berg, T.K. & Kuijpers, T.W. 2016, "How neutrophils kill fungi", *Immunological reviews,* vol. 273, no. 1, pp. 299-311.

Gazendam, R.P., van de Geer, A., van Hamme, J.L., Tool, A.T., van Rees, D.J., Aarts, C.E., van den Biggelaar, M., van Alphen, F., Verkuijlen, P., Meijer, A.B., Janssen, H., Roos, D., van den Berg, T.K. & Kuijpers, T.W. 2016, "Impaired killing of Candida albicans by granulocytes mobilized for transfusion purposes: a role for granule components", *Haematologica,* vol. 101, no. 5, pp. 587-596.

Glory, A., van Oostende, C.T., Geitmann, A. & Bachewich, C. 2017, "Depletion of the mitotic kinase Cdc5p in Candida albicans results in the formation of elongated buds that switch to the hyphal fate over time in a Ume6p and Hgc1p-dependent manner", Fungal genetics and biology : FG & B, vol. 107, pp. 51-66.

Goodridge, H.S., Underhill, D.M. & Touret, N. 2012, "Mechanisms of Fc receptor and dectin-1 activation for phagocytosis", *Traffic (Copenhagen, Denmark),* vol. 13, no. 8, pp. 1062-1071.

Gow, N.A., Netea, M.G., Munro, C.A., Ferwerda, G., Bates, S., Mora-Montes, H.M., Walker, L., Jansen, T., Jacobs, L., Tsoni, V., Brown, G.D., Odds, F.C., Van der Meer, J.W., Brown, A.J. & Kullberg, B.J. 2007, "Immune recognition of Candida albicans beta-glucan by dectin-1", *The Journal of infectious diseases,* vol. 196, no. 10, pp. 1565-1571.

Gow, N.A.R., Latge, J.P. & Munro, C.A. 2017, "The Fungal Cell Wall: Structure, Biosynthesis, and Function", *Microbiology spectrum,* vol. 5, no. 3, pp. 10.1128/microbiolspec.FUNK-0035-2016.

Graf, K., Last, A., Gratz, R., Allert, S., Linde, S., Westermann, M., Groger, M., Mosig, A.S., Gresnigt, M.S. & Hube, B. 2019, "Keeping Candida commensal: how lactobacilli antagonize pathogenicity of Candida albicans in an in vitro gut model", *Disease models & mechanisms,* vol. 12, no. 9, pp. 10.1242/dmm.039719.

Graham, L.M., Tsoni, S.V., Willment, J.A., Williams, D.L., Taylor, P.R., Gordon, S., Dennehy, K. & Brown, G.D. 2006, "Soluble Dectin-1 as a tool to detect beta-glucans", *Journal of immunological methods,* vol. 314, no. 1-2, pp. 164-169.

Grassart, A., Malarde, V., Gobaa, S., Sartori-Rupp, A., Kerns, J., Karalis, K., Marteyn, B., Sansonetti, P. & Sauvonnet, N. 2019, "Bioengineered Human Organ-on-Chip Reveals Intestinal Microenvironment and Mechanical Forces Impacting Shigella Infection", *Cell host & microbe,* vol. 26, no. 3, pp. 435-444.e4.

Gratacap, R.L., Rawls, J.F. & Wheeler, R.T. 2013, "Mucosal candidiasis elicits NF-kappaB activation, proinflammatory gene expression and localized neutrophilia in zebrafish", *Disease models & mechanisms,* vol. 6, no. 5, pp. 1260-1270.

Gratacap, R.L., Scherer, A.K., Seman, B.G. & Wheeler, R.T. 2017, "Control of Mucosal Candidiasis in the Zebrafish Swim Bladder Depends on Neutrophils That Block Filament Invasion and Drive Extracellular-Trap Production", *Infection and immunity,* vol. 85, no. 9, pp. 10.1128/IAI.00276-17. Print 2017 Sep.

Gratacap, R.L. & Wheeler, R.T. 2014, "Utilization of zebrafish for intravital study of eukaryotic pathogen-host interactions", *Developmental and comparative immunology,* vol. 46, no. 1, pp. 108-115.

Grubb, S.E., Murdoch, C., Sudbery, P.E., Saville, S.P., Lopez-Ribot, J.L. & Thornhill, M.H. 2009, "Adhesion of Candida albicans to endothelial cells under physiological conditions of flow", *Infection and immunity,* vol. 77, no. 9, pp. 3872-3878.

Gustafson, K.S., Vercellotti, G.M., Bendel, C.M. & Hostetter, M.K. 1991, "Molecular mimicry in Candida albicans. Role of an integrin analogue in adhesion of the yeast to human endothelium", *The Journal of clinical investigation,* vol. 87, no. 6, pp. 1896-1902.

Hall, R.A. 2015, "Dressed to impress: impact of environmental adaptation on the Candida albicans cell wall", *Molecular microbiology,* vol. 97, no. 1, pp. 7-17.

Han, Q., Wang, N., Pan, C., Wang, Y. & Sang, J. 2019, "Elevation of cell wall chitin via Ca(2+) - calcineurin-mediated PKC signaling pathway maintains the viability of Candida albicans in the absence of beta-1,6-glucan synthesis", *Molecular microbiology,* vol. 112, no. 3, pp. 960-972.

Hasim, S., Allison, D.P., Retterer, S.T., Hopke, A., Wheeler, R.T., Doktycz, M.J. & Reynolds, T.B. 2016, "beta-(1,3)-Glucan Unmasking in Some Candida albicans Mutants Correlates with Increases in Cell Wall Surface Roughness and Decreases in Cell Wall Elasticity", *Infection and immunity,* vol. 85, no. 1, pp. 10.1128/IAI.00601-16. Print 2017 Jan.

Hebecker, B., Vlaic, S., Conrad, T., Bauer, M., Brunke, S., Kapitan, M., Linde, J., Hube, B. & Jacobsen, I.D. 2016, "Dual-species transcriptional profiling during systemic candidiasis reveals organ-specific host-pathogen interactions", *Scientific reports,* vol. 6, pp. 36055.

Heilmann, C.J., Sorgo, A.G., Mohammadi, S., Sosinska, G.J., de Koster, C.G., Brul, S., de Koning, L.J. & Klis, F.M. 2013, "Surface stress induces a conserved cell wall stress response in the pathogenic fungus Candida albicans", *Eukaryotic cell,* vol. 12, no. 2, pp. 254-264.

Heinisch, J.J. & Rodicio, R. 2018, "Protein kinase C in fungi-more than just cell wall integrity", *FEMS microbiology reviews,* vol. 42, no. 1, pp. 10.1093/femsre/fux051.

Hernandez-Chavez, M.J., Clavijo-Giraldo, D.M., Novak, A., Lozoya-Perez, N.E., Martinez-Alvarez, J.A., Salinas-Marin, R., Hernandez, N.V., Martinez-Duncker, I., Gacser, A. & Mora-Montes, H.M. 2019, "Role of Protein Mannosylation in the Candida tropicalis-Host Interaction", *Frontiers in microbiology,* vol. 10, pp. 2743.

Hernandez-Chavez, M.J., Perez-Garcia, L.A., Nino-Vega, G.A. & Mora-Montes, H.M. 2017, "Fungal Strategies to Evade the Host Immune Recognition", *Journal of fungi (Basel, Switzerland),* vol. 3, no. 4, pp. 10.3390/jof3040051.

Herre, J., Marshall, A.S., Caron, E., Edwards, A.D., Williams, D.L., Schweighoffer, E., Tybulewicz, V., Reis e Sousa, C., Gordon, S. & Brown, G.D. 2004, "Dectin-1 uses novel mechanisms for yeast phagocytosis in macrophages", *Blood,* vol. 104, no. 13, pp. 4038-4045.

Herrero, A.B., Magnelli, P., Mansour, M.K., Levitz, S.M., Bussey, H. & Abeijon, C. 2004, "KRE5 gene null mutant strains of Candida albicans are avirulent and have altered cell wall composition and hypha formation properties", *Eukaryotic cell,* vol. 3, no. 6, pp. 1423-1432.

Ho, J., Wickramasinghe, D.N., Nikou, S.A., Hube, B., Richardson, J.P. & Naglik, J.R. 2020, "Candidalysin Is a Potent Trigger of Alarmin and Antimicrobial Peptide Release in Epithelial Cells", *Cells,* vol. 9, no. 3, pp. 10.3390/cells9030699.

Ho, J., Yang, X., Nikou, S.A., Kichik, N., Donkin, A., Ponde, N.O., Richardson, J.P., Gratacap, R.L., Archambault, L.S., Zwirner, C.P., Murciano, C., Henley-Smith, R., Thavaraj, S., Tynan, C.J., Gaffen, S.L., Hube, B., Wheeler, R.T., Moyes, D.L. & Naglik, J.R. 2019, "Candidalysin activates innate epithelial immune responses via epidermal growth factor receptor", *Nature communications,* vol. 10, no. 1, pp. 2297-019-09915-2.

Ho, V., Herman-Bausier, P., Shaw, C., Conrad, K.A., Garcia-Sherman, M.C., Draghi, J., Dufrene, Y.F., Lipke, P.N. & Rauceo, J.M. 2019, "An Amyloid Core Sequence in the Major Candida albicans Adhesin Als1p Mediates Cell-Cell Adhesion", *mBio,* vol. 10, no. 5, pp. 10.1128/mBio.01766-19.

Hohl, T.M., Feldmesser, M., Perlin, D.S. & Pamer, E.G. 2008, "Caspofungin modulates inflammatory responses to Aspergillus fumigatus through stage-specific effects on fungal beta-glucan exposure", *The Journal of infectious diseases,* vol. 198, no. 2, pp. 176-185.

Hopke, A., Brown, A.J.P., Hall, R.A. & Wheeler, R.T. 2018, "Dynamic Fungal Cell Wall Architecture in Stress Adaptation and Immune Evasion", *Trends in microbiology,* vol. 26, no. 4, pp. 284-295.

Hopke, A., Nicke, N., Hidu, E.E., Degani, G., Popolo, L. & Wheeler, R.T. 2016, "Neutrophil Attack Triggers Extracellular Trap-Dependent Candida Cell Wall Remodeling and Altered Immune Recognition", *PLoS pathogens,* vol. 12, no. 5, pp. e1005644.

Ibe, C. & Munro, C.A. 2021, "Fungal Cell Wall Proteins and Signaling Pathways Form a Cytoprotective Network to Combat Stresses", *Journal of fungi (Basel, Switzerland),* vol. 7, no. 9, pp. 10.3390/jof7090739.

Jiang, L., Wang, J., Asghar, F., Snyder, N. & Cunningham, K.W. 2018, "CaGdt1 plays a compensatory role for the calcium pump CaPmr1 in the regulation of calcium signaling and cell wall integrity signaling in Candida albicans", *Cell communication and signaling : CCS,* vol. 16, no. 1, pp. 33-018-0246-x.

Jimenez-Lopez, C., Collette, J.R., Brothers, K.M., Shepardson, K.M., Cramer, R.A., Wheeler, R.T. & Lorenz, M.C. 2013, "Candida albicans induces arginine biosynthetic genes in response to host-derived reactive oxygen species", *Eukaryotic cell,* vol. 12, no. 1, pp. 91-100.

Johnson, C.J., Cabezas-Olcoz, J., Kernien, J.F., Wang, S.X., Beebe, D.J., Huttenlocher, A., Ansari, H. & Nett, J.E. 2016, "The Extracellular Matrix of Candida albicans Biofilms Impairs Formation of Neutrophil Extracellular Traps", *PLoS pathogens,* vol. 12, no. 9, pp. e1005884.

Johnston, D.A., Tapia, A.L., Eberle, K.E. & Palmer, G.E. 2013, "Three prevacuolar compartment Rab GTPases impact Candida albicans hyphal growth", *Eukaryotic cell,* vol. 12, no. 7, pp. 1039-1050.

Jones, L.A. & Sudbery, P.E. 2010, "Spitzenkorper, exocyst, and polarisome components in Candida albicans hyphae show different patterns of localization and have distinct dynamic properties", *Eukaryotic cell,* vol. 9, no. 10, pp. 1455-1465.

Jouault, T., Sarazin, A., Martinez-Esparza, M., Fradin, C., Sendid, B. & Poulain, D. 2009, "Host responses to a versatile commensal: PAMPs and PRRs interplay leading to tolerance or infection by Candida albicans", *Cellular microbiology,* vol. 11, no. 7, pp. 1007-1015.

Kasper, L., Konig, A., Koenig, P.A., Gresnigt, M.S., Westman, J., Drummond, R.A., Lionakis, M.S., Gross, O., Ruland, J., Naglik, J.R. & Hube, B. 2018, "The fungal peptide toxin Candidalysin activates the NLRP3 inflammasome and causes cytolysis in mononuclear phagocytes", *Nature communications,* vol. 9, no. 1, pp. 4260-018-06607-1.

Kennedy, M.J. & Volz, P.A. 1985, "Ecology of Candida albicans gut colonization: inhibition of Candida adhesion, colonization, and dissemination from the gastrointestinal tract by bacterial antagonism", *Infection and immunity,* vol. 49, no. 3, pp. 654-663.

Kenny, E.F., Herzig, A., Kruger, R., Muth, A., Mondal, S., Thompson, P.R., Brinkmann, V., Bernuth, H.V. & Zychlinsky, A. 2017, "Diverse stimuli engage different neutrophil extracellular trap pathways", *eLife,* vol. 6, pp. 10.7554/eLife.24437.

Kim, H.J., Huh, D., Hamilton, G. & Ingber, D.E. 2012, "Human gut-on-a-chip inhabited by microbial flora that experiences intestinal peristalsis-like motions and flow", *Lab on a chip,* vol. 12, no. 12, pp. 2165-2174.

Kim, H.J. & Ingber, D.E. 2013, "Gut-on-a-Chip microenvironment induces human intestinal cells to undergo villus differentiation", *Integrative biology : quantitative biosciences from nano to macro,* vol. 5, no. 9, pp. 1130-1140.

Klis, F.M., de Groot, P. & Hellingwerf, K. 2001, "Molecular organization of the cell wall of Candida albicans", *Medical mycology,* vol. 39 Suppl 1, pp. 1-8.

Knafler, H.C., Smaczynska-de, R.,II, Walker, L.A., Lee, K.K., Gow, N.A.R. & Ayscough, K.R. 2019, "AP-2-Dependent Endocytic Recycling of the Chitin Synthase Chs3 Regulates Polarized Growth in Candida albicans", *mBio,* vol. 10, no. 2, pp. 10.1128/mBio.02421-18.

Kruppa, M., Greene, R.R., Noss, I., Lowman, D.W. & Williams, D.L. 2011, "C. albicans increases cell wall mannoprotein, but not mannan, in response to blood, serum and cultivation at physiological temperature", *Glycobiology,* vol. 21, no. 9, pp. 1173-1180.

LaFayette, S.L., Collins, C., Zaas, A.K., Schell, W.A., Betancourt-Quiroz, M., Gunatilaka, A.A., Perfect, J.R. & Cowen, L.E. 2010, "PKC signaling regulates drug resistance of the fungal pathogen Candida albicans via circuitry comprised of Mkc1, calcineurin, and Hsp90", *PLoS pathogens,* vol. 6, no. 8, pp. e1001069.

Lee, K.K., Maccallum, D.M., Jacobsen, M.D., Walker, L.A., Odds, F.C., Gow, N.A. & Munro, C.A. 2012, "Elevated cell wall chitin in Candida albicans confers echinocandin resistance in vivo", *Antimicrobial Agents and Chemotherapy,* vol. 56, no. 1, pp. 208-217.

Lenardon, M.D., Munro, C.A. & Gow, N.A. 2010, "Chitin synthesis and fungal pathogenesis", *Current opinion in microbiology,* vol. 13, no. 4, pp. 416-423.

Li, Y., Li, Y., Cao, X., Jin, X. & Jin, T. 2017, "Pattern recognition receptors in zebrafish provide functional and evolutionary insight into innate immune signaling pathways", Cellular & molecular immunology, vol. 14, no. 1, pp. 80-89.

Lima, S.L., Colombo, A.L. & de Almeida Junior, J.N. 2019, "Fungal Cell Wall: Emerging Antifungals and Drug Resistance", *Frontiers in microbiology,* vol. 10, pp. 2573.

Lin, J., Oh, S.H., Jones, R., Garnett, J.A., Salgado, P.S., Rusnakova, S., Matthews, S.J., Hoyer, L.L. & Cota, E. 2014, "The peptide-binding cavity is essential for Als3-mediated adhesion of Candida albicans to human cells", *The Journal of biological chemistry,* vol. 289, no. 26, pp. 18401-18412.

Liu, N.N., Acosta-Zaldivar, M., Qi, W., Diray-Arce, J., Walker, L.A., Kottom, T.J., Kelly, R., Yuan, M., Asara, J.M., Lasky-Su, J.A., Levy, O., Limper, A.H., Gow, N.A.R. & Kohler, J.R. 2020, "Phosphoric Metabolites Link Phosphate Import and Polysaccharide Biosynthesis for Candida albicans Cell Wall Maintenance", *mBio,* vol. 11, no. 2, pp. 10.1128/mBio.03225-19.

Liu, Y. & Filler, S.G. 2011, "Candida albicans Als3, a multifunctional adhesin and invasin", *Eukaryotic cell,* vol. 10, no. 2, pp. 168-173.

Lo, H., Kohler, J.R., DiDomenico, B., Loebenberg, D., Cacciapuoti, A. & Fink, G.R. 1997, "Nonfilamentous *C. albicans* mutants are avirulent", *Cells,* vol. 90, no. 5, pp. 939.

Lorenz, M.C. 2013, "Carbon catabolite control in Candida albicans: new wrinkles in metabolism", *mBio,* vol. 4, no. 1, pp. e00034-13.

Luo, S., Dasari, P., Reiher, N., Hartmann, A., Jacksch, S., Wende, E., Barz, D., Niemiec, M.J., Jacobsen, I., Beyersdorf, N., Hunig, T., Klos, A., Skerka, C. & Zipfel, P.F. 2018, "The secreted Candida albicans protein Pra1 disrupts host defense by broadly targeting and blocking complement C3 and C3 activation fragments", *Molecular immunology,* vol. 93, pp. 266-277.

Luo, S., Skerka, C., Kurzai, O. & Zipfel, P.F. 2013, "Complement and innate immune evasion strategies of the human pathogenic fungus Candida albicans", *Molecular immunology,* vol. 56, no. 3, pp. 161-169.

Maccallum, D.M. 2012, "Hosting infection: experimental models to assay Candida virulence", *International journal of microbiology,* vol. 2012, pp. 363764.

Manickam, K., Machireddy, R.R. & Seshadri, S. 2014, "Characterization of biomechanical properties of agar based tissue mimicking phantoms for ultrasound stiffness imaging techniques", *Journal of the mechanical behavior of biomedical materials,* vol. 35, pp. 132-143.

Mansour, M.K., Tam, J.M., Khan, N.S., Seward, M., Davids, P.J., Puranam, S., Sokolovska, A., Sykes, D.B., Dagher, Z., Becker, C., Tanne, A., Reedy, J.L., Stuart, L.M. & Vyas, J.M. 2013, "Dectin-1 activation controls maturation of beta-1,3-glucan-containing phagosomes", *The Journal of biological chemistry,* vol. 288, no. 22, pp. 16043-16054.

Martzoukou, O., Amillis, S., Zervakou, A., Christoforidis, S. & Diallinas, G. 2017, "The AP-2 complex has a specialized clathrin-independent role in apical endocytosis and polar growth in fungi", *eLife,* vol. 6, pp. 10.7554/eLife.20083.

Maurer, M., Gresnigt, M.S., Last, A., Wollny, T., Berlinghof, F., Pospich, R., Cseresnyes, Z., Medyukhina, A., Graf, K., Groger, M., Raasch, M., Siwczak, F., Nietzsche, S., Jacobsen, I.D., Figge, M.T., Hube, B., Huber, O. & Mosig, A.S. 2019, "A three-dimensional immunocompetent intestine-on-chip model as in vitro platform for functional and microbial interaction studies", *Biomaterials,* vol. 220, pp. 119396.

May, R.C. & Casadevall, A. 2018, "In Fungal Intracellular Pathogenesis, Form Determines Fate", *mBio,* vol. 9, no. 5, pp. 10.1128/mBio.02092-18.

McCullough, M.J., Ross, B.C. & Reade, P.C. 1996, "Candida albicans: a review of its history, taxonomy, epidemiology, virulence attributes, and methods of strain differentiation", *International journal of oral and maxillofacial surgery,* vol. 25, no. 2, pp. 136-144.

Mio, T., Yabe, T., Sudoh, M., Satoh, Y., Nakajima, T., Arisawa, M. & Yamada-Okabe, H. 1996, "Role of three chitin synthase genes in the growth of Candida albicans", *Journal of Bacteriology,* vol. 178, no. 8, pp. 2416-2419.

Miramon, P., Dunker, C., Windecker, H., Bohovych, I.M., Brown, A.J., Kurzai, O. & Hube, B. 2012, "Cellular responses of Candida albicans to phagocytosis and the extracellular activities of

neutrophils are critical to counteract carbohydrate starvation, oxidative and nitrosative stress", *PloS one,* vol. 7, no. 12, pp. e52850.

Monroy-Perez, E., Sainz-Espunes, T., Paniagua-Contreras, G., Negrete-Abascal, E., Rodriguez-Moctezuma, J.R. & Vaca, S. 2012, "Frequency and expression of ALS and HWP1 genotypes in Candida albicans strains isolated from Mexican patients suffering from vaginal candidosis", *Mycoses,* vol. 55, no. 3, pp. e151-7.

Mora-Montes, H.M., Bates, S., Netea, M.G., Castillo, L., Brand, A., Buurman, E.T., Diaz-Jimenez, D.F., Jan Kullberg, B., Brown, A.J., Odds, F.C. & Gow, N.A. 2010, "A multifunctional mannosyltransferase family in Candida albicans determines cell wall mannan structure and host-fungus interactions", *The Journal of biological chemistry,* vol. 285, no. 16, pp. 12087-12095.

Mora-Montes, H.M., McKenzie, C., Bain, J.M., Lewis, L.E., Erwig, L.P. & Gow, N.A. 2012, "Interactions between macrophages and cell wall oligosaccharides of Candida albicans", *Methods in molecular biology (Clifton, N.J.),* vol. 845, pp. 247-260.

Mora-Montes, H.M., Netea, M.G., Ferwerda, G., Lenardon, M.D., Brown, G.D., Mistry, A.R., Kullberg, B.J., O'Callaghan, C.A., Sheth, C.C., Odds, F.C., Brown, A.J., Munro, C.A. & Gow, N.A. 2011, "Recognition and blocking of innate immunity cells by Candida albicans chitin", *Infection and immunity,* vol. 79, no. 5, pp. 1961-1970.

Moreno-Ruiz, E., Galan-Diez, M., Zhu, W., Fernandez-Ruiz, E., d'Enfert, C., Filler, S.G., Cossart, P. & Veiga, E. 2009, "Candida albicans internalization by host cells is mediated by a clathrin-dependent mechanism", *Cellular microbiology,* vol. 11, no. 8, pp. 1179-1189.

Mourer, T., El Ghalid, M., d'Enfert, C. & Bachellier-Bassi, S. 2021, "Involvement of amyloid proteins in the formation of biofilms in the pathogenic yeast Candida albicans", *Research in microbiology,* vol. 172, no. 3, pp. 103813.

Moyes, D.L., Richardson, J.P. & Naglik, J.R. 2015, "Candida albicans-epithelial interactions and pathogenicity mechanisms: scratching the surface", *Virulence,* vol. 6, no. 4, pp. 338-346.

Moyes, D.L., Wilson, D., Richardson, J.P., Mogavero, S., Tang, S.X., Wernecke, J., Hofs, S., Gratacap, R.L., Robbins, J., Runglall, M., Murciano, C., Blagojevic, M., Thavaraj, S., Forster, T.M., Hebecker, B., Kasper, L., Vizcay, G., Iancu, S.I., Kichik, N., Hader, A., Kurzai, O., Luo, T., Kruger, T., Kniemeyer, O., Cota, E., Bader, O., Wheeler, R.T., Gutsmann, T., Hube, B. & Naglik, J.R. 2016, "Candidalysin is a fungal peptide toxin critical for mucosal infection", *Nature,* vol. 532, no. 7597, pp. 64-68.

Mukaremera, L., Lee, K.K., Mora-Montes, H.M. & Gow, N.A.R. 2017, "Candida albicans Yeast, Pseudohyphal, and Hyphal Morphogenesis Differentially Affects Immune Recognition", *Frontiers in immunology,* vol. 8, pp. 629.

Munawara, U., Small, A.G., Quach, A., Gorgani, N.N., Abbott, C.A. & Ferrante, A. 2017, "Cytokines regulate complement receptor immunoglobulin expression and phagocytosis of Candida albicans in human macrophages: A control point in anti-microbial immunity", *Scientific reports,* vol. 7, no. 1, pp. 4050-017-04325-0.

Munro, C.A. 2013, "Chitin and glucan, the yin and yang of the fungal cell wall, implications for antifungal drug discovery and therapy", *Advances in Applied Microbiology,* vol. 83, pp. 145-172.

Munro, C.A., Schofield, D.A., Gooday, G.W. & Gow, N.A. 1998, "Regulation of chitin synthesis during dimorphic growth of Candida albicans", *Microbiology (Reading, England),* vol. 144 (Pt 2), no. Pt 2, pp. 391-401.

Munro, C.A., Selvaggini, S., de Bruijn, I., Walker, L., Lenardon, M.D., Gerssen, B., Milne, S., Brown, A.J. & Gow, N.A. 2007, "The PKC, HOG and Ca2+ signalling pathways co-ordinately regulate chitin synthesis in Candida albicans", *Molecular microbiology,* vol. 63, no. 5, pp. 1399-1413.

Naglik, J.R., Gaffen, S.L. & Hube, B. 2019, "Candidalysin: discovery and function in Candida albicans infections", *Current opinion in microbiology,* vol. 52, pp. 100-109.

Naglik, J.R., Konig, A., Hube, B. & Gaffen, S.L. 2017, "Candida albicans-epithelial interactions and induction of mucosal innate immunity", *Current opinion in microbiology,* vol. 40, pp. 104-112.

Navarro-Garcia, F., Sanchez, M., Pla, J. & Nombela, C. 1995, "Functional characterization of the MKC1 gene of Candida albicans, which encodes a mitogen-activated protein kinase homolog related to cell integrity", *Molecular and cellular biology,* vol. 15, no. 4, pp. 2197-2206.

Neppelenbroek, K.H., Seo, R.S., Urban, V.M., Silva, S., Dovigo, L.N., Jorge, J.H. & Campanha, N.H. 2014, "Identification of Candida species in the clinical laboratory: a review of conventional, commercial, and molecular techniques", *Oral diseases,* vol. 20, no. 4, pp. 329-344.

Netea, M.G., Brown, G.D., Kullberg, B.J. & Gow, N.A. 2008, "An integrated model of the recognition of Candida albicans by the innate immune system", *Nature reviews.Microbiology,* vol. 6, no. 1, pp. 67-78.

Newman, S.L. & Holly, A. 2001, "Candida albicans is phagocytosed, killed, and processed for antigen presentation by human dendritic cells", *Infection and immunity,* vol. 69, no. 11, pp. 6813-6822.

Noble, S.M., Gianetti, B.A. & Witchley, J.N. 2017, "Candida albicans cell-type switching and functional plasticity in the mammalian host", *Nature reviews.Microbiology,* vol. 15, no. 2, pp. 96-108.

Noble, S.M. & Johnson, A.D. 2005, "Strains and strategies for large-scale gene deletion studies of the diploid human fungal pathogen Candida albicans", *Eukaryotic cell,* vol. 4, no. 2, pp. 298-309.

O'Meara, T.R., Duah, K., Guo, C.X., Maxson, M.E., Gaudet, R.G., Koselny, K., Wellington, M., Powers, M.E., MacAlpine, J., O'Meara, M.J., Veri, A.O., Grinstein, S., Noble, S.M., Krysan, D., Gray-Owen, S.D. & Cowen, L.E. 2018, "High-Throughput Screening Identifies Genes Required for Candida albicans Induction of Macrophage Pyroptosis", *mBio,* vol. 9, no. 4, pp. 10.1128/mBio.01581-18.

Padovan, A.C., Chaves, G.M., Colombo, A.L. & Briones, M.R. 2009, "A novel allele of HWP1, isolated from a clinical strain of Candida albicans with defective hyphal growth and biofilm formation, has deletions of Gln/Pro and Ser/Thr repeats involved in cellular adhesion", *Medical mycology,* vol. 47, no. 8, pp. 824-835.

Paul, D., Achouri, S., Yoon, Y.Z., Herre, J., Bryant, C.E. & Cicuta, P. 2013, "Phagocytosis dynamics depends on target shape", Biophysical journal, vol. 105, no. 5, pp. 1143-1150.

Pereira, R., Dos Santos Fontenelle, R.O., de Brito, E.H.S. & de Morais, S.M. 2021, "Biofilm of Candida albicans: formation, regulation and resistance", *Journal of applied microbiology,* vol. 131, no. 1, pp. 11-22.

Peters, B.M., Palmer, G.E., Nash, A.K., Lilly, E.A., Fidel, P.L.,Jr & Noverr, M.C. 2014, "Fungal morphogenetic pathways are required for the hallmark inflammatory response during Candida albicans vaginitis", *Infection and immunity,* vol. 82, no. 2, pp. 532-543.

Plaine, A., Walker, L., Da Costa, G., Mora-Montes, H.M., McKinnon, A., Gow, N.A., Gaillardin, C., Munro, C.A. & Richard, M.L. 2008, "Functional analysis of Candida albicans GPI-anchored proteins: roles in cell wall integrity and caspofungin sensitivity", *Fungal genetics and biology : FG & B,* vol. 45, no. 10, pp. 1404-1414.

Playfair J. H. L., Chain B. M. 2012, *Immunology at Glance,* 10th edn, Wiley-Blackwell.

Preechasuth, K., Anderson, J.C., Peck, S.C., Brown, A.J., Gow, N.A. & Lenardon, M.D. 2015, "Cell wall protection by the Candida albicans class I chitin synthases", *Fungal genetics and biology : FG & B,* vol. 82, pp. 264-276.

Prill, S.K., Klinkert, B., Timpel, C., Gale, C.A., Schroppel, K. & Ernst, J.F. 2005, "PMT family of Candida albicans: five protein mannosyltransferase isoforms affect growth, morphogenesis and antifungal resistance", *Molecular microbiology,* vol. 55, no. 2, pp. 546-560.

Puerner, C., Kukhaleishvili, N., Thomson, D., Schaub, S., Noblin, X., Seminara, A., Bassilana, M. & Arkowitz, R.A. 2020, "Mechanical force-induced morphology changes in a human fungal pathogen", *BMC biology,* vol. 18, no. 1, pp. 122-020-00833-0.

Pujol, C., Daniels, K.J. & Soll, D.R. 2015, "Comparison of Switching and Biofilm Formation between MTL-Homozygous Strains of Candida albicans and Candida dubliniensis", *Eukaryotic cell,* vol. 14, no. 12, pp. 1186-1202.

Renshaw, S.A. & Trede, N.S. 2012, "A model 450 million years in the making: zebrafish and vertebrate immunity", Disease models & mechanisms, vol. 5, no. 1, pp. 38-47.

Richardson, J.P., Ho, J. & Naglik, J.R. 2018, "Candida-Epithelial Interactions", *Journal of fungi (Basel, Switzerland),* vol. 4, no. 1, pp. 10.3390/jof4010022.

Richardson, J.P., Mogavero, S., Moyes, D.L., Blagojevic, M., Kruger, T., Verma, A.H., Coleman, B.M., De La Cruz Diaz, J., Schulz, D., Ponde, N.O., Carrano, G., Kniemeyer, O., Wilson, D., Bader, O., Enoiu, S.I., Ho, J., Kichik, N., Gaffen, S.L., Hube, B. & Naglik, J.R. 2018, "Processing of Candida albicans Ece1p Is Critical for Candidalysin Maturation and Fungal Virulence", *mBio,* vol. 9, no. 1, pp. 10.1128/mBio.02178-17.

Robertson, A.S., Smythe, E. & Ayscough, K.R. 2009, "Functions of actin in endocytosis", *Cellular and molecular life sciences : CMLS,* vol. 66, no. 13, pp. 2049-2065.

Rodriguez-Cerdeira, C., Gregorio, M.C., Molares-Vila, A., Lopez-Barcenas, A., Fabbrocini, G., Bardhi, B., Sinani, A., Sanchez-Blanco, E., Arenas-Guzman, R. & Hernandez-Castro, R. 2019, "Biofilms and vulvovaginal candidiasis", *Colloids and surfaces.B, Biointerfaces,* vol. 174, pp. 110-125.

Roman, E., Correia, I., Salazin, A., Fradin, C., Jouault, T., Poulain, D., Liu, F.T. & Pla, J. 2016, "The Cek1mediated MAP kinase pathway regulates exposure of alpha1,2 and beta1,2mannosides in the cell wall of Candida albicans modulating immune recognition", *Virulence,* vol. 7, no. 5, pp. 558-577.

Romo, J.A. & Kumamoto, C.A. 2020, "On Commensalism of Candida", *Journal of fungi (Basel, Switzerland),* vol. 6, no. 1, pp. 10.3390/jof6010016.

Rowbottom, L., Munro, C.A. & Gow, N.A. 2004, "Candida albicans mutants in the BNI4 gene have reduced cell-wall chitin and alterations in morphogenesis", *Microbiology (Reading, England),* vol. 150, no. Pt 10, pp. 3243-3252.

Rudkin, F.M., Bain, J.M., Walls, C., Lewis, L.E., Gow, N.A. & Erwig, L.P. 2013, "Altered dynamics of Candida albicans phagocytosis by macrophages and PMNs when both phagocyte subsets are present", *mBio,* vol. 4, no. 6, pp. e00810-13.

Rueda, C., Cuenca-Estrella, M. & Zaragoza, O. 2014, "Paradoxical growth of Candida albicans in the presence of caspofungin is associated with multiple cell wall rearrangements and decreased virulence", *Antimicrobial Agents and Chemotherapy,* vol. 58, no. 2, pp. 1071-1083.

Ruzicka, L., Howe, D.G., Ramachandran, S., Toro, S., Van Slyke, C.E., Bradford, Y.M., Eagle, A., Fashena, D., Frazer, K., Kalita, P., Mani, P., Martin, R., Moxon, S.T., Paddock, H., Pich, C., Schaper, K., Shao, X., Singer, A. & Westerfield, M. 2019, "The Zebrafish Information Network: new support for non-coding genes, richer Gene Ontology annotations and the Alliance of Genome Resources", *Nucleic acids research,* vol. 47, no. D1, pp. D867-D873.

Sanz, M., Carrano, L., Jimenez, C., Candiani, G., Trilla, J.A., Duran, A. & Roncero, C. 2005, "Candida albicans strains deficient in CHS7, a key regulator of chitin synthase III, exhibit morphogenetic alterations and attenuated virulence", *Microbiology (Reading, England),* vol. 151, no. Pt 8, pp. 2623-2636.

Scherer, A.K., Blair, B.A., Park, J., Seman, B.G., Kelley, J.B. & Wheeler, R.T. 2020, "Redundant Trojan horse and endothelial-circulatory mechanisms for host-mediated spread of Candida albicans yeast", *PLoS pathogens,* vol. 16, no. 8, pp. e1008414.

Segal, E. & Frenkel, M. 2018, "Experimental in Vivo Models of Candidiasis", *Journal of fungi (Basel, Switzerland),* vol. 4, no. 1, pp. 10.3390/jof4010021.

Selvaggini, S., Munro, C.A., Paschoud, S., Sanglard, D. & Gow, N.A.R. 2004, "Independent regulation of chitin synthase and chitinase activity in Candida albicans and Saccharomyces cerevisiae", *Microbiology (Reading, England),* vol. 150, no. Pt 4, pp. 921-928.

Sem, X., Le, G.T., Tan, A.S., Tso, G., Yurieva, M., Liao, W.W., Lum, J., Srinivasan, K.G., Poidinger, M., Zolezzi, F. & Pavelka, N. 2016, "beta-glucan Exposure on the Fungal Cell Wall Tightly Correlates with Competitive Fitness of Candida Species in the Mouse Gastrointestinal Tract", *Frontiers in cellular and infection microbiology,* vol. 6, pp. 186.

Seman, B.G., Moore, J.L., Scherer, A.K., Blair, B.A., Manandhar, S., Jones, J.M. & Wheeler, R.T. 2018, "Yeast and Filaments Have Specialized, Independent Activities in a Zebrafish Model of Candida albicans Infection", *Infection and immunity,* vol. 86, no. 10, pp. 10.1128/IAI.00415-18. Print 2018 Oct.

Shen, H., Chen, S.M., Liu, W., Zhu, F., He, L.J., Zhang, J.D., Zhang, S.Q., Yan, L., Xu, Z., Xu, G.T., An, M.M. & Jiang, Y.Y. 2015, "Abolishing Cell Wall Glycosylphosphatidylinositol-Anchored Proteins in Candida albicans Enhances Recognition by Host Dectin-1", *Infection and immunity,* vol. 83, no. 7, pp. 2694-2704.

Sherrington, S.L., Sorsby, E., Mahtey, N., Kumwenda, P., Lenardon, M.D., Brown, I., Ballou, E.R., MacCallum, D.M. & Hall, R.A. 2017, "Adaptation of Candida albicans to environmental pH induces cell wall remodelling and enhances innate immune recognition", *PLoS pathogens,* vol. 13, no. 5, pp. e1006403.

Singh, D.K., Toth, R. & Gacser, A. 2020, "Mechanisms of Pathogenic Candida Species to Evade the Host Complement Attack", *Frontiers in cellular and infection microbiology,* vol. 10, pp. 94.

Snarr, B.D., Qureshi, S.T. & Sheppard, D.C. 2017, "Immune Recognition of Fungal Polysaccharides", *Journal of fungi (Basel, Switzerland),* vol. 3, no. 3, pp. 10.3390/jof3030047.

Staniszewska, M., Bondaryk, M., Zukowski, K. & Chudy, M. 2015, "Role of SAP7-10 and Morphological Regulators (EFG1, CPH1) in Candida albicans' Hypha Formation and Adhesion to Colorectal Carcinoma Caco-2", *Polish journal of microbiology,* vol. 64, no. 3, pp. 203-210.

Sudbery, P., Gow, N. & Berman, J. 2004, "The distinct morphogenic states of Candida albicans", *Trends in microbiology,* vol. 12, no. 7, pp. 317-324.

Sudbery, P.E. 2011, "Growth of Candida albicans hyphae", *Nature reviews.Microbiology,* vol. 9, no. 10, pp. 737-748.

Sudoh, M., Nagahashi, S., Doi, M., Ohta, A., Takagi, M. & Arisawa, M. 1993, "Cloning of the chitin synthase 3 gene from Candida albicans and its expression during yeast-hyphal transition", *Molecular & general genetics : MGG,* vol. 241, no. 3-4, pp. 351-358.

Swidergall, M. 2019, "Candida albicans at Host Barrier Sites: Pattern Recognition Receptors and Beyond", *Pathogens (Basel, Switzerland),* vol. 8, no. 1, pp. 10.3390/pathogens8010040.

Swidergall, M., Khalaji, M., Solis, N.V., Moyes, D.L., Drummond, R.A., Hube, B., Lionakis, M.S., Murdoch, C., Filler, S.G. & Naglik, J.R. 2019, "Candidalysin Is Required for Neutrophil Recruitment and Virulence During Systemic Candida albicans Infection", *The Journal of infectious diseases,* vol. 220, no. 9, pp. 1477-1488.

Tabatabaei, F., Moharamzadeh, K. & Tayebi, L. 2020, "Three-Dimensional In Vitro Oral Mucosa Models of Fungal and Bacterial Infections", *Tissue engineering.Part B, Reviews,* .

Tams, R.N., Wagner, A.S., Jackson, J.W., Gann, E.R., Sparer, T.E. & Reynolds, T.B. 2020, "Pathways That Synthesize Phosphatidylethanolamine Impact Candida albicans Hyphal Length and Cell Wall Composition through Transcriptional and Posttranscriptional Mechanisms", *Infection and immunity,* vol. 88, no. 3, pp. 10.1128/IAI.00480-19. Print 2020 Feb 20.

Taylor, P.R., Brown, G.D., Reid, D.M., Willment, J.A., Martinez-Pomares, L., Gordon, S. & Wong, S.Y. 2002, "The beta-glucan receptor, dectin-1, is predominantly expressed on the surface of cells of the monocyte/macrophage and neutrophil lineages", *Journal of immunology (Baltimore, Md.: 1950),* vol. 169, no. 7, pp. 3876-3882.

Tebarth, B., Doedt, T., Krishnamurthy, S., Weide, M., Monterola, F., Dominguez, A. & Ernst, J.F. 2003, "Adaptation of the Efg1p morphogenetic pathway in Candida albicans by negative autoregulation and PKA-dependent repression of the EFG1 gene", *Journal of Molecular Biology,* vol. 329, no. 5, pp. 949-962.

Tessarolli, V., Gasparoto, T.H., Lima, H.R., Figueira, E.A., Garlet, T.P., Torres, S.A., Garlet, G.P., Da Silva, J.S. & Campanelli, A.P. 2010, "Absence of TLR2 influences survival of neutrophils after infection with Candida albicans", *Medical mycology,* vol. 48, no. 1, pp. 129-140.

Thomson, D.D., Wehmeier, S., Byfield, F.J., Janmey, P.A., Caballero-Lima, D., Crossley, A. & Brand, A.C. 2015, "Contact-induced apical asymmetry drives the thigmotropic responses of Candida albicans hyphae", *Cellular microbiology,* vol. 17, no. 3, pp. 342-354.

Tobin, D.M., May, R.C. & Wheeler, R.T. 2012, "Zebrafish: a see-through host and a fluorescent toolbox to probe host-pathogen interaction", *PLoS pathogens,* vol. 8, no. 1, pp. e1002349.

Trogdon, M., Drawert, B., Gomez, C., Banavar, S.P., Yi, T.M., Campas, O. & Petzold, L.R. 2018, "The effect of cell geometry on polarization in budding yeast", *PLoS computational biology,* vol. 14, no. 6, pp. e1006241.

Tronchin, G., Bouchara, J.P., Annaix, V., Robert, R. & Senet, J.M. 1991, "Fungal cell adhesion molecules in Candida albicans", *European journal of epidemiology,* vol. 7, no. 1, pp. 23-33.

Ueno, K., Namiki, Y., Mitani, H., Yamaguchi, M. & Chibana, H. 2011, "Differential cell wall remodeling of two chitin synthase deletants Deltachs3A and Deltachs3B in the pathogenic yeast Candida glabrata", *FEMS yeast research,* vol. 11, no. 5, pp. 398-407.

Vautier, S., Drummond, R.A., Chen, K., Murray, G.I., Kadosh, D., Brown, A.J., Gow, N.A., MacCallum, D.M., Kolls, J.K. & Brown, G.D. 2015, "Candida albicans colonization and dissemination from the murine gastrointestinal tract: the influence of morphology and Th17 immunity", *Cellular microbiology,* vol. 17, no. 4, pp. 445-450.

Verma, A.H., Richardson, J.P., Zhou, C., Coleman, B.M., Moyes, D.L., Ho, J., Huppler, A.R., Ramani, K., McGeachy, M.J., Mufazalov, I.A., Waisman, A., Kane, L.P., Biswas, P.S., Hube, B., Naglik, J.R. & Gaffen, S.L. 2017, "Oral epithelial cells orchestrate innate type 17 responses to Candida albicans through the virulence factor candidalysin", *Science immunology,* vol. 2, no. 17, pp. 10.1126/sciimmunol.aam8834.

Vesely, E.M., Williams, R.B., Konopka, J.B. & Lorenz, M.C. 2017, "N-Acetylglucosamine Metabolism Promotes Survival of Candida albicans in the Phagosome", *mSphere,* vol. 2, no. 5, pp. 10.1128/mSphere.00357-17. eCollection 2017 Sep-Oct.

Veses, V. & Gow, N.A. 2008, "Vacuolar dynamics during the morphogenetic transition in Candida albicans", *FEMS yeast research,* vol. 8, no. 8, pp. 1339-1348.

Vijayan, D., Radford, K.J., Beckhouse, A.G., Ashman, R.B. & Wells, C.A. 2012, "Mincle polarizes human monocyte and neutrophil responses to Candida albicans", *Immunology and cell biology,* vol. 90, no. 9, pp. 889-895.

Vylkova, S., Carman, A.J., Danhof, H.A., Collette, J.R., Zhou, H. & Lorenz, M.C. 2011, "The fungal pathogen Candida albicans autoinduces hyphal morphogenesis by raising extracellular pH", *mBio,* vol. 2, no. 3, pp. e00055-11.

Vylkova, S. & Lorenz, M.C. 2017, "Phagosomal Neutralization by the Fungal Pathogen Candida albicans Induces Macrophage Pyroptosis", *Infection and immunity,* vol. 85, no. 2, pp. 10.1128/IAI.00832-16. Print 2017 Feb.

Vylkova, S. & Lorenz, M.C. 2014, "Modulation of phagosomal pH by Candida albicans promotes hyphal morphogenesis and requires Stp2p, a regulator of amino acid transport", *PLoS pathogens,* vol. 10, no. 3, pp. e1003995.

Wagener, J., MacCallum, D.M., Brown, G.D. & Gow, N.A. 2017, "Candida albicans Chitin Increases Arginase-1 Activity in Human Macrophages, with an Impact on Macrophage Antimicrobial Functions", *mBio,* vol. 8, no. 1, pp. 10.1128/mBio.01820-16.

Wagener, J., Malireddi, R.K., Lenardon, M.D., Koberle, M., Vautier, S., MacCallum, D.M., Biedermann, T., Schaller, M., Netea, M.G., Kanneganti, T.D., Brown, G.D., Brown, A.J. & Gow, N.A. 2014, "Fungal chitin dampens inflammation through IL-10 induction mediated by NOD2 and TLR9 activation", *PLoS pathogens,* vol. 10, no. 4, pp. e1004050.

Walker, L., Sood, P., Lenardon, M.D., Milne, G., Olson, J., Jensen, G., Wolf, J., Casadevall, A., Adler-Moore, J. & Gow, N.A.R. 2018, "The Viscoelastic Properties of the Fungal Cell Wall Allow Traffic of AmBisome as Intact Liposome Vesicles", *mBio,* vol. 9, no. 1, pp. 10.1128/mBio.02383-17.

Walker, L.A., Gow, N.A. & Munro, C.A. 2010, "Fungal echinocandin resistance", *Fungal genetics and biology : FG & B,* vol. 47, no. 2, pp. 117-126.

Walker, L.A., Lenardon, M.D., Preechasuth, K., Munro, C.A. & Gow, N.A. 2013, "Cell wall stress induces alternative fungal cytokinesis and septation strategies", *Journal of cell science,* vol. 126, no. Pt 12, pp. 2668-2677.

Weiner, A., Orange, F., Lacas-Gervais, S., Rechav, K., Ghugtyal, V., Bassilana, M. & Arkowitz, R.A. 2019, "On-site secretory vesicle delivery drives filamentous growth in the fungal pathogen Candida albicans", *Cellular microbiology,* vol. 21, no. 1, pp. e12963.

Westman, J., Moran, G., Mogavero, S., Hube, B. & Grinstein, S. 2018, "Candida albicans Hyphal Expansion Causes Phagosomal Membrane Damage and Luminal Alkalinization", *mBio,* vol. 9, no. 5, pp. 10.1128/mBio.01226-18.

Westman, J., Walpole, G.F.W., Kasper, L., Xue, B.Y., Elshafee, O., Hube, B. & Grinstein, S. 2020, "Lysosome Fusion Maintains Phagosome Integrity during Fungal Infection", *Cell host & microbe,* vol. 28, no. 6, pp. 798-812.e6.

Whaley, S.G., Berkow, E.L., Rybak, J.M., Nishimoto, A.T., Barker, K.S. & Rogers, P.D. 2017, "Azole Antifungal Resistance in Candida albicans and Emerging Non-albicans Candida Species", *Frontiers in microbiology,* vol. 7, pp. 2173.

Whiley, R.A., Cruchley, A.T., Gore, C. & Hagi-Pavli, E. 2012, "Candida albicans strain-dependent modulation of pro-inflammatory cytokine release by in vitro oral and vaginal mucosal models", *Cytokine,* vol. 57, no. 1, pp. 89-97.

Wiederhold, N.P., Kontoyiannis, D.P., Prince, R.A. & Lewis, R.E. 2005, "Attenuation of the activity of caspofungin at high concentrations against candida albicans: possible role of cell wall integrity and calcineurin pathways", *Antimicrobial Agents and Chemotherapy,* vol. 49, no. 12, pp. 5146-5148.

Wiles, C.M & Mackenzie, D.W.R 1987, "**6 - Fungal diseases of the central nervous system**" in ***Infections of the Nervous System***, ed. Kennedy, Peter G.E & Johnson, Richard T., Butterworth-Heinemann, , pp. 97-117.

Witchley, J.N., Penumetcha, P., Abon, N.V., Woolford, C.A., Mitchell, A.P. & Noble, S.M. 2019, "Candida albicans Morphogenesis Programs Control the Balance between Gut Commensalism and Invasive Infection", *Cell host & microbe,* vol. 25, no. 3, pp. 432-443.e6.

Zhou, Y., Liao, M., Zhu, C., Hu, Y., Tong, T., Peng, X., Li, M., Feng, M., Cheng, L., Ren, B. & Zhou, X. 2018, "ERG3 and ERG11 genes are critical for the pathogenesis of Candida albicans during the oral mucosal infection", *International journal of oral science,* vol. 10, no. 2, pp. 9-018-0013-2.

Chapter 8: Supplementary material

Supplementary 1: CASY^{M} counter histograms

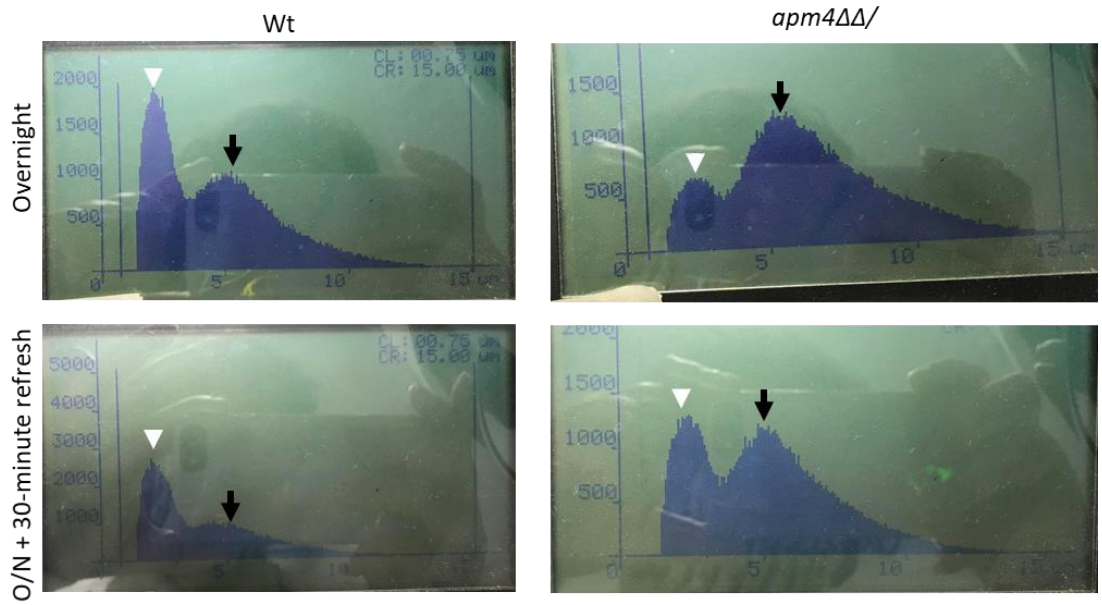

The histograms produced by the CASY$_{TM}$ counter while making the measurements. The histograms presented two peaks one for non budded cells presented with the white arrowheads and a peak for budded cells presented with black arrows. The results from the histograms give indications for the budding state of the cells during the measurements

Supplementary 2: Macrophage lysis by yeast-locked cells

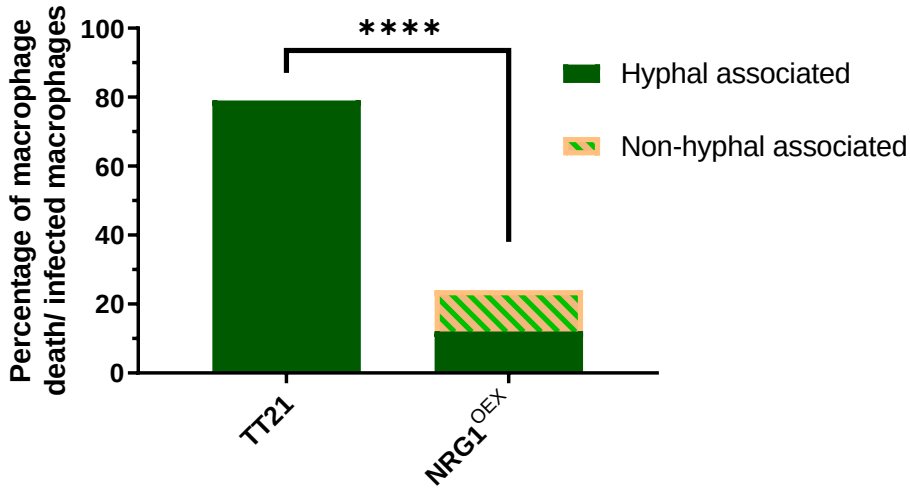

C. albicans and J774 macrophages at 1:1 ratio were co-incubated for 18 hrs. The interaction was monitored by time-lapse microscopy at Phase 20x, the results were then analyzed by single cell observations and recordings of the changes inside the phagolysosome. The statistical analysis used were both a Fisher's exact test and a Chi-square test.

The graph is a quantification of macrophage death from single cell observations during infections with *C. albicans.* Observations were recorded from 18hr time-lapse experiments using Phase 20x and capturing every 10 minutes. Hyphal associated and non-hyphal associated death are showed.